INTEGRATING MOLECULAR EVOLUTION AND MORPHOLOGY TO STUDY THE EVOLUTIONARY HISTORY OF LIZARDFISHES AND THEIR ALLIES

by

Matthew P. Davis
B.S., Regis University, 2004

Submitted to the Department of Ecology and Evolutionary Biology and the Faculty of the Graduate School of the University of Kansas in partial fulfillment of the requirements for the degree of Doctor of Philosophy

_____
Edward O. Wiley Chair

_____
C. Richard Robins

_____
Linda Trueb

_____
Mark Holder

_____
Bruce Lieberman

Date Defended: 12/04/2009

The Dissertation Committee for Matthew P. Davis certifies that this is the approved version of the following dissertation:

INTEGRATING MOLECULAR EVOLUTION AND MORPHOLOGY TO STUDY THE EVOLUTIONARY HISTORY OF LIZARDFISHES AND THEIR ALLIES

Committee:

_____
Edward O. Wiley Chair

_____
C. Richard Robins

_____
Linda Trueb

_____
Mark Holder

_____
Bruce Lieberman

Date Defended: 12/04/2009

ABSTRACT

Evolutionary relationships of the Aulopiformes (Euteleostei: Cyclosquamata) are investigated from a molecular and total evidence approach that includes previous morphological datasets. Molecular and total evidence analyses recover Aulopiformes as monophyletic and sister to a monophyletic Ctenosquamata, supporting the monophyly of Eurypterygii with molecular data.

The divergence times of Aulopiformes are estimated utilizing a Bayesian approach in combination with knowledge of the fossil record of teleosts. Also the character evolution of deep-sea evolutionary adaptations is explored. The stem species of the aulopiforms arose during the Early Cretaceous, and possibly Late Jurassic in a marine environment with separate sexes, and laterally directed, round eyes. Tubular eyes have arisen independently at different times in three deep-sea pelagic predatory aulopiform lineages. Simultaneous hermaphroditism evolved a single time in the stemspecies of the superfamily Alepisauroidei, the clade of deep-sea aulopiforms.

The BiSSE likelihood model was implemented to explore whether simultaneous hermaphroditism is affecting diversification rates within lizardfishes. The evolution of simultaneous hermaphroditism or any other codistributed character does not seem to be influencing rates of speciation or extinction. An asymmetry in rate of character change is not found to be statistically significant, however there is some evidence that this asymmetry may explain why the preponderance of aulopiform taxa are simultaneous hermaphrodites.

ACKNOWLEDGEMENTS

I would like to thank all of the people who have helped make completing my doctoral degree possible and a great experience in my life. First, I would like to thank all of the members of my dissertation committee, Edward O. Wiley, C. Richard Robins, Linda Trueb, Mark Holder, and Bruce Lieberman. I would like to extend a special acknowledgement to my three readers Ed Wiley, Linda Trueb, and Mark Holder. I thank each member of my committee for all of their helpful comments and suggestions regarding analyses, text, and figures.

I am particularly appreciative of my major adviser Ed Wiley. From the moment I started at the University of Kansas Ed has played a prominent role in my development as a scientist. I am indebted to him for the countless conversations regarding evolutionary biology, systematics, ichthyology, and whatever else the discussions of day wandered. He fostered an atmosphere in the division that made working and learning there a great place to be, and was always there for me. Ed was very supportive both mentally and monetarily, and for that I will always be grateful.

Working on a group where the majority of taxa are distributed in the deep sea meant that I had to rely heavily on specimen loans to complete this thesis. I thank the following people and institutions for providing specimen and tissue loans used in this work: E. O. Wiley and A. Bentley (University of Kansas Natural History Museum and Biodiversity Institute), H. J. Walker (Scripps Institution of Oceanography), K. Hartel (Museum of Comparative Zoology), E. J. Hilton (Virginia Institute of Marine Science), and M. Miya (Natural History Museum & Institute, Chiba, Japan). Funding

for this thesis was supported by a National Science Foundation Doctoral Dissertation Improvement Grant (DEB 0910081), NSF Euteleost Tree of Life Grant (DEB 0732819), University of Kansas Natural History Museum and Biodiversity Institute Panorama Grants, and the Wiley Laboratory. I would also like to thank the University of Kansas Natural History Museum and Biodiversity Institute for allowing me to use all the various equipment necessary to complete this work.

The KU Division of Ichthyology has been a tremendous place to work and learn for the past 5 years, which is entirely due to the people that reside there. I would like to express my thanks to Gloria Arratia, who I have had the pleasure to collaborate with on a variety of projects outside this thesis. I have learned a tremendous amount about fish morphology and paleontology from her, and I am excited to continue working with her in the future. I would also like to thank C. Richard Robins for sharing his vast expertise in ichthyology with me during many of our numerous conversations. I also greatly appreciated the many conversations I had with Hans-Peter Schultze regarding the evolution of vertebrates, ichthyology, and paleontology.

For training in molecular techniques and PCR troubleshooting, collaboration, and many interesting discussions, I want to extend a special thanks to Nancy Holcroft. I would like to thank Geff Luttrell for passing on to me a fragment of his vast knowledge about North American freshwater fishes, and for teaching me all about the art of fish identification. I want to acknowledge all of the hard work Andy Bentley did helping me process all of the specimen loans I acquired during my time at KU. I

also thank Mike Grose for all of his assistance with DNA sequencing and troubleshooting.

I am extremely grateful for all the help, assistance, and support from the ichthyology students throughout my time at KU including, Anna Clarke, Pingfu Chen, Shannon DeVaney, Francine Abe, Kathryn Mickle, Sarah Spears, and Hannah Owens. They made the Division of Ichthyology a great place to work every day. I will miss the Fish lunches, traveling the Kansas countryside seining for fish, and hanging out at Milton's grabbing coffee.

I would also like to thank members of the ichthyology community outside of the University of Kansas. First, I would like to extend a very special acknowledgement to Michael J. Ghedotti for setting me on this path during my time at Regis University. I have learned a tremendous amount about fish, biology, and academia from him over the years, and I thank him for his continued support during my time at KU. My development as an ichthyologist has been shaped by many friends and collaborators in the ichthyology community that I wish to acknowledge, including Andrew Simons, Chris Fielitz, Leo Smith, Kevin Tang, Jacob Egge, Pete Berendzen, Eric Hilton, Rick Mayden, Nick Lang, Kevin Conway, Matt Friedman, Terry Grande, and Prosanta Chakrabarty.

I did not exclusively school with fish students at KU, so I would like to acknowledge the wonderful community of graduate students, post-docs, and undergraduate researchers I had the good fortune to interact with for the past 5 years. Thanks for all the memories, the intellectual stimulating conversations, and the

occasional rocking out. While this is not a comprehensive list it still might take a while, starting with Charles Linkem, Jeff Cole, Jamie Oaks, Richard Williams, Omar Torres, Juan Manuel Guayasamin, Elisa Bonaccorso, Ismael Hinojosa, Jeet Sukumaran, Andrea Crowther, Julie Martindale, Sean Maher, Sarah Hinman, Jake Esselstyn, Stephanie Swenson, Monica Papes, Arpad Nyari, Pete Hosner, Raul Diaz, Andres Lira Noriega, Amanda Falk, Annalise Nawrocki, Anthony Barley, Blythe Alexander, Lisa Rausch, Cameron Siler, Allison Fuiten, David McLeod, Carl Oliveros, Edgar Lehr, Carola Castello, Cori Myers, Mike Anderson, Daniel Bennett, Erin Saupe, Garrett Call, Geoffrey Vincent, Katie Sparks, Grey Gustafson, Norberto Baldi, Jason Palikij, Josephine Michener, Allison Ingram, Julius Mojica, Kendra Koch, Danny Najera, Katarina Topalov, Liza Holeski, Lynn Villafuerte, Joanna Cielocha, Steve Davis, Sarah Schmidt, Ryan O'Leary, Marcos Barbeitos, Wes Gapp, Wendy Eash-Loucks, and Victor Gonzalez Betancourt. Thank you everyone, but your dissertations are in another castle. This one is mine.

A special acknowledgement goes to Francine R. Abe, who I cannot thank enough for being so supportive of me for the last 5 years. I owe her a great debt of gratitude for helping to make every day enjoyable, which even includes the day I took my qualifying exam. In 5 years we have climbed the Eiffel Tower, gone fishing for piranhas in Brazil, and watched almost everything ever made by Joss Whedon. I hope for many more adventures after graduate school.

Finally I would like to thank my family for everything they have done for me over the years. I would not be who I am without their love and support, and I want to

acknowledge my mother Tamara R. Davis and my father Danny W. Davis for the huge role they have played in life. They taught me the value of academics from an early age, supported my love of science, and went great lengths to ensure I had a high quality of education my whole life. I cannot thank them enough. I also thank my brother Mitchell D. Davis for always being there for me. I want to also acknowledge the love and support from my extended family that helped me reach this goal, including my grandparents Paul Rott, Betty Rott, Del Davis, and Carol Davis. Last but not least, I would like to thank my dogs Ash and Jet. Although they never had any idea of what I did day-to-day in graduate school—much like most people I ever tried to explain it to—they were always happy to see me which is more than enough.

TABLE OF CONTENTS

CHAPTER 1

EVOLUTIONARY RELATIONSHIPS OF THE AULOPIFORMES (EUTELEOSTEI: CYCLOSQUAMATA): A MOLECULAR AND TOTAL EVIDENCE APPROACH

INTRODUCTION

The extreme habitats of the deep sea have produced fascinating evolutionary events among the 2000 species of marine fishes that have invaded this realm. This study focuses on one such lineage, the marine order Aulopiformes (Euteleostei: Cyclosquamata), which includes 44 genera and 236 species of lizardfishes and their allies (Nelson 2006). Aulopiform fishes include some of the most bizarre deep-sea fishes, as well as key coral-reef predators, with members of the group exhibiting diverse evolutionary adaptations, such as bioluminescence, tubular eyes, and synchronous hermaphroditism (Fig. 1.1). Recent work on previously unrecognized fossil taxa supports an Early to Late Cretaceous origin for the order (e.g., Rosen 1973, Fielitz 2004) in a marine environment. Aulopiformes are classified within the Superorder Cyclosquamata, and are currently divided into four monophyletic suborders as shown in Figure 1.2 (Baldwin & Johnson 1996, Sato & Nakabo 2002).

Hypotheses regarding aulopiform relationships have been controversial since the proposal of the order by Rosen (1973), with as many as seven distinct classifications

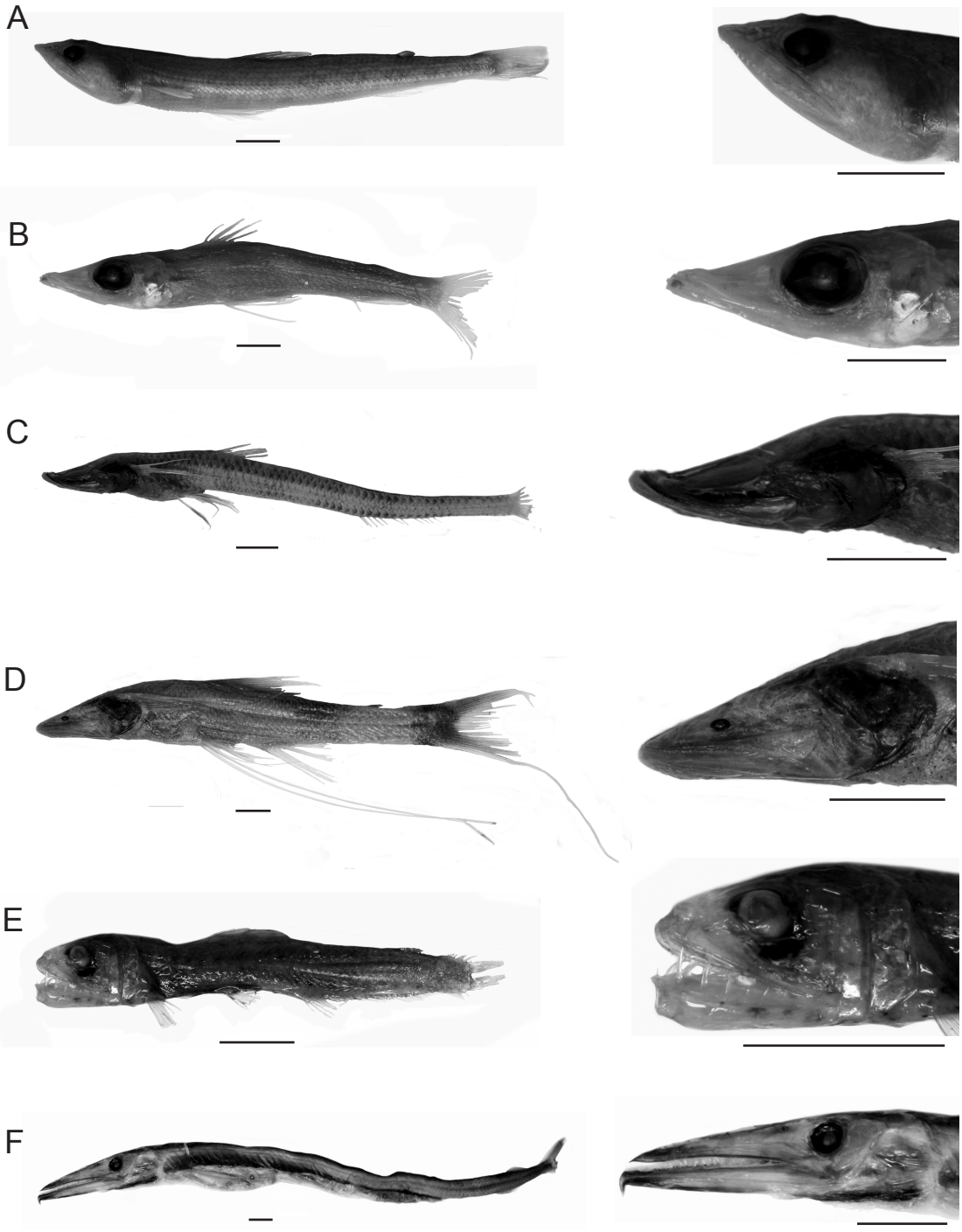

Fig. 1.1. Representatives of aulopiform diversity. (A) *Synodus foetens*, KU 18066, (B) *Parasudis truculenta*, VIMS 03261, (C) *Ipnops murrayi*, KU CI-182, (D) *Bathypterois viridensis*, VIMS 6149, (E) *Evermannella indica*, SIO 73-148, (F) *Anotopterus pharao*, KU 28218. Scale bar denotes 10 mm.

Baldwin & Johnson (1996)

Order Aulopiformes
- Suborder Synodontoidei
  - Family Aulopidae (*Aulopus*)
  - Family Pseudotrichonotidae (*Pseudotrichonotus*)
  - Family Synodontidae (*Harpadon, Saurida, Synodus, Trachinocephalus*)
- Suborder Chlorophthalmoidei
  - Family Chlorophthalmidae (*Chlorophthalmus, Parasudis*) *Bathysauropsis* (*B. gracilis*, *B. malayanus*)
  - Family Notosudidae (*Ahliesaurus, Luciosudis, Scopelosaurus*)
  - Family Ipnopidae (*Bathymicrops, Bathypterois, Bathytyphlops, Discoverichthys, Ipnops*)
- Suborder Alepisauroidei
  - Family Alepisauridae (*Alepisaurus, Omosudis*)
  - Family Paralepididae (*Anotopterus, Arctozenus, Dolichosudis, Lestidiops, Lestidium, Lestrolepis, Macroparalepis, Magnisudis, Notolepis, Paralepis, Stemnosudis, Sudis, Uncisudis*)
  - Family Evermannellidae (*Coccorella, Evermannella, Odontostomops*)
  - Family Scopelarchidae (*Benthalbella, Rosenblattichthys, Scopelarchoides, Scopelarchus*)
- Suborder Giganturoidei
  - *Bathysauroides gigas*
  - Family Bathysauridae (*Bathysaurus*)
  - Family Giganturidae (*Gigantura)*

Sato & Nakabo (2002)

Order Aulopiformes
- Suborder Synodontoidei
  - Family Paraulopidae (*Paraulopus*)
  - Family Aulopidae (*Aulopus*)
  - Family Pseudotrichonotidae (*Pseudotrichonotus*)
  - Family Synodontidae (*Harpadon, Saurida, Synodus, Trachinocephalus*)
- Suborder Chlorophthalmoidei
  - Family Bathysauroididae (*Bathysauroides*)
  - Family Chlorophthalmidae (*Chlorophthalmus, Parasudis*)
  - Family Bathysauropsidae (*Bathysauropsis)*
  - Family Notosudidae (*Ahliesaurus, Luciosudis, Scopelosaurus*)
  - Family Ipnopidae (*Bathymicrops, Bathypterois, Bathytyphlops, Discoverichthys, Ipnops*)
- Suborder Alepisauroidei
  - Family Alepisauridae (*Alepisaurus, Omosudis*)
  - Family Paralepididae (*Anotopterus, Arctozenus, Dolichosudis, Lestidiops, Lestidium, Lestrolepis, Macroparalepis, Magnisudis, Notolepis, Paralepis, Stemnosudis, Sudis, Uncisudis*)
  - Family Evermannellidae (*Coccorella, Evermannella, Odontostomops*)
  - Family Scopelarchidae (*Benthalbella, Rosenblattichthys, Scopelarchoides, Scopelarchus*)
- Suborder Giganturoidei
  - Family Bathysauridae (*Bathysaurus*)
  - Family Giganturidae (*Gigantura)*

Fig. 1.2. Recent classifications of aulopiform interrelationships. Genera within each family are listed.

proposed during the last 40 years (Gosline et al. 1966, Rosen 1973, Sulak 1977, R. K. Johnson 1982, Rosen 1985, Hartel & Stiassny 1986, Baldwin & Johnson 1996, Sato & Nakabo 2002). All previous hypotheses of aulopiform relationships have been based solely on morphological data. Disagreement and confusion regarding aulopiform morphological characters have resulted in a lack of consensus regarding relationships among aulopiform fishes as seen in Figure 1.3 (Rosen 1973, R. K. Johnson 1982, Rosen 1985, Hartel & Stiassny 1986, Johnson et al. 1996, Baldwin & Johnson 1996, Sato & Nakabo 2002), as well as confusion regarding the order's monophyly and placement among lower euteleostean fishes (Rosen 1973, R. K. Johnson 1982, Rosen 1985, Hartel & Stiassny 1986, G. D. Johnson 1992, Patterson & Johnson 1995, Baldwin & Johnson 1996, Sato & Nakabo 2002) as seen in Figure 1.4.

Prior to the proposal of the order Aulopiformes (Rosen 1973), aulopiform fishes were classified within the order Iniomi, which also included members of the order Myctophiformes (lanternfishes) (e.g., Regan 1911, Gosline et al. 1966). Rosen (1973) erected the order Aulopiformes from all previously recognized iniomous fishes *sans* the Myctophiformes, based primarily on the shared presence of an elongated uncinate process on the second epibranchial located within the gill arches of aulopiform fishes. Rosen (1973) further separated Myctophiformes from aulopiform fishes, and proposed a monophyletic Ctenosquamata based on the presence of ctenoid scales and advanced pharyngobranchial elements that lanternfishes share with members of the Acanthomorpha (spiny-rayed fishes) (Fig. 1.4A).

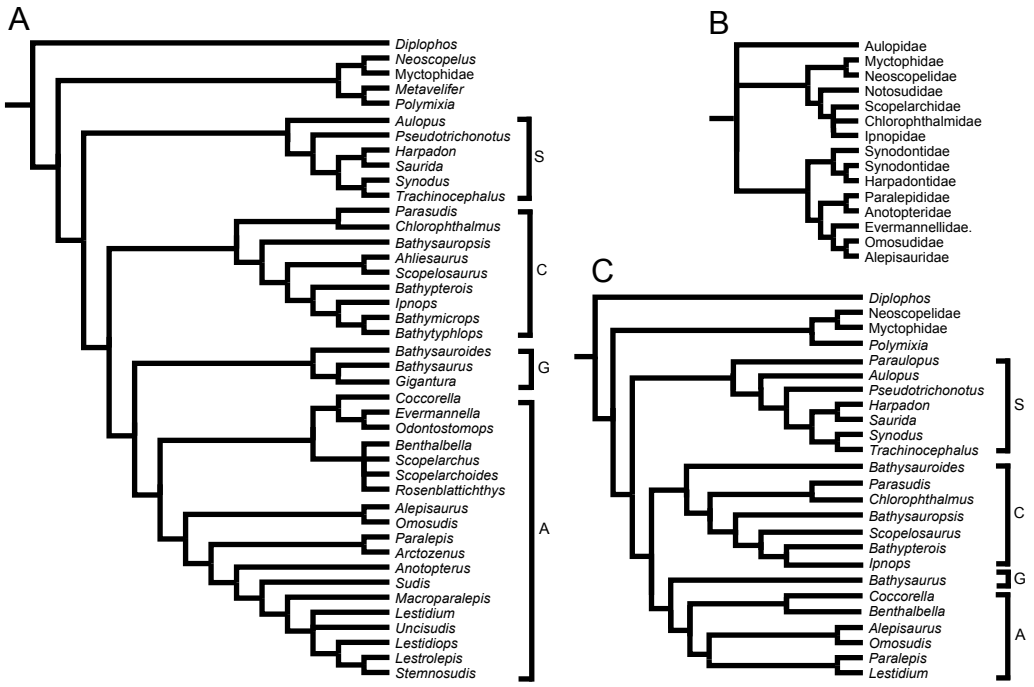

Fig. 1.3. Previous phylogenetic hypotheses of aulopiform interrelationships from (A) Baldwin and Johnson, 1996 (B) R. K. Johnson, 1982 and (C) Sato and Nakabo, 2002. Suborders include Synodontoidei (S), Chlorophthalmoidei (C), Giganturoidei (G), and Alepisauroidei (A).

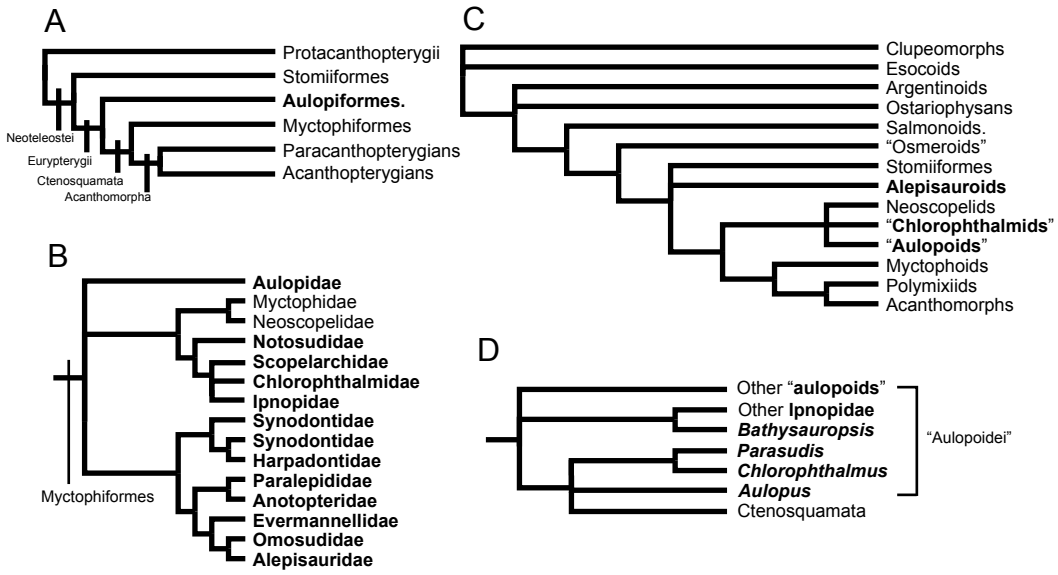

Fig. 1.4. Previous phylogenetic hypotheses of aulopiform monophyly (A) Rosen, 1973 and paraphyly (B) R.K. Johnson, 1982; (C) Rosen, 1985; (D) Hartel and Stiassny, 1986. Aulopiform taxa are bolded.

The hypothesis of aulopiform monophyly has been rejected multiple times (R. K. Johnson 1982, Rosen 1985, Hartel & Stiassny 1986). R. K. Johnson (1982) rejected aulopiform monophyly in favor of an iniomous hypothesis of relationships (Fig. 1.3B, 1.4B). He argued that the presence of an elongated uncinate process on the second epibranchial was not unique to Aulopiformes and is a primitive iniomous trait shared with the Myctophiformes. Additionally, he proposed a clade within his iniomous Myctophiformes in which lanternfishes are closely related to his chlorophthalmoids based on the shared presence of an enlarged gap between the occipital region of the neurocranium and the first centrum. Rosen (1985) proposed a revised hypothesis of euteleostean relationships that left Aulopiformes paraphyletic (Fig. 1.4C). He proposed that the genus *Aulopus* shared derived features with ctenosquamates (e.g., the presence of a median rostral cartilage) and placed the genus within Ctenosquamata along with his chlorophthalmids. Stiassny (1986) and Hartel & Stiassny (1986) corroborated this hypothesis, and placed the aulopiform genera *Aulopus*, *Parasudis*, and *Chlorophthalmus* together as the sister group to the ctenosquamates (Fig. 1.4D).

Hypotheses of aulopiform paraphyly (Rosen 1985, Hartel & Stiassny 1986) were challenged by G. D. Johnson (1992), who proposed an additional gill-arch aulopiform synapomorphy (cartilaginous condyle absent on third pharyngobranchial), and provided further support for the monophyly of Rosen's (1973) Eurypterygii (Aulopiformes + Ctenosquamata) and for Ctenosquamata (Myctophiformes + Acanthomorpha) (Fig. 1.4A). Baldwin & Johnson (1996) disagreed with R. K.

Johnson's (1982) observation that Myctophiformes posses an uncinate process on the second epibranchial, and proposed that he incorrectly identified the anterior portion of the second epibranchial as an uncinate process in the myctophiform genus *Neoscopelus*. Currently, nine morphological synapomorphies support the hypothesis of a monophyletic Aulopiformes (Baldwin & Johnson 1996, Sato & Nakabo 2002): presence of an enlarged uncinate process on second epibranchial (Rosen 1973), absence of cartilaginous condyle on third pharyngobranchial (Johnson 1992), epipleural bones extending to second or first vertebra (Patterson & Johnson 1995), absence of swimbladder (Marshall 1954), presence of peritoneal pigment in larvae (R. K. Johnson 1982), medial processes of pelvic girdle joined medially by cartilage (Baldwin & Johnson 1996), presence of fifth epibranchial (Baldwin & Johnson 1996), one or more epipleurals displaced dorsally into horizontal septum (Patterson & Johnson 1995), and palatine not expanded laterally (Sato & Nakabo 2002). Aulopiform monophyly has not been tested with molecular data utilizing the broad taxon sampling of the previous morphological studies.

Relationships within the Aulopiformes have undergone major revisions with essentially every study that has examined them. For an in-depth review of aulopiform classifications and phylogenetic studies prior to 1996, refer to the morphological study of Baldwin & Johnson (1996). Recent hypotheses of aulopiform relationships are illustrated in Figure 1.3. Baldwin & Johnson (1996) proposed a strict consensus phylogeny of nine equally parsimonious trees from 118 morphological characters that supported four major aulopiform clades as seen in Figure 1.3A. Sato & Nakabo

(2002) investigated the systematic placement of a previously unrecognized genus *Paraulopus* within a *Chlorophthalmus* species complex. Their analysis utilized 101 morphological characters, 80 from Baldwin & Johnson (1996), with revisions to 13 characters, and the addition of 21 newly considered morphological characters. While their analysis did not include all of the same taxa as Baldwin and Johnson (1996), they also recovered four major aulopiform clades (Fig. 1.3C) with a single most parsimonious tree, and made a number of small revisions to the phylogeny proposed by Baldwin & Johnson (1996) including: the recovery of *Bathysauroides* as the basal member of Chlorophthalmoidei, rather than as a member of Giganturoidei (Baldwin & Johnson 1996), and placement of the newly diagnosed genus *Paraulopus* as the basal member of Synodontoidei. Changes to the classification of Baldwin & Johnson (1996) included elevation of the genera *Bathysauropsis* and *Bathysauroides* to family level (Bathysauropsidae and Bathysauroididae respectively).

Baldwin & Johnson's (1996) study recovered a monophyletic Synodontoidei as the basal aulopiform lineage, with the genus *Aulopus* as the basal aulopiform taxon within the suborder. The placement of *Aulopus* within the suborder supports the findings of Johnson et al. (1996), but contradicts many previous hypotheses (Rosen 1973, R. K. Johnson 1982, Rosen 1985, Hartel & Stiassny 1986). Sato & Nakabo's (2002) revision of relationships recovered *Paraulopus* as the basal synodontoid. A novel hypothesis of a Notosudidae + Ipnopidae clade was proposed by Baldwin & Johnson (1996) within their monophyletic Chlorophthalmoidei. Notosudidae have previously been aligned with chlorophthalmoid taxa (Rosen 1973, Bertelsen et al.

1976, R. K. Johnson 1982) and have also been said to have a close relationship to the family Scopelarchidae (R. K. Johnson 1982, Patterson & Johnson 1995).

Another novel hypothesis from Baldwin & Johnson (1996) was the recovery of a monophyletic Alepisauroidei + Giganturoidei clade. The phylogenetic placement and classification of members within the bathypelagic suborder Giganturoidei (*Bathysaurus*, *Gigantura*) has been traditionally difficult because of highly modified morphological features. Previous studies placed *Gigantura* in its own order (e.g., Regan 1925, Walters 1961), and Rosen (1973) suggested that *Gigantura* was most closely related to members of the currently recognized family Synodontidae (*Synodus*, *Trachinocephalus*, *Harpadon*, *Saurida*). Patterson & Johnson (1995) provided support for *Gigantura* as an aulopiform and suggested *Bathysaurus* as the sister group to the genus. This result contradicts previous hypotheses that *Bathysaurus* is most closely related to synodontids (Sulak 1977, R. K. Johnson 1982). Baldwin & Johnson (1996) also included their newly described genus *Bathysauroides* as the basal giganturoid; however, Sato & Nakabo (2002) revised this relationship and found *Bathysauroides* to be the basal chlorophthalmoid.

Baldwin & Johnson's (1996) study recovered a Scopelarchidae + Evermannellidae clade sister to the remaining alepisauroid taxa (Alepisauridae + Paralepididae) which form the monophyletic suborder Alepisauroidei. Phylogenetic position and classification of Scopelarchidae have been problematic because of morphological adaptations that are potentially examples of convergence in the deep sea rather than synapomorphies. Evermannellids and scopelarchids both posses

highly modified tubular eyes, and R. K. Johnson (1982) suggested that this feature is only seemingly related in the two groups. He proposed that scopelarchids are more closely related to chlorophthalmoids than evermannellids based on the shared presence of an enlarged gap between the cranium and the first centrum. Baldwin & Johnson (1996) proposed that the tubular eyes of scopelarchids and evermannellids are a synapomorphy of that clade, although they did not further investigate the morphological characteristics of the eyes to examine the possibility of convergent structures. Evolution of tubular eyes is a common adaptation among fishes in the deep sea (Helfman et al. 1997), and tubular eyes also occur with a different morphology in *Gigantura*. Baldwin & Johnson's (1996) study supported a monophyletic Alepisauridae (*Omosudis* + *Alepisaurus*), and a monophyletic family Paralepididae, which also included the genus *Anotopterus*. These results concur with the findings of R. K. Johnson (1982).

An increasing number of works has demonstrated the utility of molecular data in providing additional insight into evolutionary relationships within and among groups that have diverse morphological variation (e.g., Holcroft 2004, Smith & Wheeler 2004, Lopez et al. 2004). Presently, there are no robust phylogenies of Aulopiformes that utilize molecular data. Such phylogenies will provide further support for hypotheses of aulopiform relationships that have been traditionally problematic (e.g., phylogenetic position and relationships of giganturids and scopelarchids). Kawaguchi et al. (2001) sequenced the whole mitochondrial genome for a single species, *Aulopus japonica*, and a rudimentary phylogeny was presented, but poor

taxon sampling of both outgroup and ingroup taxa prevented any definitive statements about the systematic position of Aulopiformes or their interrelationships. Molecular studies have recovered Aulopiformes as monophyletic (e.g., Miya et al. 2001, Miya et al. 2003) and paraphyletic (Lopez et al. 2004) although in each case aulopiform taxon sampling was extremely limited, making strong inferences about aulopiform monophyly problematic.

Morphological characters have often been ignored in systematic studies that utilize large amounts of molecular characters, especially when maximum likelihood and Bayesian methods are employed, because of skepticism surrounding the use of models with morphological data. With the increase of model development and exploration with morphological data (Lewis 2001, Nylander et al. 2004), this is no longer the case. A number of recent studies have demonstrated that morphological data can have a significant impact on hypotheses of evolutionary relationships when combined with multi-gene datasets (e.g., Nylander et al. 2004, Glenner et al. 2004, Danforth et al. 2006).

Five protein coding gene regions have been targeted and sequenced for analysis: the single-copy nuclear genes RAG1, zic1, ENC1, plagl2, and the mitochondrial gene COI. RAG1 has been demonstrated to lack paralogs and provide phylogenetic resolution among teleost groups (Holcroft 2004, Lopez et al. 2004, Li & Orti 2006). Nuclear genes zic1, ENC1, and plagl2 are part of a suite of gene regions recently described by the Ortí Laboratory that additionally produce phylogenetic resolution in teleost groups (Li et al. 2007). Finally, the mitochondrial gene COI is included

because the fast rate of mitochondrial sequence evolution is ideal for inferring relationships among species where divergence is more recent (Moritz et al. 1987, Hillis et al. 1996), allowing for increased resolution at the tips of the ingroup analysis. In an effort to fully explore the evolutionary relationships of the Aulopiformes from a total evidence approach, the morphological matrices of Baldwin & Johnson (1996) and Sato & Nakabo (2002) have been incorporated into this analysis. The goals of this study include a reexamination of (1) the systematic position of the Order Aulopiformes within Euteleostei utilizing data from nuclear gene RAG1, (2) aulopiform relationships using nuclear and mitochondrial gene sequence data and a total-evidence approach that combines a multi-gene data set with previous morphological data. These datasets (RAG1, nucDNA + mtDNA, DNA + morphology) are used to test the following hypotheses: (1) aulopiform monophyly, (2) aulopiform relationships within Euteleostei, and (3) aulopiform interrelationships.

MATERIALS AND METHODS

Taxon Sampling

Taxonomic sampling for RAG1 analysis includes 18 aulopiform species representing all 4 suborders and 11 of 14 aulopiform families. Outgroup sampling includes 54 species representing 28 actinopterygiian orders (Table 1.1). Outgroups were chosen in order to maintain a broad taxonomic sampling of groups hypothesized to be basal or closely related to Aulopiformes (e.g., Rosen 1973, Johnson 1992, Arratia 2004) including members of the following groups (Nelson 2006):

TABLE 1.1: List of species examined in this study. Classification follows Nelson (2006) with GenBank accession numbers.

	Baldwin & Johnson	Sato & Nakabo			Accession Nos.			
Taxon	(1996)	(2002)	Catalog	RAG1	zic1	ENC1	plagl2	COI
Order Amiiformes								
Family Amiidae								
Amia calva	NA	NA	Various	AY430199	EF032909	EF032974	EF033013	AB042952
Order Hiodontiformes								
Family Hiodontidae								
Hiodon alosoides	NA	NA	Various	AY430200	EU366766	—	—	AP004356
Order Elopiformes								
Family Megalopidae								
*Megalops atlanticus***	NA	NA		AY430204	—	—	—	—
Order Clupeiformes								
Family Engraulidae								
*Coilia mystus***	NA	NA		DQ912126	—	—	—	—
*Engraulis encrasicolus***	NA	NA		DQ912103	—	—	—	—
Family Clupeidae								
Dorosoma cepedianum	NA	NA	KU T7841	DQ912099	EU366767	—	—	EU366583
*Harengula jaguana***	NA	NA		DQ912122	—	—	—	—
Order Gonorynchiformes								
Family Chanidae								
*Chanos chanos***	NA	NA		AY430207	—	—	—	—
Order Cypriniformes								
Family Cyprinidae								
Danio rerio	NA	NA	Various	U71093	EF032910	EF032975	EF033014	NC002333
*Pimephales promelas***	NA	NA		AY430210	—	—	—	—
Order Characiformes								
Family Characidae								
*Catoprion mento***	NA	NA		AY430212	—	—	—	—
Order Siluriformes								
Family Ictaluridae								
*Pylodictis olivaris***	NA	NA		DQ492619	—	—	—	—
Order Gymnotiformes								
Family Gymnotidae								
*Gymnotus sp.***	NA	NA		DQ492427	—	—	—	—
Order Argentiniformes								
Family Argentinidae								
Argentina sialis	NA	NA	KU T519	AY430228	EU366773	EU366634	EU366680	—
Order Osmeriformes								
Family Osmeridae								
Thaleichthys pacificus	NA	NA	KU T3135	AY380537	EU366774	EU366635	EU366681	—
*Salangichthys microdon***	NA	NA		AY380539	—	—	—	—
*Mallotus villosus***	NA	NA		DQ836486	—	—	—	—
Order Salmoniformes								
Family Salmonidae								
Oncorhynchus mykiss	NA	NA		U15663	EF032911	EF032976	EF033015	NC001717
Order Esociformes								
Family Esocidae								
*Esox americanus***	NA	NA		AY380541	—	—	—	—
Order Stomiiformes								
Family Gonostomatidae								
Diplophos taenia		*D. orientalis*	KU T3781	EU366724	EU366768	EU366630	EU366676	EU366584
Family Gonostomatidae								
*Gonostoma bathyphilum***	NA	NA		AY438703	—	—	—	—
Order Ateleopodiformes								
Family Ateleopodidae								
Ijimaia antillarum	NA	NA	KU T5411	EU366725	EU366769	EU366631	EU366677	EU366585
Order Aulopiformes								
Suborder Synodontoidei								
Family Paraulopidae								
Paraulopus oblongus	NA		C T99-109	EU366709	EU366752	EU366615	EU366664	EU366568
Family Aulopidae								
Aulopus filamentosus		*A. japonicus*	U T3816	EU366688	EU366733	EU366593	EU366642	EU366546
Aulopus japonicus			C T99-124	EU366687	EU366732	EU366592	EU366641	EU366545
Hime sp.	—	—	SIO T02-68	EU366701	EU366746	EU366606	EU366654	EU366559
Family Pseudotrichonotidae								
Pseudotrichonotus altivelis			C T99-156	EU366711	EU366754	EU366617	—	EU366570
Family Synodontidae								
Synodus kaianus	—	—	C T99-128	EU366719	EU366761	EU366625	EU366672	EU366578
Synodus variegatus		*S. ulae**	KU T6901	EU366720	EU366762	EU366626	EU366673	EU366579
Synodus intermedius	—	—	KU T5219	EU366721	EU366763	EU366627	EU366674	EU366580
Trachinocephalus myops			KU T5225	EU366723	EU366765	EU366629	—	EU366582
Saurida undosquamis		*S. gracilis**	C T99-162	EU366712	EU366755	EU366618	EU366665	EU366571
Harpadon microchir	*H. nehereus**	*H. nehereus*	C T99-148	EU366700	EU366745	EU366605	EU366653	EU366558
Suborder Chlorophthalmoidei								
Family Bathysauroididae								
Bathysauroides			NA	NA	NA	NA	NA	NA

TABLE 1.1 Continued: List of species examined in this study.

Taxon	Baldwin & Johnson (1996)	Sato & Nakabo (2002)	Accession Nos. Catalog	RAG1	zic1	ENC1	plagl2	COI
Family Chlorophthalmidae								
Chlorophthalmus agassizi			KU T3759	EU366695	EU366740	EU366600	—	EU366553
Parasudis truculenta			KU T959	EU366710	EU366753	EU366616	—	EU366569
Family Bathysauropsidae								
Bathysauropsis			NA	NA	NA	NA	NA	NA
Family Notosudidae								
Ahliesaurus berryi		NA	KU T5285	EU366685	EU366731	EU366590	EU366639	EU366544
Scopelosaurus harryi	—	—	KU T3244	EU366713	EU366756	EU366619	EU366666	EU366572
Scopelosaurus lepidus	*S. argenteus**		KU T3641	EU366714	EU366757	EU366620	EU366667	EU366573
Family Ipnopidae								
Bathypterois grallator	*B. pectinatus**	*B. atricolor**	KU T5935	EU366690	EU366735	EU366595	EU366644	EU366548
Bathypterois mediteraneus	—	—	C T99-139	EU366691	EU366736	EU366596	EU366645	EU366549
Bathypterois phenax	—	—	KU T3625	EU366692	EU366737	EU366597	EU366646	EU366550
Ipnops sp.	*I. murrayi**	*I. murrayi*	C T99-144	EU366702	EU366747	EU366607	EU366655	EU366560
Bathymicrops		NA	NA	NA	NA	NA	NA	NA
Bathytyphlops		NA	NA	NA	NA	NA	NA	NA
Suborder Alepisauroidei								
Family Scopelarchidae								
Benthalbella dentata			KU T3239	EU366693	EU366738	EU366598	EU366647	EU366552
Benthalbella macropinna		*B. dentate*	KU T926	EU366694	EU366739	EU366599	EU366648	EU366552
Scopelarchus sp.	*S. analis*	NA	KU T3783	EU366715	EU366758	EU366621	EU366668	EU366574
Scopelarchoides		NA	NA	NA	NA	NA	NA	NA
Rosenblattichthys		NA	NA	NA	NA	NA	NA	NA
Family Evermannellidae								
Coccorella atlantica			KU T5314	EU366696	EU366741	EU366601	EU366649	EU366554
Evermannella indica		NA	KU T3790	EU366697	EU366742	EU366602	EU366650	EU366555
Odontostomops sp.	*O. normalops*	NA	C T99-129	EU366706	EU366749	EU366612	EU366661	EU366565
Family Alepisauridae								
Alepisaurus brevirostris		*A. ferox*	KU T5258	EU366684	EU366730	EU366589	EU366638	EU366543
Alepisaurus ferox	—	—	KU T5395	EU366683	EU366729	—	EU366637	EU366542
Omosudis lowei			KU T5909	EU366707	EU366750	EU366613	EU366662	EU366566
Family Paralepididae								
Anotopterus pharao		NA	KU T2305	EU366686	—	EU366591	EU366640	—
Lestidiops jayakari	*L. affinis**	NA	KU T3792	EU366705	—	EU366610	EU366658	EU366562
Lestidiops ringens	—	—	SIO T93-297	—	—	—	EU366659	EU366563
Lestidium atlanticum			KU T3544	EU366703	—	EU366608	EU366656	EU366561
Lestrolepis intermedia		NA	KU T3557	EU366704	—	EU366609	EU366657	—
Macroparalepis johnfitchi	*M. affine*	NA	SIO T94-266	EU366722	EU366764	EU366628	EU366675	EU366581
Magnisudis atlantica	NA	NA	KU T5928	—	EU366748	EU366611	EU366660	EU366564
Paralepis coregonoides			KU T3719	EU366708	EU366751	EU366614	EU366663	EU366567
Stemonosudis macrurus	*S. rothschildi**	NA	KU T93-238	EU366716	—	EU366622	EU366669	EU366575
Sudis atrox		NA	KU T3107	EU366717	EU366759	EU366623	EU366670	EU366576
Sudis sp.	—	—	KU T3798	EU366718	EU366760	EU366624	EU366671	EU366577
Arctozenus		NA	NA	NA	NA	NA	NA	NA
Uncisudis		NA	NA	NA	NA	NA	NA	NA
Suborder Giganturoidei								
Family Bathysauridae								
Bathysaurus ferox		*B. mollis*	KU T5934	EU366689	EU366734	EU366594	EU366643	EU366547
Family Giganturidae								
Gigantura chuni		NA	KU T6533	EU366698	EU366743	EU366603	EU366651	EU366556
Gigantura indica		NA	KU T5270	EU366699	EU366744	EU366604	EU366652	EU366557
Order Myctophiformes								
Family Neoscopelidae								
Neoscopelus macrolepidotus			KU T3297	EU366727	EU366771	EU366632	EU366678	EU366587
Family Myctophidae								
Benthosema glaciale	*L. cuprarius**		KU T3734	EU366728	EU366775	—	—	—
Nannobrachium lineatum	—	—	KU T3634	EU366726	EU366770	—	—	EU366586
*Diaphus effulgens***	NA	NA		EU477496	—	—	—	—
*Lampanyctus macdonaldi***	NA	NA		EU477497	—	—	—	—
*Notoscopelus kroyeri***	NA	NA		AY430221	—	—	—	—
*Notoscopelus caudispinosus***	NA	NA		EF094948	—	—	—	—
*Hygophum hygomii***	NA	NA		EF094947	—	—	—	—
Order Polymixiiformes								
Family Polymixiidae								
Polymixia japonicus	*P. lowei*		KU T258	AY308765	EU366776	EU366636	EU366682	AB034826
Order Lampriformes								
Family Veliferidae								
Metavelifer multiradiatus		NA	KU T1252	EF094949	EU366772	EU366633	EU366679	EU366588
Family Lampridae								
*Lampris guttatus***	NA	NA		AY308764	—	—	—	—
Order Ophidiiformes								
Family Ophidiidae								
*Neobythites stigmosus***	NA	NA		EF033043	—	—	—	—
*Petrotyx sanguineus***	NA	NA		AY308782	—	—	—	—
Order Mugiliformes								
Family Mugilidae								
*Mugil curema***	NA	NA		AY308783	—	—	—	—

TABLE 1.1 Continued: List of species examined in this study.

Taxon	Baldwin & Johnson (1996)	Sato & Nakabo (2002)	Catalog	Accession Nos. RAG1	zic1	ENC1	plagl2	COI
Order Atheriniformes								
Family Atherinopsidae								
*Menidia menidia***	NA	NA		AY430225	—	—	—	—
Order Cyprinodontiformes								
Family Fundulidae								
*Fundulus heteroclitus***	NA	NA		EF033040	—	—	—	—
Order Beryciformes								
Family Holocentridae								
*Sargocentron vexillarium***	NA	NA		AY308770	—	—	—	—
*Sargocentron punctatissimum***	NA	NA		AY430223	—	—	—	—
Order Zeiformes								
Family Oreosomatidae								
*Allocyttus verrucosus***	NA	NA		AY308781	—	—	—	—
Family Grammicolepididae								
*Grammicolepis brachiusculus***	NA	NA		AY308780	—	—	—	—
Family Zeidae								
*Zenopsis conchifer***	NA	NA		AY308778	—	—	—	—
Order Scorpaeniformes								
Family Peristediidae								
*Peristedion miniatum***	NA	NA		AY308774	—	—	—	—
Order Perciformes								
Family Percidae								
*Perca flavescens***	NA	NA		AY308768	—	—	—	—
Family Moronidae								
Morone chrysops	NA	NA	Various	AY308767	EF032917	EF032982	EF033021	—
Family Carangidae								
*Caranx latus***	NA	NA		EU477492	—	—	—	—
Family Pomacanthidae								
*Holacanthus bermudensis***	NA	NA		EF530081	—	—	—	—
Family Elassomatidae								
*Elassoma evergladei***	NA	NA		AY308784	—	—	—	—
Family Ephippidae								
*Chaetodipterus faber***	NA	NA		AY308773	—	—	—	—
Family Sphyraenidae								
*Sphyraena argentea***	NA	NA		EU477494	—	—	—	—
Family Scombridae								
*Scomber scombrus***	NA	NA		EU477493	—	—	—	—
Order Pleuronectiformes								
Family Psettodidae								
*Psettodes erumei***	NA	NA		EU477495	—	—	—	—

Species are labeled for morphology if different from species sequenced. NA = Not applicable, species or genus was not utilized in previous morphological study or molecular analysis. * = multiple species of the same genus were examined in previous morphological study. — = Morphology not coded for species in total evidence data set or DNA data not collected. ** = species only used in RAG1 analysis. Catalog C refers to CBM-ZF. Catalog U refers to USNM.

Neopterygii, Osteoglossomorpha, Elopomorpha, Otocephala, Protacanthopterygii, Sternopterygii, Ateleopodomorpha, Scopelomorpha, and Acanthomorpha. Where possible, RAG1 sequences were obtained from previous phylogenetic analyses from GenBank. RAG1 data collected in the Wiley Lab by N. Holcroft (*Caranx latus*, *Sphyraena argentea*, and *Scomber scombrus*) and E. O. Wiley (*Psettodes erumei*) were donated to this study.

Taxon sampling for multi-gene DNA analysis (nucDNA + mtDNA) includes tissue samples for 43 ingroup species representing 32 of 44 aulopiform genera and every family with the exception of the recently elevated Bathysauropsidae and Bathysauroididae (Sato & Nakabo 2002). Outgroup sampling includes tissue samples for 15 species representing 13 actinopterygiian orders (Table 1.1). Outgroups were chosen in order to maintain a broad sampling of groups hypothesized to be basal to or closely related to Aulopiformes (e.g., Rosen 1973, Johnson 1992, Arratia 2004) including members of the following groups (Nelson 2006): Neopterygii, Osteoglossomorpha, Otocephala, Protacanthopterygii, Sternopterygii, Ateleopodomorpha, Ctenosquamata, and Acanthomorpha. A list of tissue samples included in this analysis is located in Table 1.1. Total evidence analyses included 8 additional aulopiform genera that have data for morphology only (Baldwin & Johnson 1996; Sato & Nakabo 2002) (Table 1.1). Outgroups used in Baldwin & Johnson (1996) and Sato & Nakabo (2002) that were also sequenced for DNA included *Diplophos taenia* (Stomiiformes), *Neoscopelus macrolepidotus* (Myctophiformes), *Polymixia japonicus* (Polymixiiformes), and *Metavelifer*

multiradiatus (Lampriformes). For all analyses, the only taxon designated as the outgroup was *Amia calva* (Amiiformes).

DNA Extraction, Amplification, and Sequencing

DNA was extracted with a Guanidine Thiocyanate protocol from tissue samples frozen and stored at -70°C, with some samples being initially preserved in 95% ethanol. Polymerase chain reaction procedures (PCR) (Saiki 1990) were used to amplify an approximately 1500-bp region of RAG1, 900-bp regions of zic1, ENC1, and plagl2, and a 900-bp region of the mitochondrial gene COI. Amplification of RAG1 was performed using a 25 μL PCR cocktail which included approximately 10-60 ng template DNA, 1x PuReTaq Ready-To-Go PCR Beads, and 200 pmol of each primer (Lopez et al. 2004, Holcroft 2004). Nested-PCR was used to amplify RAG1 in taxa that did not amplify with the first PCR. Products of the first PCR were diluted 100 times, and used as the template for the Nested-PCR. Primers that were internal to the primers from the first PCR were used for the Nested-PCR. The thermal cycling profile used to amplify RAG1 fragments for both rounds of PCR is as follows: 10 cycles of 94˚C denaturing for 45 s, 53-58˚C annealing for 45 s, 72˚C extension for 1 m 15 s, followed by 30 cycles of 94˚C denaturing for 45 s, 50-53˚C annealing for 45 s, and 72˚C extension for 1 m 15 s followed by a final extension step of 72˚C for 7 m.

Amplification of nucDNA gene fragments zic1, ENC1, plagl2, and mtDNA gene fragment COI was performed using a 10 μL PCR cocktail including approximately 1-60 ng template DNA, 1x TaKaRa Ex Taq PCR buffer, 200 pmol of each dNTP, 6.4 pmol of each primer (Miya & Nishida 2000, Inoue et al. 2001, Li et al. 2007), and

0.25 units of TaKaRa Ex Taq (TaKaRa). Nested-PCR was used to amplify these genes in taxa that did not amplify with the first PCR, and followed the same procedure as discussed above. The thermal cycling profile used to amplify zic1, ENC1, and plagl2 fragments for both rounds of PCR is as follows: 30 cycles of 98˚C denaturing for 10 s, 53-61˚C annealing for 30 s, and 72˚C extension for 1 m followed by a final extension step of 72˚C for 5 m. The thermal cycling profile used to amplify COI fragments for both rounds of PCR is as follows: 35 cycles of 95˚C denaturing for 15 s, 53-55˚C annealing for 15 s, and 72˚C extension for 55 s followed by a final extension step of 72˚C for 7 m.

Purification of PCR products was done using ExoSAP-IT (USB) following instructions given by the manufacturer. Light and Heavy strands of PCR products were sequenced at the University of Kansas DNA Sequencing Laboratory using an Applied Biosystems 3130XL automated sequencer. Primers used for sequencing included the amplification primers. The program Sequencher was used to inspect sequences and create a consensus sequence from the light and heavy strands. All sequences used in this analysis are available on GenBank (Table 1.1).

Sequence alignment and analysis

Alignment was done by creating a separate NEXUS file for each gene, and sequences were aligned by eye with comparison to published GenBank sequences as an alignment template. Consensus sequences from Sequencher were checked in order to verify the existence of observed differences from the alignment template (e.g.,

insertion/deletion events, heterozygosities). Aligned RAG1 and nucDNA + mtDNA datasets are available upon request.

In order to test for the amount of saturation as a result of substitutions, sequences were analyzed using pair-wise Tamura-Nei distances (Tamura and Nei 1993) for each gene (all positions) and third positions. Tamura-Nei distances were calculated with PAUP*4.0b10 (Swofford 2002). If saturation is not present, a linear relationship is expected between the absolute observed number of nucleotide substitutions and the Tamura-Nei distances.

The presence of heterogeneous base composition can result in misleading phylogenetic signals across taxa. Base compositional stationarity was analyzed with the Chi-square test in PAUP*4.0b10 (Swofford 2002). GC content was determined using the program CodonW (Peden 2005) for each gene (all positions) and third positions. This program was also used to measure Wright's (1990) ENC (effective number of codons), which helps identify codon bias across taxa (e.g., 20 is high codon bias, 61 is no bias) for each gene (all positions) and third positions.

Phylogenetic Analyses, Hypothesis Testing, and Partitioning of RAG1 Data Set

Bayesian analyses of the RAG1 nucDNA data set were carried out in MrBayes v3.1 (Ronquist and Huelsenbeck 2003). The program MrModeltest v2.0 (Nylander 2004) was used to determine the best-fit model for each data partition using the Akaike information criterion (AIC). The data set was partitioned by codon position with a total of 3 partitions. A GTR+I+G model was selected by MrModeltest v2.0 (Nylander 2004) for all 3 RAG1 codon position partitions. Gaps were coded as

missing rather than a fifth character state for all methods (Bayesian, Maximum Likelihood). Four simultaneous runs were conducted utilizing four chains for 10 million generations with a tree and parameter sampling frequency of every 100 generations. Trees sampled before stationarity (the first 10,000 trees) were excluded as burn-in, with the remaining 360,000 post-burn-in trees used to compute the consensus tree and posterior probabilities. *A priori* alternative phylogenetic hypotheses of aulopiform relationships were tested (Table 1.2). Topological constraint trees were produced with the program Treeview 1.6.6. (Page 1996). Posterior probabilities of the constraint tree hypothesis were then calculated. Post burn-in trees were loaded into PAUP*4.0b10 (Swofford 2002) and filtered to keep only trees consistent with the constraint topology. The total number of trees remaining was then divided by the total number of post stationarity trees (360,000), resulting in the posterior probability of the constraint hypothesis.

Maximum likelihood (ML) analyses were carried out in GARLI v0.95 (Zwickl 2006). Codon partitions were not incorporated in the ML analyses, and a GTR+I+Γ model was used. Ten independent analyses were conducted, with tree searching concluding if either of the two criteria were reached: a maximum of 5 million generations were generated, or when no significance between tree likelihood scores was obtained for a maximum of 10,000 generations. The tree with the best likelihood score from the ten independent runs was used to evaluate evolutionary relationships. A nonparametric bootstrap analysis was performed for 100 random pseudoreplicates using the recommended default settings in the GARLI manual. Bootstrap support

TABLE 1.2: List of *a priori* maximum likelihood Shimodaira-Hasegawa tests (SH) and Bayesian posterior probabilities (PP) based on RAG1 nucDNA analyses.

Hypothesis Tested	References	RAG1 Analyses	
		PP%	SH
Order Iniomi (Aulopiformes+Myctophiformes) Monophyly	Gosline et al. (1966)	2.289	0.245
Aulopiformes Monophyly	Rosen (1973)	100.0*	1.000
Aulopiform Paraphyly	Rosen (1985)	0.000	0.000*
Ateleopodiformes + Lampriformes+ Myctophiformes	Miya et al. (2003)	0.000	0.013*
Aulopus + *Chlorophthalmus* + *Parasudis* sister to Ctenosquamata	Hartel and Stiassny (1986)	0.000	0.000*

* Significant difference at $p < 0.05$ (SH)
* Significant PP Support at $p \geq 95\%$

values for the ML topology are shown in Fig. 1.5, with a bootstrap value of ≥ 70 regarded as significantly supported. Alternative hypotheses were tested with a one-tailed Shimodaira and Hasegawa (SH) test with 1000 RELL bootstrap replicates (Shimodaira and Hasegawa 1999) (Table 1.2). SH tests were performed in PAUP*, and GARLI v0.95 was used to obtain the best tree that corroborated the constraint topology for each alternative hypothesis. Topologies recovered from the 100 random pseudoreplicates (nonparametric bootstrap) were included in all SH tests, along with topologies representing alternative hypotheses of aulopiform placement (Table 1.2).

Phylogenetic Analyses, Hypothesis Testing, and Data Partitioning of nucDNA and mtDNA Data Set

Bayesian analyses of the nucDNA and mtDNA concatenated data set were carried out in MrBayes v3.1 (Ronquist & Huelsenbeck 2003). The program MrModeltest v2.0 (Nylander 2004) was used to determine the best-fit model for each data partition using the Akaike information criterion (AIC). The concatenated data set was partitioned by both gene and codon position for the five genes, with a total of 15 partitions. A total of four models were selected by MrModeltest v2.0 (Nylander 2004) for the following 15 codon position partitions: GTR+I+G, RAG1 (1^{st}, 2^{nd}, 3^{rd}), zic1 (1^{st}), COI (1^{st}, 2^{nd}), ENC1 (1^{st}); GTR+G, zic1 (2^{nd}), ENC1 (3^{rd}), plagl2 (2^{nd}, 3^{rd}); HKY+G, zic1 (3^{rd}), COI (3^{rd}), ENC1 (2^{nd}); HKY+I+G, plagl2 (1^{st}). Gaps were coded as missing rather than as a fifth character state for all methods (Bayesian, Maximum Parsimony, Maximum Likelihood). Four simultaneous runs were conducted utilizing four chains for 10 million generations with a tree and parameter sampling frequency

of every 100 generations. Trees sampled before stationarity (the first 10,000 trees) were excluded as burn-in, with the remaining 360,000 post-burn-in trees used to compute the consensus tree and posterior probabilities. *A priori* alternative phylogenetic hypotheses of aulopiform relationships were tested (Table 1.3) following the same procedure described for the RAG1 analysis.

Maximum likelihood (ML) analyses were carried out in GARLI v0.95 (Zwickl 2006). Data partitions were not incorporated in the ML analyses, and a GTR+I+Γ model was used. Ten independent analyses were conducted, with tree searching concluding if either of the two criteria were reached; a maximum of 5 million generations were generated, or when no significance between tree likelihood scores was obtained for a maximum of 10,000 generations. The tree with the best likelihood score from the ten independent runs was used to evaluate evolutionary relationships. A nonparametric bootstrap analysis was performed for 100 random pseudoreplicates using the recommended default settings in the GARLI manual. Alternative hypotheses were tested with a one-tailed Shimodaira and Hasegawa (SH) test with 1000 RELL bootstrap replicates (Shimodaira & Hasegawa 1999) following the same procedure described for the RAG1 analysis (Table 1.3).

Maximum parsimony analyses were conducted on the concatenated data set of all five genes with PAUP*. Heuristic searches were replicated 100 times with a step-wise addition using tree-bisection-reconnection (TBR) branch swapping. All characters were unweighted. Statistical support was estimated using a bootstrap analysis with 1000 replicates, each with 30 random step-wise addition sequence

TABLE 1.3: List of *a priori* maximum parsimony Wilcozon-signed-ranks tests (WS-R), maximum likelihood Shimodaira-Hasegawa tests (SH), and Bayesian posterior probabilities (PP) based on combined nucDNA and mtDNA and total evidence analyses.

Hypothesis Tested	References	DNA Only			Total Evidence	
		WS-R	SH	PP%	WS-R	PP%
Order Iniomi (Aulopiformes+Myctophiformes) Monophyly	Gosline et al. (1966)	0.2504	0.381	0.00	0.3110	0.00
Aulopiformes Monophyly	Rosen (1973)	1.0000	1.000	99.80*	1.00	99.95*
Aulopiformes Interrelationships	Rosen (1973)	<0.0001*	0.000*	0.00	<0.0001*	0.00
Order Myctophiformes Interrelationships (Includes Aulopiformes)	Johnson (1982)	<0.0001*	0.000*	0.00	<0.0001*	0.00
Aulopiform Paraphyly	Rosen (1985)	<0.0001*	0.000*	0.00	<0.0001*	0.00
Aulopiform Interrelationships	Baldwin & Johnson (1996)	<0.0001*	0.000*	0.00	0.0001*	0.00
Aulopiform Suborder Interrelationships	Baldwin & Johnson (1996)	<0.0001*	0.000*	0.00	<0.0001*	0.00
Aulopiform Interrelationships	Sato & Nakabo (2002)	<0.0001*	0.000*	0.00	<0.0001*	0.00
Aulopiform Suborder Interrelationships	Sato & Nakabo (2002)	<0.0001*	0.000*	0.00	0.0043*	0.00
Synodontoidei Monophyly	Baldwin & Johnson (1996)	0.4255	0.047*	67.28	0.4311	99.44*
Synodontoidei Monophyly	Sato & Nakabo (2002)	0.5842	0.310	0.00	0.7679	0.81
Chlorophthalmoidei Monophyly	Baldwin & Johnson (1996)	0.0078*	0.000*	0.00	0.0006*	0.00
Chlorophthalmoidei Monophyly	Sato & Nakabo (2002)	0.0078*	0.000*	0.00	<0.0001*	0.00
Giganturoidei Monophyly	Baldwin & Johnson (1996)	0.2059	0.148	58.07	0.3020	78.69
Giganturoidei Monophyly	Sato & Nakabo (2002)	0.2059	0.148	58.07	0.3692	39.61
Alepisauroidei Monophyly	Baldwin & Johnson (1996)	0.0610	0.130	0.00	1.0000	97.52*
Alepisauroidei Monophyly	Sato & Nakabo (2002)	0.0610	0.130	0.00	1.0000	97.52*
Synodontidae Monophyly	Baldwin & Johnson (1996)	1.0000	0.185	0.02	1.0000	90.99
Aulopidae Monophyly	Baldwin & Johnson (1996)	1.0000	1.000	30.24	1.0000	55.67
Chlorophthalmidae Monophyly	Baldwin & Johnson (1996)	0.1917	0.234	0.00	1.0000	98.65*
Notosudidae Monophyly	Baldwin & Johnson (1996)	1.0000	1.000	99.99*	1.0000	99.95*
Ipnopidae Monophyly	Baldwin & Johnson (1996)	0.8981	0.140	54.00	1.0000	94.34*
Scopelarchidae Monophyly	Baldwin & Johnson (1996)	0.1917	0.139	0.05	1.0000	99.14*
Alepisauridae Monophyly	Baldwin & Johnson (1996)	1.0000	1.000	99.98*	1.0000	99.98*
Paralepididae Monophyly	Baldwin & Johnson (1996)	0.0092*	0.222	0.00	0.4194	0.00
Evermannellidae Monophyly	Baldwin & Johnson (1996)	1.0000	1.000	99.98*	1.0000	100.00*
Giganturoidei +Alepisauroidei	Baldwin & Johnson (1996)	0.0039*	0.002*	0.00	0.0002*	0.00
Paraulopus + Synodontidae	Sato & Nakabo (2002)	0.1567	0.311	0.00	0.3930	0.78
Scopelarchidae + Evermannellidae	Baldwin & Johnson (1996)	0.0136*	0.012*	0.00	0.2023	0.00
Notosudidae + Ipnopidae	Baldwin & Johnson (1996)	0.0003*	0.002*	0.00	0.0693	0.00
Alepisauridae + Paralepididae	Baldwin & Johnson (1996)	0.0092*	0.222	0.00	0.6295	0.00
Anotopterus + "Paralepididae"	Baldwin & Johnson (1996)	<0.0001*	0.000*	0.00	0.0121*	0.00
Evermannella + *Odontostomops*	Baldwin & Johnson (1996)	0.0076*	0.005*	0.00	0.1246	0.00
Ateleopodiformes + Lampriformes+ Myctophiformes	Miya et al. (2003)	0.5410	0.271	0.00	0.4688	0.00

* Significant difference at $p < 0.05$ (WS-R, SH)
* Significant PP Support at $p \geq 95\%$

replicates, to generate bootstrap values (Felsenstein 1985). Alternative hypotheses were tested using Wilcoxon signed-ranks (WS-R) tests performed in PAUP* (Table 1.3). Heuristic parsimony searches were used to generate the most parsimonious topology that fit the alternative hypothesis constraint.

Phylogenetic Analysis of Concatenated Morphological Data Set

The concatenated morphological data set included 118 characters from Baldwin & Johnson (1996), and 21 newly considered characters from Sato & Nakabo (2002). Sato & Nakabo (2002) made revisions to 13 characters (Appendix 1.1; 1, 15, 18, 52, 53, 69, 71, 79, 81, 96, 104, 105, 113) from Baldwin & Johnson (1996) with revisions incorporated into the concatenated data set. For a detailed description of all characters and revisions, refer to Baldwin & Johnson (1996) and Sato & Nakabo (2002). An abbreviated list of characters can be found in Appendix 1.1.

Maximum parsimony analysis of the concatenated morphological data set was performed in PAUP*. Parsimony tree searching procedures and bootstrap replicates followed the same guidelines as the nucDNA and mtDNA analysis. Polymorphisms were not ordered. The concatenated morphological data set can be found in Appendix 1.2.

Phylogenetic Analyses, Hypothesis Testing, and Data Partitioning of Total Evidence Data Set

Morphological data sets from Baldwin & Johnson (1996) and Sato & Nakabo (2002) were concatenated with the five gene molecular data set. Where possible, morphological data were matched to the same species used for DNA sequences. For

cases where multiple species of the same genus were examined with molecular data, only species that matched a species used in previous morphological studies were coded for morphological characters. For example, as seen in Table 1.1, *Synodus variegatus* was examined in Baldwin & Johnson (1996), so morphological data were coded for that species, but not for *Synodus kaianus* or *Synodus intermedius* since they were not examined in either previous morphological study. In instances where an exact match was not possible, morphological data from a close relative (e.g., the same genus) were utilized following the recommendations of Nylander et al. (2004) (Table 1.1). The morphological studies of Baldwin & Johnson (1996) and Sato & Nakabo (2002) presented their results at the level of genera for ingroup taxa, and did not identify differences in transformation series for each species examined. For the outgroup member of the family Myctophidae, morphological data from the myctophid genera *Lampanyctus* and *Myctophum* (Baldwin & Johnson 1996) were concatenated to the molecular data for the genus *Benthosema* (Table 1.1) as morphological data for Myctophidae were generalized to the level of family in Baldwin and Johnson (1996). All other outgroup taxa with morphological data were either concatenated with the same species, or a member from the same genus.

Bayesian analyses of the total evidence data set utilized the same partitions and models for the five gene fragments as the nucDNA and mtDNA data set. Morphological data were analyzed within a single partition, and a MK (Markov) model was implemented as recommended by Lewis (2001) and Nylander et al. (2004). All morphological characters were unweighted, with coding sites variable

and equal rates employed. Polymorphisms are treated as uncertainties in Bayesian analysis. Four simultaneous runs were conducted utilizing four chains for 15 million generations with tree and parameter sampling frequencies of every 100 generations. Trees sampled before stationarity (the first 15,000 trees) were excluded as burn-in, with the remaining 540,000 post-burn-in trees used to compute the consensus tree and posterior probabilities. Bayesian hypothesis testing followed the same procedures as outlined previously (Table 1.3).

Maximum parsimony analyses and morphological character distributions (Appendix 1.3) of the total evidence data set were performed in PAUP*. Phylogenetic analysis and hypothesis testing followed the same procedures as the nucDNA and mtDNA analysis. Maximum Likelihood analyses were not performed on the total evidence data set.

RESULTS

Sequence Analysis and Data Partitions of RAG1 Data Set

The RAG1 data matrix included the 1479 base positions. Mutational site saturation was not apparent across codon positions when all three positions were analyzed together, but the third codon position alone did show slight saturation for transversions and transitions. All codon positions were included in all analyses based on the recommendations of Källersjö et al. (1999), where saturated data were demonstrated to provide phylogenetic signal.

The null hypothesis of base compositional stationarity was not rejected for the first (χ^2 =79.28, df = 213, P = 1.000) and second (χ^2 = 26.01, df = 213, P = 1.000)

codon positions of RAG1, but it was rejected for the third position (χ^2 = 1396.77, df = 213, *P* = 0.000). The average GC content of RAG1 was 56.41% with a range from 47.6% in *Pylodictis olivaris* to 68.2% in *Coilia mystus*.

Nuclear gene RAG1 possessed little codon bias, with an average ENC coefficient of 49.33. Of the 11 taxa out of 72 with ENCs < 45, 4 were Clupeiformes, 3 were Osmeriformes, and the remaining four were from various orders (Argentiniformes, Stomiiformes, Ateleopodiformes, and Myctophiformes).

Phylogenetic Analysis of RAG1 Data Set and *A Priori* Hypothesis Tests

The Bayesian analysis produced a majority-rule consensus topology as shown in Figure 1.5, where posterior probabilities (PP) are considered significant if PP≥95%. The four simultaneous runs reached convergence (PSRF = 1.009–1.000, s.d. = 0.01-0.00), with each run obtaining the same consensus tree topology. Of the 67 nodes represented in the analysis, 49 were significantly supported (PP≥95%). The PP of *a priori* hypotheses is shown in Table 1.2. The only *a priori* hypothesis that was significantly supported (PP≥95%) was monophyly of the order Aulopiformes.

Of the 10 independent maximum likelihood analyses performed, all 10 topologies were identical with likelihood scores ranging from –33440.787 to –33440.798. Topology likelihood scores were verified with PAUP*. The likelihood topology was identical to the Bayesian majority-rule consensus topology as seen in Figure 1.5. The following *a priori* hypotheses of evolutionary relationships were rejected by SH tests (p≤0.05); aulopiform paraphyly (Rosen 1985), an *Aulopus, Chlorophthalmus* + *Parasudis* clade, and Ctenosquamata polytomy (Hartel and Stiassny 1986), and a

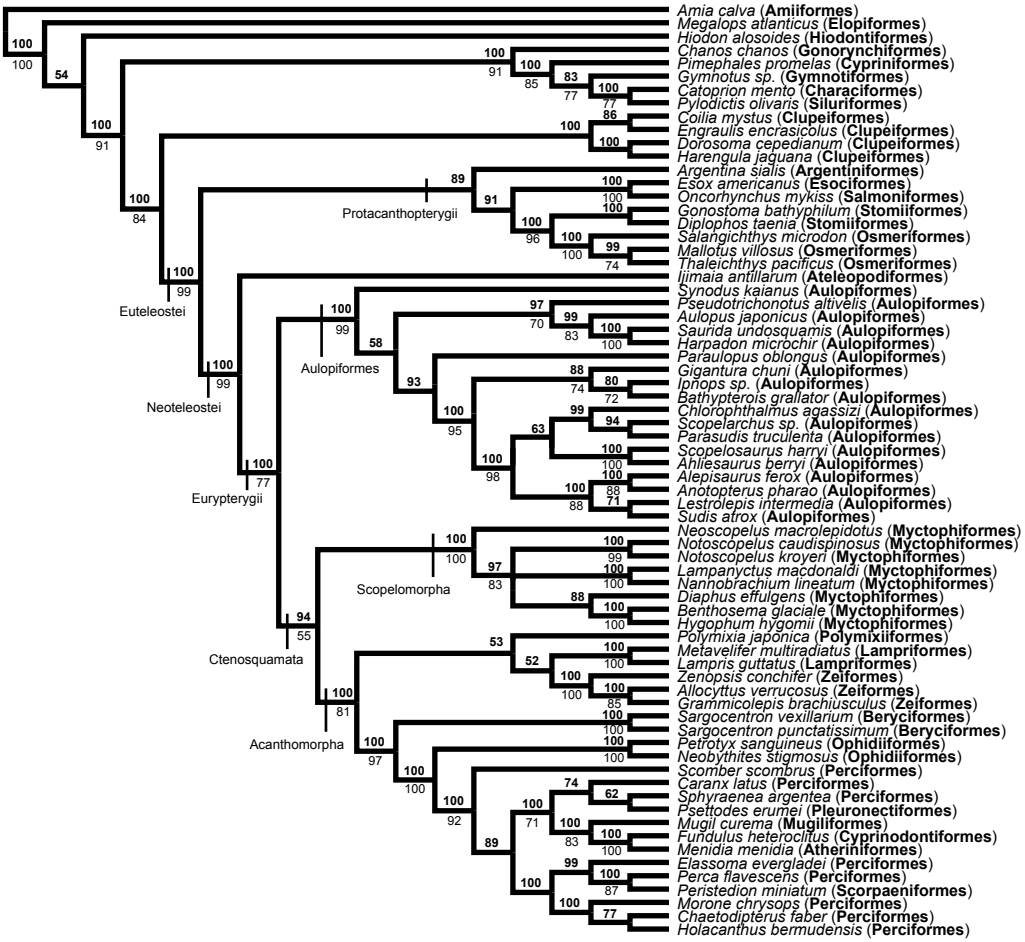

Fig. 1.5. Systematic placement of the Aulopiformes based on Bayesian and Maximum Likelihood analysis of nuclear gene RAG1. Bayesian posterior probabilities denoted by bold numbers above node, with significant support ≥ 95. Likelihood bootstrap support values denoted by numbers below node, with significant support ≥ 70. Likelihood values below 70 not shown.

sister-group relationship between Myctophiformes and an Ateleopodiformes + Lampriformes clade within Scopelomorpha (Miya et al. 2003). An *a priori* hypothesis of Order Iniomi (Aulopiformes + Myctophiformes) failed to be rejected by SH tests (Goseline et al. 1966, R.K. Johnson 1982) as seen in Table 1.2.

Sequence Analysis and Data Partitions of nucDNA and mtDNA Data Set

The five-gene data matrix included the following 4898 base positions; RAG1 (1498 bp), zic1 (916 bp), ENC1 (845bp), plagl2 (858bp), and COI (781). A total of 1947 characters were parsimony-informative. As a result of amplification and sequencing difficulties, data were not obtained for a few taxa with regards to certain genes (Table 1.1). The data for these taxa were coded as missing in the five-gene data matrix, and these taxa were not excluded from any analyses following the recommendation of Wiens (2003, 2006).

Mutational site saturation was not apparent across all codon positions for any of the sequenced gene regions (RAG1, zic1, ENC1, plagl2, and COI). Nuclear gene RAG1 showed slight saturation for transversions and transitions in only the third codon position. The third codon position of COI and plagl2 showed evidence of transitional saturation. All codon positions were included in all analyses based on the recommendations of Källersjö et al. (1999), where saturated data were demonstrated to provide phylogenetic signal.

The null hypothesis of base compositional stationarity was not rejected for the following first and second codon positions of all genes; RAG1 1^{st} ($\chi^2 = 53.47$, df = 165, $P = 1.000$), RAG1 2^{nd} ($\chi^2 = 20.54$, df = 165, $P = 1.000$), zic1 1^{st} ($\chi^2 = 18.19$, df

= 150, $P = 1.000$), zic1 2nd ($\chi^2 = 2.37$, df = 150, $P = 1.000$), ENC1 1st ($\chi^2 = 15.45$, df = 153, $P = 1.000$), ENC1 2nd ($\chi^2 = 3.04$, df = 153, $P = 1.000$), plagl2 1st ($\chi^2 = 74.09$, df = 150, $P = 0.999$), plagl2 2nd ($\chi^2 = 37.67$, df = 150, $P = 1.000$), COI 1st ($\chi^2 = 4.01$, df = 153, $P = 1.000$), and COI 2nd ($\chi^2 = 24.20$, df = 153, $P = 1.000$). Base compositional stationarity was rejected for the following third codon positions; RAG1 3rd ($\chi^2 = 897.52$, df = 165, $P = 0.000$), zic1 3rd ($\chi^2 = 674.54$, df = 150, $P = 0.000$), ENC1 3rd ($\chi^2 = 799.01$, df = 153, $P = 0.000$), plagl2 3rd ($\chi^2 = 710.41$, df = 150, $P = 0.000$), and COI 3rd ($\chi^2 = 468.67$, df = 153, $P = 0.000$).

The ranges of GC content varied in each gene. The average GC content of RAG1 was 57.45%, with a range from 49.1% in *Danio rerio* to 66.9% in *Coccorella atlantica*. For zic1, the average GC content was 57.85%, ranging from 50.5% in *Hiodon alosoides* to 66.9% in *Metavelifer multiradiatus*. For ENC1, the average GC content was slightly higher at 58.2%, with a range of 51% in *Metavelifer multiradiatus* to 66.7% in *Diplophos taenia*. For plagl2, the average GC content was the highest at 61.32%, ranging from 53.1% in *Danio rerio* to 67.1% in *Diplophos taenia*. Finally, for COI, the average GC content was lower than all other genes at 48.96%, with a range of 39.7% in *Danio rerio* to 53.9% in *Gigantura indica*.

Nuclear gene RAG1 possessed some codon bias, with an average ENC coefficient of 47.98. Of the ten taxa out of 56 with ENCs < 45, two were from the family Evermannellidae, four from the family Paralepididae, and the remaining four taxa included various orders (Salmoniformes, Argentiniformes, Ateleopodiformes, and Myctophiformes). ENC was higher overall for zic1, with an average ENC of 53.33.

Seven taxa out of 52 possessed ENCs < 45 (*Metavelifer multiradiatus*, *Paralepis coregonoides*, *Scopelosaurus lepidus*, *Scopelosaurus harryi*, *Benthosema glaciale*, *Paraulopus oblongus*, and *Harpadon microchir*) although codon bias was not limited to any particular order or family with the exception of the genus *Scopelosaurus*. The ENC1 gene possessed some codon bias with an average ENC across taxa of 46.74. From the 14 taxa out of 52 with ENCs < 45, two were from the family Scopelarchidae, three from family Evermannellidae, three from the family Notosudidae, and three were from the family Paralepididae, suggesting codon bias was limited to these particular families. Only three taxa had ENCs < 40, *Thaleichthys pacificus* (31.18), *Oncorhynchus mykiss* (33.68), and *Argentina sialis* (37.8), demonstrating strong codon bias among the protacanthopterygian taxa included in this analysis. Codon bias was most prevalent with the plagl2 gene, with an average ENC of 45.01 across taxa. Of the 50 taxa sequenced for ENC1, 20 had ENCs < 45, with the strongest bias appearing in *Synodus indicus* (29.35) and *Evermannella indica* (29.66). Mitochondrial gene COI also possessed some codon bias with an average ENC of 47.25. From the 11 taxa out of 52 with ENCs < 45 only two had ENCs < 40, *Danio rerio* (39.24) and *Lestidum atlanticum* (39.33).

Phylogenetic Analysis of nucDNA and mtDNA Data Set and *A Priori* Hypothesis Tests

The Bayesian analysis produced a majority-rule consensus topology as shown in Figure 1.6, where posterior probabilities (PP) are considered significant if PP≥95%. The four simultaneous runs reached convergence (PSRF = 1.008–1.000, s.d. = 0.01-

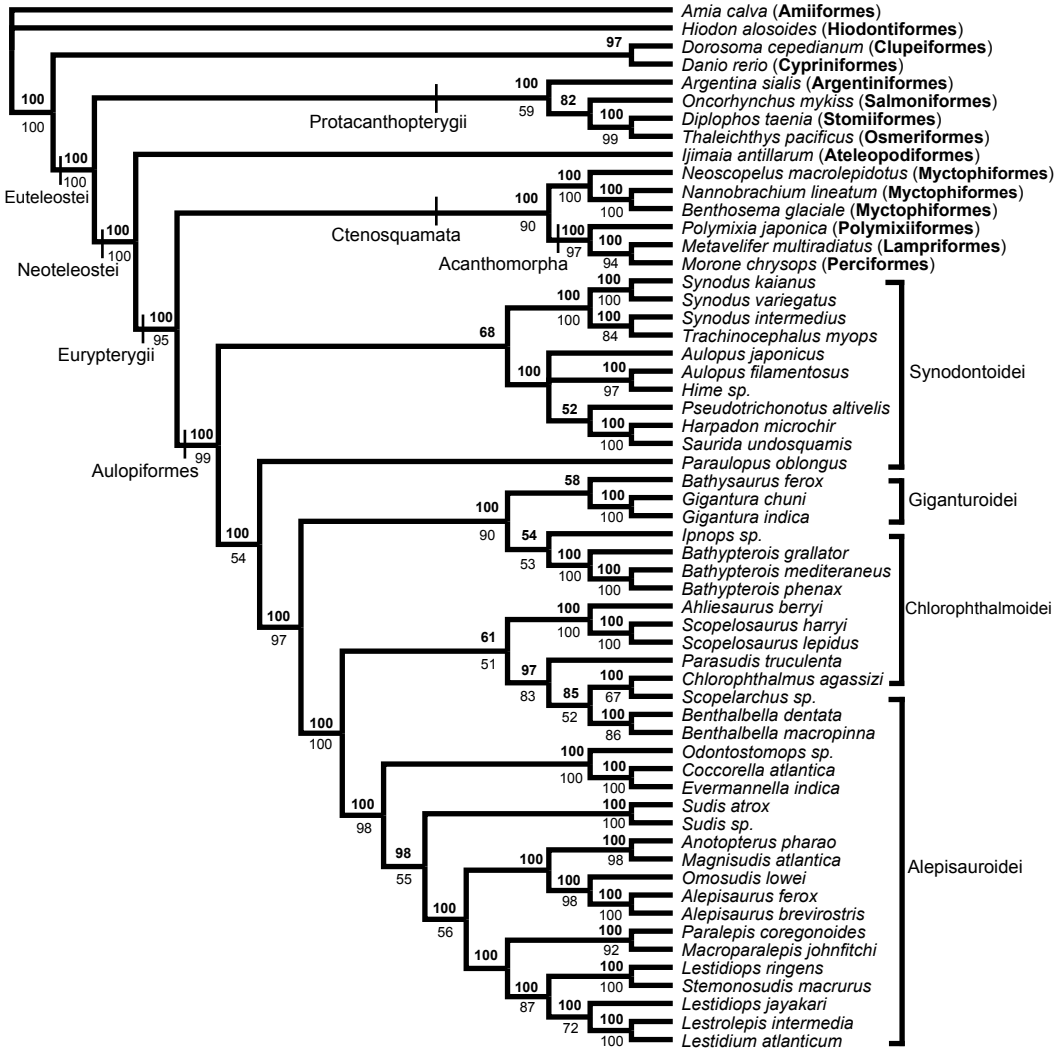

Fig. 1.6. Relationships of the Aulopiformes based on Bayesian and Maximum Likelihood analysis of five genes (RAG1, zic1, ENC1, plagl2, COI). Bayesian posterior probabilities denoted by bold numbers above node, with significant support ≥ 95. Likelihood bootstrap support values denoted by numbers below node, with significant support ≥ 70. Values below 50 not shown. Bars denote aulopiform suborders as described by Baldwin and Johnson (1996) and Sato and Nakabo (2002).

0.00), with each run obtaining the same consensus tree topology. Of the 54 nodes represented in the analysis, 47 were significantly supported (PP≥95%). The PP of *a priori* hypotheses is shown in Table 1.3. The following four hypotheses were significantly supported (PP≥95%): monophyly of Aulopiformes (Rosen 1973), monophyly of Notosudidae (Baldwin & Johnson 1996), monophyly of Alepisauridae (Baldwin & Johnson 1996), and monophyly of Evermannellidae (Baldwin & Johnson 1996).

Of the ten independent maximum-likelihood analyses performed, nine topologies were identical with likelihood scores ranging from –72686.62 to –72687.96. The one differing topology had the worst likelihood score of –72692.205. Topology likelihood scores were verified with PAUP*. The topology of the group composed of the nine best likelihood scores was identical to the Bayesian majority-rule consensus topology, with a few exceptions involving taxa within the suborder Synodontoidei. The clade comprised of Baldwin & Johnson's (1996) Synodontoidei, which was not significantly supported in the Bayesian analysis, was not recovered in the ML topology. The ML topology recovered a *Synodus* + *Trachinocephalus* clade as the basal aulopiform lineage, with a clade containing the genera *Harpadon*, *Saurida*, *Pseudotrichonotus*, *Aulopus*, and *Hime* being sister to all remaining aulopiform taxa. Additionally, the family Aulopidae (*Aulopus* + *Hime*) was monophyletic in the ML topology. Bootstrap support values for the ML topology are shown in Figure 1.6, with a bootstrap value of ≥70 regarded as significantly supported.

Maximum parsimony analysis obtained two equally parsimonious trees of 15774 steps (CI = 0.2853, HI = 0.7147, RI = 0.3858, RC = 0.1101). Clade bootstrap support values were considered significant if ≥70, following the recommendation of Hillis & Bull (1993). The parsimony consensus topology, not presented here, differed in a few relationships from the Bayesian and ML topologies. Unlike the Bayesian and ML topologies, the family Synodontidae (*Synodus*, *Trachinocephalus*, *Harpadon*, and *Saurida*) was recovered as monophyletic, but with no significant bootstrap support (<70). The genus *Paraulopus* was recovered as the sister taxon of *Pseudotrichonotus*, rather than of all remaining aulopiforms, but also with no significant bootstrap support (<70). A clade consisting of the family Aulopidae sister to all remaining aulopiform taxa was recovered with no significant bootstrap support (<70). Also unlike the Bayesian and ML topologies, the family Evermannellidae was not recovered as the basal member of the suborder Alepisauroidei, but was obtained within a clade consisting of the genera *Lestidiops*, *Lestidium*, *Lestrolepis* and *Stemnosudis*. This clade was significantly supported by bootstrap values (84), but may be an artifact of strong codon bias evident in these taxa for nuclear genes RAG1 and plagl2. Finally, the clade consisting of *Paralepis* + *Macroparalepis* was recovered as the sister group of the *Anotopterus* + *Magnisudis* clade, with that clade sister to the family Alepisauridae. This grouping was significantly supported (94) and may also be an artifact of codon bias, as the genera *Paralepis*, *Macroparalepis*, *Anotopterus*, and *Magnisudis* all demonstrated strong codon bias in nuclear genes ENC1 and plagl2.

As seen in Table 1.3, both WS-R and SH tests failed to reject the following *a priori* hypotheses not recovered in ML or MP analyses ($p \geq 0.05$): Order Iniomi monophyly (Gosline et al. 1966), a clade of Ateleopodiformes + Lampriformes sister to Myctophiformes (Miya et al. 2003), monophyly of Synodontoidei (Sato & Nakabo 2002), monophyly of Giganturoidei (Baldwin & Johnson 1996), monophyly of Alepisauroidei (Baldwin & Johnson 1996), monophyly of Chlorophthalmidae (Baldwin & Johnson 1996), monophyly of Scopelarchidae (Baldwin & Johnson 1996), and *Paraulops* as the basal member of the Synodontoidei (Sato & Nakabo 2002). The following *a priori* hypotheses of evolutionary relationships were rejected by both WS-R and SH tests ($p \leq 0.05$): interrelationships of Aulopiformes (Rosen 1973), Order Myctophiformes and interrelationships (R.K. Johnson 1982), aulopiform paraphyly (Rosen 1985), aulopiform interrelationships (Baldwin & Johnson 1996), aulopiform suborder relationships (Baldwin & Johnson 1996), aulopiform interrelationships (Sato & Nakabo 2002), aulopiform suborder relationships (Sato & Nakabo 2002), monophyly of Chlorophthalmoidei (Baldwin & Johnson 1996, Sato & Nakabo 2002), a Giganturoidei + Alepisauroidei clade (Baldwin & Johnson 1996), a Notosudidae + Ipnopidae clade (Baldwin & Johnson 1996), an *Anotopterus* + Paralepididae clade (Baldwin & Johnson 1996), and an *Evermannella* + *Odontostomops* clade (Baldwin & Johnson 1996). Monophyly of Synodontoidei (Baldwin & Johnson 1996) was rejected by SH, but not WS-R. The hypotheses of a monophyletic Paralepididae (Baldwin & Johnson 1996) and an Alepisauridae +

Paralepididae clade (Baldwin & Johnson 1996) were rejected by WS-R, but not SH tests.

Phylogenetic Analysis of Morphological Data Set

Maximum parsimony analysis of the concatenated morphological data set from Baldwin & Johnson (1996) and Sato & Nakabo (2002) generated eleven equally parsimonious trees of 485 steps (CI = 0.4928, HI = 0.5381, RI = 0.7659, RC = 0.3774). All 139 characters were parsimony informative. The MP consensus tree, not presented here, differed from the relationships presented by Baldwin & Johnson (1996) and Sato & Nakabo (2002) in the following ways: Giganturoidei is the sister group to Chlorophthalmoidei (*sensu* Sato and Nakabo 2002) although without significant bootstrap support; a Scopelarchidae + Evermannellidae clade is less resolved, and Scopelarchidae are no longer monophyletic with the scopelarchid + evermannellid clade forming a polytomy among *Benthalbella*, Evermannellidae, and a *Scopelarchus* + *Scopelarchoides* + *Rosenblattichthys* clade.

Phylogenetic Analyses of Total Evidence Data Set and *A Priori* Hypothesis Tests

The Bayesian majority consensus topology is shown in Figure 1.7. The four simultaneous runs reached convergence (PSRF = 1.022–1.000, s.d. = 0.08-0.00), with each run generating the same consensus tree topology. Of the 64 clades present in the analysis, 47 had significant support (PP≥95%). Clades of *a priori* hypotheses that possessed significant support (PP≥95%) include the following (Table 1.3): monophyly of Aulopiformes (Rosen 1973), monophyly of Synodontoidei (Baldwin & Johnson 1996), monophyly of Alepisauroidei (Baldwin & Johnson 1996, Sato &

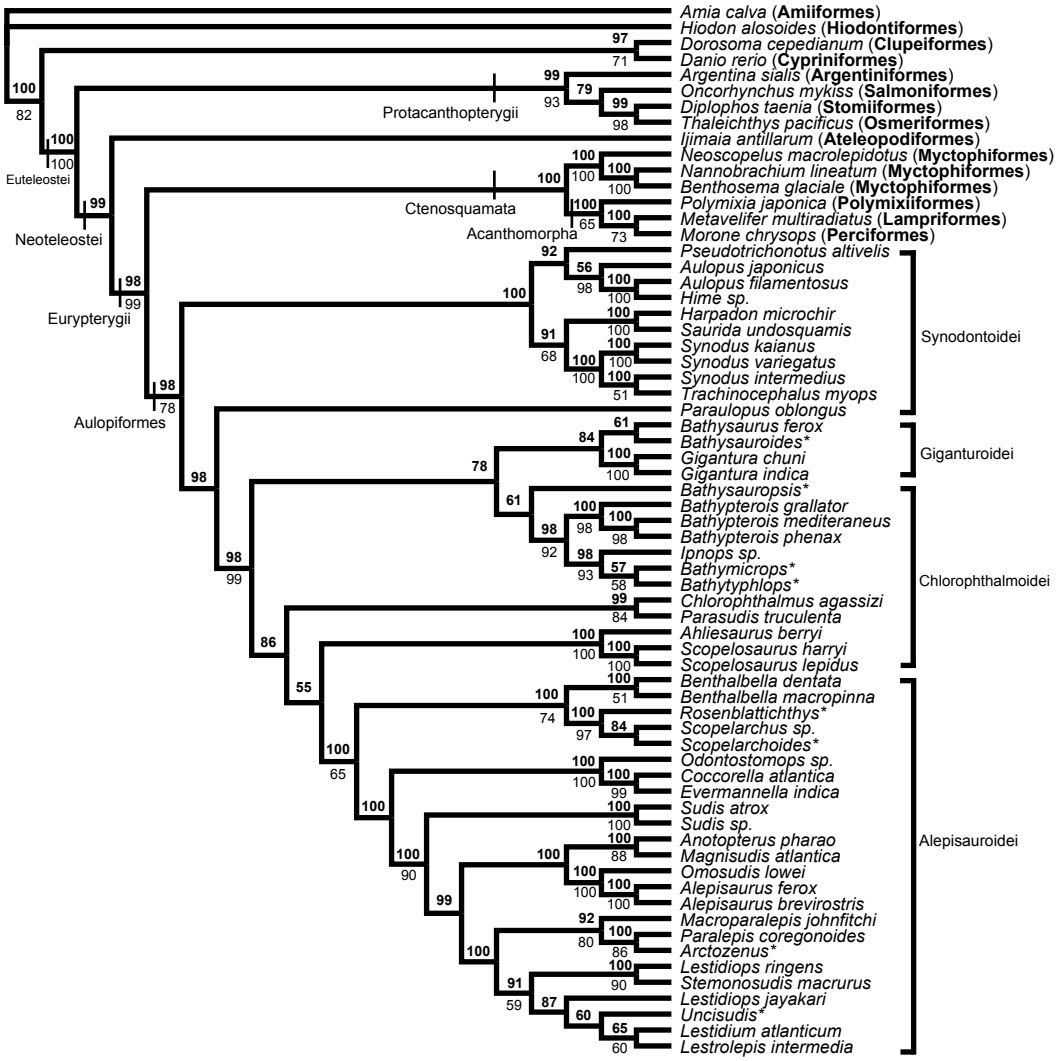

Fig. 1.7. Relationships of the Aulopiformes based on Bayesian analysis of five genes (RAG1, zic1, ENC1, plagl2, COI) and 138 morphological characters (Baldwin and Johnson 1996; Sato and Nakabo 2002). Bayesian posterior probabilities denoted by bold numbers above node, with significant support ≥ 95. Parsimony bootstrap support values denoted by numbers below node, with significant support ≥ 70. Values below 50 not shown. Bars denote aulopiform suborders as described by Baldwin and Johnson (1996) and Sato and Nakabo (2002). * indicates taxa represented by morphological data only.

Nakabo 2002), monophyly of Chlorophthalmidae (Baldwin & Johnson 1996), monophyly of Notosudidae (Baldwin & Johnson 1996), monophyly of Ipnopidae (Baldwin & Johnson 1996), monophyly of Scopelarchidae (Baldwin & Johnson 1996), monophyly of Alepisauridae (Baldwin & Johnson 1996), and Evermannellidae monophyly (Baldwin & Johnson 1996).

Maximum-parsimony analysis generated five equally parsimonious trees of 16358 steps (CI = 0.2902, HI = 0.7107, RI = 0.4016, RC = 0.1165). Of the 5036 included characters (4898 DNA, 138 morphological), 2086 characters were parsimony informative. Differences among the five equally parsimonious trees involved the phylogenetic relationships and placement of the genera *Lestidium*, *Lestrolepis*, and *Uncisudis*. The strict consensus parsimony tree, not presented here, differed from the Bayesian reconstruction of relationships in a few ways. The same differences discussed previously between the Bayesian and maximum parsimony consensus topologies for the nucDNA and mtDNA data set were observed in the total evidence analyses, with no significant bootstrap support values (≥70) for any discrepant parsimony clades. Unlike the Bayesian analysis, the genus *Bathysauroides* was not recovered within the suborder Giganturoidei, and instead was recovered as the sister group to the Alepisauroidei, although with no significant bootstrap support (≥70). Additionally, in the parsimony analysis the genus *Bathysauropsis* was sister to a clade consisting of Chlorophthalmidae, Bathysauroididae, and Alepisauroidei, with no significant bootstrap support. Clades with significant bootstrap support (≥70) that are congruent with the Bayesian majority consensus topology are presented in Figure 1.7.

The WS-R test failed to reject the following *a priori* hypotheses not recovered in the MP analysis ($p \geq 0.05$) as seen in Table 1.3: monophyly of Order Iniomi (Gosline et al. 1966), a Mytophiformes + Ateleopodiformes + Lampriformes clade (Miya et al. 2003), monophyly of Synodontoidei (Baldwin & Johnson 1996), monophyly of Synodontoidei (Sato & Nakabo 2002), monophyly of Giganturoidei (Baldwin & Johnson 1996), monophyly of Giganturoidei (Sato & Nakabo 2002), monophyly of Paralepididae (Baldwin & Johnson 1996), a *Paraulopus* + Synodontoidei clade (Sato & Nakabo 2002), a Scopelarchidae + Evermannellidae clade (Baldwin & Johnson 1996), a Notosudidae + Ipnopidae clade (Baldwin & Johnson 1996), an Alepisauridae + Paralepididae clade (Baldwin & Johnson 1996), and an *Evermannella* + *Odontostomops* clade (Baldwin & Johnson 1996). The following *a priori* hypotheses of evolutionary relationships were rejected by WS-R tests ($p \leq 0.05$): Aulopiformes interrelationships (Rosen 1973), Order Myctophiformes and interrelationships (R.K. Johnson 1982), aulopiform paraphyly (Rosen 1985), aulopiform interrelationships (Baldwin & Johnson 1996), aulopiform suborder relationships (Baldwin & Johnson 1996), aulopiform interrelationships (Sato & Nakabo 2002), aulopiform suborder relationships (Sato & Nakabo 2002), monophyly of Chlorophthalmoidei (Baldwin & Johnson 1996), monophyly of Chlorophthalmoidei (Sato & Nakabo 2002), a Giganturoidei + Alepisauroidei clade (Baldwin & Johnson 1996), and an *Anotopterus* + Paralepididae clade (Baldwin & Johnson 1996).

DISCUSSION

Monophyly of the Aulopiformes and their Systematic Placement within Euteleostei

Monophyly of the Aulopiformes as first proposed by Rosen (1973) was strongly supported in all analyses (RAG1, nucDNA + mtDNA, morphology only, DNA + Morphology) (Fig. 1.5, 1.6, 1.7). This result is in disagreement with the works of R.K. Johnson (1982), Rosen (1985), and Hartel & Stiassny (1986), but corroborates recent studies based on morphological data alone (Johnson 1992, Patterson & Johnson 1995, Johnson et al. 1996, Baldwin & Johnson 1996, Sato & Nakabo 2002). While an *a priori* hypothesis of iniomous relationships (Gosline et al. 1966) could not be significantly rejected, an aulopiform + myctophiform clade was not recovered in any analysis, and an iniomous hypothesis of relationships possessed a 0% posterior probability for Bayesian topologies (nucDNA + mtDNA, DNA + morphology). Aulopiform relationships as proposed by R.K. Johnson (1982) and Rosen (1985) were significantly rejected for all analyses. Aulopiform monophyly is supported by fourteen morphological synapomorphies in this study (Appendix 1.3; 1–1, 2–1, 16–2, 18–1, 58–1, 59–1, 69–1, 70–1, 89–1, 93–1, 104–1, 120–1, 133–1, 137–1), including six recovered in both ACCTRAN and DELTRAN optimizations; presence of an enlarged second epibranchial uncinate process (1–1), presence of a fifth epibranchial (18–1), lateral expansion of the palatine absent (58–1), palatinad cartilaginous facet for articulation with lateral ethmoid located on posterior portion of palatine (59–1), posterior processes of pelvic girdle elongate and widely separated (104–1), and absence of swimbladder (133–1).

Aulopiformes were recovered as the sister group to a monophyletic Ctenosquamata (Myctophiformes + Acanthomorpha) in all analyses (RAG1, nucDNA + mtDNA, DNA + morphology) with high statistical support for the nucDNA + mtDNA and total evidence analyses (Fig. 1.6, 1.7). The sister-group relationship with ctenosquamates supports the monophyly of Rosen's (1973) Eurypterygii. Miya et al. (2003) also found support for a monophyletic Eurypterygii with whole mitochondrial genomes; however, their Ctenosquamata consisted of a Myctophiformes + Ateleopodiformes + Lampriformes clade sister to the remaining Acanthomorpha. In all analyses (RAG1, nucDNA + mtDNA, DNA + morphology), Ateleopodiformes were recovered as the sister group to the eurypterygians with strong statistical support (Fig. 1.5, 1.6, 1.7). This result partially corroborates the placement by Olney et al. (1993) of Ateleopodiformes in a trichotomy with Stomiiformes and Eurypterygii. An *a priori* hypothesis of a Myctophiformes + Ateleopodiformes + Lampriformes clade (Miya et al. 2003) was not significantly rejected with the nucDNA + mtDNA dataset across parsimony (WS-R) and likelihood analyses (SH), but possessed a 0% posterior probability among Bayesian topologies (nucDNA + mtDNA, DNA + Morphology), and was additionally significantly rejected with the RAG1 dataset likelihood analysis (SH).

Monophyly of Rosen's (1973) Ctenosquamata was strongly supported across all nucDNA + mtDNA and total evidence analyses, with high statistical support for a monophyletic Scopelomorpha (Myctophiformes) sister to a strongly supported Acanthomorpha (Fig. 1.6, 1.7). Within the monophyletic Myctophiformes, the family

Neoscopelidae was recovered as sister to a strongly supported clade comprised of species within the family Myctophidae (Fig. 1.5). This result corroborates previous myctophiform morphological studies (e.g., Paxton 1972, Stiassny 1996) but contradicts the findings of Rosen (1985) in which Neoscopelidae formed a clade with aulopoid and chlorophthalmoid aulopiforms as the sister group to Ctenosquamata including the family Myctophidae. While 11 of the 20 orders of Acanthomorpha (Nelson 2006) were sampled in the RAG1 analysis (Fig. 1.5), a discussion on the phylogenetic relationships of acanthomorphs is beyond the scope of this study and would require greater taxon sampling of this extremely diverse group.

Of the included taxa within this analysis, monophyly of Neoteleostei was highly supported with the exception of the Order Stomiiformes, which was recovered as the sister group to Osmeriformes within Protacanthopterygii with high statistical support across all analyses (RAG1, nucDNA + mtDNA, DNA + morphology) (Fig. 1.5, 1.6, 1.7). The RAG1 analysis included representatives of two stomiiform families, Gonostomatidae and Diplophidae (Nelson 2006), while the combined DNA and total evidence analyses included only *Diplophos taenia*. While this result is in disagreement with the vast majority of morphological studies (e.g., Rosen 1973, Johnson 1992, Johnson and Patterson 1993), it corroborates other recent molecular studies examining protacanthopterygian relationships (e.g., Lopez et al. 2004), which recovered Stomiiformes closely related to Osmeriformes. While the mitochondrial study of Miya et al. (2003) recovered a more traditional Neoteleostei with

Stomiiformes sister to the eurypterygians, their analysis did not include any Osmeriformes.

Monophyly of Aulopiform Suborders

Relationships within the order Aulopiformes have recently been classified in four monophyletic suborders (Synodontoidei, Chlorophthalmoidei, Alepisauroidei, and Giganturoidei) following the studies of Baldwin & Johnson (1996) and Sato & Nakabo (2002). The results of the nucDNA + mtDNA only analyses do not support the monophyly of either the Chlorophthalmoidei or Alepisauroidei as described by Baldwin & Johnson (1996) and Sato & Nakabo (2002) (Fig. 1.6). Bayesian reconstructions (nucDNA + mtDNA) recovered a monophyletic Synodontoidei *sensu* Baldwin & Johnson (1996) without any statistical support. The genus *Paraulopus* was not recovered as a member of the Synodontoidei (Sato & Nakabo 2002) in any of the DNA analyses. The suborder Giganturoidei was recovered as monophyletic with no statistical support in the nucDNA + mtDNA analyses. Total evidence (DNA + morphology) analyses recovered monophyletic suborders Synodontoidei, Giganturoidei, and Alepisauroidei *sensu* Baldwin & Johnson (1996) with strong statistical support for Synodontoidei and Alepisauroidei (Fig. 1.7). The results of the total evidence analyses and *a priori* hypothesis tests suggest that the suborder Chlorophthalmoidei as currently recognized is not monophyletic. Systematic placement of taxa within the monophyletic and paraphyletic suborders, revised classification, and morphological evidence supporting previously unrecognized clades

are discussed below. A complete list of morphological character optimizations for each node and terminal can be found in Appendix 1.3.

Aulopiform Relationships

The results of the molecular (nucDNA + mtDNA) and total evidence (DNA + morphology) analyses suggest that the taxa within the suborder Synodontoidei (Baldwin & Johnson 1996, Sato & Nakabo 2002), classified in this study as the Aulopoidei, are the basal lineages of aulopiform fishes (Fig. 1.6, 1.7). This result concurs with the hypotheses of Baldwin & Johnson (1996) and Sato & Nakabo (2002). The newly recognized genus *Paraulopus*, diagnosed from a *Chlorophthalmus* species complex, was not recovered in any analysis as the basal aulopoid lineage as hypothesized by Sato & Nakabo (2002). However, an *a priori* hypothesis of a *Paraulopus* + Aulopoidei clade was not significantly rejected for parsimony and ML analyses (Table 1.3). The results from the DNA and total evidence analyses suggest that *Paraulopus*, recognized here as the sole member of the suborder Paraulopoidei (*sensu novo*), is the sister group of a clade consisting of taxa from the suborders Chlorophthalmoidei, Alepisauroidei, and Giganturoidei *sensu* Baldwin & Johnson (1996), classified in this study as the suborder Alepisauroidei (*sensu novo*) as seen in Fig. 1.8. This hypothesis of the systematic placement of the genus *Paraulopus* had high statistical support for nucDNA + mtDNA and total evidence analyses, and is a novel reconstruction of relationships.

Taxa within the suborder Aulopoidei were recovered as monophyletic and as the basal aulopiform lineage (Fig. 1.6, 1.7), with both strong (DNA + morphology) and

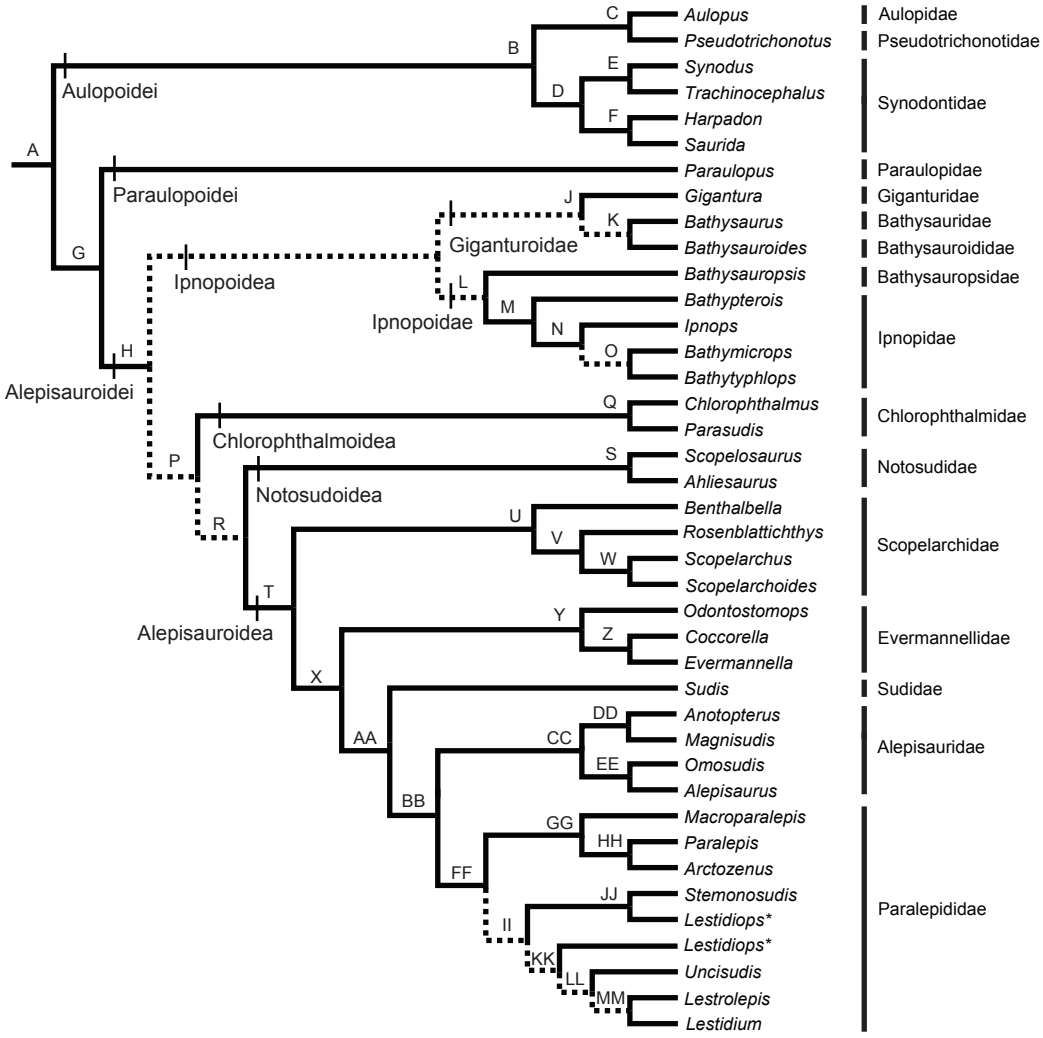

Fig. 1.8. Classification of the Aulopiformes based on Bayesian total evidence topology (Fig. 1.7). Solid lines denote nodes with strong statistical support in either Bayesian or parsimony reconstructions. Dashed lines indicate nodes with weak support. For morphological character distributions please see Appendix 3.

weak (nucDNA + mtDNA) statistical support. Two distinct aulopoid clades were recovered with the DNA analyses. A clade comprising *Synodus* + *Trachinocephalus* was sister to a clade consisting of the genera *Aulopus*, *Hime*, *Pseudotrichonotus*, *Harpadon*, and *Saurida*. Molecular data alone did not recover a monophyletic Synodontidae (*Synodus*, *Trachinocephalus*, *Harpadon*, and *Saurida)* or Aulopidae (*Aulopus* and *Hime*) with Bayesian reconstructions. A clade consisting of *Harpadon* + *Saurida* was recovered with high statistical support corroborating many previous studies (e.g., Rosen 1973, Sulak 1977, R. K. Johnson 1982, Baldwin & Johnson 1996). Results from the total evidence analyses also suggest two aulopoid clades, although with different taxonomic composition. The family Synodontidae is monophyletic with high statistical support and sister to a clade consisting of Pseudotrichonotidae + Aulopidae. The results of the total evidence analysis concur with the nucDNA + mtDNA only analysis in recognizing a *Harpadon* + *Saurida* clade with strong statistical support.

For both nucDNA + mtDNA and total evidence analyses, a *Synodus* + *Trachinocephalus* clade was recovered where *Trachinocephalus* is placed within the genus *Synodus*, sister to *Synodus intermedius* with high statistical support. The monotypic genus *Trachinocephalus* shares all of its morphological character transformation series with *Synodus,* with one exception (Baldwin & Johnson 1996). *Trachinocephalus myops* possesses a reduced fifth epibranchial that is present as a small cartilage, with fifth epibranchials absent in *Synodus* (18–0). The results of this study suggest that *Trachinocephalus myops* is a member of the genus *Synodus*,

although further study is needed that would include a broader taxonomic sampling of the approximately 36 species of *Synodus* (Nelson 2006).

The genus *Hime* was recovered within the genus *Aulopus* across both nucDNA + mtDNA (ML and MP) and total evidence (Bayesian and MP) topologies with high statistical support (Fig. 1.7). The genus *Hime* is recognized by Parin and Kotlyar (1989) and Thompson (1998) to include all former species of *Aulopus* that are distributed in the Pacific Ocean (e.g., *Aulopus japonicus*, *Aulopus purpurissatus*), with Atlantic-distributed species remaining in the genus *Aulopus* (e.g., *Aulopus filamentosus*). Baldwin & Johnson (1996) rejected the use of *Hime* as a valid genus because of a lack of significant morphological differences between Atlantic and Pacific species, and *Aulopus* is the currently accepted generic name. The results of the nucDNA + mtDNA and total evidence analyses show strong support for the recognition of a single genus *Aulopus*, as the Atlantic *Aulopus filamentosus* was found to be more closely related to the specimen of *Hime sp*. collected in the Pacific Ocean than either were to the specimen of *Aulopus japonicus*, previously regarded as a member of the genus *Hime*. The nucDNA + mtDNA and total evidence analyses support the inclusion of Aulopidae within the aulopoids (e.g., Johnson et al. 1996, Baldwin & Johnson 1996), and not the sister group of the Ctenosquamata (Stiassny 1986, Hartel & Stiassny 1986) (Figs. 1.6, 1.7). The results of the total evidence Bayesian reconstruction suggest a sister-group relationship between Aulopidae and the Pacific and Indian Ocean distributed genus *Pseudotrichonotus*, which is a novel hypothesis of aulopiform relationships, although it is not statistically supported. An

Aulopus + *Pseudotrichonotus* clade is supported by four morphological synapomorphies (60–1, 77–1, 120–1, 121–1).

The suborder Chlorophthalmoidei, including the families Chlorophthalmidae, Bathysauropsidae, Notosudidae, and Ipnopidae (Baldwin & Johnson 1996, Sato & Nakabo 2002) was not recovered as monophyletic. The results of the nucDNA + mtDNA and total evidence analyses strongly support a Giganturoidei (*Gigantura* + *Bathysaurus* + *Bathysauroides*) + Bathysauropsidae + Ipnopidae clade sister to all remaining chlorophthalmoids + Alepisauroidei taxa (Fig. 1.6, 1.7). Support for a Giganturoidei (*Bathysaurus* + *Gigantura*) + Ipnopidae (*Ipnops* + *Bathypterois*) clade was strong for nucDNA + mtDNA analyses, but weak with total evidence analyses where the genera *Bathysauroides* and *Bathysauropsis* were added with morphological data alone. A sister group relationship between giganturids and ipnopids has never been proposed, and contradicts previous placement of the suborder Giganturoidei as the sister group to the suborder Alepisauroidei (Baldwin & Johnson 1996, Sato & Nakabo 2002). *A priori* hypothesis tests of a Giganturoidei + Alepisauroidei clade were significantly rejected for all analyses (Table 1.3). A giganturid + ipnopid clade was supported by multiple morphological characters (26–1, 27–1, 113–2, 128–1, 134–1), including two recovered in both ACCTRAN and DELTRAN optimizations, the number of postcleithra (113–2), and eye morphology (128–1).

Within the giganturid + ipnopid clade, recognized in this study as the superfamily Ipnopoidea (*sensu novo*), the suborder Giganturoidei (Baldwin & Johnson 1996) was recovered as monophyletic in both nucDNA + mtDNA and total evidence analyses

(Bayesian reconstruction), although without statistical support (Fig. 1.6, 1.7, 1.8). Taxa within the suborder Giganturoidei *sensu* Baldwin & Johnson (1996) are classified in this study within the epifamily Giganturoidae (*sensu novo*). A sister group relationship between *Bathysaurus* and *Gigantura*, first suggested by Patterson & Johnson (1995), was supported by molecular data, although without strong support. When the genus *Bathysauroides* was included in the total evidence analyses, it was recovered within the epifamily Giganturoidae as suggested by Baldwin & Johnson (1996), although only in Bayesian reconstructions where a clade consisting of *Bathysauroides* + *Bathysaurus* was sister to *Gigantura* (Fig. 1.7, 1.8).

The family Ipnopidae was recovered as monophyletic in all analyses with high statistical support (DNA + morphology). Relationships within the family corroborate those of Baldwin & Johnson (1996). Total evidence analyses (Bayesian) recover the genus *Bathysauropsis* as the sister group to the family Ipnopidae, a result which corroborates Hartel & Stiassny's (1986) systematic placement of the genus, and its inclusion within their Ipnopidae based on the shared presence of a small obliquely aligned basihyal. Sulak (1977) also recovered *Bathysauropsis* as the sister group to his subfamily Ipnopinae, which included all currently recognized members of Ipnopidae. Baldwin & Johnson (1996) hypothesized that *Bathysauropsis* was the sister group to a Notosudidae + Ipnopidae clade, and removed *Bathysauropsis* from the family Ipnopidae. Sato & Nakabo (2002) subsequently elevated *Bathysauropsis* to family level (Bathysauropsidae). This study concurs with the elevation of *Bathysauropsis* to family level as the *Bathysauropsis* + Ipnopidae clade is weakly

supported, while the Ipnopidae clade *sensu* Baldwin & Johnson (1996) has strong statistical support (Fig. 1.7, 1.8). For nucDNA + mtDNA and total evidence analyses, *a priori* hypothesis tests of a Notosudidae + Ipnopidae clade were significantly rejected (Table 1.3).

Relationships among the remaining chlorophthalmoid taxa were less resolved. Molecular analyses recovered a Notosudidae + Chlorophthalmidae + Scopelarchidae clade as the sister group to all remaining alepisauroid taxa with high statistical support, however the Notosudidae + Chlorophthalmidae + Scopelarchidae clade itself was weakly supported (Fig. 1.6). Within this clade, the family Notosudidae (*Ahliesaurus* and *Scopelosaurus*) was recovered as monophyletic and the sister group to a well supported Chlorophthalmidae + Scopelarchidae clade, where neither family was monophyletic. R. K. Johnson (1982), considered the family Scopelarchidae within his chlorophthalmoid group in a clade consisting of the families Chlorophthalmidae + Ipnopidae based on the shared presence of a gap in ossification between the first centrum and the skull (R. K. Johnson 1982; 40). Prior to this reconstruction, Scopelarchids had been thought to be more closely related to the family Evermannellidae (e.g., Gosline et al. 1966), and Baldwin & Johnson (1996) recovered an Evermannellidae + Scopelarchidae clade as the sister group of all remaining alepisauroid taxa. Baldwin & Johnson (1996) suggested that scopelarchids and evermannellids share five synapomorphies (82–1; 84–2; 117–1; 128–3; 135–2); however, two of these synapomorphies (128–3; 135–2) are directly related to the shared feature of tubular eyes. R. K. Johnson (1982) identified that the tubular eyes

of scopelarchids and evermannellids may be a result of convergence, and that the morphological characteristics of the tubular eyes are potentially not homologous. While it is interesting that molecular data supports R. K. Johnson's (1982) hypothesis that scopelarchids are more closely related to chlorophthalmoids than alepisauroids, further molecular and morphological analysis is needed to further investigate these relationships.

Total evidence analyses recover a monophyletic Notosudidae, Chlorophthalmidae and Scopelarchidae with high statistical support for each family (Fig. 1.7). Systematic positions of the Chlorophthalmidae and Notosudidae are not well supported, with superfamily Chlorophthalmoidea (*sensu novo*) sister to a clade consisting of superfamilies Notosudoidea (*sensu novo*) + Alepisauroidea (*sensu novo*). Scopelarchidae are recovered as the basal group within the Alepisauroidea with strong statistical support, but are not recovered as the sister group of the Evermannellidae, as hypothesized by Baldwin & Johnson (1996). An *a priori* hypothesis test of an Evermannellidae + Scopelarchidae clade was significantly rejected for all analyses with the exception of total evidence parsimony tests (Table 1.3).

The results of the total evidence analyses (Bayesian reconstruction) strongly suggest that Evermannellidae are the sister group to all remaining taxa of Alepisauroidea (Sudidae, Alepisauridae, Paralepididae) (Fig. 1.7, 1.8). Under total evidence and nucDNA + mtDNA only parsimony analysis, evermannellids were recovered within a clade of paralepidids; however, this result was most likely the

result of significant codon bias in these taxa for nuclear genes RAG1 and plagl2. Relationships within the Evermannellidae for both DNA and total evidence analyses corroborate those of R. K. Johnson (1982), with *Odontostomops* sister to a strongly supported *Evermannella* + *Coccorella* clade (Fig. 1.6, 1.7). The genera *Evermannella* and *Coccorella* share the possession of tubular eyes (128–3), which are absent in *Odontostomops*. Baldwin & Johnson (1996) hypothesized a sister-group relationship between *Evermannella* + *Odontostomops* that required a reversal in *Odontostomops* for possession of tubular eyes. An *Evermannella* + *Odontostomops* clade was significantly rejected in all *a priori* hypothesis tests with the exception of total evidence parsimony (Table 1.3).

A strongly supported clade consisting of the families Sudidae, Alepisauridae, and Paralepididae includes the remainder of the Alepisauroidea. The family Paralepididae *sensu* Baldwin and Johnson (1996; *Sudis*, *Anotopterus*, *Magnisudis*, *Paralepis*, *Macroparalepis*, *Lestidiops*, *Lestrolepis*, *Lestidium*, *Stemonosudis*, *Arctozenus*, *Uncisudis*) was recovered as paraphyletic for nucDNA + mtDNA and total evidence analyses (Fig. 1.6, 1.7, 1.8). This result contradicts the findings of Patterson & Johnson (1996), Baldwin & Johnson (1996), and Sato & Nakabo (2002), where an Alepisauridae + Paralepididae clade was hypothesized. Null hypotheses of an Alepisauridae + Paralepididae clade were significantly rejected for all analyses with the exception of nucDNA + mtDNA maximum likelihood, and total evidence parsimony (Table 1.3). The results of all analyses strongly support *Sudis* as the sister group to a clade consisting of the family Alepisauridae (*sensu novo*; [*Omosudis* +

Alepisaurus] + [*Anotopterus* + *Magnisudis*]) and the remaining paralepidids (Fig. 1.6, 1.7, 1.8). The genus *Sudis* is re-elevated to the family Sudidae which is distinguished by multiple morphological apomorphies (Appendix 1.3), including enlarged pectoral fins in larvae (134–1), and larval head spines (136–1).

A monophyletic Alepisauridae (*sensu novo*) consisting of *Anotopterus* + *Magnisudis* sister to *Alepisaurus* + *Omosudis*, was recovered with strong support as sister to all remaining paralepidid taxa (Bayesian and ML topologies) (Fig. 1.6, 1.7, 1.8). Monophyly of the family Alepisauridae was recovered with high statistical support by both nucDNA + mtDNA and total evidence analyses. This corroborates the sister-group relationship between *Omosudis* and *Alepisaurus* first proposed by R. K. Johnson (1982), and its sister group, the *Anotopterus* + *Magnisudis* clade, is a novel hypothesis of relationships with strong support. The genera *Anotopterus* and *Magnisudis* are recognized here within the family Alepisauridae (*sensu novo*), and members of this family share a third pharyngobranchial toothplate (UP3) that is restricted to the lateral edge of the ventral surface of pharyngobranchial 3 (11–1), and a supracleithrum that is equal to or longer than the cleithrum (99–1), along with other apopmorphies (Appendix 1.3). Baldwin & Johnson (1996) recovered *Anotopterus* within a monophyletic Paralepididae, corroborating the hypothesis of R. K. Johnson (1982). This relationship between *Anotopterus* and paralepidids was significantly rejected across all hypothesis tests (Table 1.3). The genus *Magnisudis* was not included in the studies of Baldwin & Johnson (1996) or Sato & Nakabo (2002), but

had previously been hypothesized to be closely related to the paralepidid genera *Arctozenus*, *Paralepis*, and *Notolepis* (Post 1987).

The remaining paralepidids are recovered within a strongly supported clade in all analyses, recognized here as the family Paralepididae (*sensu novo*) (Fig. 1.6, 1.7, 1.8). A clade including the genera *Paralepis* + *Macroparalepis* was strongly recovered in nucDNA + mtDNA analyses. When the genus *Arctozenus* was included in total evidence analyses, it was recovered as the sister group to *Paralepis* within the *Macroparlepis* + *Paralepis* clade. A sister group relationship between *Paralepis* and *Arctozenus* corroborates the findings of Baldwin & Johnson (1996). In parsimony analyses (nucDNA + mtDNA and total evidence), the *Macroparalepis* + *Paralepis* + *Arctozenus* clade is recovered as the sister group to the *Anotopeterus* + *Magnisudis* clade, with this entire clade sister to Alepisauridae (*sensu* Baldwin & Johnson 1996). However, this parsimony relationship may be an artifact of strong codon bias as the genera *Paralepis*, *Macroparalepis*, *Anotopterus*, and *Magnisudis* all possess strong codon bias in nuclear genes ENC1 and plagl2.

The results of this study support the recovery of a clade consisting of the genera *Lestidiops*, *Stemonosudis*, *Lestrolepis*, *Lestidium*, and *Uncisudis*; this result corroborates relationships recovered by Baldwin & Johnson (1996). However, relationships within this clade differ slightly from those of their study, and resolution among the taxa was poorly supported for total evidence analyses, but strongly supported for nucDNA + mtDNA analyses (Fig. 1.6, 1.7). For nucDNA + mtDNA analyses, a sister-group relationship was recovered between *Stemonosudis* and

Lestidiops ringens, with the genus *Lestidiops* paraphyletic. This clade was sister to a clade consisting of *Lestidiops jayakari* sister to a *Lestrolepis* + *Lestidium* clade. In total evidence analyses, the genus *Uncisudis* was recovered as the sister group to the *Lestrolepis* + *Lestidium* clade. Further work and broader taxon sampling is necessary in order to satisfactorily resolve relationships among the paralepidids.

Morphological Signal in Total Evidence Analyses

In general, concerns that morphological data would be overshadowed by a large multi-gene data set were not observed in this study. Analyses utilizing the five nuclear and mitochondrial gene data-set were well resolved, with 47 of 54 nodes significantly supported with posterior probabilities of ≥95% in the Bayesian topology reconstruction. Even with well resolved topologies based on molecular data, morphological characters from Baldwin & Johnson (1996) and Sato & Nakabo (2002) were able to significantly influence aulopiform evolutionary relationships recovered by the total evidence analyses, regardless of the fact that morphological characters contributed < 3% of the total evidence data matrix. The results of this study support the recommendations of Nylander et al. (2004) that morphological signal can contribute important information to molecular systematic analyses, and should be considered when morphological information is applicable and available.

Comment on Extinct Aulopiform Taxa

Currently the study of Fielitz (2004), focusing on the Late Cretaceous marine enchodontids, is the only phylogenetic study that incorporates both extinct and extant aulopiform taxa. Fielitz (2004) proposed a monophyletic Superfamily

†Enchodontoidea (families †Cimolichthyidae and †Enchodontidae) as the sister group to Alepisauridae *sensu* Baldwin and Johnson (1996), with that clade sister to Paralepididae. While fossil taxa were not included in this analysis, it is likely that the systematic position of the enchodontids would remain within Alepisauroidea, sister to Alepisauridae. Monophyly and relationships to extant taxa of the remaining aulopiform fossil taxa (e.g., Suborder †Ichthyotringoidei, Suborder †Halecoidei) are questionable (e.g., Rosen 1973, Chalifa 1989, De Figueiredo & Gallo 2005, Nelson 2006). Additional robust systematic studies that include both extinct and extant aulopiforms are needed to further elucidate the evolutionary relationships of fossil aulopiform taxa.

CLASSIFICATION

A new classification of extant aulopiform genera and families is presented. Asterisks indicate taxa not included in analyses. Classification follows phyletic sequence, and reflects the total evidence hypothesis of relationships (Fig. 1.8).

Order Aulopiformes

- Suborder Aulopoidei *sens. nov.*
  - Family Synodontidae (*Synodus, Trachinocephalus, Harpadon, Saurida*)
  - Family Aulopidae (*Aulopus*)
  - Family Pseudotrichonotidae (*Pseudotrichonotus*)
- Suborder Paraulopoidei *taxon nov.*
  - Family Paraulopidae (*Paraulopus*)
- Suborder Alepisauroidei *sens. nov.*
  - Superfamily Ipnopoidea *sens. nov.*
    - Epifamily Giganturoidae *sens. nov.*
      - Family Giganturidae (*Gigantura*)
      - Family Bathysauridae (*Bathysaurus*)
      - Family Bathysauroididae (*Bathysauroides*)
    - Epifamily Ipnopoidae *sens. nov.*
      - Family Bathysauropsidae (*Bathysauropsis*)
      - Family Ipnopidae (*Bathypterois, Ipnops*, *Bathymicrops, Bathytyphlops, Discoverichthys**)
  - Superfamily Chlorophthalmoidea *sens. nov.*
    - Family Chlorophthalmidae (*Chlorophthalmus, Parasudis*)
  - Superfamily Notosudoidea *sens. nov.*
    - Family Notosudidae (*Scopelosaurus*, *Ahliesaurus, Luciosudis**)
  - Superfamily Alepisauroidea *sens. nov.*
    - Family Scopelarchidae (*Benthalbella, Rosenblattichthys, Scopelarchus, Scopelarchoides*)
    - Family Evermannellidae (*Odontostomops*, *Coccorella*, *Evermannella*)
    - Family Sudidae (*Sudis*)
    - Family Alepisauridae *sens. nov.* (*Anotopterus, Magnisudis*, *Omosudis*, *Alepisaurus*)
    - Family Paralepididae *sens. nov.* (*Macroparalepis*, *Paralepis*, *Arctozenus*, *Stemonosudis*, *Lestidiops*, *Uncisudis*, *Lestrolepis*, *Lestidium, Dolichosudis**)

CONCLUSIONS

In summary, DNA and total evidence analyses strongly support monophyly of the Aulopiformes. Aulopiformes are recovered as the sister group to Rosen's (1973) Ctenosquamata with high statistical support. This result corroborates monophyly of Eurypterygii (e.g., Rosen 1973, Johnson 1993) with nuclear and mitochondrial gene data. Ateleopodiformes were recovered as the sister group to the Eurypterygii with high statistical support using molecular data. Within Aulopiformes, the suborders Synodontoidei and Giganturoidei *sensu* Baldwin & Johnson (1996) were recovered as monophyletic with DNA data, but without statistical support. Total evidence analyses recovered monophyletic suborders Synodontoidei, and Alepisauroidei *sensu* Baldwin & Johnson (1996) with statistical support. The suborder Chlorophthalmoidei was not recovered as monophyletic. DNA analyses recovered the following families as paraphyletic: Synodontidae (Bayesian, ML), Scopelarchidae (Bayesian, ML, MP), Chlorophthalmidae (Bayesian, ML, MP), and Paralepididae (Bayesian, ML, MP). All families were recovered as monophyletic with high statistical support in total evidence analyses with the exception of the paraphyletic Paralepididae (Bayesian, ML, MP).

DNA analyses corroborated Sato & Nakabo (2002) in recovering *Paraulopus* outside of *Chlorophthalmus*, but did not support their hypothesis that *Paraulopus* is the basal member of the suborder Aulopoidei. The genus was recovered as the sister group to all chlorophthalmoid + giganturoid + alepisauroid taxa with strong statistical support, and is recognized here as the sole member of suborder Paraulopoidei. The

monotypic genus *Trachinocephalus* was recovered within the genus *Synodus* (nucDNA + mtDNA, DNA + morphology), and further research is needed to determine whether *Trachinocephalus myops* should be assigned to *Synodus*. Recognition of the genus *Hime* was not supported by molecular data and a single genus *Aulopus* is recommended, although further research is needed to properly assess the potential of genetic and morphological diversity between Atlantic and Pacific species of the genus *Aulopus*.

Taxa within the Giganturoidae were recovered as the sister group of Ipnopoidae within the superfamily Ipnopoidea, rather than of the suborder Alepisauroidei (Baldwin & Johnson 1996; Sato & Nakabo 2002) with high statistical support. The genus *Bathysauroides* was recovered within Giganturoidae, corroborating Baldwin & Johnson (1996). The genus *Bathysauropsis* was recovered as the sister group of Ipnopidae (total evidence Bayesian, ML) without statistical support, and remains assigned to its own family Bathysauropsidae. The results of the nucDNA + mtDNA and total evidence analyses suggest that the family Notosudidae is not the sister group of the ipnopids as hypothesized by Baldwin & Johnson (1996).

DNA analyses recovered a Notosudidae + Chlorophthalmidae + Scopelarchidae clade without support. Scopelarchidae was recovered with Chlorophthalmidae within a clade where both families were paraphyletic with high statistical support for molecular data. While this result corroborates the placement of scopelarchids with chlorophthalmoids suggested by R. K. Johnson (1982), total evidence analyses recover Scopelarchidae as the basal family in the Alepisauroidea lineage. In either

case, Scopelarchidae are not recovered as the sister group to Evermannellidae (Baldwin & Johnson, 1996), and further research into the morphologies of these groups is needed to ascertain whether a number of derived features are truly shared (e.g., tubular eyes) or are the result of convergence in the deep sea. The systematic position of Chlorophthalmidae and Notosudidae is weakly supported for total evidence analyses, but Chlorophthalmoidea are sister to a Notosudoidea + Alepisauroidea clade.

Evermannellidae were recovered as the sister group to a clade consisting of alepisauroid taxa in the families Sudidae, Alepisauridae (*sensu novo*) and Paralepididae (*sensu novo*). Relationships within Evermannellidae corroborate R. K. Johnson (1982) in recovering *Coccorella* and *Evermannella* as sister groups. The genus *Sudis* is the sister group to a clade comprised of two distinct lineages of parelepidid and alepisaurid fishes, and is re-elevated here to the family Sudidae. The first lineage includes the family Alepisauridae, with an *Alepisaurus* + *Omosudis* clade sister to an *Anotopterus* + *Magnisudis* clade (Bayesian, ML). The genera *Anotopterus* and *Magnisudis* were previously recognized as members of the family Paralepididae, and are recognized here as belonging to the family Alepisauridae. The second distinct lineage includes the remaining genera of the family Paralepididae, including *Paralepis*, *Macroparalepis*, *Arctozenus*, *Lestidiops*, *Stemonosudis*, *Lestrolepis*, *Uncisudis*, and *Lestidium*. Resolution of this clade is strongly supported by molecular data, but weakly supported by the total-evidence analyses. Further

research is needed with broader taxon sampling to further investigate relationships among the lineages of Paralepididae.

CHAPTER 2

ESTIMATING DIVERGENCE TIMES OF LIZARDFISHES AND THEIR ALLIES (EUTELEOSTEI: AULOPIFORMES) AND THE TIMING OF DEEP-SEA ADAPTATIONS

INTRODUCTION

The order Aulopiformes (Euteleostei: Cyclosquamata) includes 44 genera and approximately 236 species of lizardfishes and their allies (Nelson, 2006). Taxa within the order include predatory marine fishes that range in habitat from inshore coastal systems to the deep sea. The order has been recovered as monophyletic with both morphological (e.g., Rosen, 1973; Baldwin and Johnson, 1996; Sato and Nakabo, 2002) and molecular data (Davis, 2009). The fossil record for aulopiform fishes is robust. Extinct taxa have been described from two of the three suborders, the Aulopoidei and the Alepisauroidei; most fossil taxa are associated with the crown aulopiform clade of alepisauroids (Lancetfishes) from Late Cretaceous deposits. This study explores the divergence times of aulopiform fishes and character evolution of deep-sea adaptations within a robust molecular phylogenetic framework. I investigate the divergence times of: (1) the common ancestor of aulopiforms, (2) the major aulopiform lineages, and (3) two aulopiform deep-sea evolutionary adaptations.

The results of this study will provide a temporal framework for further macroevolutionary studies of aulopiform diversification.This study concentrates on the timing of the evolutionary diversification of aulopiform lineages, eye specializations, and reproductive strategies.

The oldest complete aulopiform fossil is †*Atolvorator longipectoralis* from the Sergipe-Alagoas Basin in northeastern Brazil (Gallo and Coelho, 2008). This formation is dated to the Barremian of the Lower Cretaceous and is estimated to be 125 million years old. Gallo and Coelho (2008) did not conduct a phylogenetic study to explore the relationship of †*A. longipectoralis* to other aulopiform taxa, but hypothesized that the taxon was closely aligned to other extinct alepisauoids (e.g, †Cimolichthyidae, †Serrilepidae). Additionally, isolated tooth elements were suggested to belong to an unidentified alepisauroid taxon which has been described from Barremian deposits of Alcaine in northeastern Spain (Kriwet, 2003).

While there have been many studies focused on the evolutionary relationships of extant aulopiforms (e.g., Rosen, 1973; Johnson, 1982; Baldwin and Johnson, 1996; Sato and Nakabo, 2002, Davis, 2009), relationships within the group including extinct aulopiforms are unclear with the exception of the family †Enchodontidae. Currently, the only phylogenetic study of aulopiform fishes to include both extant and extinct taxa is that of Fielitz (2004), which examined the interrelationships of the family †Enchodontidae. Fielitz (2004) recovered a trichotomous clade consisting of the extant family Alepisauridae (*Alepisaurus* and *Omosudis*) and the extinct families †Cimolichthyidae and †Enchodontidae, classified under the superfamily

Alepisauroidea (Fig 2.1; Fielitz, 2004). The oldest specimen analyzed in this study was from the Lower Cenomanian Stage of the Late Cretaceous, approximately 100 million years ago. All other studies examining aulopiform fossils have assigned taxa to extant families based on morphological characteristics with no systematic analysis (e.g., Rosen, 1973), or have left the taxa *incertae sedis* within the order (e.g., Taverne, 2004; 2005).

Hypotheses of aulopiform divergence times never have been explored with molecular data from a robust dataset with comprehensive aulopiform taxonomic sampling. Alfaro et al. (2009) included two aulopiform taxa (*Synodus intermedius and Chlorophthalmus* sp.*)* in their analysis of divergence and diversification rates among vertebrates, and recovered a mean divergence time for the aulopiform clade of 102 Ma (95% HPD 96–138 Ma). Overall, the young mean age recovered for the divergence of the entire clade certainly was the result of their calibration of the aulopiform node. Alfaro et al. (2009) placed a minimum age for the aulopiform clade at 96 Ma, based on fossil representatives †*Nematonotus* spp. (Aulopididae) and †*Acrognathus dodgei* (Chlorophthalmidae), and a maximum age of 128–130 Ma based on teeth from an undetermined fossil taxon (Kriwet, 2003). Their calibration scheme for aulopiforms is problematic as the minimum age imposed for the clade is nearly 30 Ma younger than the oldest complete aulopiform fossil †*Atolvorator longipectoralis* (Gallo and Coelho, 2008) and they imposed a maximum clade age based on fossil teeth elements from an undetermined taxon that was hypothesized to be closely related to the crown aulopiform lineage of alepisauroids (Kriwet, 2003).

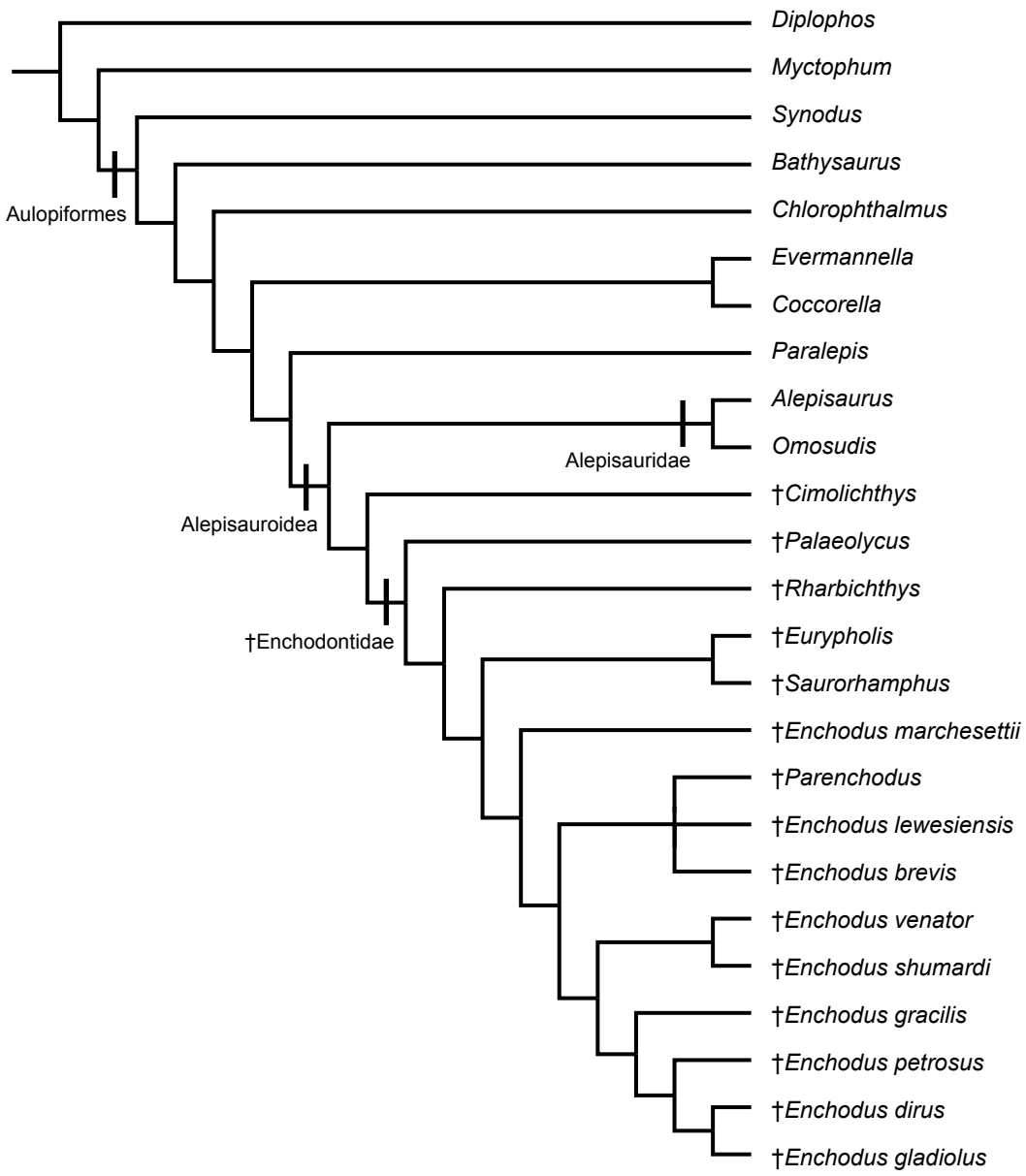

Fig. 2.1. Evolutionary relationships of the †Enchodontidae. Reproduced from Fieltiz (2004). Consensus of three equally parsimonious trees.

Deep-sea fishes are subject to similar selective pressures as a result of the extreme habitat; thus, convergent adaptations, such as bioluminescence, thin bones, tubular or greatly reduced eyes, hermaphroditism, and large mouths with daggerlike teeth, are extremely common (Marshall, 1954; Helfman et al., 1997). The eye modifications that are a common evolutionary adaptation in deep-sea teleost lineages can be attributed to the two main sources of illumination in the deep sea—residual sunlight and bioluminescence (Douglas et al., 1998). At depths greater than 1000 m, teleosts cannot detect residual sunlight; hence, the fish depend solely on bioluminescence for any visual functions, such as identifying predators and prey, and finding mates (Denton, 1990). While most deep-sea fishes possess large eyes with a large pupils (Fig 2.2 A) that aid in detecting distinct sources of residual or biolumenescent light (Land, 1981; 1990), numerous lineages have evolved highly modified morphological specializations of the eyes (e.g., Stomiiformes, Osmeriformes, Lampridiformes, Lophiformes).

The eyes of deep-sea aulopiform fishes possess some of the most bizzare modifications any teleost lineage, making them ideal candidates for studying the character evolution of various eye morphologies (Fig 2.2). Three families (Giganturidae, Evermannellidae, and Scopelarchidae) have taxa with tubular eyes—a highly specialized type of eye usually characterized by a large spherical lense, large pupil, a thick main retina, and often an accessory retina (Fig 2.2 D, E). Species of *Gigantura* have rostrally directed and elongated tubular/telescopic eyes (Fig 2.2 E),

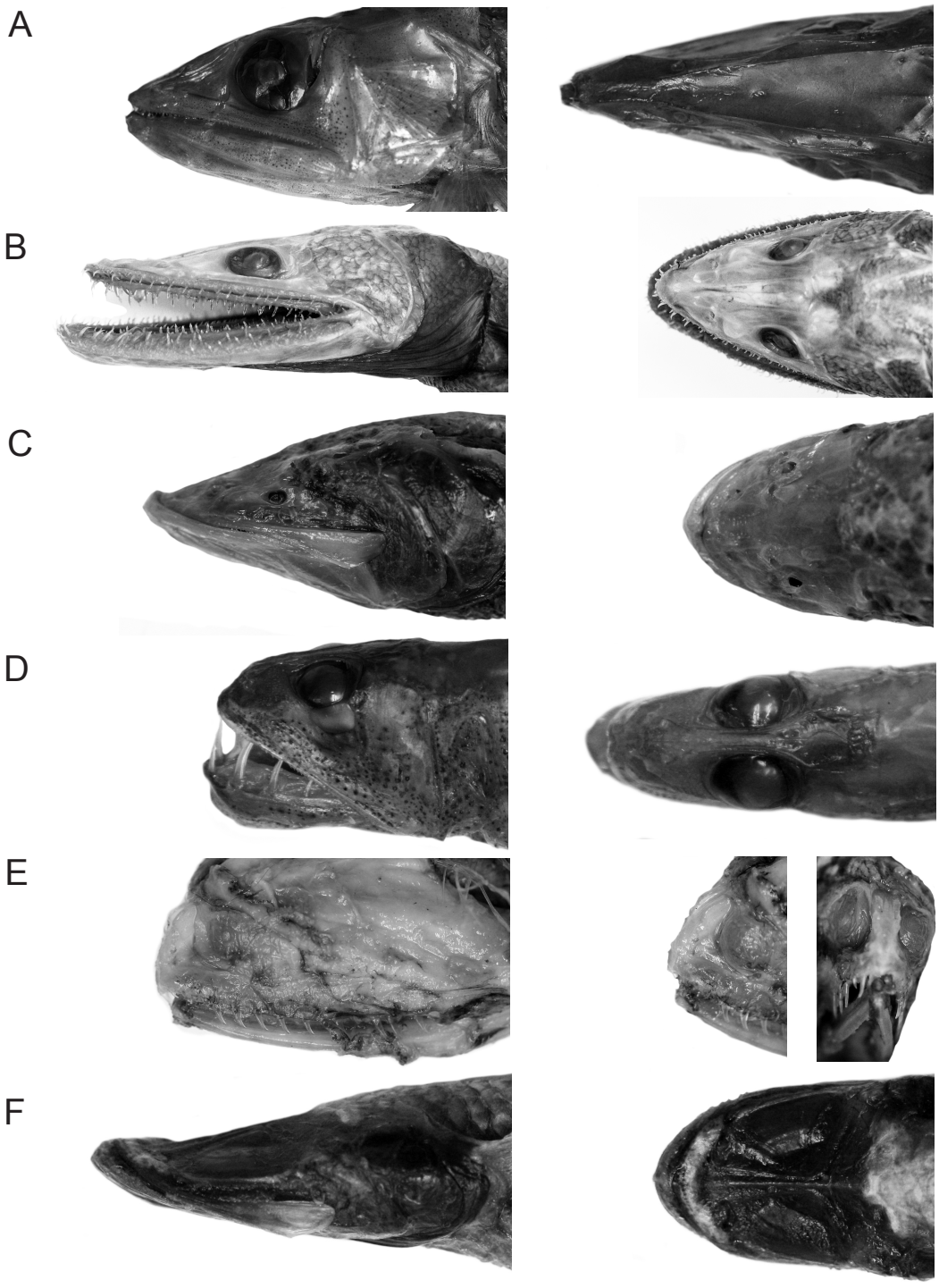

Fig. 2.2. Aulopiform eye specializations. A - Round and laterally directed (0), *Alepisaurus brevirostris*, MCZ 43134. B - Slightly flattened to elliptical (1), *Bathysaurus ferox*, MCZ 165208. C - Minute or absent (2), *Bathypterois longipes*, MCZ 36634. D - Dorsally directed tublar/semitublar (3), *Evermannella balbo*, MCZ 101362. E - Anteriorlly directed tubular/telescopic (4), *Gigantura chuni*, MCZ 59485. F - Broad lensless plates on dorsal surface of head (5), *Ipnops murrayi*, KU-CI-159. Scale bar denotes 10 mm.

whereas species of *Evermannella*, *Coccorella*, *Benthalbella*, *Rosenblattichthys*, *Scopelarchoides*, and *Scopelarchus* have dorsally directed tubular eyes (Fig 2.2 D).

Two genera within the family Ipnopidae have greatly reduced (*Bathytyphlops*, *Bathypterois)* eyes, and one (*Bathymicrops*) lacks eyes (Fig 2.2 C); another genus, *Ipnops*, has one of the most bizarre eye adaptations among fishes. Prior to the work of Munk (1959), members of *Ipnops* had been reported to be the only vertebrate that lacked every trace of an eye (e.g., optic nerve, rods, cones, muscle attachments). Munk (1959) documented that *Ipnops* possessed highly modified eyes in the form of a flattened, upward-directed cephalic organ that was innervated by optic nerves, and a retinal layer with typical rods. This modified eye is covered by transparent, fused frontal bones (Fig 2.2 F).

In addition to modified eye structures, deep-sea aulopiform fishes also are hermaphroditic. Sequential hermaphroditism is a common reproductive strategy among deep-sea teleost fishes, and has evolved independently in multiple lineages (e.g., Stomiiformes). However, aulopiforms are one of only four teleostean clades that have evolved synchronous hermaphroditism (Mank et al., 2006) and are the only deep-sea fish lineage in which this strategy has evolved. Synchronous hermaphrodites can produce functional male and female gametes at the same time; however, there is no evidence that any aulopiform taxa are capable of self-fertilization. Of the other three lineages, two are coral-reef predators (Muraenidae: Elopiformes; Serranidae: Perciformes) and one is found in neotropical freshwaters (Rivulidae: Cyprinodontiformes). Because of their diverse habitat and reproductive

strategies, aulopiform fishes offer a unique opportunity to study the evolution of this rare adaptation within a phylogenetic context.

MATERIALS AND METHODS

Phylogenetic Analyses

Molecular data included four nuclear genes (RAG1, 1498 bp; zic1, 916 bp; ENC1, 845 bp; plagl2, 858 bp) and one mitochondrial gene (COI, 781 bp), for a total of 4898 base pairs from my previous study of aulopiform interrelationships (Davis, 2009). The alignment used was identical to the alignment of Davis (2009). Taxonomic sampling included 43 aulopiform species representing 32 of 44 aulopiform genera (Table 2.1) and every family with the exception of the recently elevated Bathysauropsidae and Bathysauroididae (Sato and Nakabo 2002). Outgroup sampling included tissue samples for 15 species representing 13 actinopterygiian orders (Table 2.1). Outgroups were chosen in order to maintain a broad sampling of groups hypothesized to be basal to or closely related to Aulopiformes (e.g., Rosen, 1973; Johnson, 1992; Arratia, 2004) including members of the following groups (Nelson, 2006): Neopterygii, Osteoglossomorpha, Otocephala, Protacanthopterygii, Sternopterygii, Ateleopodomorpha, Ctenosquamata, and Acanthomorpha.

A Bayesian phylogenetic analysis was performed in BEAST (Drummond and Rambaut, 2007), which simultaneously estimates topology and divergence times. Each codon position was assigned a separate GTR + I + G model. Mean substitution rates were not fixed, with substitution rates estimated under a relaxed uncorrelated lognormal clock that allows for independent rates to vary on different branches in the

TABLE 2.1: List of species examined in this study. Classification follows Nelson (2006) with GenBank accession numbers.

		Accession Nos.				
Taxon	Catalog Number	RAG1	zic1	ENC1	plagl2	COI
Order Amiiformes						
Family Amiidae						
Amia calva	Various	AY430199	EF032909	EF032974	EF033013	AB042952
Order Hiodontiformes						
Family Hiodontidae						
Hiodon alosoides	Various	AY430200	EU366766	—	—	AP004356
Order Clupeiformes						
Family Clupeidae						
Dorosoma cepedianum	KU T7841	DQ912099	EU366767	—	—	EU366583
Order Cypriniformes						
Family Cyprinidae						
Danio rerio	Various	U71093	EF032910	EF032975	EF033014	NC002333
Order Argentiniformes						
Family Argentinidae						
Argentina sialis	KU T519	AY430228	EU366773	EU366634	EU366680	—
Order Osmeriformes						
Family Osmeridae						
Thaleichthys pacificus	KU T3135	AY380537	EU366774	EU366635	EU366681	—
Order Salmoniformes						
Family Salmonidae						
Oncorhynchus mykiss		U15663	EF032911	EF032976	EF033015	NC001717
Order Stomiiformes						
Family Gonostomatidae						
Diplophos taenia	KU T3781	EU366724	EU366768	EU366630	EU366676	EU366584
Order Ateleopodiformes						
Family Ateleopodidae						
Ijimaia antillarum	KU T5411	EU366725	EU366769	EU366631	EU366677	EU366585
Order Aulopiformes						
Suborder Synodontoidei						
Family Paraulopidae						
Paraulopus oblongus	CBM-ZF T99-109	EU366709	EU366752	EU366615	EU366664	EU366568
Family Aulopidae						
Aulopus filamentosus	USNM T3816	EU366688	EU366733	EU366593	EU366642	EU366546
Aulopus japonicus	CBM-ZF T99-124	EU366687	EU366732	EU366592	EU366641	EU366545
Hime sp.	SIO T02-68	EU366701	EU366746	EU366606	EU366654	EU366559
Family Pseudotrichonotidae						
Pseudotrichonotus altivelis	CBM-ZF T99-156	EU366711	EU366754	EU366617	—	EU366570
Family Synodontidae						
Synodus kaianus	CBM-ZF T99-128	EU366719	EU366761	EU366625	EU366672	EU366578
Synodus variegatus	KU T6901	EU366720	EU366762	EU366626	EU366673	EU366579
Synodus intermedius	KU T5219	EU366721	EU366763	EU366627	EU366674	EU366580
Trachinocephalus myops	KU T5225	EU366723	EU366765	EU366629	—	EU366582
Saurida undosquamis	CBM-ZF T99-162	EU366712	EU366755	EU366618	EU366665	EU366571
Harpadon microchir	CBM-ZF T99-148	EU366700	EU366745	EU366605	EU366653	EU366558
Suborder Chlorophthalmoidei						
Family Chlorophthalmidae						
Chlorophthalmus agassizi	KU T3759	EU366695	EU366740	EU366600	—	EU366553
Parasudis truculenta	KU T959	EU366710	EU366753	EU366616	—	EU366569
Family Notosudidae						
Ahliesaurus berryi	KU T5285	EU366685	EU366731	EU366590	EU366639	EU366544
Scopelosaurus harryi	KU T3244	EU366713	EU366756	EU366619	EU366666	EU366572
Scopelosaurus lepidus	KU T3641	EU366714	EU366757	EU366620	EU366667	EU366573
Family Ipnopidae						
Bathypterois grallator	KU T5935	EU366690	EU366735	EU366595	EU366644	EU366548
Bathypterois mediteraneus	CBM-ZF T99-139	EU366691	EU366736	EU366596	EU366645	EU366549
Bathypterois phenax	KU T3625	EU366692	EU366737	EU366597	EU366646	EU366550
Ipnops sp.	CBM-ZF T99-144	EU366702	EU366747	EU366607	EU366655	EU366560
Suborder Alepisauroidei						
Family Scopelarchidae						
Benthalbella dentata	KU T3239	EU366693	EU366738	EU366598	EU366647	EU366552
Benthalbella macropinna	KU T926	EU366694	EU366739	EU366599	EU366648	EU366552
Scopelarchus sp.	KU T3783	EU366715	EU366758	EU366621	EU366668	EU366574
Family Evermannellidae						
Coccorella atlantica	KU T5314	EU366696	EU366741	EU366601	EU366649	EU366554
Evermannella indica	KU T3790	EU366697	EU366742	EU366602	EU366650	EU366555
Odontostomops sp.	CBM-ZF T99-129	EU366706	EU366749	EU366612	EU366661	EU366565
Family Alepisauridae						
Alepisaurus brevirostris	KU T5258	EU366684	EU366730	EU366589	EU366638	EU366543
Alepisaurus ferox	KU T5395	EU366683	EU366729	—	EU366637	EU366542
Omosudis lowei	KU T5909	EU366707	EU366750	EU366613	EU366662	EU366566
Family Paralepididae						
Anotopterus pharao	KU T2305	EU366686	—	EU366591	EU366640	—
Lestidiops jayakari	KU T3792	EU366705	—	EU366610	EU366658	EU366562
Lestidiops ringens	SIO T93-297	—	—	—	EU366659	EU366563
Lestidium atlanticum	KU T3544	EU366703	—	EU366608	EU366656	EU366561
Lestrolepis intermedia	KU T3557	EU366704	—	EU366609	EU366657	—
Macroparalepis johnfitchi	SIO T94-266	EU366722	EU366764	EU366628	EU366675	EU366581
Magnisudis atlantica	KU T5928	—	EU366748	EU366611	EU366660	EU366564

TABLE 2.1 Continued: List of species examined in this study. Classification follows Nelson (2006) with GenBank accession numbers.

		Accession Nos.				
Taxon	Catalog Number	RAG1	zic1	ENC1	plagl2	COI
Paralepis coregonoides	KU T3719	EU366708	EU366751	EU366614	EU366663	EU366567
Stemonosudis macrurus	KU T93-238	EU366716	—	EU366622	EU366669	EU366575
Sudis atrox	KU T3107	EU366717	EU366759	EU366623	EU366670	EU366576
Sudis sp.	KU T3798	EU366718	EU366760	EU366624	EU366671	EU366577
Suborder Giganturoidei						
Family Bathysauridae						
Bathysaurus ferox	KU T5934	EU366689	EU366734	EU366594	EU366643	EU366547
Family Giganturidae						
Gigantura chuni	KU T6533	EU366698	EU366743	EU366603	EU366651	EU366556
Gigantura indica	KU T5270	EU366699	EU366744	EU366604	EU366652	EU366557
Order Myctophiformes						
Family Neoscopelidae						
Neoscopelus macrolepidotus	KU T3297	EU366727	EU366771	EU366632	EU366678	EU366587
Family Myctophidae						
Benthosema glaciale	KU T3734	EU366728	EU366775	—	—	—
Nannobrachium lineatum	KU T3634	EU366726	EU366770	—	—	EU366586
Order Polymixiiformes						
Family Polymixiidae						
Polymixia japonicus	KU T258	AY308765	EU366776	EU366636	EU366682	AB034826
Order Lampriformes						
Family Veliferidae						
Metavelifer multiradiatus	KU T1252	EF094949	EU366772	EU366633	EU366679	EU366588
Order Perciformes						
Morone chrysops	Various	AY308767	EF032917	EF032982	EF033021	—

topology (Drummond et al., 2006). Under this model there is no *a priori* correlation between any rates in the tree. Four separate analyses were performed with 100 million generations each, with a burn-in of 10 million generations for each analysis. Parameters and trees were sampled every 1000 iterations for a total of 400,000 trees, 360,000 post-burnin. The program Tracer v 1.41 (Rambaut and Drummond, 2007) was used to inspect the effective sample size (ESS) of all parameters in each analysis and check for parameter stationarity. All parameters appeared to converge on a stationary distribution, and possessed ESS's greater than 200, suggesting that all analyses sampled the posterior distributions of each parameter satisfactorily. Two clades were constrained in the BEAST analysis, including a monophyletic suborder Aulopoidei and a sister relationship between the family Scopelarchidae and the remaining alepisaurid taxa (families Evermannellidae, Alepisauridae, Sudidae, Paralepididae) (Table 2.2). A monophyletic Aulopoidei was recovered with weak (DNA only) and strong support (Total Evidence) in Davis's (2009) analysis. The scopelarchid + alepisaurid clade was not recovered with DNA evidence alone in Davis's (2009) analysis, but was recovered with strong statistical support in the total evidence analysis when morphological data was considered in combination with DNA.

Fossil Calibrations

Fossil calibrations were done using a lognormal prior, with only hard minimum ages of clades set *a priori*. Minimum dates were based on the oldest known representative of each of the teleost clades discussed bellow (Fig 2.3, Table 2.2). In

TABLE 2.2: Divergence times of Aulopiformes. Clades with (C#) were constrained to a minimum age; see Figure 2.3. An * indicates minimum age constrained. Bold posterior probabilities (PP) indicate the clade was constrained as monophyletic.

Clade/Node		Posterior Probability	Mean Age (Ma)	95% HPD Age
1	Neopterygii	1.00	264	220–337
2	Teleostei (C1)	1.00	222	220*–226
3		1.00	193	171–212
4	Ostarioclupeomorpha (C2)	1.00	148	146*–151
5	Euteleostei (C3)	1.00	165	150*–186
6	Protacanthopterygii	1.00	138	99–174
7		0.88	120	79–161
8	Stomiiformes + Osmeriformes	1.00	82	35–126
9	Neotelostei	1.00	155	139–176
10	Eurypterygii	1.00	148	133–166
11	Ctenosquamata	1.00	124	101–147
12	Order Myctophiformes (C4)	1.00	74	72*–77
13	Family Myctophidae	1.00	41	19–62
14	Acanthomorpha (C5)	1.00	96	94*–100
15		1.00	75	52–94
16	Order Aulopiformes	1.00	140	127–156
17	Suborder Aulopoidei	**1.00**	133	115–152
18	*Synodus* + *Trachinocephalus*	1.00	85	55–115
19		1.00	56	27–88
20		1.00	56	25–86
21		1.00	118	93–143
22		0.61	104	74–134
23	*Harpadon* + *Saurida*	1.00	60	26–97
24	Family Aulopidae	0.95	95	60–127
25		1.00	53	20–87
26	Paraulopoidei + Alepisauroidei	0.98	135	123–149
27	Alepisauroidei	1.00	128	118–140
28	Superfamily Ipnopoidea	1.00	102	72–129
29	Family Giganturidae	1.00	35	10–65
30		0.74	91	62–120
31	Family Ipnopidae	0.90	80	50–112
32	*Bathypterois*	1.00	49	23–78
33		1.00	26	7–46
34		1.00	121	113–131
35	Family Chlorophthalmidae	1.00	101	65–127
36		1.00	120	112–130
37	Family Notosudidae	1.00	67	31–106

TABLE 2.2 Continued: Divergence times of Aulopiformes. Clades with (C#) were constrained to a minimum age, see Figure 2.3. An * indicates minimum age constrained. Bold posterior probabilities (PP) indicate clade was constrained as monophyletic.

Clade/Node		Posterior Probability	Mean Age (Ma)	95% HPD Age
38	*Scopelosaurus*	1.00	24	6 –47
39	Superfamily Alepisauroidea	1.00	119	111–129
40	Family Scopelarchidae	**1.00**	88	50–119
41	*Benthalbella*	1.00	67	26–107
42		1.00	115	108–123
43	Family Evermannellidae	1.00	56	27–88
44		1.00	34	12–60
45		1.00	113	106–120
46	Family Sudidae	1.00	61	26–95
47		1.00	109	104–116
48	Family Alepisauridae	1.00	105	101–109
49		1.00	33	7–67
50	*Omosudis* + *Alepisaurus* + Family †Enchodontidae (C6)	1.00	101	100*–102
51	*Alepisuarus*	1.00	41	12–74
52	Family Paralepididae	1.00	95	75–110
53		1.00	63	33–91
54		1.00	74	47–98
55		1.00	3	1–8
56		1.00	55	30–81
57		1.00	27	7–47

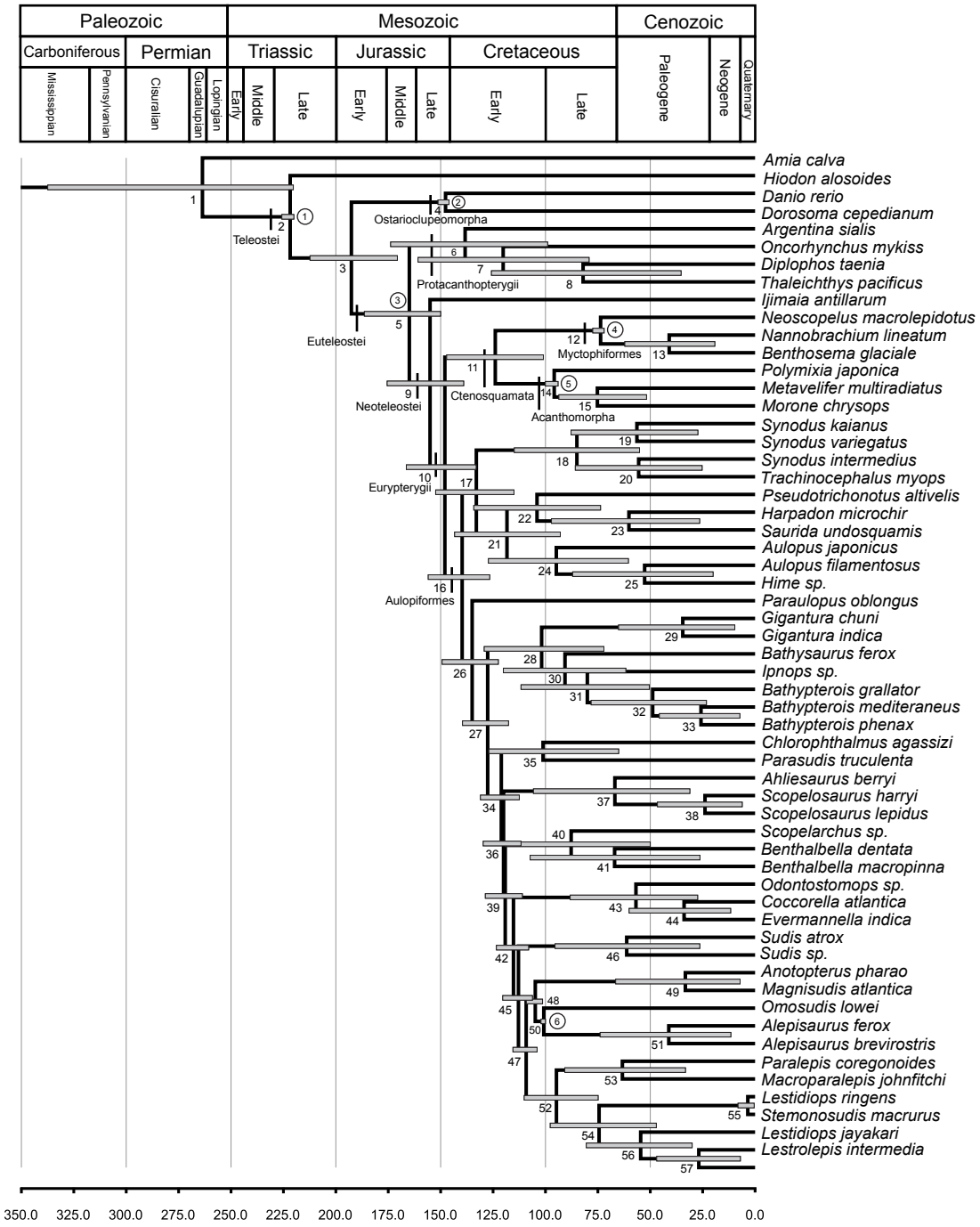

Fig. 2.3. Divergence time estimations. Bars denote 95% HPD. Numbers at nodes refer to clades in Table 2, which includes information on mean clade age, 95% HPD, and posterior probabilities. Circled numbers refer to calibration points, see materials and methods for discussion on calibrations. Scale is in millions of years.

order to be conservative with calibrations, dates were based on taxa attributed to the following nodes in previous phylogenetic analyses.

Teleostei – The fossil taxon used to date the clade Teleostei was †*Pholidophorus bechei*, recovered as the basal teleost lineage in Arratia's (2000b, 2001) phylogenetic study of lower teleost relationships. The taxon †*Pholidophorus bechei* is known from the Early Jurassic, with the fossil dated at approximately 220 Ma (Arratia, 2000a). Thus, 220 Ma was set as the minimum age for the most recent common ancestor (MRCA) of the clade Teleostei.

Ostarioclupeomorpha – The systematic placement of genus †*Tischlingerichthys* (Arratia, 1997; Arratia, 1999; Arratia, 2000b) as the stem ostariophysan was used to date the MRCA of the clade Ostarioclupeomorpha at 146 Ma. Specimens of †*Tischlingerichthys* examined by Arratia (1997, 1999, 2000b) are from the Late Jurassic, Upper Tithonian (Malm Z3) of Mühlheim, Bavaria, Germany.

Euteleostei – The age of †*Leptolepides sprattiformis*, the oldest member of a stem extinct euteleostean clade recovered as the sister group to extant eutelosts in Arratia's (1997, 1999) phylogenetic study on the relationships of lower teleosts was used to date the MRCA of euteleosts at a minimum age of 150 Ma. Specimens of †*Leptolepides sprattiformis* are known from Solenhofen, Germany, in Late Jurassic, Early Tithonian (Malm Z2) deposits (Arratia, 1997).

Acanthomorpha – The node representing the MRCA of acanthomorphs was given a minimum age of 94 Ma, following the recommendations of Hurley et al. (2007). Fossil taxa attributed to extant stem acanthomorph lineages (e.g., *Polymixia*)

are known from Cenomanian deposits dated to approximately 94 Ma (Patterson 1993; Hurley et al., 2007).

Order Myctophiformes – The oldest representatives of Mycthophiformes are known from the Campanian in the Early Cretaceous from the extinct genus †*Sardinioides*, which has been recovered as the stem myctophid taxon (Rosen, 1973; Prokofiev, 2006). The minimum age for the MRCA of Myctophiformes was dated to 72 Ma.

Family Alepisauridae – The systematic placement of a clade including the families †Enchodontidae and †Cimolichthyidae sister to Alepisauridae *sensu* Fielitz (2004) (Fig 2.1), was used to date a minimum age for the MRCA of the *Alepisaurus* + *Omosudis* clade at 100 Ma (Fig 2.3, Table 2.2), the approximate age of the oldest taxa in that systematic analysis, †*Enchodus brevis* and †*Saurorhamphus freyeri* (Fielitz, 2004). Although the oldest aulopiform fossil is dated at approximately 125 Ma (Gallo and Coelho, 2008), its current systematic position among extant taxa is unknown, therefore the age of †*A. longipectoralis* was not utilized for dating any nodes within Aulopiformes in an effort to have the most accurate calibrations possible.

Ancestral Character State Reconstruction

Ancestral character states were reconstructed in Mesquite 2.7 (Maddison and Maddison, 2009). Reconstruction methods included likelihood and parsimony procedures. The Mk1 model (Lewis, 2001), was used to identify the state at each node that maximizes the probability of the states observed in the terminal taxa under

the likelihood framework. All character states were unordered for the parsimony analysis. Character states for eye morphologies and reproductive strategies were taken from Baldwin and Johnson (1996), and modified by Davis (2009). Character states were reconstructed on the total evidence Bayesian phylogeny presented by Davis (2009).

RESULTS

Divergence Time Estimation

The time tree based on Bayesian diverge time analysis of four nuclear (RAG 1, Zic1, Enc1, Plagl2) and one mitochondrial (COI) gene is shown in Figure 2.3. Information on lineage divergences including posterior probabilities, mean clade age, and 95% highest posterior densities can be found in Table 2.2. Highest posterior densities (HPD) include the interval of age ranges from which 95% of all sampled ages were found during the divergence analysis. The reconstructed phylogeny in BEAST was identical to the topology recovered by Mr. Bayes analysis of DNA alone in Davis (2009), with the exception of the constraints enforced and the movement of *Bathysaurus* as the sister group of the family Ipnopidae rather than Giganturidae. A relationship between *Bathysaurus* and *Gigantura* had low statistical support in Davis (2009), and it is unsurprising that its systematic position changed within the well-supported superfamily Ipnopoidea clade that includes these taxa.

Teleostei is recovered as monophyletic, with a mean clade age of 222 Ma (95% HPD 220–226), suggesting a Late Triassic origin. The divergence date for a lineage split between Ostarioclupeomorpha and Euteleostei is 193 Ma (95% HPD 171–212;

Early Jurassic–Late Triassic). Dates for Ostarioclupeomorpha include a mean age of 148 Ma in the Late Jurassic (95% HPD 146–151) and Euteleostei with a mean age of 165 Ma and a Middle Jurassic origin with a range of possible origin from the Early to Late Jurassic (95% HPD 150–186). The estimated age of Protacanthopterygii is 138 Ma (95% HPD 99–174), with a lineage split between Stomiiformes and Osmeriformes at 82 Ma (95% HPD 35–126). The mean date of divergence for Neoteleostei is 155 Ma (95% HPD 139–176), with the divergence of Eurypterygii at 148 Ma (95% HPD 133–166). The divergence date of Ctenosquamata is estimated at 124 Ma in the Early Cretaceous (95% HPD 101–147), with Myctophiformes diverging at 74 Ma in the Late Cretaceous (95% HPD 72–77) and Acanthomorpha diverging at 96 Ma, also in the Late Cretaceous (95% HPD 94–100).

The origin of the Aulopiformes clade is estimated at 140 Ma in the Early Cretaceous, with a possible range into the Late Jurassic (95% HPD 127–156). The suborder Aulopoidei has a divergence date of 133 Ma (95% HPD 115–152), with the origin of the common ancestor of Paraulopoidei and Alepisauroidei occurring at 135 Ma (95% HPD 123–149). Suborder Alepisauroidei has an estimated origin at 128 Ma (95% HPD 118–140) in the Early Cretaceous. The superfamily Ipnopoidea has an origin at 102 Ma (95% HPD 72–129), with a possible range from the Late to Early Cretaceous. The superfamily Chlorophthalmoidea has an estimated divergence date of 101 Ma (95% HPD 65–127). This is followed by a series of rapid divergences, including the lineage split between the superfamilies Notosudoidea and Alepisauroidea, at 120 Ma (95% HPD 112–130), and the origin of Alepidauroidea at

119 MY (95% HPD 111–129). Notosudoidea is found to have an origin at 67 MY (95% HPD 31–106).

Within Alepisauroidea, the family Scopelarchidae has a mean age of divergence of 88 Ma (95% HPD 50–119), while the family Evermannellidae has a younger estimated divergence of 56 Ma (95% HPD 27–88). The origin of the family Sudidae was estimated at 61 Ma (95% HPD 26-95), with the family Alepisauridae having an older estimated divergence date in the Early Cretaceous at 105 Ma (95% HPD 101–109). The crown aulopiform family Paralepididae has a mean origin of 95 Ma in the Late Cretacteous with its range extending into the Early Cretaceous (95% HPD 75–110).

Character Evolution: Eye Morphology

Ancestral character state reconstructions of aulopiform eye morphological specializations in the likelihood analysis are shown in figure 2.4. The same states identified as most likely are also found to be most parsimonious, with no equivocally parsimonious states found for any node. Of 42 nodes, 37 are found to have a state that was greater than 95% likely for that nodal reconstruction, with the other five nodes having a state greater than 90% likely (Fig 2.4 A, B, C, D, E). In the following account, “stem species” refers to the inferred ancestor and first member of a particular clade.

Round, laterally directed eyes (State 0) are assigned to the stem species of Aulopiformes, and are common throughout the order. Slightly flattened to elliptical eyes (State 1) arose twice—once in the stem species of Ipnopoidea, and again in the

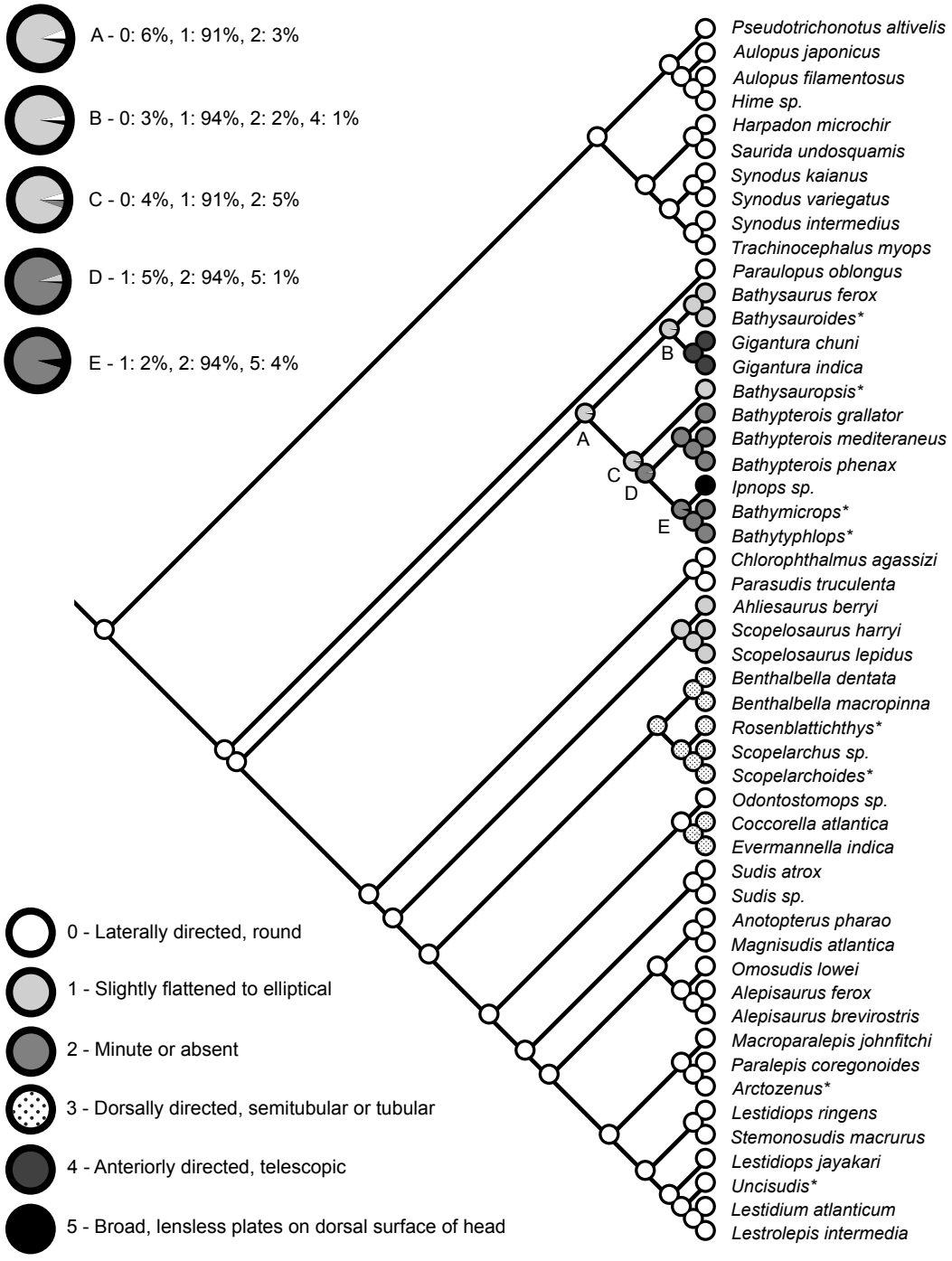

Fig. 2.4. Likelihood character evolution of aulopiform eye specializations. Tree used for ancestral character state reconstruction taken from Davis's (2009) Bayesian total evidence analysis, with * taxa including only morphological data. Circles are pie charts representing probabilites of character state likelihoods. There was no difference between parsimony and likelihood reconstructions. Character states adopted from Baldwin and Johnson (1996).

stem species of the Notosudoidea. A single evolutionary event is identified for the origin minute or absent eyes (State 2) in the stem species of Ipnopidae; within Ipnopidae, there is a single evolutionary event of the highly modified broad lensless plates (State 5) in *Ipnops*.

Anteriorly directed, tubular/telescopic eyes evolved once in the stem species of *Gigantura*. In contrast, dorsally directed tubular eyes have multiple evolutionary origins, once in the stem species of Scopelarchidae, and separately in the stem species of the *Coccorella + Evermannella* clade within Evermannellidae.

Character Evolution: Reproductive Strategies

Reconstruction of ancestral character states for reproductive strategies is shown in Figure 2.5. There are no differences between likelihood and parsimony reconstructions, and no equivocal states are identified with parsimony. All nodes showed a likelihood probability for their respective nodes greater than 99% for the reconstructed state.

The evolution of separate sexes (State 0) is reconstructed as the reproductive strategy for the stem species of Aulopiformes, and is the method of reproduction found in Aulopoidei and Paraulopoidei. A single evolutionary event of synchronous hermaphroditism occurs in the stem species of Alepisauroidei, permeating all members of this clade.

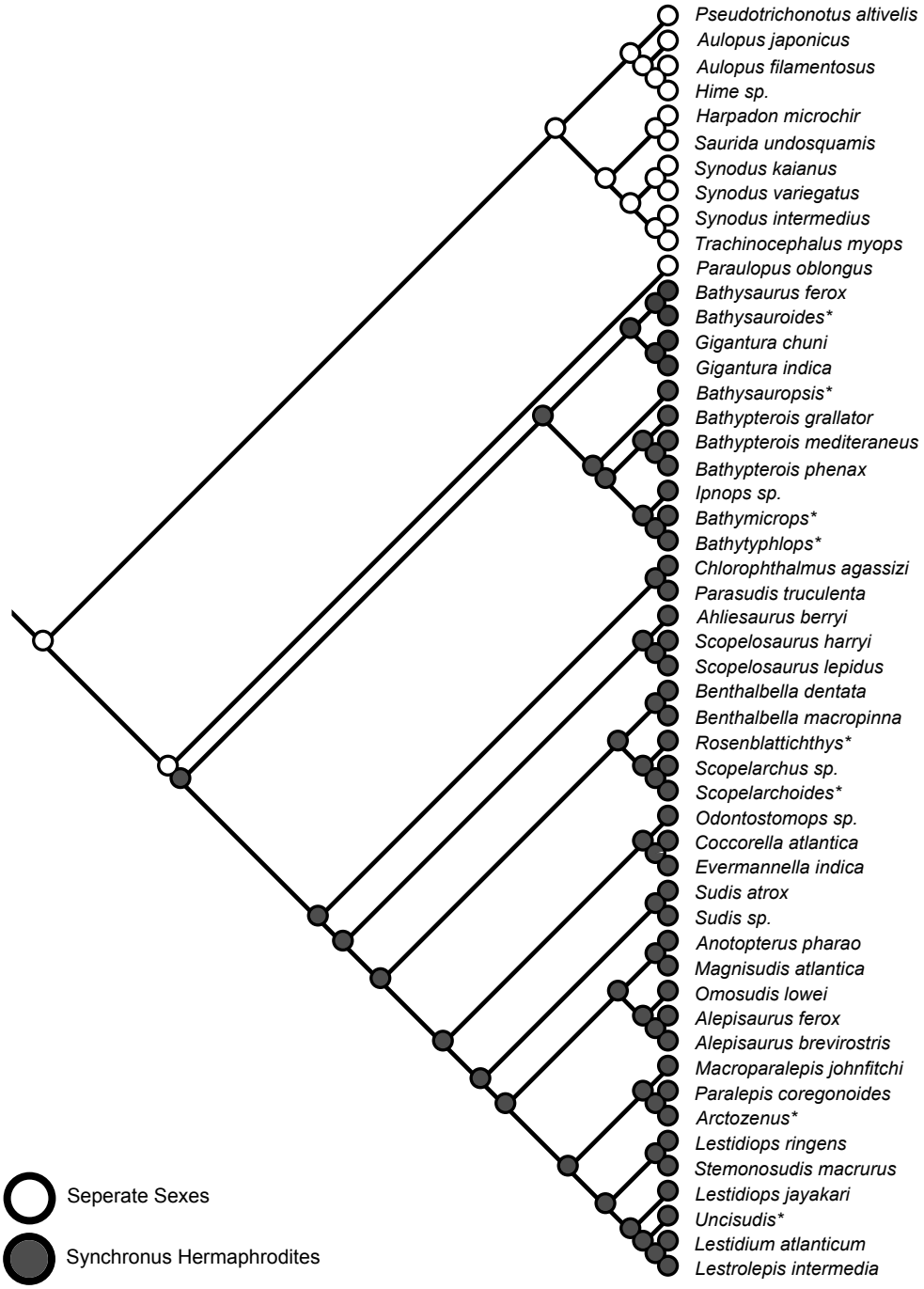

Fig. 2.5. Likelihood character evolution of aulopiform reproductive strategies. Tree used for ancestral character state reconstruction taken from Davis's (2009) Bayesian total evidence analysis, with * taxa including only morphological data. Circles are pie charts representing probabilites of character state likelihoods. There was no difference between parsimony and likelihood reconstructions. Character states adopted from Baldwin and Johnson (1996).

DISCUSSION

Origin of the Aulopiformes

Fielitz (2004) hypothesized that the common ancestor of aulopiforms must have arisen prior to the Late Cretaceous because most aulopiform fossil taxa are derived forms found in Late Cretaceous deposits. This hypothesis is supported by the divergence times recovered (Fig 2.3, 2.6; Node 16), in which the common ancestor of Aulopiformes is estimated to have an origin in the Early Cretaceous (140 Ma), possibly even the Late Jurassic. Currently, there are no fossils known from this time range, with the oldest complete fossil aulopiform †*Atolvorator longipectoralis* having been found in deposits from the Barremian of the Early Cretaceous (Fig 2.6) at 125 Ma (Gallo and Coelho, 2008). While the systematic position of †*A. longipectoralis* is unknown, Gallo and Coelho (2008) suggested that the taxon shared some morphological similarities with members if Alepisauroidea. This hypothesis was also supported by the divergence time estimation, as the age of †*A. longipectoralis* falls within the range of possible divergence dates for the origin of Alepisauroidea (95% HPD 111–129). However, a full systematic study is necessary to elucidate further the relationships of †*A. longipectoralis* to the remaining extant and extinct aulopiform taxa.

Divergence of Aulopiform Lineages

The roots of all major aulopiform lineages were estimated to have arisen within a span of about 30 Ma in the Early Cretaceous (Fig 2.6). Divergence time estimations place the origin of Aulopoidei into the Early Cretaceous (133 Ma), with a possible

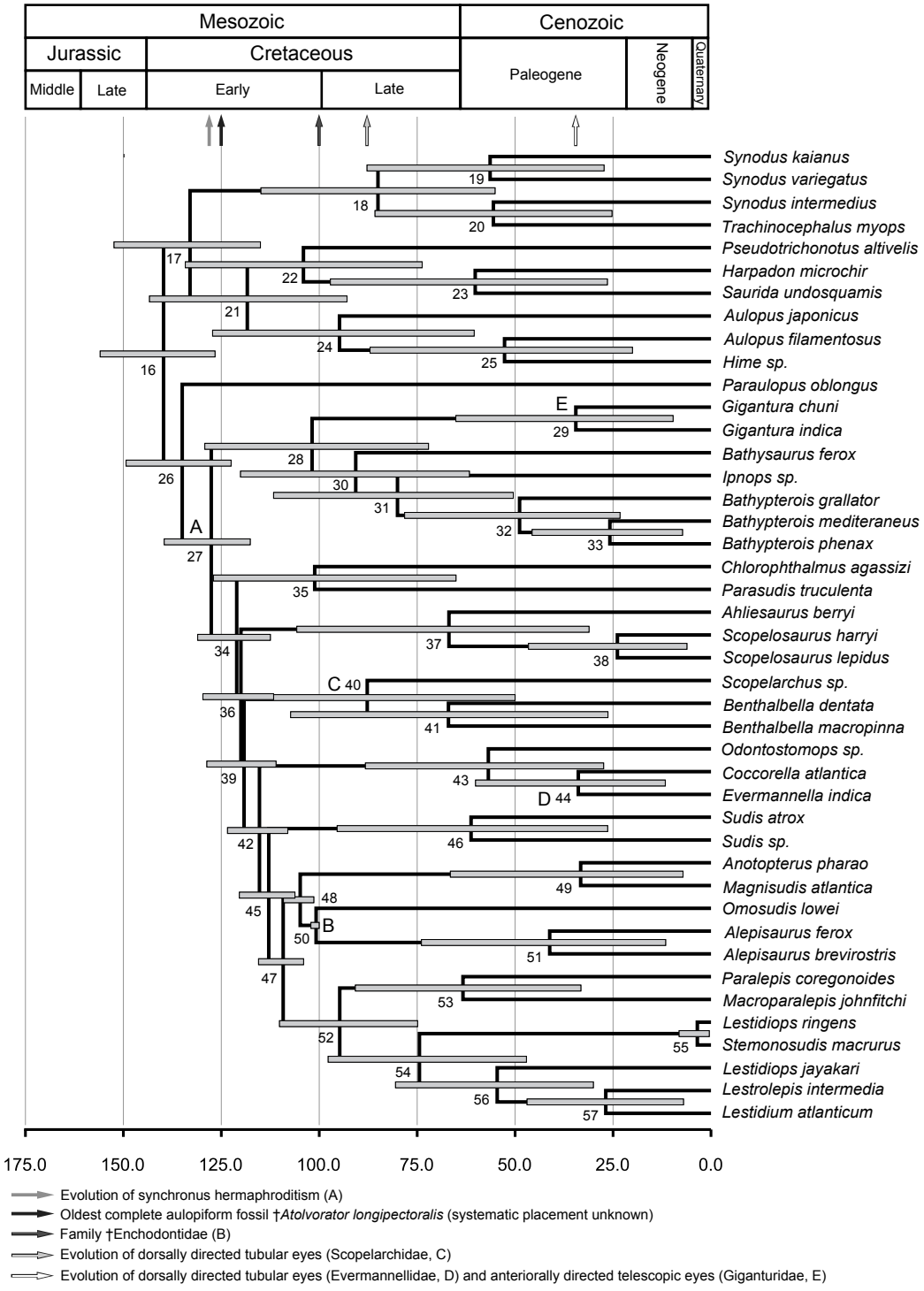

Fig. 2.6. Aulopiform divergence times. Bars denote 95% HPD. Numbers at nodes refer to clades in Table 2, which includes information on mean clade age, 95% HPD, and posterior probabilities. Scale is in millions of years.

origin in the Late Jurassic (Fig 2.6; Node 17). Aulopoid fishes consist predominantly of coral-reef and continental, shelf-inhabiting benthic fishes, including the lizardfishes (e.g., *Synodus*, *Saurida*) and the flagfin fishes (*Aulopus*). During the Late Jurassic and Early Cretaceous there was tremendous coral reef diversity (Vernon, 1995), and it is likely that the common ancestor of Aulopoidei inhabited coral-reef or continental-shelf environments. The oldest fossil taxon attributed to Aulopoidei, †*Nematonotus* spp., was placed in the family Aulopidae by Rosen without a systematic analysis (1973). Fossil specimens of †*Nematonotus* spp. are known from the Campanian of the Late Cretaceous (96 Ma), which is near the mean age Aulopidae estimated by divergence data at 95 Ma (Fig 2.6), and falls within the range of possible origin dates (95% HPD 60–127).

There are no known fossil representatives of the suborder Paraulopoidei, although divergence time estimations suggest that the lineage dates to at least the Early Cretaceous, and potentially the Late Jurassic (Fig 2.6). Paraulopoidei includes a single genus *Paraulopus,* a benthic group found on the continental shelf in the Indo-Pacific (Sato and Nakabo, 2002).

Most fossil aulopiforms have been attributed to Alepisauroidei within the Alepisauroidea. Within the superfamily Ipnopoidea, there are no known fossil representatives. Taxa within Ipnopoidea include predominantly benthic-oriented deep-sea fishes, with the exception of the genus *Gigantura* which is bathypelagic. Divergence time estimations recover an Ipnopoidea origin near the end of the Early Cretaceous, with possible ranges extending into the Late Cretaceous (Fig 2.6). The

family Giganturidae (*Gigantura*) is estimated to have a date of divergence in the Paleogene of the Cenozoic, with a possible origin in the Neogene. *Gigantura* includes highly specialized deep-sea aulopiform fishes that were a systematic and taxonomic mystery for centuries (e.g., Regan, 1911; Walters, 1961), before being recognized as aulopiforms by Rosen (1973) and Patterson and Johnson (1995). The origin of Ipnopidae is recovered in the middle of the Late Cretaceous (Fig 2.6; node 31), but with a broad possible range extending from the Early Cretaceous to the Paleogene. Ipnopids are composed of benthic deep-sea fishes, including the bizarre tripodfishes and the highly specialized *Ipnops*.

The superfamily Chlorophthalmoidea includes one known extinct aulopiform genus, †*Acrognathus*, which is known from deposits of 96 Ma and associated with the family Chlorophthalmidae. †*Acrognathus* is recognized as a chlorophthalmid (Patterson, 1993), although there has been no systematic analysis that has placed †*Acrognathus* within the family. Chlorophthalmids have an estimated origin of 101 Ma, with a possible range from 65–127 Ma, which corroborates with †*Acrognathus* position in the fossil record. The superfamily Notosudidae, which consists of bathy- and mesopelagic waryfishes, is hypothesized to have originated toward the end of the Late Cretaceous with a broad possible range from the Early Cretaceous to the Paleogene. The oldest fossil representative of the family, †*Scopelosaurus brevirostris*, is known from the Bartonian of the Eocene at 42 MY (Patterson, 1993).

The superfamily Alepisauroidea, includes five extant families—Scopelarchidae, Evermannellidae, Sudidae, Alepisauridae, and Paralepididae. Scopelarchids include

bathy-mesopelagic predatory fishes, with the oldest fossil representative †*Scopelarchus nolfi* known from the Chattian of the Paleogene (23–30 Ma, Patterson, 1993). The date of divergence for the scopelarchid lineage is estimated to be in the Late Cretaceous, with a broad range extending from the Early Cretaceous to the Paleogene (Fig 2.6: Node 40, Table 2.2). Evermannellidae (sabertooth fishes), which also includes bathy-to mesopelagic predatory fishes, does not have any fossil representatives. The origin of the evermannellid lineage is estimated in the Ypresian of the Paleogene, with a range extending into the Late Cretaceous (Fig 2.6: Node 43, Table 2.2).

Sudidae has an estimated origin in the Danian of the Paleogene, with a range that extends into the Late Cretaceous. Currently, Sudidae has no fossil record. Alepisauridae include meso- to bathypelagic predators and a rich fossil record. In a systematic study of extant and extinct taxa, Fielitz (2004) recovered the families †Cimolichthyidae + †Enchodontidae as the sister group to his Alepisauridae (*Omosudis* + *Alepisaurus*) in his superfamily Alepisauroidea (Alepisauridae *sensu* Davis, 2009). As discussed previously, this information was used to date the minimum age of an *Alepisaurus* + *Omosudis* clade at 100 Ma (Fig 2.3, 6: Node 50, Table 2.2). The estimated divergence date for the Alepisauridae is in the Early Cretaceous. The oldest fossil attributed to Paralepididae is †*Lestidiops ypresiensis* from the Ypresian of the Paleogene (Patterson, 1993). Paralepididae has an estimated origin in the Late Cretaceous, with a range extending into the Early Cretaceous.

There are also a number of extinct aulopiform families that are presently regarded as *incertae sedis*, including †Ichthyotringidae, †Dercetidae, and †Nardorexidae. All three have taxa that are known from the Late Cretaceous, with †Nardorexidae and †Deretidae found in Campanian-Maastrichtian deposits (e.g., Taverne 2004, 2005), and †Ichthyotringidae dating to the Albian-Cenomanian (Fielitz and González Rodríguez, 2008). Taxa in these families have been hypothesized to be related to extant taxa within Alepisauroidea, although none has been examined in a systematic study that includes both extant and extinct taxa, so phylogenetic position is unclear (e.g., Chalifa, 1989).

Evolution and Timing of Deep-sea Eye Adaptations

The evolution of laterally directed round eyes (Fig 2.2 A) seems to have been present in the stem species of aulopiforms and permeates the majority of the clades (Fig 2.4; State 0). The remaining eye morphologies all evolved in taxa inhabiting the deep-sea in meso- to bathypelagic habitats. The superfamily Ipnopoidea, in particular represents a "hotspot" for eye evolution within the aulopiforms, with ipnopoids possessing four of the five deep-sea eye adaptations represented in this study.

Slightly flattened to elliptical eyes (Fig 2.2 B) has evolved multiple times, once in the stem species of the superfamily Ipnopoidea in the Early Cretaceous, and again in the stem species of the superfamily Notosudoidea in the Late Cretaceous. The phylogenic analysis indicates that, with this particular morphology in the two clades is a result of convergent evolution (Fig 2.4, 2.6; State 1). A reduction in eyes (Fig 2.2 C) occurs in the stem species of the family Ipnopidae during the Late Cretaceous (Fig

2.4, 2.6; State 2), with the further evolution to the flattened, upward directing cephalic organ (Fig 2.2 F) isolated to the genus *Ipnops* following the reduction in eyes, which is the most likely trait observed in the stem species of a clade *Ipnops* + *Bathymicrops* + *Bathytyphlops* (Fig 2.4; State 5). It is difficult to ascertain the timing of the evolutionary appearance of this peculiar feature without molecular data for *Bathytyphlops* and *Bathymicrops*, however, it would most likely trace back to the Late Cretaceous or Paleogene (Fig 2.6).

Tubular eyes has evolved many times in deep-sea aulopiforms. Dorsally directed tubular eyes (Fig 2.2 D) has evolved independently in two lineages, one each within the families Scopelarchidae and Evermannellidae, both of which include deep-sea vertically migrating predators found in the meso- to bathypelagic zone (Fig 2.4; State 3). Baldwin and Johnson (1996) recovered dorsally directed tubular eyes as a synapomorphy of a Scopelarchidae + Evermannellidae Clade, however, this study suggests that this trait has independently evolved within these families. Tubular eyes are a common eye specialization among members of teleost lineages inhabiting the deep sea, and convergence of this trait is likely in these two lineages as first suggested by R. K. Johnson (1982). Dorsally directed tubular eyes probably arose first in the stem species of Scopelarchidae in the Late Cretaceous, with the trait common among species in this clade (Fig 2.4; State 3).

Within Evermannellidae, tubular eyes most likely evolved once in the stem species of the *Evermannella* + *Coccorella* Clade (Fig 2.4, 2.6; State 3). The genus *Odontostomops* has lateral, round eyes typical of other alepisaurids, and R. K.

Johnson (1982) hypothesized that *Odontostomops* was the sister group to an *Evermannella* + *Coccorella* Clade, this relationship is corroborated in this study. Baldwin and Johnson (1996) recovered *Coccorella* as the basal evermannellid, and suggested that the lack of tubular eyes was a reversal in *Odontostomops,* this reversal is not supported by this work. Tubular eyes evolved in the Paleogene in evermannellids, whereas they evolved in the Late Cretaceous in scopelarchids. The results of this study indicate that the dorsally tubular eyes of scopelarchids and evermannellids are not homologous structures, and are, in fact, the result of convergent evolution.

Anteriorly directed tubular/telescopic eyes (Fig 2.2 E) seem to have evolved once within deep-sea aulopiforms in the stem species of Giganturidae, within the superfamily Ipnopoidea (Fig 2.4, 6; State 4). This eye specialization is estimated to have evolved in the Paleogene. *Gigantura* is the only pelagic member of Ipnopoidea, and is not known to migrate vertically. Among aulopiform lineages, anterior or dorsally directed tubular eyes have only evolved in deep-sea fishes with pelagic lifestyles, and dorsally directed tubular eyes has evolved in predatory taxa that are predominantly vertically migratory.

Evolution and Timing of Synchronous Hermaphroditism

The stem species of aulopiforms most likely had separate sexes, with this trait found in the stem lineages of the suborders Aulopoidei and Paraulopoidei (Fig 2.5, 2.6). The evolution of synchronous hermaphroditism is hypothesized to have evolved in the stem species of the Alepisauroidei, probably during the Early Cretaceous,

between the Berriasian and the Barremian stages. This estimate suggests the oldest known date and lineage for the evolution of simultaneous hermaphroditism among vertebrates. Other simultaneous hermaphroditic teleost lineages are younger and are generally known from the Paleogene (Patterson, 1993). Additional synchronous hermaphroditic teleost lineages include a few species of muraenid eels (e.g., *Siderea grisea*), serranid sea basses (e.g., *Serranus fasciatus*), and killifishes (*Kryptolebias marmoratus*) (Mank et al., 2006). Approximately two thirds of aulopiform fishes (~158 species) are simultaneous hermaphrodites, making aulopiforms the largest vertebrate clade with this reproductive strategy. Determining whether this feature represents a key innovation for aulopiform speciation in the deep sea is beyond the scope of this study and further morphological work is needed to explore the specifics of the reproductive systems across aulopiforms in order to better understand this rare and unique reproductive strategy among vertebrates.

CONCLUSIONS

The stem species of the aulopiforms arose during the Early Cretaceous, and possibly Late Jurassic in a marine environment that was most likely in an inshore contintental shelf habitat, with separate sexes, and laterally directed, round eyes. The major aulopiform lineages originated during the Early Cretaceous, with most extant families appearing by the Late Cretaceous to the Eocene.

There have been multiple independent evolutionary events of flattened elliptical eyes in the stem species of the superfamilies Ipnopoidea and Notosudoidea. Tubular eyes have arisen independently at different times in three deep-sea pelagic predatory

aulopiform lineages. Dorsally directed tubular eyes have evolved independently, once in the stem species of Scopelarchidae during the Late Cretaceous, and once within Evermannellidae in the stem species of the *Evermannella* + *Omosudis* clade during the Paleogene. Anteriorly directed tubular eyes evolved a single time in Giganturidae during the Paleogene. Eyes are reduced in the stem species of Ipnopidae during the Late Cretaceous, with the highly specialized, upward-directed cephalic organ evolving in *Ipnops*.

Simultaneous hermaphroditism evolved a single time in the stemspecies of the superfamily Alepisauroidei, the clade of deep-sea aulopiforms. This feature most likely arose in the Early Cretaceous, and is the oldest known simultaneous hermaphroditic strategy among vertebrates. The superfamily Alepisauroidei is the largest vertebrate clade possessing this reproductive strategy with approximately 158 species.

CHAPTER 3

EXPLORING THE PREPONDERANCE OF SIMULTANEOUS HERMAPHRODITES IN LIZARDFISHES (EUTELEOSTEI: AULOPIFORMES) WITH COMMENTS ON THE POWER AND LIMITATIONS OF THE BiSSE METHOD

INTRODUCTION

Lizardfishes (Cyclosquamata: Aulopiformes) are unique among teleost fishes in that two thirds of their taxonomic diversity (ca. 147 species) is represented by simultaneous hermaphrodites that occupy a deep-sea habitat. Simultaneous hermaphrodites can produce functional male and female gametes at the same time, as opposed to sex-switching hermaphroditic strategies, such as protoandry, in which male gamete production switches to female gamete production, and protogyny, in which female gamete production switches to male game production. Aulopiform fishes comprise the only lineage in which simultaneous hermaphroditism evolved in the deep sea and in which the strategy was not evolutionarily short-lived. Three other teleost lineages have simultaneous hermaphroditic taxa; two are composed of coral reef predators (Muraenidae: Elopiformes; Serranidae: Perciformes) and the third is a single neotropical freshwater species *Kryptolebias marmoratus* (Rivulidae:

Cyprinodontiformes) (Mank et al. 2006). In each case, the richness of simultaneous hermaphroditic taxa accounts for less than 1% of the diversity of each lineage.

Lizardfishes have the highest species diversity of any vertebrate clade with this reproductive strategy. Mead et al. (1964) hypothesized that the evolution of simultaneous hermaphroditism in the deep-sea lizardfishes was related to low population densities and possibly lower mate success, thereby making the ability to produce both gametes evolutionarily advantageous. Davis' (Chapter 2, 2009) study on the evolution of deep-sea character adaptations in lizardfishes suggested that the stem aulopiform species most likely had separate sexes, and that simultaneous hermaphroditism evolved once in the stem Alepisauroidei species, probably during the Early Cretaceous (Chapter 2, Fig 2.5, 2.6). This study explores why such a high number of lizardfish taxa possess this reproductive strategy. The BiSSE (binary-state speciation and extinction) likelihood model (Maddison et al., 2007) is ideal for addressing this question, because it is the only method that fully integrates and simultaneously estimates rates of speciation, extinction, and character state change.

A number of possibilities may explain the disparity in aulopiform clade size between taxa with separate sexes and simultaneous hermaphroditism. This work addresses hypotheses that may explain this disparity, including the following. (1) Speciation rates are higher in aulopiform taxa with simultaneous hermaphroditism. (2) Extinction rates are higher in taxa with separate sexes. (3) Rates of character change are asymmetrical, with the rate of transition from simultaneous hermaphroditism to separate sexes being less than from separate sexes to

simultaneous hermaphroditism. Additionally, little is known about how the BiSSE method performs when estimating parameters under extreme rate asymmetries or the ways in which power (probability of rejecting a false null hypothesis) is affected by tree size and rate asymmetries. Thus, a primary goal of this study is to explore the power and parameter estimation of the BiSSE method. To investigate power levels and parameter estimations, BiSSE likelihoods and parameter values are compared from a variety of asymmetrical and corresponding symmetrical simulations under different tree sizes and rate variations.

MATERIALS AND METHODS

Parameter Estimation and Hypothesis Testing of Lizardfish Data

The BiSSE likelihood calculation and parameter estimations were done in the Diverse package of Mesquite (2.7). The temporal mean clade age tree of lizardfish relationships from Davis' divergence time study (Chapter 2, Fig 2.6) was used as a phylogenetic framework for rate estimation of speciation (λ), extinction (μ), and character state change (q). BiSSE estimates six parameters: speciation rate under state 0 (λ_0); speciation rate under state 1 (λ_1); extinction rate under state 0 (μ_0); extinction rate under state 1 (μ_1); rate of character change from state 0 to 1 (q_{01}); and rate of character change from state 1 to 0 (q_{10}). Binary character information for simultaneous hermaphroditism was taken from the character coding of Baldwin and Johnson (1996) and Sato and Nakabo (2002) (Chapter 2, Fig 2.5).

Data were first collected under an unconstrained model in which all six parameters were freely estimated and the BiSSE likelihood was calculated. The

BiSSE likelihood was then estimated for each of three constrained models ($\lambda_0 = \lambda_1, \mu_0 = \mu_1, q_{01} = q_{10}$) representing a null hypotheses that rates are symmetrical. The difference in likelihood calculations between the unconstrained six parameter model and the constrained five parameter model can then be utilized as a metric for accepting or rejecting the null hypothesis that parameter values are symmetrical.

In order to explore what Ln likelihood difference represented a significant value, 500 trees and characters were simulated under each null model. First, the parameter values were estimated from the lizardfish data under the null model (e.g., $\lambda_0 = \lambda_1$). These values were then used to simulate trees and characters simultaneously in Mesquite. For each tree and corresponding character data matrix, the BiSSE likelihood was calculated under the unconstrained and appropriate constrained model, and the likelihood difference was recorded. The result is a distribution of likelihood differences estimated under a symmetrical null hypothesis that gives a possible range of values expected if the null is true, allowing for the calculation of a 5% cutoff value that can be used to test for significance. To explore whether the number of taxa had an influence on the power of the lizardfish data analysis, simulations of 500 trees and characters were done for groups of 43, 100, 300, and 500 taxa for each null hypothesis and an alternate hypothesis using the parameter values from the estimated unconstrained data (Table 3.1). For the lizardfish data, simulations were constrained to have a root starting state of 0, as this characteristic (separate sexes) has been inferred to be the ancestral character state of the inferred stem ancestor of aulopiform fishes with high likelihood (Davis, Chapter 2).

TABLE 3.1: Simulations of varying tree size using estimated parameters from lizardfish data. The 5% cutoff represents a significant BiSSE likelihood difference recovered from the null hypothesis simulations where the corresponding rate was constrained to be equal. Power was calculated as the percentage of BiSSE likelihood difference values for the asymmetrical simulations above this critical value. Power is plotted in Fig 3.1.

Rates	5% Cutoff	Power	Percent State 0
Speciation ($\lambda_0 = 0.133$, $\lambda_1 = 0.114$)			
500 taxa	6.509	3.5%	82.55%
300 taxa	8.301	4.0%	83.98%
100 taxa	3.574	6.7%	86.402%
43 taxa	3.178	4.0%	88.30%
Extinction ($\mu_0 = 0.0018$, $\mu_1 = 0.000064$)			
500 taxa	2.734	5.8%	82.77%
300 taxa	2.513	5.6%	84.36%
100 taxa	4.413	4.8%	86.32%
43 taxa	2.760	5.3%	88.85%
Character change ($q_{01} = 0.0055$, $q_{10} = 0.00001$)			
500 taxa	2.525	25.0%	82.77%
300 taxa	2.577	11.6%	83.25%
100 taxa	2.028	4.3%	85.65%
43 taxa	1.818	5.0%	87.91%

Power of BiSSE Method

Maddison et al. (2007) suggested that the probability of rejecting a false null hypothesis (power) may vary with the number of species in an analysis, and with the degree of rate difference among parameters. To explore the power of the BiSSE method, trees were simulated under a variety of tree sizes and parameter combinations that introduced an asymmetry in one set of rates, and a corresponding null simulation where all rates are symmetrical. Each parameter combination was tested under tree sizes of 50, 100, 300, and 500 taxa, respectively, in which the probability or the root state was stationary (Felsenstein, 1981) unless otherwise noted. Power was determined as the percentage of likelihood difference scores in the asymmetrical simulation that was above the 5% cutoff value in the corresponding null hypothesis simulation, as seen in Tables 3.2, 3.3, and 3.4. Power levels of parameter asymmetries with a large magnitude of difference but smaller rate values were also explored for tree sizes of 500 taxa. To explore the potential impact constraining the root state may have on the power of the analysis, these low rate values were simulated once with stationary root states, and again with the root state constrained to 0. Additionally for all simulations the average percentage of taxa with each character state was calculated, and can be seen in all tables.

Asymmetries in Speciation—For rates of speciation, the null hypothesis of rate symmetry ($\lambda_0 = 0.1$, $\lambda_1 = 0.1$) and alternative asymmetry hypotheses were simulated for the following parameter combinations where speciation rates are higher under state 1; one and a quarter times ($\lambda_0 = 0.1$, $\lambda_1 = 0.125$), one and a half times ($\lambda_0 = 0.1$, λ_1

TABLE 3.2: Power of asymmetrical speciation rate simulations. Remaining parameters were symmetrical for each simulation (q_{01} = 0.01, q_{10} = 0.01, μ_0 = 0.03, μ_1 = 0.03). Power is plotted in Fig 3.2. The percent of terminal taxa with State 0 is the average value of 500 simulations.

Rate of Speciation	5% Cutoff	Power	Percent State 0
1.25× (λ_0 = 0.1, λ_1= 0.125)			
500 taxa	1.875	20.88%	29.23%
300 taxa	2.107	11.20%	28.74%
100 taxa	2.818	8.60%	30.86%
50 taxa	4.575	3.21%	28.39%
1.5× (λ_0 = 0.1, λ_1= 0.15)			
500 taxa	1.875	40.72%	19.33%
300 taxa	2.107	25.85%	18.85%
100 taxa	2.818	14.60%	10.47%
50 taxa	4.575	3.20%	19.26%
2× (λ_0 = 0.1, λ_1= 0.2)			
500 taxa	1.875	57.00%	9.90%
300 taxa	2.107	42.40%	10.79%
100 taxa	2.818	12.60%	11.60%
50 taxa	4.575	2.60%	11.24%
3× (λ_0 = 0.1, λ_1= 0.3)			
500 taxa	1.875	72.40%	4.94%
300 taxa	2.107	47.20%	4.64%
100 taxa	2.818	12.00%	5.02%
50 taxa	4.575	1.80%	4.85%
4× (λ_0 = 0.1, λ_1= 0.4)			
500 taxa	1.875	69.00%	3.19%
300 taxa	2.107	49.00%	3.38%
100 taxa	2.818	9.80%	3.36%
50 taxa	4.575	1.80%	4.72%
5× (λ_0 = 0.1, λ_1= 0.5)			
500 taxa	1.875	71.00%	2.50%
300 taxa	2.107	42.80%	2.55%
100 taxa	2.818	10.20%	2.84%
50 taxa	4.575	1.80%	3.04%
10× (λ_0 = 0.1, λ_1= 1.0)			
500 taxa	1.875	53.60%	1.13%
300 taxa	2.107	24.40%	3.05%
100 taxa	2.818	2.60%	1.28%
50 taxa	4.575	1.40%	1.07%
20× (λ_0 = 0.1, λ_1= 2.0)			
500 taxa	1.875	29.80%	0.51%
300 taxa	2.107	8.15%	0.54%
100 taxa	2.818	1.20%	0.51%
50 taxa	4.575	1.00%	0.86%

TABLE 3.3: Power of simulations for character rate change. Remaining parameters were symmetrical for each simulation ($\mu_0 = 0.03$, $\mu_1 = 0.03$, $\lambda_0 = 0.1$, $\lambda_1 = 0.1$). Power is plotted in Fig 3.3. The percent of terminal taxa with State 0 is the average value of 500 simulations.

Rate of Character Change	5% Cutoff	Power	Percent State 0
2× ($q_{01} = 0.01$, $q_{10} = 0.005$)			
500 taxa	2.149	19.19%	33.96%
300 taxa	2.048	13.40%	31.97%
100 taxa	2.379	5.80%	32.65%
50 taxa	5.661	4.00%	31.63%
3× ($q_{01} = 0.015$, $q_{10} = 0.005$)			
500 taxa	2.149	39.67%	24.01%
300 taxa	2.048	28.08%	25.53%
100 taxa	2.379	7.40%	26.60%
50 taxa	5.661	5.00%	26.10%
4× ($q_{01} = 0.02$, $q_{10} = 0.005$)			
500 taxa	2.149	53.63%	20.57%
300 taxa	2.048	33.46%	20.17%
100 taxa	2.379	9.80%	20.43%
50 taxa	5.661	3.80%	19.11%
5× ($q_{01} = 0.025$, $q_{10} = 0.005$)			
500 taxa	2.149	62.47%	16.69%
300 taxa	2.048	43.72%	16.78%
100 taxa	2.379	11.20%	14.78%
50 taxa	5.661	5.21%	16.45%
10× ($q_{01} = 0.05$, $q_{10} = 0.005$)			
500 taxa	2.149	63.36%	9.14%
300 taxa	2.048	42.28%	9.46%
100 taxa	2.379	13.4%	8.81%
50 taxa	5.661	5.00%	8.96%
20× ($q_{01} = 0.1$, $q_{10} = 0.005$)			
500 taxa	2.149	38.91%	4.69%
300 taxa	2.048	26.02%	4.75%
100 taxa	2.379	8.6%	4.60%
50 taxa	5.661	3.00%	4.79%
40× ($q_{01} = 0.2$, $q_{10} = 0.005$)			
500 taxa	2.149	15.04%	2.39%
300 taxa	2.048	11.71%	2.41%
100 taxa	2.379	4.42%	2.32%
50 taxa	5.661	2.60%	2.42%

TABLE 3.4: Power of asymmetrical extinction rate simulations. Remaining parameters were symmetrical for each simulation (q_{01} = 0.01, q_{10} = 0.01, λ_0 = 0.1, λ_1 = 0.1). Power is plotted in Fig 3.4. The percent of terminal taxa with State 0 is the average value of 500 simulations.

Rate of Extinction	5% Cutoff	Power	Percent State 0
2× (μ_0 = 0.06, μ_1 = 0.03)			
500 taxa	2.128	11.47%	23.85%
300 taxa	2.443	7.22%	24.22%
100 taxa	2.869	4.60%	23.99%
50 taxa	5.567	4.00%	24.33%
3× (μ_0 = 0.09, μ_1 = 0.03)			
500 taxa	2.128	20.00%	13.21%
300 taxa	2.443	10.02%	13.16%
100 taxa	2.869	5.00%	13.01%
50 taxa	5.567	4.00%	12.69%
4× (μ_0 = 0.12, μ_1 = 0.03)			
500 taxa	2.128	20.78%	9.29%
300 taxa	2.443	6.70%	9.15%
100 taxa	2.869	5.62%	9.05%
50 taxa	5.567	1.20%	8.91%
5× (μ_0 = 0.15, μ_1 = 0.03)			
500 taxa	2.128	15.87	7.12%
300 taxa	2.443	4.47%	7.17%
100 taxa	2.869	2.60%	7.00%
50 taxa	5.567	1.40%	7.05%
10× (μ_0 = 0.3, μ_1 = 0.03)			
500 taxa	2.128	3.71%	3.40%
300 taxa	2.443	2.5%	3.37%
100 taxa	2.869	1.40%	3.41%
50 taxa	5.567	0.20%	3.04%

= 0.15), two times ($\lambda_0 = 0.1$, $\lambda_1 = 0.2$), three times ($\lambda_0 = 0.1$, $\lambda_1 = 0.3$), four times ($\lambda_0 = 0.1$, $\lambda_1 = 0.4$), five times ($\lambda_0 = 0.1$, $\lambda_1 = 0.5$), ten times ($\lambda_0 = 0.1$, $\lambda_1 = 1.0$), and twenty times ($\lambda_0 = 0.1$, $\lambda_1 = 2.0$) (Table 3.2). For each of the speciation rate asymmetry simulations, the remaining four parameters were symmetrical ($\mu_0 = \mu_1 = 0.03$, $q_{01} = q_{10} = 0.01$).

Asymmetries in Character Rate Change—Transition rates were simulated under a null hypothesis ($q_{01} = 0.005$, $q_{10} = 0.005$) and the following parameter combinations where the transition from q_{01} is greater than q_{10}; two times ($q_{01} = 0.01$, $q_{10} = 0.005$), three times ($q_{01} = 0.015$, $q_{10} = 0.005$), four times ($q_{01} = 0.02$, $q_{10} = 0.005$), five times ($q_{01} = 0.025$, $q_{10} = 0.005$), ten times ($q_{01} = 0.05$, $q_{10} = 0.005$), twenty times ($q_{01} = 0.1$, $q_{10} = 0.005$), and forty times ($q_{01} = 0.2$, $q_{10} = 0.005$) (Table 3.3). The remaining four parameters were symmetrical for each simulation ($\mu_0 = \mu_1 = 0.03$, $\lambda_0 = \lambda_1 = 0.1$). The 5% cutoff rate for the significance of the BiSSE likelihood difference was calculated for the null hypothesis ($q_{01} = 0.005$, $q_{10} = 0.005$, $\mu_0 = \mu_1 = 0.03$, $\lambda_0 = \lambda_1 = 0.1$) with the same procedure described above.

Asymmetries in Extinction—Rates were estimated for the following asymmetries where extinction is greater under state 0; two times ($\mu_0 = 0.06$, $\mu_1 = 0.03$), three times ($\mu_0 = 0.09$, $\mu_1 = 0.03$), four times ($\mu_0 = 0.12$, $\mu_1 = 0.03$), five times ($\mu_0 = 0.15$, $\mu_1 = 0.03$), and ten times ($\mu_0 = 0.3$, $\mu_1 = 0.03$). For each simulation, the remaining parameters were the same ($q_{01} = q_{10} = 0.01$, $\lambda_0 = \lambda_1 = 0.1$).

Low Rates with Stationary and Constrained Root State—Decreasing levels of speciation rates were simulated for the following combinations under stationary and

constrained (state 0) roots; 1/2 times ($\lambda_0 = 0.05$, $\lambda_1 = 0.1$), 1/4 times ($\lambda_0 = 0.025$, $\lambda_1 = 0.1$), 1/10 times ($\lambda_0 = 0.01$, $\lambda_1 = 0.1$), and 1/50 times ($\lambda_0 = 0.0025$, $\lambda_1 = 0.1$) (Table 3.5). The null hypothesis and remaining parameters had the same values as the previously described speciation simulations.

Character state asymmetries were simulated with a stationary root probability and an analogous simulation where the root was constrained to State 0 for the following parameter combinations of; 1/2 times ($q_{01} = 0.005$, $q_{10} = 0.0025$), 1/5 times ($q_{01} = 0.005$, $q_{10} = 0.0001$), 1/10 times, ($q_{01} = 0.005$, $q_{10} = 0.0005$), 1/100 times ($q_{01} = 0.005$, $q_{10} = 0.00005$), and 1/500 times ($q_{01} = 0.005$, $q_{10} = 0.00001$) (Table 3.6).

Asymmetrical rates of extinction with low values were simulated for the following parameter combinations; 1/2 times ($\mu_0 = 0.03$, $\mu_1 = 0.015$), 1/10 times ($\mu_0 = 0.03$, $\mu_1 = 0.003$), 1/50 times ($\mu_0 = 0.03$, $\mu_1 = 0.0006$), and 1/100 times ($\mu_0 = 0.03$, $\mu_1 = 0.0003$) (Table 3.7). The remaining parameter values and the null hypothesis were the same as the previously described extinction simulations.

Testing Rates Similar to Lizardfish Data with Multiple Asymmetries—An additional set of simulations explored conditions similar to the parameters estimated by the lizardfish data and investigated the effect of multiple parameter asymmetries on the power of testing hypotheses. For each analysis, a specific asymmetry was set (e.g., $\lambda_0 > \lambda_1$), and the power was first investigated with symmetrical rates in the additional parameters. This was followed by analyses in which an additional asymmetry was added in an increasing magnitude of difference, with analogous simulations conducted that included the same magnitude of difference but with rates

TABLE 3.5: Simulations with low values of speciation rate asymmetry with stationary and constrained root states.

Rate of Speciation	5% Cutoff	Power	Percent State 0
Root state stationary			
1/2× ($\lambda_0 = 0.05$, $\lambda_1 = 0.1$)			
500 taxa	1.875	70.47%	15.13%
1/4× ($\lambda_0 = 0.025$, $\lambda_1 = 0.1$)			
500 taxa	1.875	95.55%	10.46%
1/10× ($\lambda_0 = 0.01$, $\lambda_1 = 0.1$)			
500 taxa	1.875	100.00%	8.86%
1/50× ($\lambda_0 = 0.0025$, $\lambda_1 = 0.1$)			
500 taxa	1.875	100.00%	8.17%
Root state 0			
1/2× ($\lambda_0 = 0.05$, $\lambda_1 = 0.1$)			
500 taxa	1.851	82.51%	16.76%
1/4× ($\lambda_0 = 0.025$, $\lambda_1 = 0.1$)			
500 taxa	1.851	96.40%	10.60%
1/10× ($\lambda_0 = 0.01$, $\lambda_1 = 0.1$)			
500 taxa	1.851	99.56%	8.84%
1/50× ($\lambda_0 = 0.0025$, $\lambda_1 = 0.1$)			
500 taxa	1.851	100.00%	8.12%

TABLE 3.6: Simulations with low values of character change asymmetry with stationary and constrained root states.

Rate of Character Change	5% Cutoff	Power	Percent State 0
Root state stationary			
1/2× (q_{01} = 0.005, q_{10} = 0.0025)			
500 taxa	2.149	10.32%	33.36%
1/5× (q_{01} = 0.005, q_{10} = 0.001)			
500 taxa	2.149	18.29%	14.70%
1/10× (q_{01} = 0.005, q_{10} = 0.0005)			
500 taxa	2.149	36.07%	7.93%
1/100× (q_{01} = 0.005, q_{10} = 0.00005)			
500 taxa	2.149	5.55%	0.67%
1/500× (q_{01} = 0.005, q_{10} = 0.00001)			
500 taxa	2.149	5.22%	0.42%
Root state 0			
1/2× (q_{01} = 0.005, q_{10} = 0.0025)			
500 taxa	2.214	13.44%	71.13%
1/5× (q_{01} = 0.005, q_{10} = 0.001)			
500 taxa	2.214	33.61%	69.62%
1/10× (q_{01} = 0.005, q_{10} = 0.0005)			
500 taxa	2.214	45.21%	70.77%
1/100× (q_{01} = 0.005, q_{10} = 0.00005)			
500 taxa	2.214	58.00%	69.76%
1/500× (q_{01} = 0.005, q_{10} = 0.00001)			
500 taxa	2.214	59.91%	67.77%

TABLE 3.7: Simulations with low values of extinction rate asymmetry with stationary and constrained root states.

Rate of Extinction	5% Cutoff	Power	Percent State 0
Root state stationary			
1/2× ($\mu_0 = 0.03$, $\mu_1 = 0.015$)			
500 taxa	2.128	6.02%	36.53%
1/10× ($\mu_0 = 0.03$, $\mu_1 = 0.003$)			
500 taxa	2.128	6.61%	28.71%
1/50× ($\mu_0 = 0.03$, $\mu_1 = 0.0006$)			
500 taxa	2.128	6.80%	26.48%
1/100× ($\mu_0 = 0.03$, $\mu_1 = 0.0003$)			
500 taxa	2.128	6.21%	26.54%
Root state 0			
1/2× ($\mu_0 = 0.03$, $\mu_1 = 0.015$)			
500 taxa	2.051	2.02%	51.52%
1/10× ($\mu_0 = 0.03$, $\mu_1 = 0.003$)			
500 taxa	2.051	2.40%	44.36%
1/50× ($\mu_0 = 0.03$, $\mu_1 = 0.0006$)			
500 taxa	2.051	3.40%	43.42%
1/100× ($\mu_0 = 0.03$, $\mu_1 = 0.0003$)			
500 taxa	2.051	4.25%	42.46%

reversed (e.g., $\mu_0 = 0.03$, $\mu_1 = 0.015$, and $\mu_0 = 0.015$, $\mu_1 = 0.03$). These analyses were conducted with a tree size of 500 taxa and a root state constrained to State 0.

Speciation rates were fixed at $\lambda_0 = 0.125$ and $\lambda_1 = 0.1$. An additional asymmetry was added to the rate of character state change (Table 3.8) and then to the rate of extinction (Table 3.9). Rates of character state change were fixed at $q_{01} = 0.005$ and $q_{10} = 0.00001$, with an additional asymmetry introduced to either the rate of speciation (Table 3.10) or extinction (Table 3.11). Extinction rates were fixed at $\mu_0 = 0.03$ and $\mu_1 = 0.0006$, with an additional asymmetry added to rates of speciation (Table 3.12) and extinction (Table 3.13). While these specific parameters combinations were similar to values estimated under the lizardfish data, they provide a glimpse at the impact multiple asymmetries may have on the power of testing hypotheses of rate asymmetry.

Estimating Parameters in Asymmetrical Scenarios

Rate parameters for unconstrained and constrained models were tabulated in an effort to elucidate BiSSE's ability to estimate parameters under a variety of scenarios ranging from low, medium, and high rate asymmetry with tree sizes of 500 taxa. Parameters estimated under a constrained model were generally identical to those under the unconstrained model. Only the unconstrained results are discussed. Parameters were estimated from the same 500 trees and respective characters that were used to calculate the BiSSE likelihood difference in the following simulations: one and a quarter times speciation ($\lambda_0 = 0.1$, $\lambda_1 = 0.1.25$); five times speciation ($\lambda_0 = 0.1$, $\lambda_1 = 0.5$); twenty times speciation ($\lambda_0 = 0.1$, $\lambda_1 = 2.0$); one fiftieth time speciation

TABLE 3.8: Power for a speciation rate difference of 1.25× when a additional asymmetry is introduced to the rate of character change.

Rate of Speciation with Character Change Asymmetry	5% Cutoff	Power	Percent State 0
No additional Asymmetry			
($\lambda_0 = 0.125$, $\lambda_1 = 0.1$, $q_{01} = 0.005$, $q_{10} = 0.005$, $\mu_0 = 0.03$, $\mu_1 = 0.03$)	2.16	11.42%	86.28%
Root state 0 $q_{01} > q_{10}$			
q 1/2×			
($\lambda_0 = 0.125$, $\lambda_1 = 0.1$, $q_{01} = 0.005$, $q_{10} = 0.0025$, $\mu_0 = 0.03$, $\mu_1 = 0.03$)	2.47	7.81%	85.41%
q 1/10×			
($\lambda_0 = 0.125$, $\lambda_1 = 0.1$, $q_{01} = 0.005$, $q_{10} = 0.0005$, $\mu_0 = 0.03$, $\mu_1 = 0.03$)	3.08	5.80%	84.10%
q 1/500×			
($\lambda_0 = 0.125$, $\lambda_1 = 0.1$, $q_{01} = 0.005$, $q_{10} = 0.00001$, $\mu_0 = 0.03$, $\mu_1 = 0.03$)	3.30	4.00%	83.32%
Root state 0 $q_{01} < q_{10}$			
q 1/2×			
($\lambda_0 = 0.125$, $\lambda_1 = 0.1$, $q_{01} = 0.0025$, $q_{10} = 0.005$, $\mu_0 = 0.03$, $\mu_1 = 0.03$)	2.92	7.00%	92.65%
q 1/10×			
($\lambda_0 = 0.125$, $\lambda_1 = 0.1$, $q_{01} = 0.0005$, $q_{10} = 0.005$, $\mu_0 = 0.03$, $\mu_1 = 0.03$)	3.69	6.48%	98.35%
q 1/500×			
($\lambda_0 = 0.125$, $\lambda_1 = 0.1$, $q_{01} = 0.00001$, $q_{10} = 0.005$, $\mu_0 = 0.03$, $\mu_1 = 0.03$)	1.38	0.2%	99.96%

TABLE 3.9: Power for a speciation rate difference of 1.25× when a additional asymmetry is introduced to the rate of extinction.

Rate of Speciation with Extinction Asymmetry	5% Cutoff	Power	Percent State 0
No additional Asymmetry			
($\lambda_0 = 0.125$, $\lambda_1 = 0.1$, $q_{01} = 0.005$, $q_{10} = 0.005$, $\mu_0 = 0.03$, $\mu_1 = 0.03$)	2.16	11.42%	86.28%
Root state 0 $\mu_0 > \mu_1$			
μ 1/2×			
($\lambda_0 = 0.125$, $\lambda_1 = 0.1$, $q_{01} = 0.005$, $q_{10} = 0.005$, $\mu_0 = 0.03$, $\mu_1 = 0.015$)	2.08	3.41%	82.38%
μ 1/10×			
($\lambda_0 = 0.125$, $\lambda_1 = 0.1$, $q_{01} = 0.005$, $q_{10} = 0.005$, $\mu_0 = 0.03$, $\mu_1 = 0.003$)	2.83	4.40%	77.25%
μ 1/50×			
($\lambda_0 = 0.125$, $\lambda_1 = 0.1$, $q_{01} = 0.005$, $q_{10} = 0.005$, $\mu_0 = 0.03$, $\mu_1 = 0.0006$)	2.63	5.00%	75.89%
Root state 0 $\mu_0 < \mu_1$			
μ 1/2×			
($\lambda_0 = 0.125$, $\lambda_1 = 0.1$, $q_{01} = 0.005$, $q_{10} = 0.005$, $\mu_0 = 0.015$, $\mu_1 = 0.03$)	2.15	12.20%	89.53%
μ 1/10×			
($\lambda_0 = 0.125$, $\lambda_1 = 0.1$, $q_{01} = 0.005$, $q_{10} = 0.005$, $\mu_0 = 0.003$, $\mu_1 = 0.03$)	2.37	10.00%	91.62%
μ 1/50×			
($\lambda_0 = 0.125$, $\lambda_1 = 0.1$, $q_{01} = 0.005$, $q_{10} = 0.005$, $\mu_0 = 0.0006$, $\mu_1 = 0.03$)	3.66	9.00%	91.99%

TABLE 3.10: Power for a character rate difference of 500× when a additional asymmetry is introduced to the rate of speciation.

Rate of Character Change with Speciation Asymmetry	5% Cutoff	Power	Percent State 0
No additional Asymmetry			
(q_{01} = 0.005, q_{10} = 0.00001, μ_0 = 0.03, μ_1 = 0.03, λ_0 = 0.1, λ_1 = 0.1)	2.214	59.91%	67.77%
Root state 0 $\lambda_0 < \lambda_1$			
λ 1.1×			
(q_{01} = 0.005, q_{10} = 0.00001, λ_0 = 0.1, λ_1 = 0.11, μ_0 = 0.03, μ_1 = 0.03)	2.334	64.40%	60.70%
λ 1.25×			
(q_{01} = 0.005, q_{10} = 0.00001, λ_0 = 0.1, λ_1 = 0.125, μ_0 = 0.03, μ_1 = 0.03)	1.921	75.00%	51.31%
λ 1.5×			
(q_{01} = 0.005, q_{10} = 0.00001, λ_0 = 0.1, λ_1 = 0.15, μ_0 = 0.03, μ_1 = 0.03)	1.822	73.52%	41.11%
λ 2×			
(q_{01} = 0.005, q_{10} = 0.00001, λ_0 = 0.1, λ_1 = 0.2, μ_0 = 0.03, μ_1 = 0.03)	1.633	71.00%	26.26%
Root state 0 $\lambda_0 > \lambda_1$			
λ 1.1×			
(q_{01} = 0.005, q_{10} = 0.00001, λ_0 = 0.11, λ_1 = 0.1, μ_0 = 0.03, μ_1 = 0.03)	1.747	50.02%	76.62%
λ 1.25×			
(q_{01} = 0.005, q_{10} = 0.00001, λ_0 = 0.125, λ_1 = 0.1, μ_0 = 0.03, μ_1 = 0.03)	1.656	29.52%	83.22%
λ 1.5×			
(q_{01} = 0.005, q_{10} = 0.00001, λ_0 = 0.15, λ_1 = 0.1, μ_0 = 0.03, μ_1 = 0.03)	1.736	12.80%	90.06%
λ 2×			
(q_{01} = 0.005, q_{10} = 0.00001, λ_0 = 0.2, λ_1 = 0.1, μ_0 = 0.03, μ_1 = 0.03)	1.047	4.80%	95.32%

TABLE 3.11: Power for a character rate difference of 500× when a additional asymmetry is introduced to the rate of extinction.

Character Change with Extinction Asymmetry	5% Cutoff	Power	Percent State 0
No additional Asymmetry ($q_{01} = 0.005$, $q_{10} = 0.00001$, $\mu_0 = 0.03$, $\mu_1 = 0.03$, $\lambda_0 = 0.1$, $\lambda_1 = 0.1$)	2.214	59.91%	67.77%
Root state 0 $\mu_0 < \mu_1$ μ 1/2×, ($q_{01} = 0.005$, $q_{10} = 0.00001$, $\lambda_0 = 0.1$, $\lambda_1 = 0.1$, $\mu_0 = 0.015$, $\mu_1 = 0.03$)	2.218	39.34%	78.38%
μ 1/30× ($q_{01} = 0.005$, $q_{10} = 0.00001$, $\lambda_0 = 0.1$, $\lambda_1 = 0.1$, $\mu_0 = 0.001$, $\mu_1 = 0.03$)	3.118	15.67%	85.6%
μ 1/100×, ($q_{01} = 0.005$, $q_{10} = 0.00001$, $\lambda_0 = 0.1$, $\lambda_1 = 0.1$, $\mu_0 = 0.0003$, $\mu_1 = 0.03$)	2.908	16.32%	84.96%
Root state 0 $\mu_0 > \mu_1$ μ 1/2× ($q_{01} = 0.005$, $q_{10} = 0.00001$, $\lambda_0 = 0.1$, $\lambda_1 = 0.1$, $\mu_0 = 0.03$, $\mu_1 = 0.015$)	2.321	65.60%	59.58%
μ 1/30× ($q_{01} = 0.005$, $q_{10} = 0.00001$, $\lambda_0 = 0.1$, $\lambda_1 = 0.1$, $\mu_0 = 0.03$, $\mu_1 = 0.001$)	2.172	73.30%	49.12%
μ 1/100× ($q_{01} = 0.005$, $q_{10} = 0.00001$, $\lambda_0 = 0.1$, $\lambda_1 = 0.1$, $\mu_0 = 0.03$, $\mu_1 = 0.0003$)	2.052	74.60%	49.20%

TABLE 3.12: Power for an extinction rate difference of 50× when a additional asymmetry is introduced to the rate of speciation.

Rate of Extinction with Speciation Asymmetry	5% Cutoff	Power	Percent State 0
No additional Asymmetry ($\mu_0 = 0.03$, $\mu_1 = 0.0006$, $q_{01} = 0.005$, $q_{10} = 0.005$, $\lambda_0 = 0.1$, $\lambda_1 = 0.1$)	2.16	3.80%	57.69%
Root state 0 $\lambda_0 < \lambda_1$			
λ 1.25× ($\mu_0 = 0.03$, $\mu_1 = 0.0006$, $q_{01} = 0.005$, $q_{10} = 0.005$, $\lambda_0 = 0.1$, $\lambda_1 = 0.125$)	2.18	3.60%	44.58%
λ 1.5× ($\mu_0 = 0.03$, $\mu_1 = 0.0006$, $q_{01} = 0.005$, $q_{10} = 0.005$, $\lambda_0 = 0.1$, $\lambda_1 = 0.15$)	2.77	1.20%	32.82%
λ 2× ($\mu_0 = 0.03$, $\mu_1 = 0.0006$, $q_{01} = 0.005$, $q_{10} = 0.005$, $\lambda_0 = 0.1$, $\lambda_1 = 0.2$)	2.88	1.00%	22.78%
Root state 0 $\lambda_0 > \lambda_1$			
λ 1.25× ($\mu_0 = 0.03$, $\mu_1 = 0.0006$, $q_{01} = 0.005$, $q_{10} = 0.005$, $\lambda_0 = 0.125$, $\lambda_1 = 0.1$)	1.86	3.40%	76.90%
λ 1.5× ($\mu_0 = 0.03$, $\mu_1 = 0.0006$, $q_{01} = 0.005$, $q_{10} = 0.005$, $\lambda_0 = 0.15$, $\lambda_1 = 0.1$)	1.74	3.00%	85.55%
λ 2× ($\mu_0 = 0.03$, $\mu_1 = 0.0006$, $q_{01} = 0.005$, $q_{10} = 0.005$, $\lambda_0 = 0.2$, $\lambda_1 = 0.1$)	1.18	5.60%	93.19%

TABLE 3.13: Power for an extinction rate difference of 50× when a additional asymmetry is introduced to the rate of character change.

Rate of Extinction with Character Change Asymmetry	5% Cutoff	Power	Percent State 0
No additional Asymmetry			
($\mu_0 = 0.03$, $\mu_1 = 0.0006$, $q_{01} = 0.005$, $q_{10} = 0.005$, $\lambda_0 = 0.1$, $\lambda_1 = 0.1$)	2.16	3.80%	57.69%
Root state 0 $q_{01} < q_{10}$			
q 1/2×			
($\mu_0 = 0.03$, $\mu_1 = 0.0006$, $q_{01} = 0.0025$, $q_{10} = 0.005$, $\lambda_0 = 0.1$, $\lambda_1 = 0.1$)	2.01	4.70%	71.66%
q 1/10×			
($\mu_0 = 0.03$, $\mu_1 = 0.0006$, $q_{01} = 0.0005$, $q_{10} = 0.005$, $\lambda_0 = 0.1$, $\lambda_1 = 0.1$)	4.43	3.60%	92.16%
q 1/500×			
($\mu_0 = 0.03$, $\mu_1 = 0.0006$, $q_{01} = 0.00001$, $q_{10} = 0.005$, $\lambda_0 = 0.1$, $\lambda_1 = 0.1$)	1.44	1.0%	99.94%
Root state 0 $q_{01} > q_{10}$			
q 1/2×			
($\mu_0 = 0.03$, $\mu_1 = 0.0006$, $q_{01} = 0.005$, $q_{10} = 0.0025$, $\lambda_0 = 0.1$, $\lambda_1 = 0.1$)	2.32	1.80%	52.31%
q 1/10×			
($\mu_0 = 0.03$, $\mu_1 = 0.0006$, $q_{01} = 0.005$, $q_{10} = 0.0005$, $\lambda_0 = 0.1$, $\lambda_1 = 0.1$)	3.34	6.00%	48.14%
q 1/500×			
($\mu_0 = 0.03$, $\mu_1 = 0.0006$, $q_{01} = 0.005$, $q_{10} = 0.00001$, $\lambda_0 = 0.1$, $\lambda_1 = 0.1$)	3.49	4.00%	48.11%

(λ_0 = 0.0025, λ_1= 0.1); two times rate change (q_{01} = 0.01, q_{10} = 0.005); ten times rate change (q_{01} = 0.05, q_{10} = 0.005); forty times rate change (q_{01} = 0.2, q_{10} = 0.005); two times extinction (μ_0 = 0.06, μ_1 = 0.03); three times extinction (μ_0 = 0.09, μ_1 = 0.03); and ten times extinction (μ_0 = 0.3, μ_1 = 0.03).

RESULTS

Parameter Rate Estimations and Hypothesis Testing of Lizardfish Data

Asymmetries in Lizardfish Speciation Rates—Rates of speciation are slightly asymmetrical, with taxa under state 0 (λ_0) having a rate of 0.1327, while taxa under state 1 (λ_1) have a smaller rate of 0.1142. The BiSSE likelihood difference between the unconstrained model and the constrained null hypothesis ($\lambda_0 = \lambda_1$) is 0.3783, which is not recovered as a significant value. The 5% cutoff for a significant value based on simulations from the symmetrical null hypothesis ($\lambda_0 = \lambda_1$) was 3.178. Simulations of 43 taxa with the asymmetrical rates estimated above recovered a power of only 4.024%. Asymmetrical simulations with different tree sizes recovered similarly low powers when compared to their respective null simulations (Table 3.1). Power levels varying with tree size are plotted in Figure 3.1.

Asymmetries in Lizardfish Rates of Character Change—Rates of character change are higher from 0 to 1 (q_{01}) than from 1 to 0 (q_{10}), with respective rates of 0.0055 and 0.00001. The BiSSE likelihood difference between the unconstrained model and the constrained null hypothesis ($q_{01} = q_{01}$) is 0.6151, which was not above the 5% cutoff estimated from the symmetrical simulations of 1.8183. With 43 taxa,

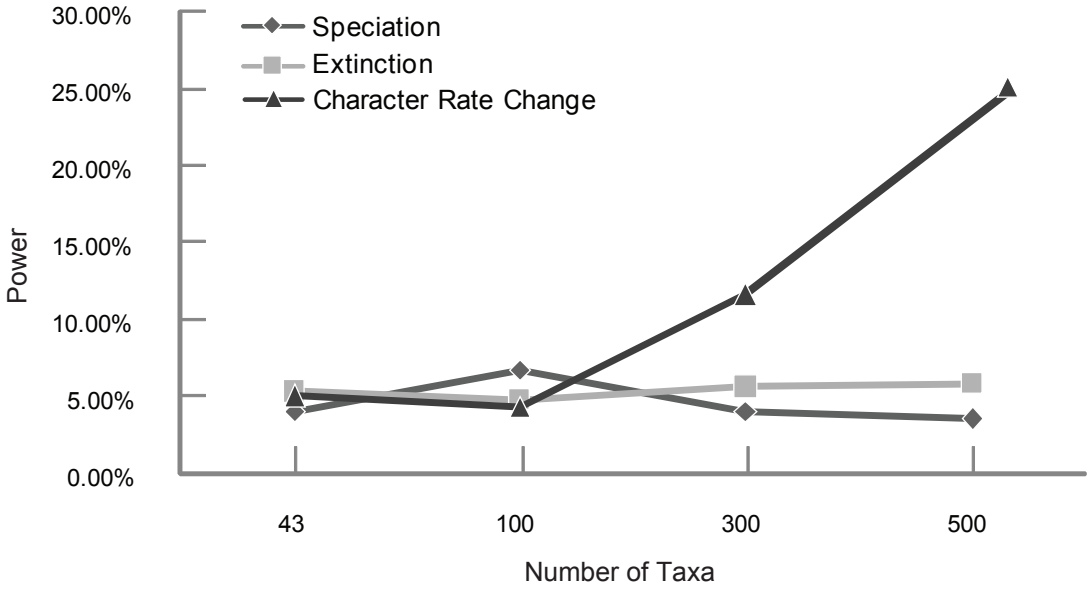

Fig. 3.1. Power of varying tree sizes with paramters estimated from lizardfish data. See Table 3.1 and text for discussion.

the estimated parameters have a 5.06% power, and this power increased as tree size increased to approximately 25 % in tree sizes of 500 taxa (Table 3.1, Fig 3.1).

Asymmetries in Lizardfish Extinction Rates—Extinction rates under State 0 are higher than under state 1 at 0.0018 and 0.0000664, respectively. Although extinction rates are slightly higher for taxa under state 0, the BiSSE likelihood difference of 0.0657 is not significant, with the 5% cutoff being 2.7603, with a power of 5.2694% under a 43 taxa asymmetrical simulation. Simulations of varying tree sizes recovered similar low powers (Table 3.1, Fig. 3.1).

Power of BiSSE Method

Asymmetries in Speciation Rate—Tree sizes of 50 taxa exhibited low powers of approximately 5% regardless of difference in speciation rates (Table 3.2, Fig 3.2 A, B). Power levels marginally improved for tree sizes of 100 taxa, to about 12%, but decreased significantly with a 10 and 20× rate difference to below 3% (Fig 3.2 A, B). Tree sizes of 300 have higher overall powers for each difference in rate than powers observed in 50 or 100 taxa, and power increased as the degree of difference in rate increased, until reaching a power of 49% at four times the speciation rate difference. Power levels significantly decreased as the rate difference grew beyond 4×.

In simulations with 500 taxa, power is again higher than in analogous simulations with a smaller tree size (Fig 3.2 A, B). The power curve followed a similar pattern as that shown from 300 taxa, with power increasing as rate difference increased to around 70%, leveling off, and then decreasing after a rate difference of about 5×. In general, for each difference in rates, power increased as tree size increased (Fig 3.2

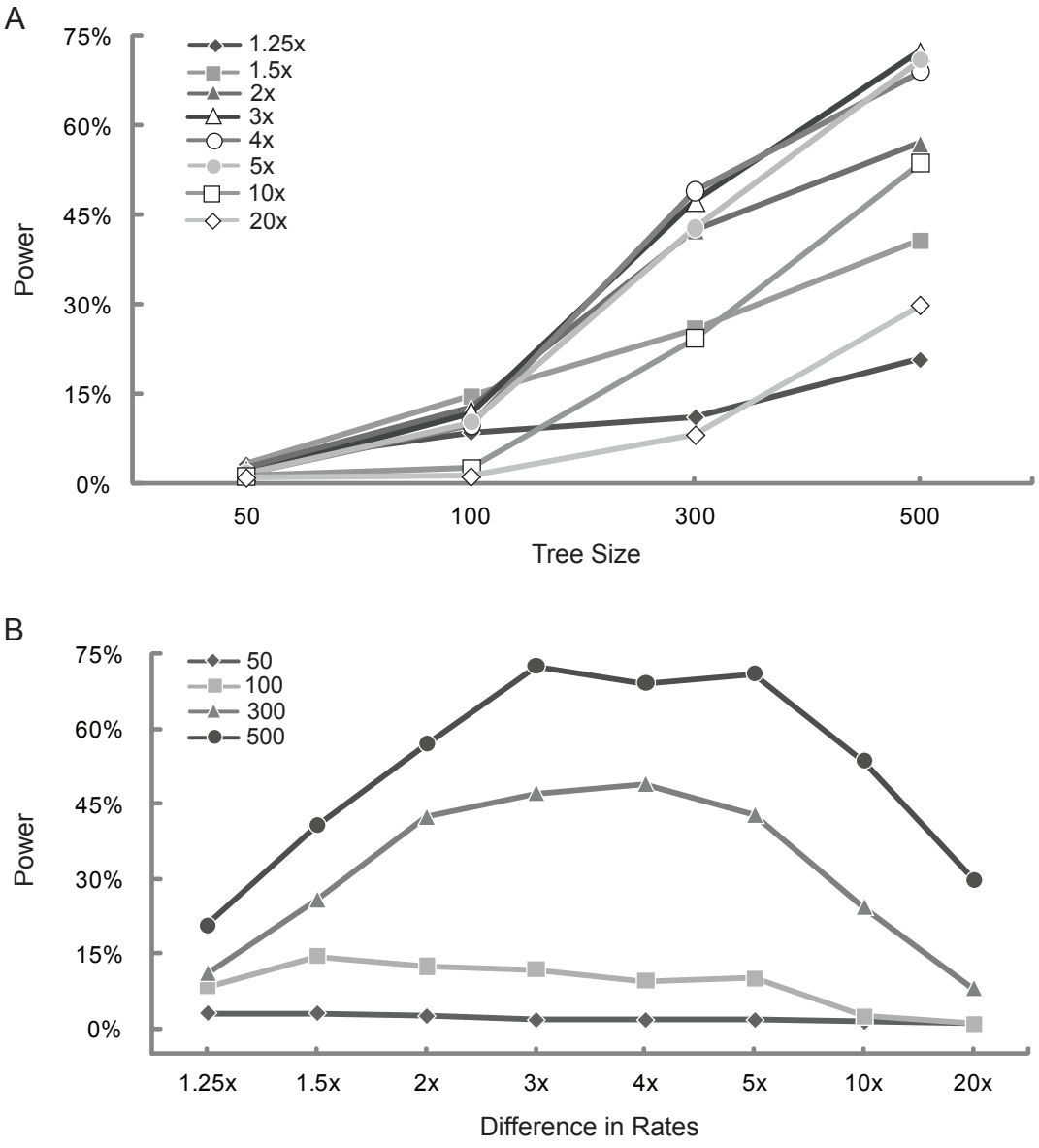

Fig. 3.2. Power of simulations with asymmetrical rates of speciation. See Table 3.2 for list of rate values.

A), and in simulations with tree sizes of 100, 300, and 500 taxa, a common pattern of power decreasing after a 5× difference in rate was observed (Fig 3.2 B). The average percentage of simulated taxa with a character State of 0 also steadily decreased across all tree sizes as the asymmetry of higher speciation under State 1 increased, with State 0 occurring in less than 5% of the taxa after a 3× difference in rates.

Asymmetries in Rate of Character State Change—Table 3.3 shows the power results from the asymmetrical character rate model simulations and their respective symmetrical simulations, including the 5% significance cutoff and power. In general, for each asymmetrical model of character change (e.g., 2×, 5×), power increased with an increase in tree size (Fig 3.3 A). Power did not increase with a difference in rates when the tree size was 50 taxa, with power recovered at approximately 5%. There was a slight increase in power as the degree of difference in rates increased with tree sizes of 100 taxa, but power was still relatively low with a range from 5.8 (2×) to 13.4% (10×). Power was higher for simulations with 300 taxa for each respective difference in rates compared to the same simulations with 100 and 50 taxa. Power increased as the rate difference increased to 5× then leveled off to 10×, followed by a strong decrease in power as the difference in rates increased to 20× and 40× (Fig 3.3 B). This same pattern was observed in simulations of 500 taxa, and in general there was a decrease in power that was observed in all tree sizes beyond a 10x difference in rates of character change (Fig 3.3 B). The average percentage of terminal taxa with State 0 unsurprisingly decreased as the rate of character change from State 0 to 1 increased.

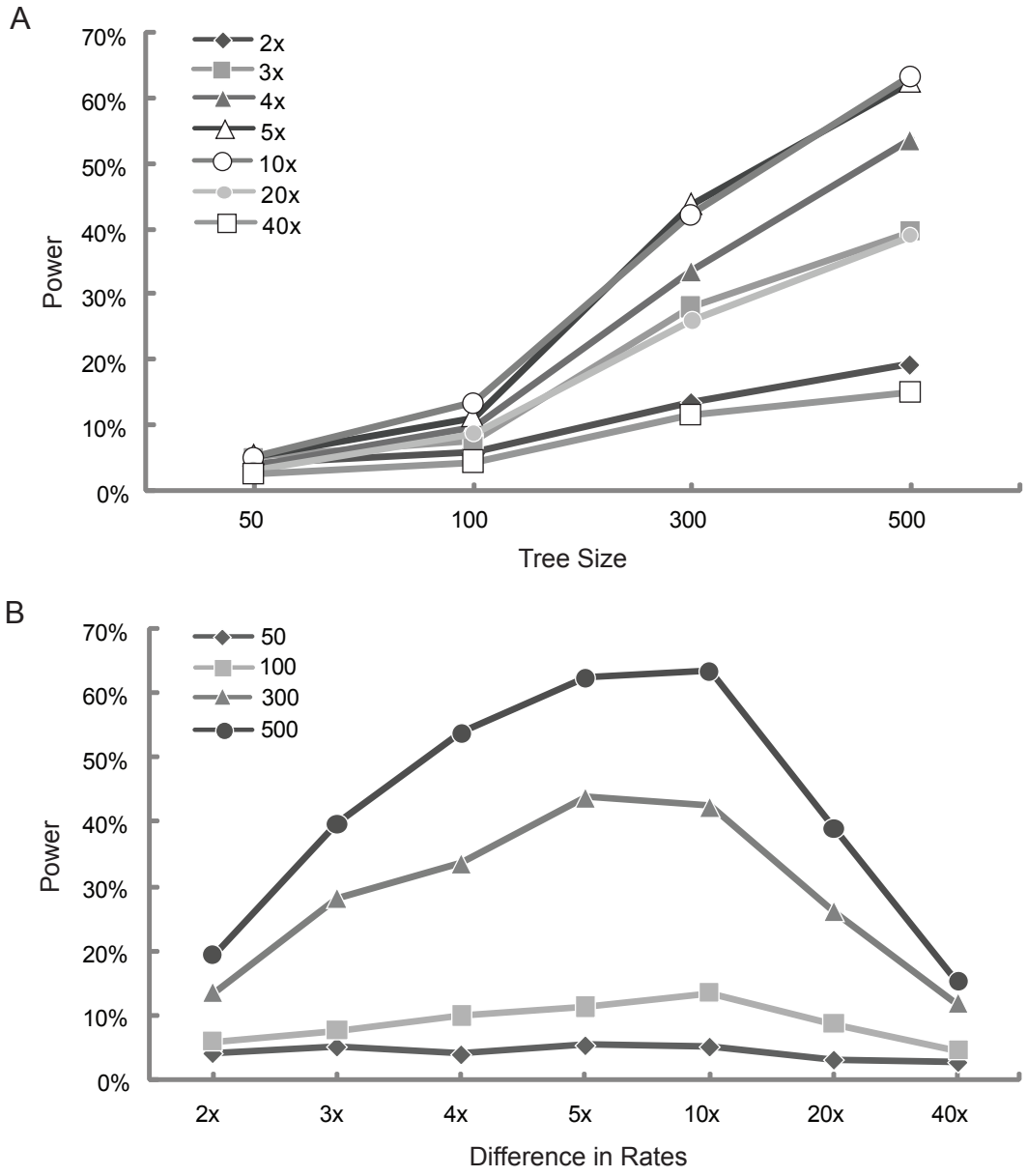

Fig. 3.3. Power of simulations with asymmetrical rates of character change. See Table 3.3 for list of rate values.

Asymmetries in Extinction Rate—As with rates of speciation and character state change, power increased as tree size increased regardless of the amount of difference in extinction rate (Table 3.4; Fig 3.4 A). With tree sizes of 50 taxa, power levels are at 4% for 2 and 3× difference in rates, but then decreased to approximately 2%. With 100 taxa, power levels hovered around 5%, decreasing steadily after a 4× rate difference. The highest power achieved with tree sizes of 300 taxa is 10% at a rate difference of 3×, followed by a decrease in power. With 500 taxa, power increased to approximately 20% for rate differences of 3 and 4× followed by a sharp decline in power. Statistical power associated with estimating differences in extinction rates are lower overall than those of speciation or character state change (Fig 3.4 A, B). As extinction rates under state 0 increased, the average percentage of taxa with State 0 decreased.

Power of Low Rates with Stationary and Constrained Roots—A similar trend in power is observed between stationary and constrained (State 0) roots with rates of speciation higher under State 1 than 0 when the rates of State 0 are small. As the rate of speciation decreased under State 0 relative to State 1, power increased to 100 percent (Table 3.5, Fig 3.5 A). The percentage of terminal taxa with State 0 was also similar under both root analyses decreasing as the speciation rate of State 0 decreased. This decrease did not lead to the severe rarity of State 0 observed when the magnitude of difference increased with higher speciation rate values. Correspondingly, a decrease in power is not observed as rates became increasingly asymmetrical, as was the case with the analyses of higher rate values (Table 3.2, Fig 3.2).

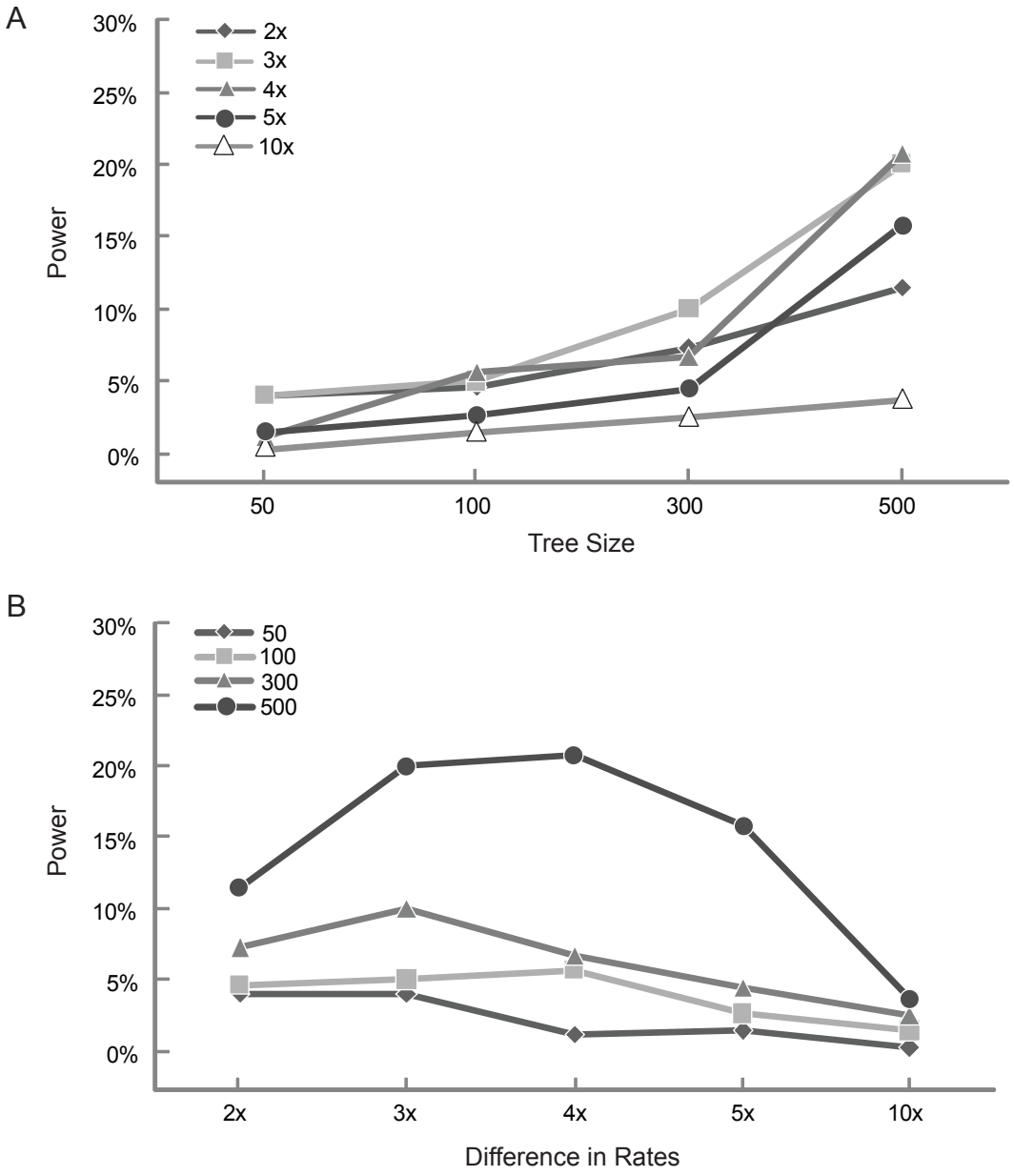

Fig. 3.4. Power of simulations with asymmetrical rates of extinction. See Table 3.4 for list of rate values.

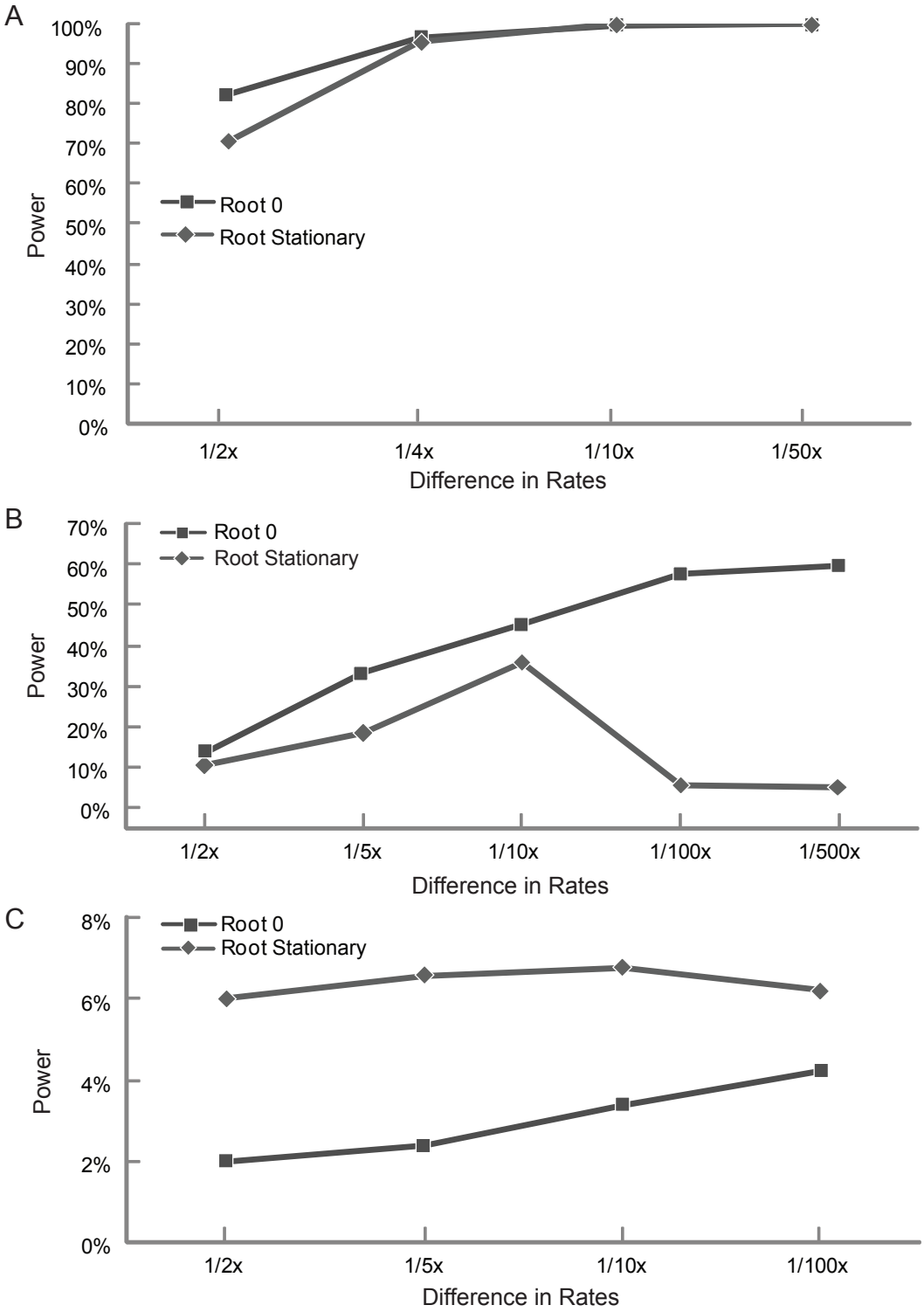

Fig. 3.5. Power of low rates of A. speciation, B. character change, and C. extinction under a stationary root state probability and with the root constrained to state 0. See Table 3.5 and text for discussion.

When the rate of character change from 0 to 1 was higher than 1 to 0, but the rate differences are small values, the same decrease in power as rate difference increased is observed with tree sizes of 500 taxa (Table 3.6, Fig 3.5 B). From 1/2 times the rate difference (q_{01} = 0.005, q_{10} = 0.0025) to 1/10x (q_{01} = 0.005, q_{10} = 0.0005), power increased to 36.07%, but by 1/100× and 1/500× power decreased to near 5%. When the root of the tree is constrained to State 0 rather than a stationary probability, the power curve did not show the same pattern with power continuing to increase as the degree of rate difference increased (Fig 3.5 B), reaching nearly 60% for a 1/500× rate difference (q_{01} = 0.005, q_{10} = 0.00001). In this case, when the root is stationary, the percent of taxa with State 0 dramatically decreases as the rate of change from 1 to 0 decreases, and in both cases in which power drops substantially the percent of taxa with State 0 is extremely small. When the root is constrained to be State 0, rarity of State 0 is not observed, and the power of identifying rate asymmetry increases.

Power is small as the magnitude of difference in extinction increased as the extinction rate under State 1 decreased for both stationary and constrained roots (Table 3.7, Fig 3.5 C). When a large magnitude of difference between the extinction rates is observed, power never increased beyond 7%. In general, the power of testing for extinction asymmetry when rates are low is worse than when testing for higher values of extinction, even when the magnitude of difference was greater. Character state rarity was not observed with low extinction rates and high magnitude of rate difference and the decline in overall power may be the result of poor extinction parameter estimation of low rates.

Power of Multiple Asymmetry Simulations Related to Lizardfish Data—With a 1.25× difference in speciation rates ($\lambda_0 = 0.125$, $\lambda_1 = 0.1$) and symmetrical character state change and extinction rates, the power was a relatively small 11.42% (Table 3.8). Power decreased to 4% as the rate of character change from 1 to 0 decreased to 500 times. When the decrease in character change was from 0 to 1, the percent of terminal taxa with State 0 became highly asymmetrical and the power decreased dramatically (Fig 3.6 A). When an asymmetry was introduced to extinction rates, an overall drop in power was observed, although the drop was more pronounced when extinction rates under State 0 were greater than State 1 (Table 3.9, Fig 3.6 B). There is a slight decrease in power when extinction under State 1 is greater than State 0. Overall, the power of testing hypotheses of asymmetrical speciation rates can be effected by additional rate asymmetries.

Introducing an additional asymmetry to either speciation or extinction for simulations of 1/500 times character rate difference with the root state constrained to 0 shows that multiple asymmetries can have a strong impact on the power associated with testing for asymmetries in rates of character change. For introduced asymmetries of speciation, power marginally increased from 60% and then leveled off when the asymmetry in speciation is higher for taxa under State 1 (Fig 3.7 A). However, when speciation rates are higher under State 0 rather than State 1, the power of rejecting a null hypothesis of symmetry in rate of character change drops dramatically to approximately 5% as the degree of rate difference between 0 and 1 increases (Table 3.10). A similar pattern is seen for extinction rates (Table 3.11), in

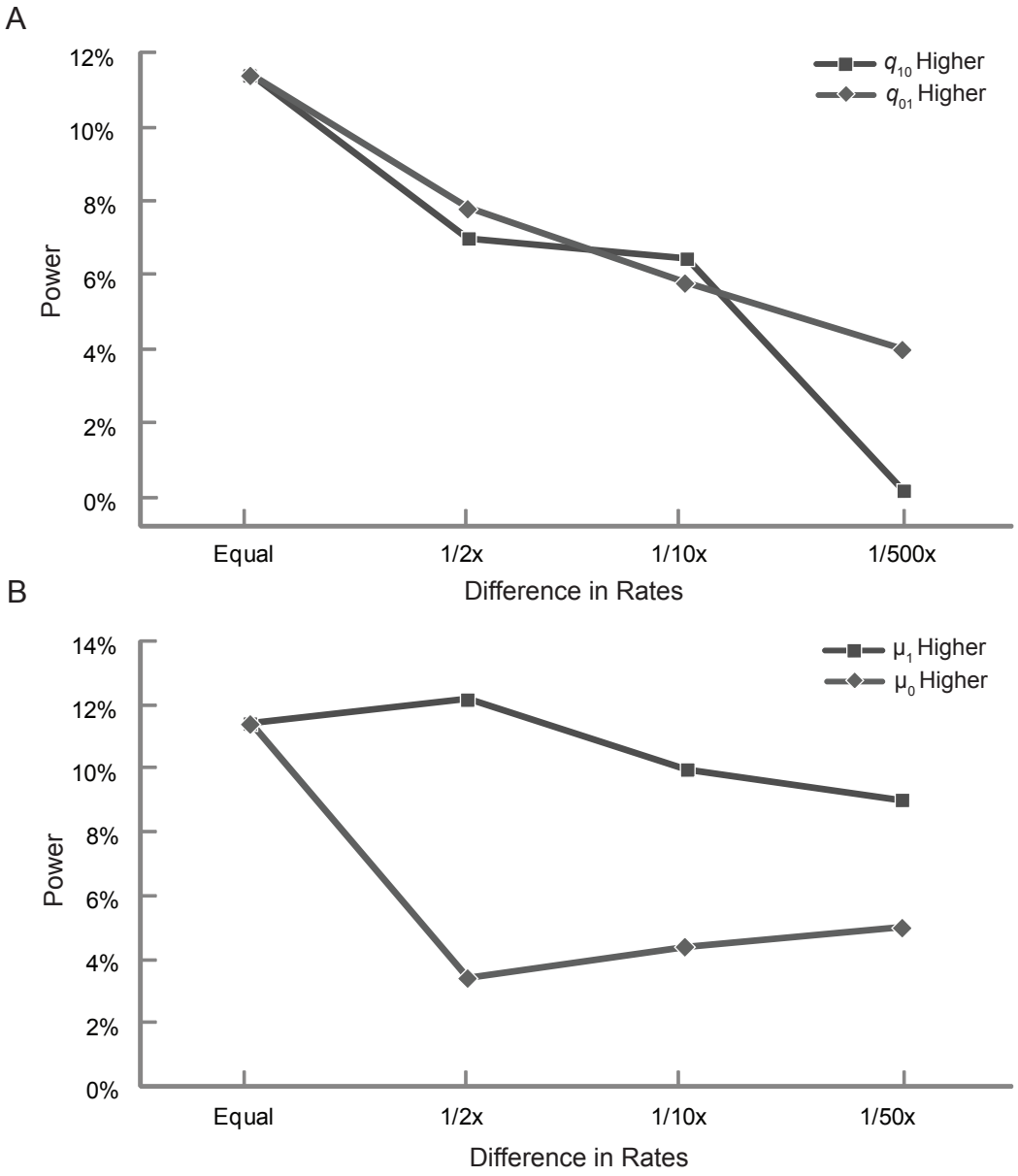

Fig. 3.6. Power of 1.25x speciation rate asymmetry ($\lambda_0 = 0.125$, $\lambda_1 = 0.1$) when an additional set of asymmetries are introduced. A. Character change. B. Extinction. See Table 3.8 and 3.9 for list of rate values and text for discussion.

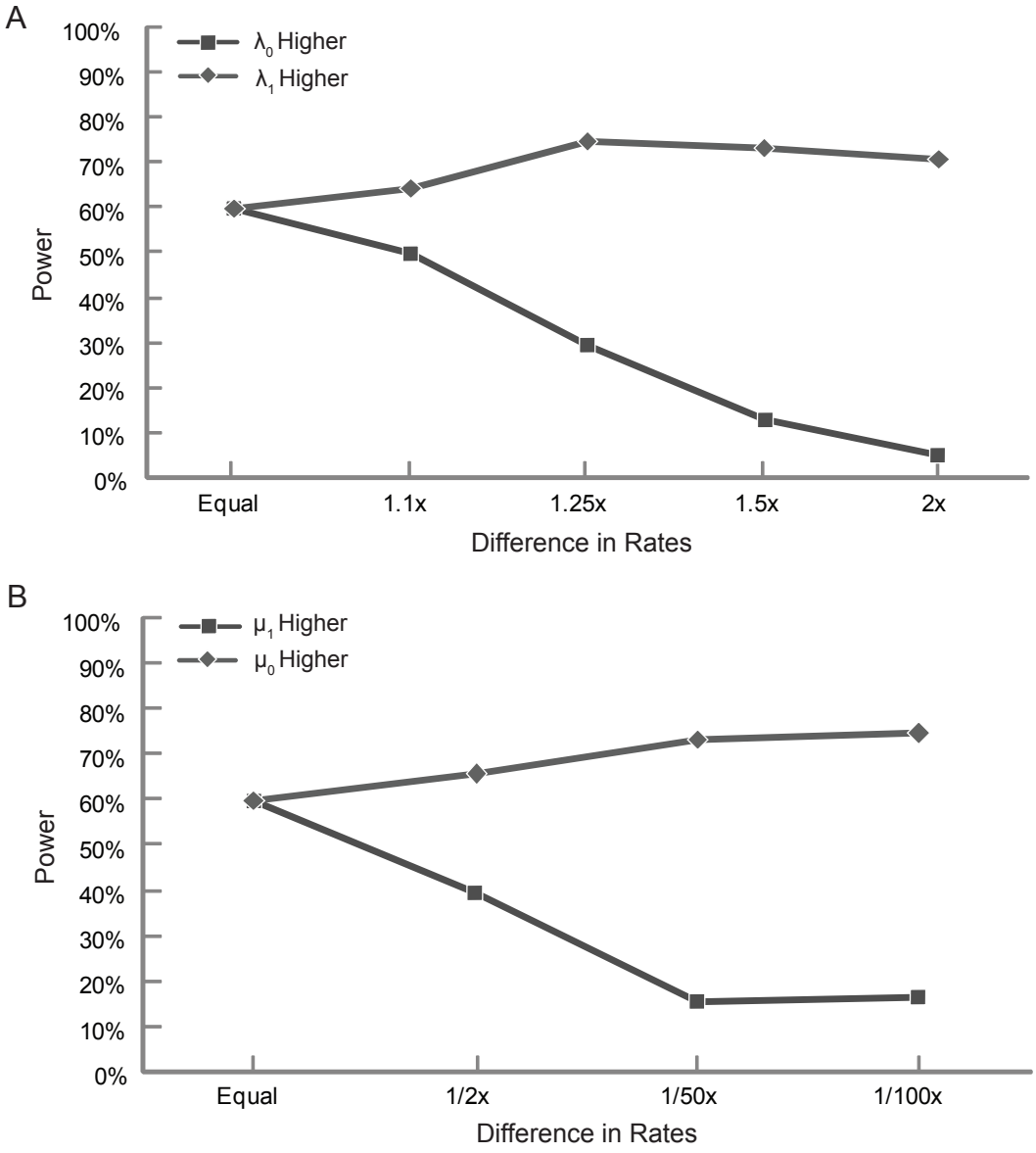

Fig. 3.7. Power of 500 times character change rate asymmetry (q_{01} = 0.005, q_{10} = 0.00001) when an additional set of asymmetries are introduced. A. Speciation. B. Extinction. See Table 3.10 and 3.11 for list of rate values and text for discussion.

which an asymmetry of higher extinction rates under State 0 leads to a small increase in the starting power of 60% from which extinction rates are equal, but an increase in extinction rates under State 1 resulted in a dramatic decrease in the power of testing hypotheses of character change symmetry (Fig 3.7 B).

A fixed extinction asymmetry of a 50 times difference in magnitude has a low power of approximately 4% when rates of speciation and extinction are symmetrical. When an additional asymmetry is introduced to speciation rates, power slightly decreases as speciation rates under State 1 increase, and also slightly increases when speciation under State 0 increases (Table 3.12, Fig 3.8 A). When an asymmetry is introduced to character change, power declined as the rate of change from 0 to 1 decreases, which also corresponded with a large increase in the rarity of character State 1 (Table 3.13, Fig 3.8 B). Power remained near the levels of no additional asymmetry when the rate of change from 1 to 0 decreases with the small rate of changing to State 1 not having much impact on character state rarity.

Parameter Estimation

Estimating Parameters Under Asymmetrical Speciation—As described by Maddison et al. (2007), estimation of speciation rates are good, with strong delimitation of known asymmetrical rates (Fig 3.9), although precision seems to decrease as the rate difference of speciation increases. For estimates of symmetrical rates of character change under asymmetrical speciation rates, accuracy and precision of estimating known rates are worse for the higher magnitude of speciation rate asymmetry in the twenty times difference (Fig 3.10 A). However, a 1/50x difference

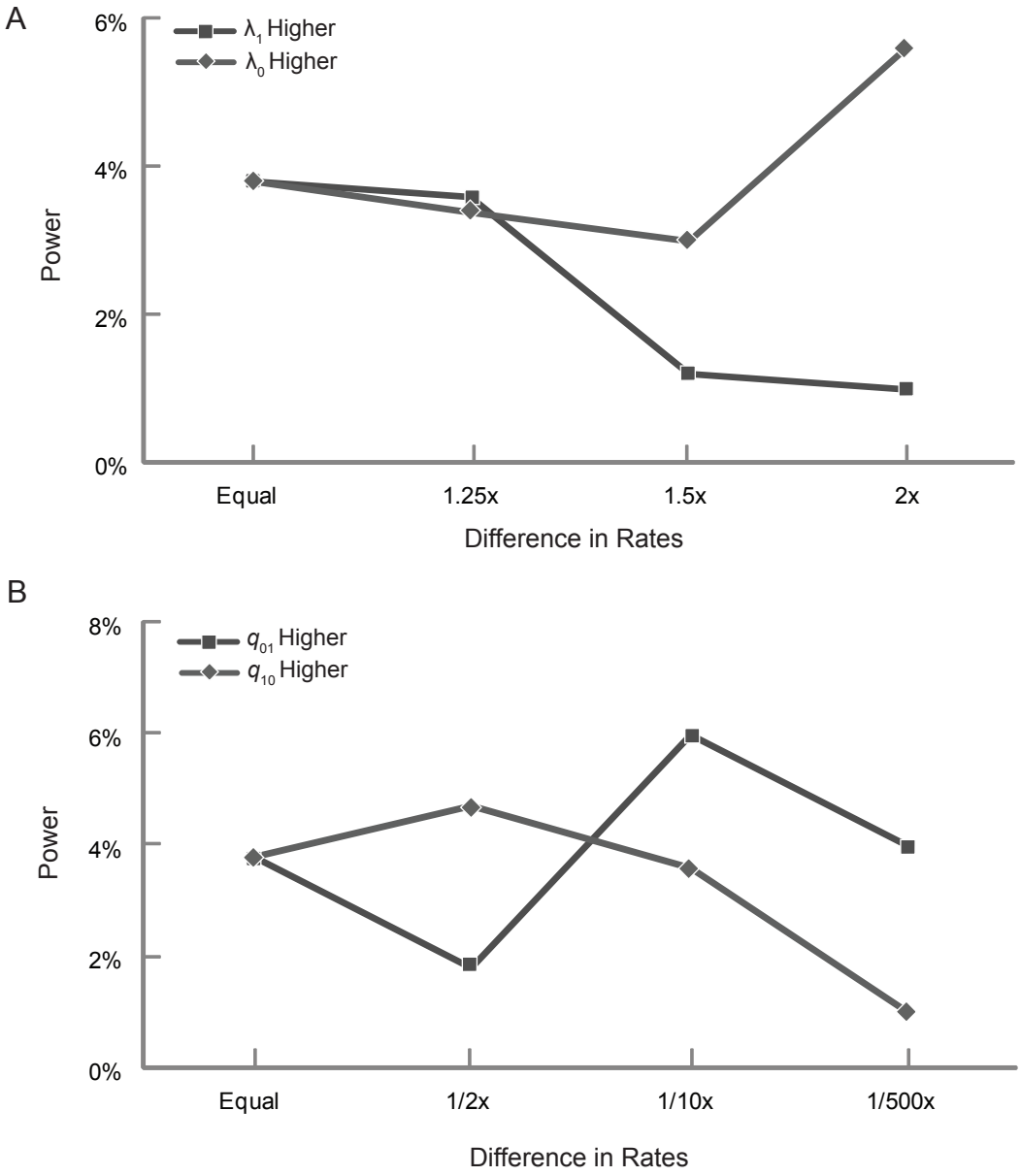

Fig. 3.8. Power of 50x speciation rate asymmetry ($\mu_0 = 0.03$, $\mu_1 = 0.0006$) when an additional set of asymmetries are introduced. A. Speciation. B. Character Change. See Table 3.12 and 3.13 for list of rate values and text for discussion.

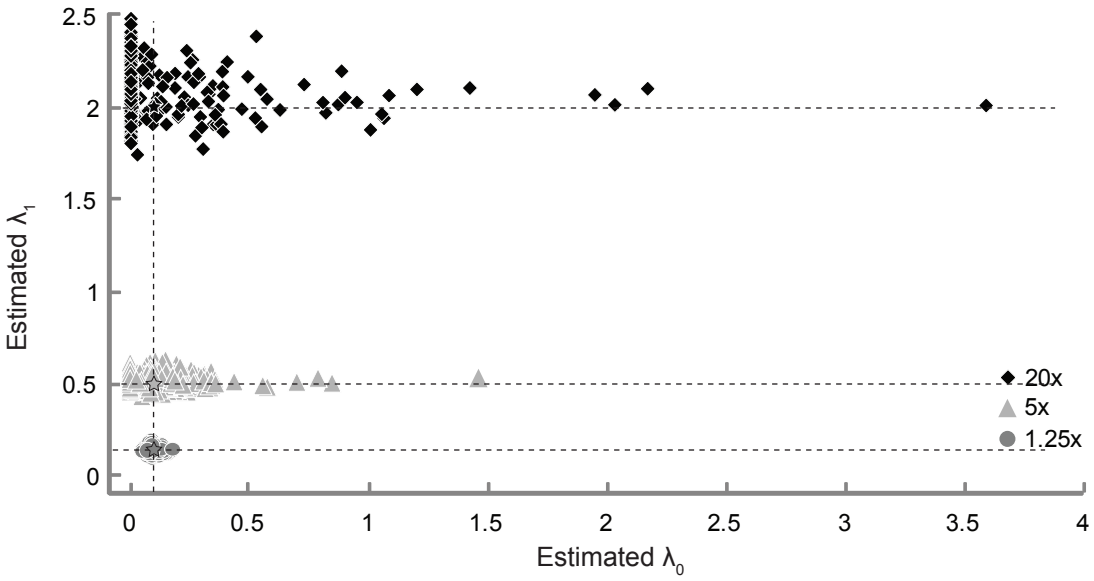

Fig. 3.9. Parameter estimations of speciation under different degrees of asymmetry in speciation rates. See text for discussion. Star symbols inside clusters represent known values.

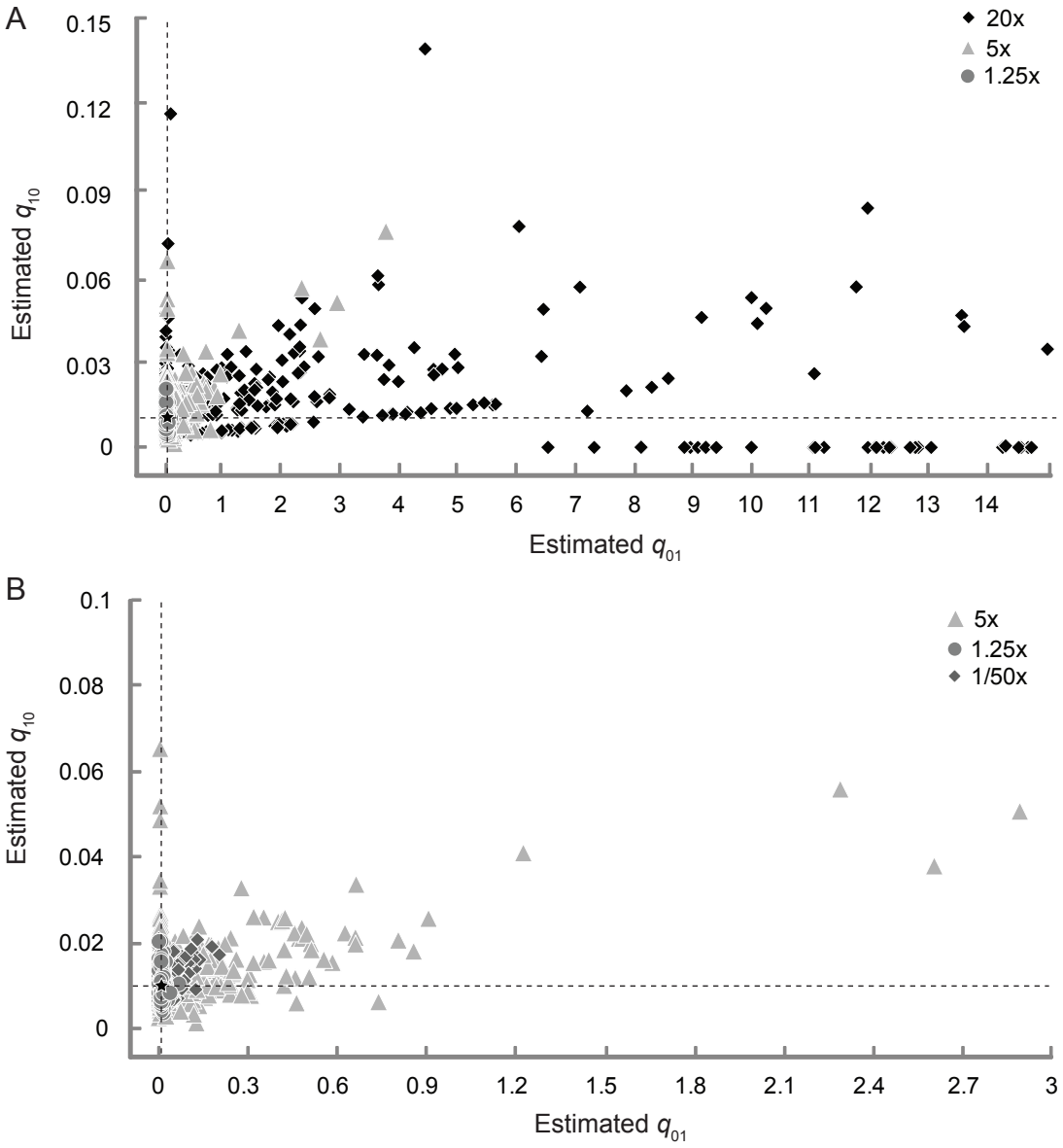

Fig. 3.10. Parameter estimations of character change under different degrees of asymmetry in speciation rates. See text for discussion. Star symbols inside clusters represent known values.

recovered similar accuracy and precision of estimated rates as 1.25× and 5× speciation difference (Fig 3.10 B). A similar pattern is shown for estimates of known symmetrical extinction values, in which speciation rates of 1.25, 5, and 1/50 times had similar estimates of extinction (Fig 3.11 A, B), but 20×speciation estimated rates of extinction poorly with high rate asymmetry of extinction rates (Fig 3.11 A).

Estimating Parameters Under Asymmetrical Character Change—Estimates of asymmetries in character change are not as precise to the known values as with estimates of asymmetries in speciation (Fig 3.12). In general, precision seems to decrease as the rate difference increased, with a 40× rate difference fitting the known estimates particularly poorly. Symmetrical speciation rates ($\lambda_0 = 0.1$, $\lambda_1 = 0.1$) are well estimated when the rate of character change is 2× (low power) and 10× (high power) (Fig. 3.13 A, B). However, with a 40× (low power) difference in the rate of character change the precision of parameter estimation appears to decrease, and the number of estimates for highly asymmetrical speciation rates increases (Fig 3.13 A). Parameter estimation of known extinction rates ($\mu_0 = 0.03$, $\mu_1 = 0.03$) are similar for character rate changes of 2 and 10× (Fig 3.14 A, B). Estimates of known extinction values are very poor under a 40× rate difference.

Estimating Parameters Under Asymmetrical Extinction—As was described by Maddison et al (2007), estimates of known extinction values are poor and seem to lack precision, which seems to decrease as the difference in extinction rates increase (Fig 3.15). Speciation values are well estimated to the known values ($\lambda_0 = 0.1$, $\lambda_1 = 0.1$) when the difference between extinction rates is 2× (low power) and 3× (high

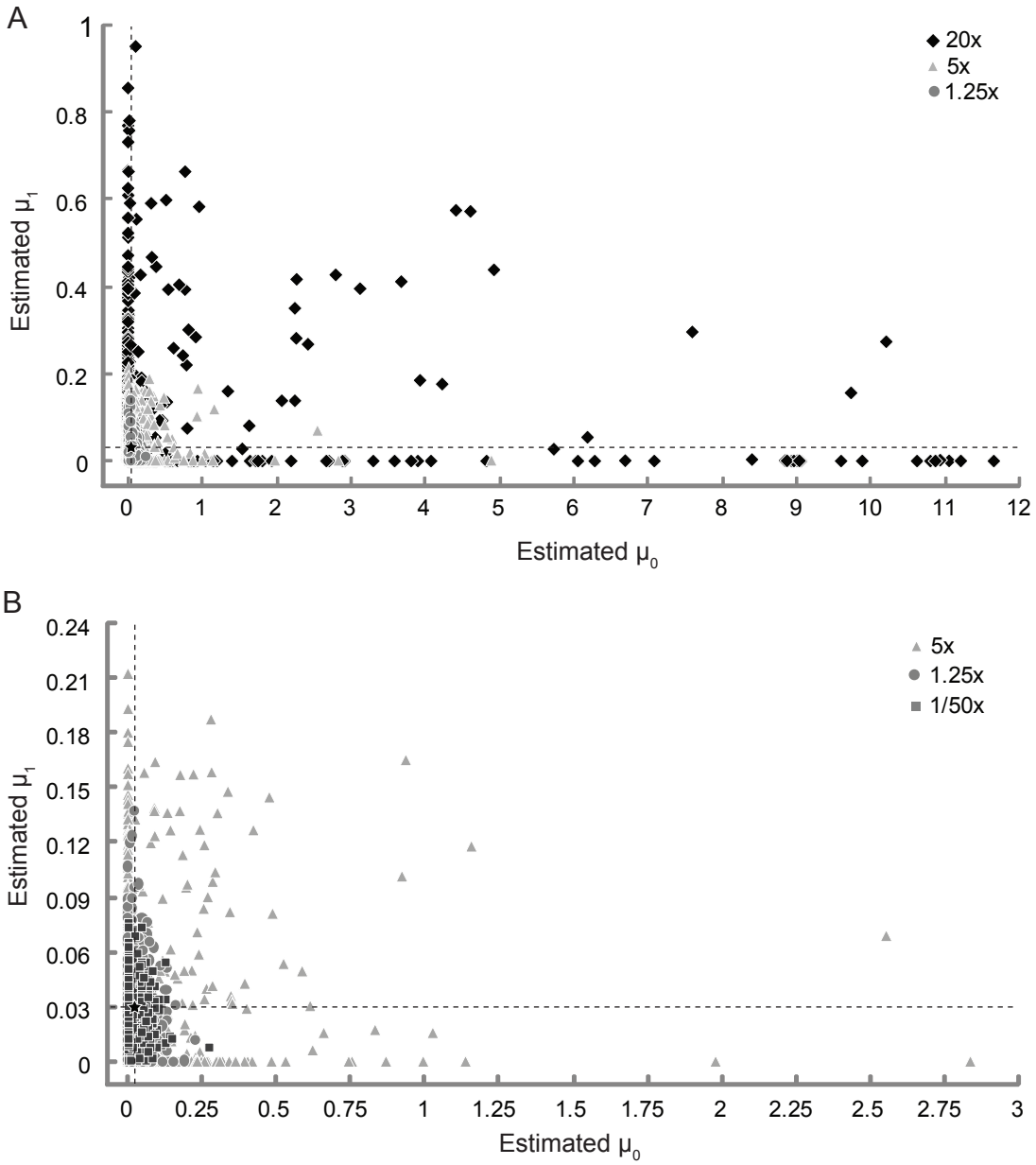

Fig. 3.11. Parameter estimations of extinction under different degrees of asymmetry in speciation rates. See text for discussion. Star symbols inside clusters represent known values.

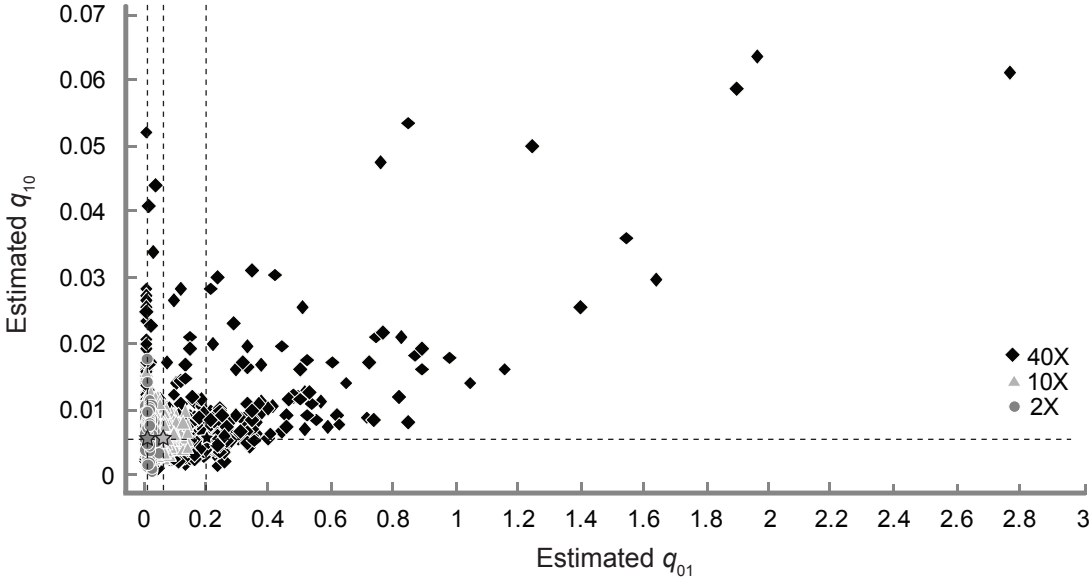

Fig. 3.12. Parameter estimations of character change under different degrees of asymmetry in rates of character change. See text for discussion. Star symbols inside clusters represent known values.

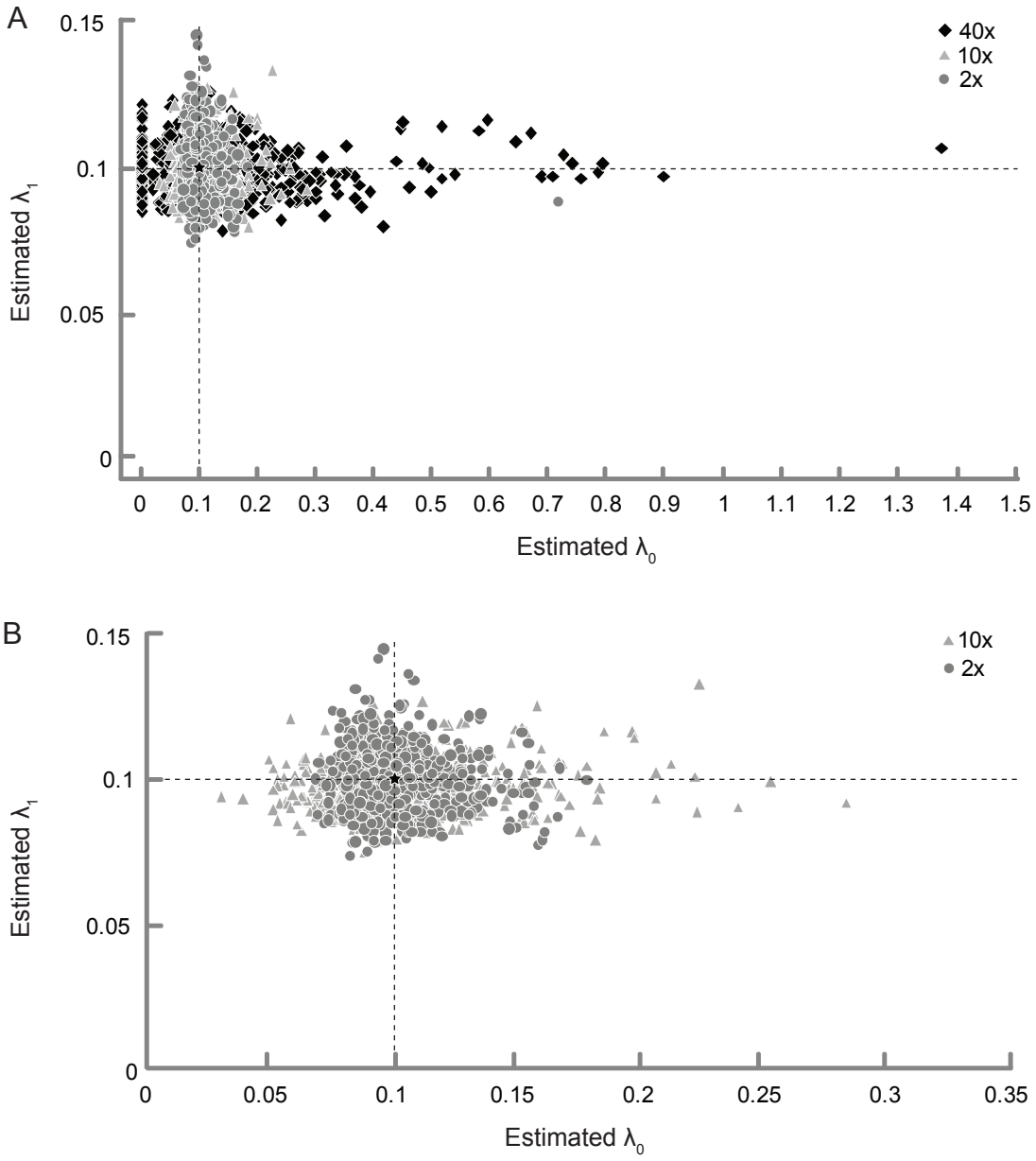

Fig. 3.13. Parameter estimations of speciation under different degrees of asymmetry in rates of character change. See text for discussion. Star symbols inside clusters represent known values.

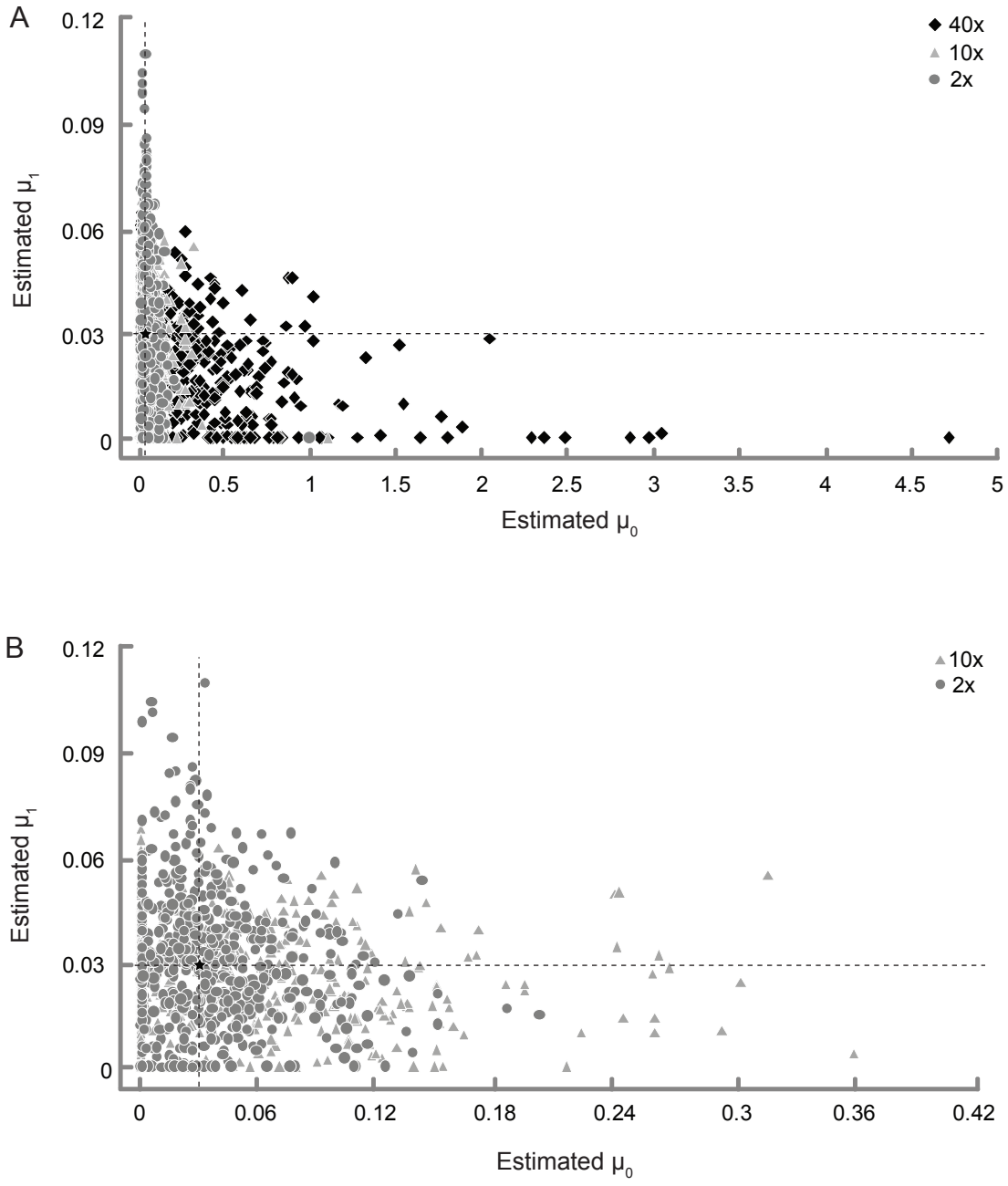

Fig. 3.14. Parameter estimations of extinction under different degrees of asymmetry in rates of character change. See text for discussion. Star symbols inside clusters represent known values.

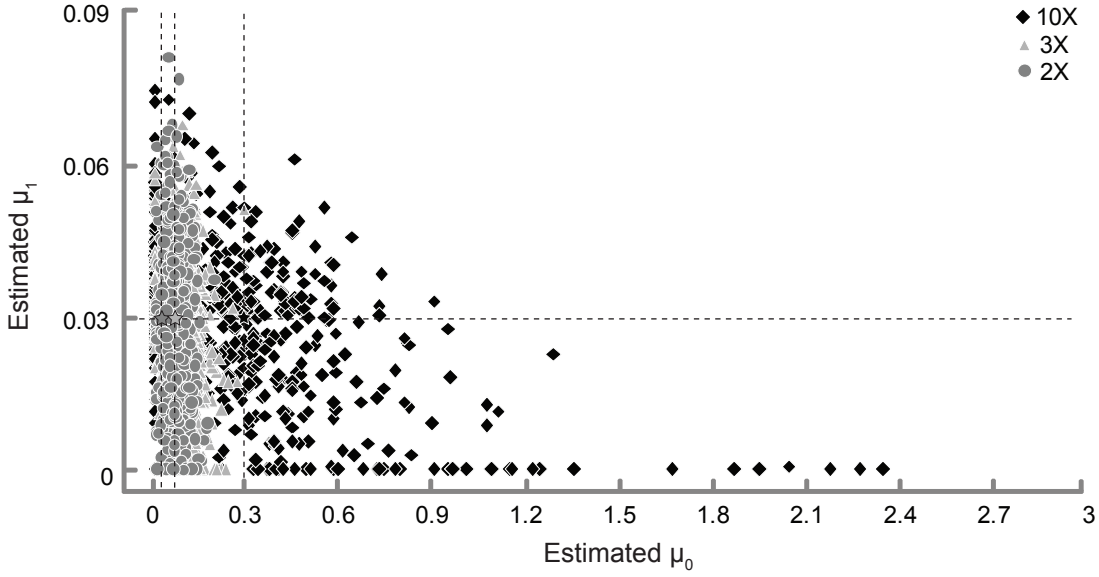

Fig. 3.15. Parameter estimations of extinction under different degrees of asymmetry in rates of extinction. See text for discussion. Star symbols inside clusters represent known values.

power) (Fig 3.16 A, B), but accuracy and precision seems to decrease dramatically as the extinction rate asymmetry increases, leading to an abundance of highly asymmetrical speciation rates (Fig 3.16 A). Parameter estimation of character change has the same pattern, in which the known rate (q_{01} = 0.01, q_{10} = 0.01) is well estimated under 2 and 3× extinction rate differences (Fig 3.17 A, B), but is poorly estimated under an increased difference in extinction rate asymmetry (Fig. 3.17 A). This poor estimation leads to a dramatic increase in the estimation of highly asymmetrical rates of character change favoring rapid transitions from State 0 to 1.

DISCUSSION

The statistical power of the BiSSE method seems to be highly sensitive to changes in the number of taxa and asymmetries in rates of speciation, extinction, and character state change. In terms of tree size, BiSSE recovers extremely low power when testing hypotheses of rate asymmetry for each rate parameter if fewer than 100 taxa are used in the analysis, even when rates are known to be highly asymmetrical (Fig 3.2, 3.3, 3.4). As a result, the potential for a Type II error (failing to reject the null hypothesis when the alternate hypothesis is true) is extremely high. The highest power attributed to any rate asymmetry associated with 300 taxa is still only 50 percent (Fig 3.2). Caution should be taken by researchers that attempt to utilize the BiSSE method with fewer than 300 taxa. Below 100 taxa there is essentially no guarantee of any significant statistical power associated with identifying rate asymmetries, regardless of whether strong asymmetries exist at all. Maddison et al. (2007) hypothesized that power levels would potentially decrease with tree size

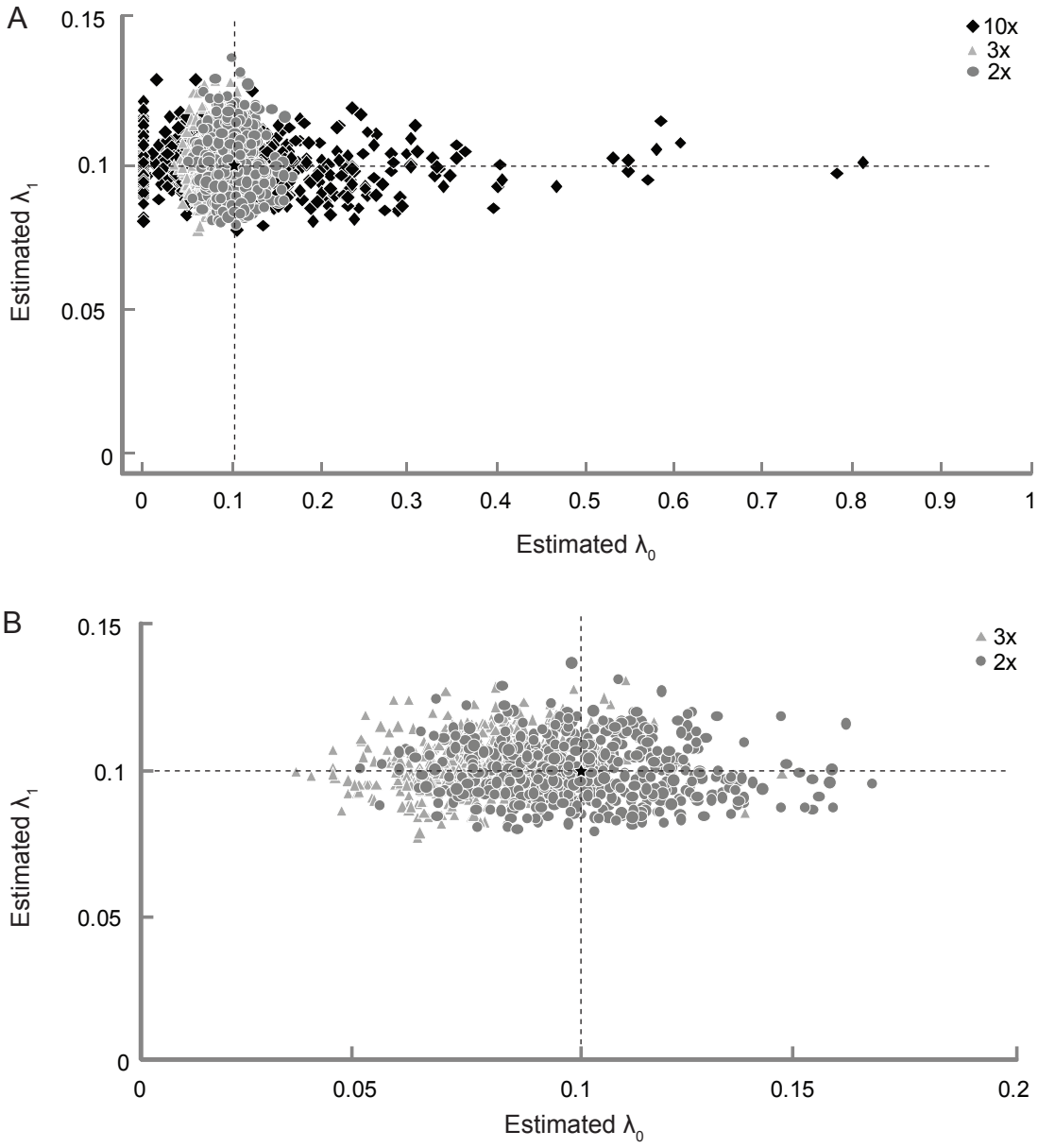

Fig. 3.16. Parameter estimations of speciation under different degrees of asymmetry in rates of extinction. See text for discussion. Star symbols inside clusters represent known values.

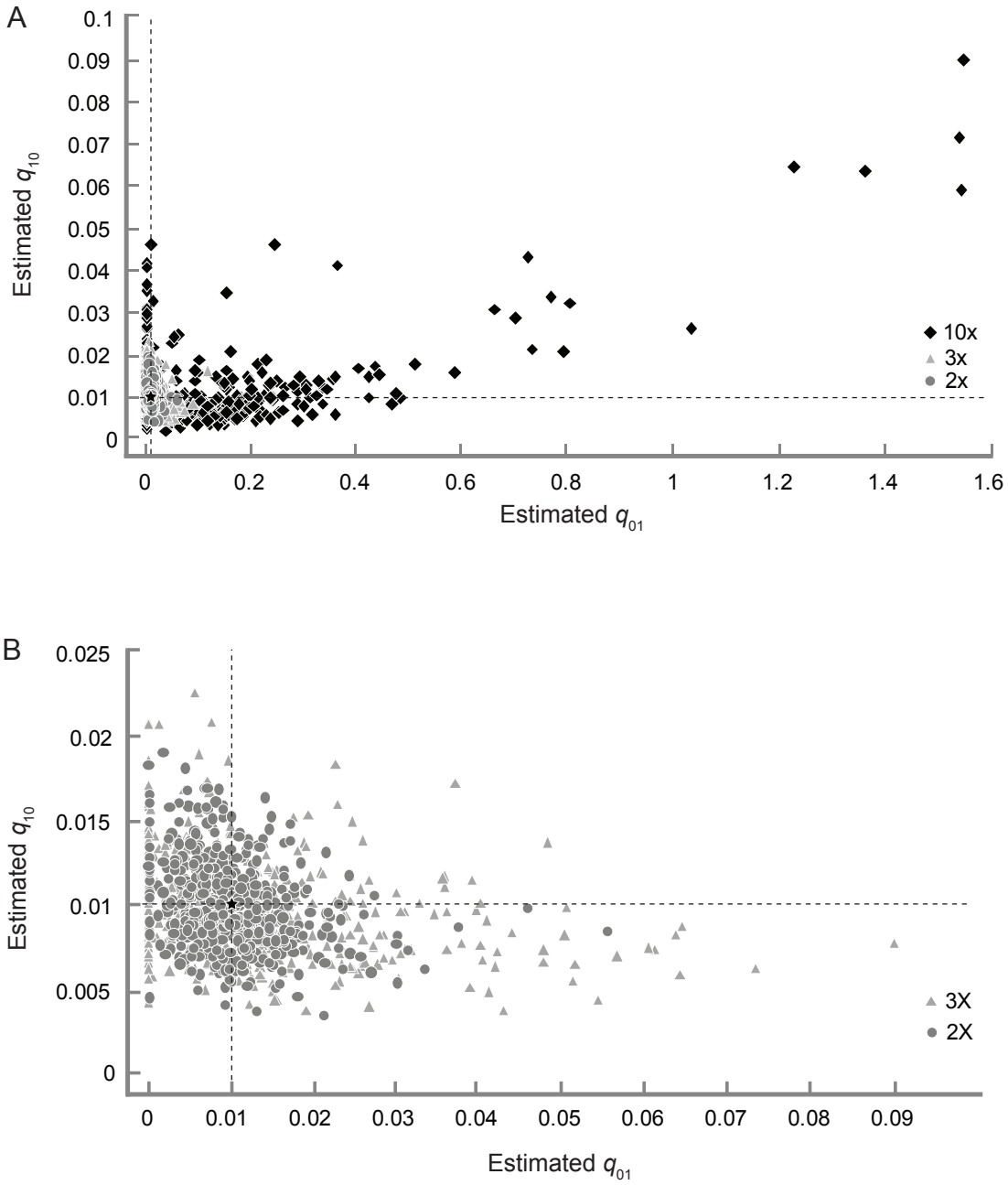

Fig. 3.17. Parameter estimations of character change under different degrees of asymmetry in rates of extinction. See text for discussion. Star symbols inside clusters represent known values.

because there are many ways to arrive at a given phylogeny, and large amounts of data would be needed to distinguish significant asymmetries.

The common pattern of extreme power decreases associated with speciation, extinction, and character change when rates become increasingly asymmetrical also is troubling (Fig 3.2–3.4). This crash in power seems to be related to a phenomenon described by Maddison (2006), in which he showed that estimating rates of character state change decoupled from speciation could lead to erroneous conclusions if the tree is too asymmetrical for a particular character. Strong asymmetries in speciation rates or character state change resulted in the same pattern of taxonomic excess with a single character in his study, and Maddison (2006) hypothesized that teasing apart parameters that are the cause of taxonomic character asymmetry is difficult and that simultaneously estimating these parameters may help address this issue. However, it seems that high rate asymmetries are a problem even when these parameters are simultaneously estimated using the BiSSE method.

When either the rate of speciation, extinction, or character change reached a high degree of rate difference, power began to decrease. In each case in which power decreased because of high rate asymmetry, one of the binary character states is becoming increasingly rare (Table 3.2, 3.3, 3.4). High asymmetrical rates led to similar simulation results in which taxa are saturated with one of the binary character states. For example, when rates of speciation are 20× higher under State 1 than State 0, the number of taxa in a 500 tree size data set with State 0 is disproportionately low, often only 0.5%. The reason for the decrease in power as rate asymmetry increases

seems to be attributed to the difficulty BiSSE has in estimating rate parameters with any accuracy or precision as binary characters begin to be saturated in one direction as seen in Figures 3.10, 3.11, 3.13, 3.14, 3.16, and 3.17.

When taxa are extremely saturated for a particular state, the BiSSE method begins estimating high asymmetries in rates to explain this pattern, even when rates are known to be low and symmetrical. For example, when extinction is 10× higher for State 0 than State 1, the rate of character change is estimated to be highly asymmetrical for a rapid change from State 0 to 1 (Fig 3.17 A) when in fact, the known rates were fairly low and symmetrical ($q_{01} = 0.01$, $q_{10} = 0.01$). When data are not saturated in one direction, BiSSE estimates known parameters with similar accuracy and precision under low, medium, and high rate asymmetries regardless of power (e.g., Fig 3.16 B, 3.17 B). Additionally, when a high magnitude of difference in rate asymmetry is present that did not lead to trait rarity, power levels did not decrease as the asymmetry grew (e.g., Table 3.5, 3.6, Fig 3.5 A, B).

In general, investigators who wish to explore parameter asymmetries when binary characters are exceedingly rare in their data sets should be cautious using the BiSSE method and may want to follow the likelihood ratio test methodology suggested by Paradis (2008) to try and untangle which parameters acting alone or in combination are contributing to the rarity of states. Because BiSSE has difficulties with identifying high rate asymmetries in a given parameter accurately, it may mistakenly estimate the wrong parameter (or combination of parameters) to be the cause of

taxonomic excess. But what state rarity is too rare for the BiSSE method to remain effective?

The power of testing hypotheses for asymmetrical speciation rates is less affected by trait rarity bias and power remains high even when only 2.5% of the taxa have one of the binary traits (Table 3.2, Fig 3.2). Power begins to sharply decrease, when the percentage of taxa with one trait falls below this value. Power of character change and extinction rates is more affected by trait rarity with a decrease in power occurring as rate asymmetry causes one trait to be below about 8–10% of the terminal taxa (e.g., Table 3.3, 3.4, Fig 3.3, Fig 3.4). It is likely that a higher percentage of trait rarity is needed to decrease power in speciation rate studies relative to character state change and extinction because speciation rates are more accurately and precisely estimated by the BiSSE method (Maddison et al., 2007). Caution is recommend when trying to use the BiSSE method when there is a 10–90% ratio of binary character states or lower in terminal taxa, as this level of trait rarity may have a negative impact on the power of the analysis and the accuracy and precision of parameter estimation.

One potential method of dealing with this character state bias is to incorporate knowledge of ancestral character state reconstructions of the organisms being studied if sufficient data are available. When rates of character change are highly asymmetrical with the root state stationary and inferred from the model, a decreasing rate of character change from State 1 to 0 recovered an increase of power as the asymmetry grew to 10×, followed by a power decrease to approximately 5% as the asymmetry increased to 100 and 500× (Table 3.6, Fig 3.5 B). As states changed from

0 to 1 in this system the ability to change from 1 to 0 became increasingly small, leading to a rarity of State 0 in the highly asymmetrical simulations. However, if the root is constrained to start at State 0 (assuming State 0 is the known state of the stem ancestor) the bias caused by extreme excess of character State 1 is lessened, and power increases as the rate asymmetry increases (Fig. 3.5 B).

Because stationary frequencies of the root are based on equilibrium frequencies deduced from the rate parameter values of the model, it is possible that highly asymmetrical character rate values may bias the root towards a single state (Goldberg and Igic, 2008), further leading to increased rarity of one character state in certain situations, followed by a decrease in power. If enough information is present, constraining the root to a character state may improve the accuracy and precision of the BiSSE method, assuming that constraint does not bias it further. In the case discussed above, if the root is constrained to State 1, power would be extremely low as the probability of returning to State 0 would be small and few terminal taxa would evolve State 0. In other cases in which the power of a stationary root was compared to a constrained root, the power is not dramatically different between the two root constraints (Table 3.5, Table 3.7). However, in these cases, rates of character change are symmetrical, which would decrease the potential bias associated with stationary rates if the rates of character change are asymmetrical.

Further work is needed to explore the effect of multiple rate asymmetries on the power of the BiSSE method. A subset of simulations were performed to test the effect of multiple asymmetries on the power of rate estimates associated with the

empirical lizardfish data, and the results from these analyses provide evidence that multiple rate asymmetries can have a significant impact on the power of testing a hypothesis of a given parameter. Two things seem to cause a decrease in power when an additional asymmetry is introduced. The first occurs when the additional asymmetry increases the frequency of a state that is counter to the state being increased by the original asymmetry. For example, when the power of an asymmetrical speciation rate of 1.25× is tested with rates of speciation higher under State 0, an additional asymmetry to the rate of character change where the rate from 1 to 0 is smaller than from 0 to 1 caused the percentage of terminal taxa with State 0 to decrease as well as a decrease in power (Table 3.8, Fig 3.6 A).

Second, power decreases when the combinations of multiple rate asymmetries are asymmetrical enough in a particular direction that one of the binary characters is driven to be exceedingly rare. This can occur when the additional asymmetry increases the frequency of the same character state as the initial asymmetry, or when the additional asymmetry overrides the state direction of the initial asymmetry enough that one state becomes rare. When the rate of character change is higher from 1 to 0 than 0 to 1 in combination with a higher rate of speciation under State 0, the percent of taxa with State 0 increased dramatically, leading to an extreme rarity in State 1, and a huge decrease in power (Table 3.8, Fig 3.6 A). Finally, power seems to increase if an asymmetry in the additional rate causes the frequency of a state to grow in combination with the initial rate asymmetry, but to an extent that does not cause a rarity of states. For example, when the extinction rate under State 0 is higher than

State 1 and the rate of character change is higher from 0 to 1 than from 1 to 0, the power of detecting a higher rate of character change from 0 to 1 increases (Table 3.11, Fig 3.7 B).

Returning to the empirical lizardfish data and the question of why two thirds of aulopiform taxa are simultaneous hermaphrodites, a bit of caution must be taken with the results. It has been clearly demonstrated that power levels of any test of rate asymmetry with a smaller data set (in this case 43 taxa) are poor and that the possibility of Type II error is likely. Also, there is a caveat that the unmodified BiSSE likelihood method for estimating rates of diversification assumes complete taxonomic sampling. The sampling of aulopiform taxa represents a good random subset of total aulopiform diversity, and character state bias is not high enough to appear to have an impact on the power of the analysis (26% State 0, 74% State 1). It would be more appropriate to estimate parameter values using the unresolved tree method proposed by Fitzjohn et al. (2009), in which additional taxa not included in the systematic analysis could be grafted to their respective monophyletic groups, thereby increasing taxonomic sampling and parameter estimation. However, this method is currently computationally limited to data sets of fewer than 200 taxa, and an aulopiform analysis conducted in this fashion would have nearly 260 taxa. When the modified BiSSE likelihood method of Fitzjohn et al. (2009) becomes available for larger datasets, the estimated paramaters from this study will be revisited and compared to this alternate method.

The likelihood difference between the unconstrained and constrained (symmetrical) models of speciation are below the significant value produced from null hypothesis simulations, suggesting that rates of speciation in lizardfishes under States 0 and 1 are not significantly asymmetrical. Taxa under State 0 ($\lambda_0 = 0.133$) have a speciation rate approximately 1.2× higher than under State 1 ($\lambda_1 = 0.114$), however, this rate difference recovered a consistently low power across simulations of 43, 100, 300, and 500 taxa (Table 3.1, Fig 3.3), suggesting that the low power for this asymmetry is not caused simply by low tree size, and that the failure to reject the null hypothesis of rate symmetry is potentially not a type II error. Results of a similar difference in speciation rate of 1.25× with symmetrical rates of extinction and character change have a slightly higher power of near 12%, with power decreasing to levels similar to those observed in the tree simulations with 500 taxa of the estimated lizardfish parameters when an additional asymmetry was introduced to character change or extinction that closely mirrored the estimated lizardfish parameters (Table 3.1, 3.8, 3.9). This suggests that the multiple asymmetries have slightly affected the power of the lizardfish speciation rate parameters when estimated with a 500-taxa tree size, but only slightly, with a reduction from 12–4%. Currently it seems unlikely that the estimated speciation rates are significantly different for taxa with separate sexes and simultaneous hermaphroditism.

This same result is recovered for tests of asymmetry in extinction under States 0 and 1. Extinction rates are both estimated to be very low and nearing 0, with extinction rates higher under State 0 than State 1. The likelihood difference between

the values is extremely small (0.065), and the null hypothesis that rates are symmetrical is not rejected. Hypothesis testing with the same rate values for tree sizes of 43, 100, 300, and 500 taxa recovered similarly low powers ranging from 4.8–5.8% again suggesting that the inability to reject the null hypothesis is not simply an issue related to tree size. Rates are similarly low when additional asymmetries were added to speciation and character change (Table 3.12, 3.13).

Extinction rates recovered from molecular data alone have traditionally been difficult to estimate with any certainty and often approach 0 (e.g., Nee et al., 1994, Paradis, 2005) as the only events that are directly interpreted from molecular phylogenies currently are cladogenetic, although signal of extinction may be present. In general, the BiSSE method has a difficult time estimating rates of extinction with any accuracy or precision (Maddison et al., 2007), and extinction rates near 0 also may result from using the BiSSE likelihood method with incomplete taxonomic sampling (FitzJohn et al., 2009). Aulopiform fishes have a rich fossil record, particularly of taxa associated with extant clades that are simultaneous hermaphrodites, and it is quite probable that the extinction rates within aulopiformes are not as small as estimated. While rates of extinction are found to not be significantly asymmetrical, it is difficult to make any definitive statements about extinction rates in lizardfishes without further study.

Rates of character change in lizardfish are higher from 0 to 1 (q_{01} = 0.0055) than from 1 to 0 (q_{10} = 0.00001), although the likelihood difference (0.615) is not recovered as significant being below the 5% cutoff estimated from simulations of the

symmetrical null hypothesis. While the power of rejecting a null hypothesis of rate symmetry is expectedly small with a tree size of 43 taxa, power increased as tree size increased (Fig 3.1) to approximately 25% in 500 taxa. This suggests that there is some possibility of a Type II error. Additionally, this difference in rates is comparable to the simulations of character rate change where rates from 0 to 1 were 0.005 and rates from 1 to 0 were 0.00001. In those simulations power of this 500 times difference is nearly 60% when all other rate parameters are symmetrical (Fig 3.5 B).

In the character state simulations in which a 500 times difference in rates is simulated with the rate of 1 to 0 being smaller than the rate of 0 to 1, an increase in speciation under State 0 relative to State 1 caused power to decrease rapidly (Table 3.10, Fig 3.13). Power levels decreased to levels near those observed in the lizardfish simulation of 500 taxa in which speciation under state 0 is 1.2 times greater than under state 1 (Table 3.1, 3.10). These results suggest that the inability to reject the null hypothesis with the estimated rate difference from the lizardfish data set may be a Type II error resulting from low tree size, and that this asymmetry may be playing a role in the excess of lizardfish taxa with simultaneous hermaphroditism.

If this is the case, it is possible that simultaneous hermaphroditism evolved once with a very small rate (q_{01} = 0.0055) and the rate of change back to separate sexes (q_{10} = 0.00001) is so small that it has yet occurred, accounting for the excess of lizardfish diversity with this reproductive strategy, as well as the singular evolutionary event of this trait observed in aulopiforms. It is also not unexpected that

the rate of change from separate sexes to simultaneous hermaphroditism would be small, as this reproductive strategy is exceedingly rare among vertebrates. Additionally, because there is only a single evolutionary event of simultaneous hermaphroditism, any codistributed character would possess the same rates of character change, and results described above.

It is also possible that the excess of taxa can be explained through other evolutionary situations not explored by the BiSSE method. There is a possibility that the net rate of diversification is highly heterogeneous among aulopiform lineages (Rabosky et al., 2007), or that the taxonomic excess is simply a factor of clade age rather than diversification (McPeek and Brown, 2007). These potential factors are outside the scope of the current study, and will be addressed by future papers.

CONCLUSIONS

The power of the BiSSE likelihood method to test hypotheses of rate asymmetry is highly susceptible to both tree size and variation in parameter rates. If parameter values are too asymmetrical, BiSSE is unable to accurately estimate rates when the asymmetry results in one of the binary character states being exceedingly rare, which in turn, results in a dramatic decrease of power. In such cases, it may be advantageous to constrain the root to an estimated state if enough information is available to make a strong prediction of ancestral state, as this may help increase power. Preliminary simulations examining the impact of multiple rate asymmetries demonstrate that power of estimating symmetry of a given parameter can be effected by additional asymmetries in other parameters, and further exploration of the impact

of multiple asymmetries is needed. Overall, caution should be exercised when using the BiSSE method, as statistical power can be severely affected by a number of variables.

Within lizardfishes, the evolution of simultaneous hermaphroditism or any other codistributed character does not seem to be influencing rates of speciation or extinction. While power is small for tree sizes used in this study potentially increasing the chances of a Type II error, the estimated rates display similarly low powers when applied to tree sizes of 100, 300, and 500 taxa. This suggests that tree size is not the principal factor for the low power, and that the rates themselves are simply not large enough to be significantly asymmetrical. While the rate of character change from separate sexes to simultaneous hermaphroditism is 500 times lower than from simultaneous hermaphroditism to separate sexes, the difference is not found to be statistically significant. However, this rate difference is shown to have higher power in simulations with larger tree sizes, and low power of estimating character state change in this case is potentially the result of an asymmetry in speciation where State 0 has slightly higher speciation than State 1. This suggests that the failure to reject the null hypothesis in this case is potentially a Type II error, and that this rate asymmetry may be playing a factor in the excess of aulopiform taxa that are simultaneous hermaphrodites.

LITERATURE CITED

Alfaro, M. E., Santini, F., Brock, C., Alamillo, H., Domburg, A., Rabosky, D.L., Carnevale, G., & Harmon, L.J. (2009): Nine exceptional radiations plus high turnover explain species diversity in jawed vertebrates. – Proc. Nat. Acad. Sci. **106**: 13410–13414.

Arratia, G. (1997): Basal teleosts and teleostean phylogeny. – Palaeo. Ichthy. **7**: 5–168.

Arratia, G. (1999): The monophyly of Teleostei and stem-group teleosts, consensus and disagreements. – In: G. Arratia, & H.P. Schultze (eds.). *Mesozoic Fishes 2 and Fossil Record*. 265–334. München (Verlag Dr. F. Pfeil).

Arratia, G. (2000a): New teleostean fishes from the Jurassic of southern Germany and the systematic problems concerning the 'pholidophoriforms'. – Paleo. Zeits. **74**(1/2): 113–143.

Arratia, G. (2000b): Phylogenetic relationships of teleostei past and present. – Estud. Oceanol. **19**: 19–51.

Arratia, G. (2001): The sister-group of teleostei: consensus and disagreements. – Jour. Vert. Paleo. **21**(4): 767–773.

Arratia, G. (2004): Mesozoic halecostomes and the early radiation of teleosts. – In: G. Arratia & A. Tintori (eds.). Mesozoic Fishes 3 – Systematics, Paleoenvironments, and Biodiversity: 279–315; München (Verlag Dr. F. Pfeil).

Baldwin, C. C. & Johnson, G. D. (1996): Aulopiform interrelationships. In: – Stiassny, M. L. J., Parenti, L. R., & Johnson, G. D. (eds.). Interrelationships of Fishes: 355–404; San Diego (Academic Press).

Bertelsen, E., Krefft, G. & Marshall, N. B. (1976): The fishes of the family Notosudidae. – Dana. Rep. **86**: 1–114.

Chalifa, Y. (1989): Two new species of longirostrine fishes from the early Cenomanian (Late Cretaceous) of Ein-Yabrud, Israel, with comments on the phylogeny of the Dercetidae. – J. Vertebr. Paleontol. **9**(3):314–328.

Danforth, B. N., Sipes, S., Fang, J. & Brady, S. G. (2006): The history of early bee diversification based on five genes plus morphology. – Proc. Natl. Acad. Sci. **103**(41): 15118–23.

Davis, M. P. (2010). Evolutionary relationships of the Aulopiformes (Euteleostei: Cyclosquamata): a molecular and total evidence approach. In: Nelson, J. S., Schultze, H.-P., and Wilson, M. V. H. (Eds.), Origin and phylogenetic interrelationships of teleosts. München (Verlag Dr. F. Pfeil). In press.

De Figueiredo, F. J. & Gallo, V. (2005): A new dercetid fish (Neoteleostei: Aulopiformes) from the Turonian of the Pelotas Basin, southern Brazil. – Palaeontol. **49**(2): 445–456.

Denton, E. J. (1990): Light and vision at depths greater than 200 metres. In: Herring, P.J., Campbell, A.K., Whitfiield, M., & Maddock, L. (Eds.), *Light and life in the sea*. 127–148. Cambridge University Press, Cambridge, New York.

Douglas, R. H., Partridge, J. C., & Marshall, N. J. (1998): The eyes of deep-sea fish I: lens pigmentation, tapeta and visual pigments. – Prog. Retin. Eyes. Res. **17**(4): 597–636.

Drummond A. J, Ho S. Y. W., Phillips M. J. & Rambaut A (2006): *PLoS Biology* **4**, e88

Drummond A. J, & Rambaut A (2007) "BEAST: Bayesian evolutionary analysis by sampling trees." *BMC Evolutionary Biology* **7**:214

Felsenstein, J. (1981): Evolutionary trees from DNA sequences: A maximum likelihood approach. – J. Mol. Evol. **17**: 368–376.

Felsenstein, J. (1985): Confidence limits on phylogenies: an approach using the bootstrap. – Evol. **39**: 783–791.

Fielitz, C. (2004): The phylogenetic relationships of the Enchodontidae (Teleostei: Aulopiformes). – In: Arratia, G., Wilson, M. V. H., & Cloutier, R. (eds.). *Recent Advances in the Origin and Early Radiation of Vertebrates*: 619–634. München (Verlag Dr. F. Pfeil).

Fielitz, C., & González Rodríguez, K. (2008): A new species of *Ichthyotringa* from the El Doctor Formation (Cretaceous), Hidalgo, Mexico. – In: Arratia, G., Schultze, H. P., & Wilson, M. V. H. (eds.). *Mesozoic Fishes 4 – Homology and Phylogeny*: 373–388. München (Verlag Dr. F. Pfeil).

FitzJohn, R. G., Maddison, W. P., & Otto, S. P. (2009): Estimating Trait-Dependent Speciation and Extinction Rates from Incompletely Resolved Phylogenies. – Syst. Biol. **58(6)**: 595–611.

Gallo, V., & Coelho, P. M. (2008): First occurrence of an aulopiform fish in the Barremian of the Sergipe-Alagoas Basin, northeastern Brazil. – In: Arratia, G., Schultze, H. P., & Wilson, M. V. H. (eds.). *Mesozoic Fishes 4*: 351–371. München (Verlag Dr. F. Pfeil).

Glenner, H., Hansen, A., Sorensen, M., Ronquist, F., Huelsenbeck, J. & Willerslev, E. (2004): Bayesian inference of the metazoan phylogeny: A combined molecular and morphological approach. – Curr. Biol. **14**(18): 1644–1649.

Goldberg, E. E., & Igic, B. (2008): On phylogenetic tests of irreversible evolution. – Evol. **62**: 2727–2741.

Gosline, W. A., Marshall, N. B. & Mead, G. W. (1966): Order Iniomi. Characters and synopsis of families. – In: Fishes of the Western North Atlantic. – Sears Found. Mar. Res., Mem. **1**(5): 1–18. New Haven, CT. (Yale University).

Hartel, K. E. & Stiassny, M. L. J. (1986): The identification of larval *Parasudis* (Teleostei, Chlorophthalmidae); with notes on the anatomy and relationships of aulopiform fishes. –Breviora **487**: 1–23.

Helfman, G. S., Collette, B. B. & Facey, D. E. (1997): The Diversity of Fishes. – 544 pp.; Maiden, Massachusetts (Blackwell Science, Inc.).

Hillis, D. M. & Bull, J. J., (1993): An empirical test of bootstrapping as a method for assessing confidence in phylogenetic analysis. – Syst. Biol. **42**: 182–192.

Hillis, D. M., Mable, B. K., Larson, A., Davis, S. & Zimmer, E. A. (1996): Nucleic acids IV: Sequencing and cloning. – In: Hillis, D. M., Moritz, C., & Mable, B. K. (eds.). Molecular Systematics: 321–385. Sunderland, MA (Sinauer Associates).

Holcroft, N. I. (2004): A molecular test of alternative hypotheses of tetraodontiform (Acanthomorpha: Tetraodontiformes) sister group relationships using data from the RAGI gene. – Molec. Phylo. Evol. **32**: 749-760.

Hurley, I. A., Mueller, R. L., Dunn, K. A., Schmidt, E. J., Friedman, M., Ho, R. K., Prince, V. E., Yang, Z., Thomas, M.G., & Coates, M.I. (2007): A new time-scale for ray-finned fish evolution. – Proc. R. Soc. B. **274**: 489–498.

Inoue, J. G., Miya, M., Tsukamoto, K. & Nishida, M. (2001): A mitogenomic perspective on the basal teleostean phylogeny: resolving higher-level relationships with longer DNA sequences. – Molec. Phylo. Evol. **20**: 275–285.

Johnson, R. K. (1982): Fishes of the families Evermannellidae and Scopelarchidae (Pisces, Myctophiformes). – Field. Zool. **66**: 1–249.

Johnson, G. D. (1992): Monophyly of the euteleostean clades—Neoteleostei, Eurypterygii, and Ctenosquamata. – Copeia **1992**: 8–25.

Johnson, G. D., Baldwin, C. C., Okiyama, M., & Tominaga, Y. (1996): Osteology and relationships of *Pseudotrichonotus altivelis* (Teleostei: Aulopiformes: Pseudotrichonotidae). – Ichthyol. Res. **43**: 17–45.

Källersjö, M., Albert, V. A. & Farris, J. S. (1999): Homoplasy increases phylogenetic structure. – Cladistics **15**: 91–93.

Kawaguchi, A., Miya, M. & Nishida, M. (2001): Complete mitochondrial DNA sequence of *Aulopus japonicus* (Teleostei: Aulopiformes), a basal Eurypterygii: longer mDNA sequences and higher-level relationships. – Ichyol. Res. **48**(3): 213–223.

Kriwet, J. (2003): Lancetfish teeth (Neoteleostei, Alepisauroidei) from the Early Cretaceous of Alcaine, NE Spain. – Lethaia. **36**: 323–332.

Land, M. F. (1981): Optics and vision in invertebrates. In: Autrum, H. (Eds.), *Handbook of sensory physiology*. 471–592. Springer Verlag, Berlin.

Land, M. F. (1990): Optics of the eyes of marine animals. In: Herring, P.J., Campbell, A.K., Whitfiield, M., & Maddock, L. (Eds.), *Light and life in the sea*. 149–166. Cambridge University Press, Cambridge, New York.

Lewis, P. (2001): A likelihood approach to estimating phylogeny from discrete morphological character data. – Syst. Biol. **50**(6): 913–925.

Li, C. & Ortí, G. (2006): Molecular phylogeny of Clupeiformes (Actinopterygii) inferred from nuclear and mitochondrial DNA sequences. – Molec. Phylo. Evol. **44**: 386–398.

Li, C., Ortí, G., Zhang, G. & Lu., G. (2007): A practical approach to phylogenomics: the phylogeny of ray-finned fish (Actinopterygii) as a case study. – BMC. Evol. Biol. **7**(44) 1–11.

López, J. A., Chen, W–J. & Ortí., G. (2004): Esociform phylogeny. – Copeia **3**(2004): 449–464.

Maddison, W. P. (2006): Confounding asymmetries in evolutionary diversification and character change. – Evol. **60**: 1743–1746.

Maddison, W. P., Midford, P. E., & Otto, S. P. (2007): Estimating a Binary Character's Effect on Speciation and Extinction. – Syst. Biol. **56(5)**: 701–710.

Maddison, W. P. & D.R. Maddison. (2009). Mesquite: a modular system for evolutionary analysis. Version 2.7 http://mesquiteproject.org.

Mank, J. E., Promislow, D. E., & Avise, J. C. (2006): Evolution of alternative sex-determining mechanisms in teleost fishes. – Biol. J. Linn. Soc. **87**: 83–93.

Marshall, N. B. (1954): Aspects of Deep Sea Biology. – 380 pp.; London (Hutchinsons).

McPeek, M. A., & Brown, J. M. (2007): Clade age and not diversification rate explains species richness among animal taxa. – Amer. Natur. **169(4)**: E97–E106.

Mead, G. W., Bertelsen, E., and& Cohen, D. M. (1964): Reproduction amoung Deep Sea Fishes. – Deep. Sea. Res. **11**: 569–596.

Miya, M. & Nishida, M. (2000): Use of mitogenomic information in teleostean molecular phylogenetics: a tree-based exploration under the maximum-parsimony optimality criterion. – Molec. Phylo. Evol. **17**: 437–455.

Miya, M., Kawaguchi, A. & Nishida, M. (2001): Mitogenomic exploration of higher teleostean phylogenies: a case study for moderate-scale evolutionary genomics with 38 newly determined complete mitochondrial DNA sequences. – Molec. Biol. Evol. **18**: 1993-2009.

Miya, M., Takeshima, H., Endo, H., Naoya, I., Inoue, G., Mukai, T., Satoh, T., Yamaguchi, M., Kawaguchi, A., Mabuchi, K., Shirai, S. & Nishida, M. (2003): Major patterns of higher teleostean phylogenies: A new perspective based on 100 complete mitochondrial DNA sequences. – Molec. Phyl. Evol. **26**: 121–138.

Moritz, C., Dowling, T.E. & Brown, W. M. (1987): Evolution of animal mitochondrial DNA: Relevance for population biology and systematics. – Ann. Rev. Ecol. Syst. **18**: 269–292.

Munk, O. (1959): The eyes of *Ipnops murrayi*. – Galathea. **3**: 79–87.

Nee, E. C., Holmes, E. C., May, R. M., & Harvery, P. H. (1994): Extinction Rates can be estimated from molecular phylogenies. – Phil. Trans. Biol. Sci. **344(1307)**: 77–82.

Nelson J. S.(2006): Fishes of the World, 4th ed. – 624 pp.; New York (Wiley).

Nylander, J. A. A. (2004): MrModeltest 2.0. – Distributed by the author. Uppsala.

Nylander, J. A., Ronquist, F., Huelsenbeck, J. P. & Nieves-Aldrey, J. L. (2004): Bayesian phylogenetic analysis of combined data. – Syst. Biol. **53**(1): 47–67.

Olney, J. E., Johnson, G. D. & Baldwin, C.C. (1993): Phylogeny of lampridiform fishes. Bull. Mar. Sci. **52**(1): 137–169.

Page, R. D. (1996): Treeview: an application to display phylogenetic trees on personal computers. – Comput. Appl. Biosci. **12**: 357–358.

Paradis, E. (2005): Statistical analysis of diversification with species traits. – Evol. **59**: 1–12.

Paradis, E. (2008): Asymmetries in phylogenetic diversification and character change can be untangled. – Evol. **62**: 241–247.

Parin, N. V. & Kotlyar, A. N. (1989): A new aulopodid species, *Hime microps*, from the eastern South Pacific, with comments on geographic variation of *H. japonica*. – Jpn. J. Ichthyol. **35**: 407–413.

Patterson, C. (1993): Osteichthyes: Teleostei. – In Benton, M. (eds.) *The Fossil Record 2*. 621–656. Chapman and Hall, London.

Patterson, C. & Johnson, G. D. (1995): The intermuscular bones and ligaments of teleostean fishes. – Smithson. Contrib. Zool. **559**: 1–83.

Paxton, J. R. (1972): Osteology and relationships of the lanternfishes (Family Myctophidae). – Bull. Nat. Hist. Mus. L.A. Cty. **13**: 1–81.

Peden, J. (2005): CodonW 1.4.2. – Distributed by the author. Nottingham.

Post, A. (1987): Results of the research cruises of FRV "Walther Herwig" to South America. LXVII. Revision of the subfamily Paralepidinae (Pisces, Aulopiformes, Alepisauroidei, Paralepididae). I. Taxonomy, morphology and geographical distribution. – Arch. Fischer. **38**: 75–131.

Prokofiev, A. M. (2006): Fossil myctophoid fishes (Myctophiformes: Myctophoidei) from Russia and adjacent regions. – Jour. Ichthy. **46**: 38–83.

Rabosky, D. L., Donellan, S. C., Talaba, A. L., & Lovette, I. J. (2007): Exceptional among-lineage variation in diversification rates during the radiation of Australia's most diverse vertebrate clade. – Proc. R. Soc. B. **274**: 2915–2923.

Rambaut, A., & Drummond, A.J. (2007): Tracer v1.4.

Regan, C. T. (1911): The anatomy and classification of the teleostean fishes of the Order Iniomi. – Ann. Mag. Nat. Hist. **7**: 120–133.

Regan, C. T. (1925): The fishes of the genus *Gigantura,* A. Brauer; based on specimens collected in the Atlantic by the "Dana" expeditions, 1920-22. – Ann. Mag. Nat. Hist. **15**: 53–59.

Ronquist, F., & Huelsenbeck, J. P. (2003): MrBayes 3: Bayesian phylogenetic inference under mixed models. – Bioinfor. **19**: 1572–1574.

Rosen, D. E. (1973): Interrelationships of higher euteleosteans. – In: Greenwood, P. H., Miles, R. S. & Patterson, C. (eds.). Interrelationships of Fishes: 397–513. London (Academic Press).

Rosen, D. E. (1985): An essay on euteleostean classification. – Am. Mus. Novit. **2827**:1–57.

Saiki, R. K. (1990): Amplification of genomic DNA. In: Innis. M. A., Gelfand, D. H., Sninsky, J. J. & White, T. J. (eds.). PCR Protocols: A Guide to Methods and Applications: 13-20. New York (Academic Press).

Sato, T., & Nakabo, T. (2002): Paraulopidae and *Paraulopus*, a new family and genus of aulopiform fishes with revised relationships within the order. – Ichthyol. Res. **49**: 25–46.

Shimodaira, H., & Hasegawa, M. (1999): Multiple comparisons of log-likelihoods with applications to phylogenetic inference. – Mol. Biol. Evol. **16**: 1114–1116.

Smith, W. L. & Wheeler, W. C. (2004): Polyphyly of the mail-cheeked fishes (Teleostei: Scorpaeniformes): Evidence from mitochondrial and nuclear sequence data. – Molec. Phyl. Evol. **32**: 627–646.

Stiassny, M. L. J. (1986): The limits and relationships of acanthomorph teleosts. – J. Zool. (B) **1**: 411–460.

Sulak, K. J. (1977): The systematics and biology of *Bathypterois* (Pisces: Chlorophthalmidae) with a revised classification of benthic myctophiform fishes. – Galath. Rep. **14**: 49–108.

Swofford, D. L. (2002: PAUP*. Phylogenetic Analysis Using Parsimony (*and Other Methods). Version 4. – Sunderland (Sinauer Associates).

Tamura, T., & Nei, M. (1993): Estimation of the number of nucleotide substitutions in the control region of mitochondrial DNA data. – Mol. Biol. Evol. **10**: 512–526.

Taverne. L. (2004): Les poissons crétacés de Nardò. 19º. *Nardorex zorzoni* gen. et sp. nov. (Teleostei, Aulopiformes, Alepisauroidei). – Bollet. Mus. Civ. Stor. Natu. Ver., Geolo. Paleon. Preist. **28**: 29–40.

Taverne, L. (2005): Les poissons crétacés de Nardò. 21º. *Ophidercetis italiensis* gen. et sp. nov. (Teleostei, Aulopiformes, Dercetidae). Une solution ostéologique au problème des genres *Dercetis* et *Benthesikyme* (= *Leptotrachelus*). Bollet. Mus. Civ. Stor. Natu. Ver., Geolo. Paleon. Preist. **29**: 55–79.

Thompson, B. A. (1998): Redescription of *Aulopus bajacali* Parin & Kotlyar, 1984, comments on its relationship and new distribution records. – Ichthol. Res. **45**(1): 43–51.

Vernon, J. E. (1995): Corals in space and time: the biogeography and evolution of the Scleractinia. – UNSW Press, Sydney, Australia.

Walters, V. (1961): A contribution to the biology of the Giganturidae, with description of a new genus and species. – Bull. Mus. Comp. Zool. **125**: 297–319.

Wiens, J. J. (2003): Missing data, incomplete taxa, and phylogenetic accuracy. – Syst. Biol. **52**: 528–538.

Wiens, J. J. (2006): Missing data and the design of phylogenetic analyses. – J. Biomed. Infor. **39**: 34–42.

Wright, F. (1990): The ‘effective number of codons’ used in a gene. – Gene **87**: 23–29.

Zwickl, D. J. (2006): Genetic algorithm approaches for the phylogenetic analysis of large biological sequence datasets under the maximum likelihood criterion. – Ph.D. dissertation, The University of Texas at Austin.

APPENDIX 1.1: Abbreviated List of Morphological Characters. Reproduced and modified from Baldwin and Johnson (1996) and Sato and Nakabo (2002). For full descriptions and figures, please see the respective studies.

Gill Arches

1.– Second epibranchial uncinate process: absent (0), present, enlarged (1), present, not enlarged, end of second pharyngobranchial displaced posterolaterally (2), present, not enlarged, end of second pharyngobranchial displaced posteriorly (3), (Baldwin and Johnson [1], 1996; Sato and Nakabo [32], 2002).

2.– Cartilaginous condyle on dorsal surface of third pharyngobranchial: PB3 with cartilaginous condyle articulating with EB2 (0), PB3 without cartilaginous condyle articulating with EB2 (1), (Baldwin and Johnson [2], 1996).

3.– Fourth pharyngobranchial toothplate: UP4 present (0), UP4 absent (1), (Baldwin and Johnson [3], 1996).

4.– Articulation of first pharyngobranchial: PB1 articulates at distal tip of EB1 (0), PB1 articulates at proximal base of cartilaginous tip of EB1 (1), (Baldwin and Johnson [4], 1996).

5.– Gill rakers or toothplates: Gill rakers long, lathlike (0), gill rakers present as toothplates (1), single elongate gill raker on EB1 (2), (Baldwin and Johnson [5], 1996).

6.– Second pharyngobranchial with extra uncinate process: PB2 without extra uncinate process (0), PB2 without extra uncinate process but with expanded proximal base (1), PB2 with extra uncinate process (2), (Baldwin and Johnson [6], 1996).

7.– Second pharyngobranchial toothplate: UP2 present (0), UP2 absent (1), (Baldwin and Johnson [7], 1996).

8.– Second pharyngobranchial uncinate process: PB2 with short uncinate process (0), PB2 with long uncinate process (1), (Baldwin and Johnson [8], 1996).

9.– Uncinate process of second epibranchial adjacent to second epibranchial: EB2 uncinate process diverges from EB2 as it approaches PB3; PB2 oriented anteromedial to posterolateral (0), EB2 uncinate process adjacent to EB2 as both approach PB3; PB2 oriented anterior to posterior (1), (Baldwin and Johnson [9], 1996).

10.– Articulation between uncinate processes of first epibranchial and second pharyngobranchial: EB1 and PB2 articulate via uncinate processes (0), uncinate process of EB1 does not articulate with that of PB2 (1), uncinate process on EB1 absent (2), (Sato and Nakabo [43], 2002).

11.– Third pharyngobranchial produced: PB3 not extending anteriorly beyond the tips of EB1 and PB2 (0), PB3 extending anteriorly beyond the tips of EB1 and PB2 (1), (Baldwin and Johnson [10], 1996).

12.– Bony ridge on dorsal surface of third pharyngobranchial: absent (0), present (1), (Sato and Nakabo [34], 2002).

13.– Distribution of PB3 teeth: UP3 covering large area of ventral surface of PB3 (0), UP3 restricted to lateral edge of ventral surface of PB3 (1), UP3 absent (2), (Baldwin and Johnson [11], 1996).

14.– Size of PB3 teeth: small (0), large (1), (Baldwin and Johnson [12], 1996).

15.– First pharyngobranchial: PB1 normal or reduced (0), PB1 very long (1), PB1 absent (2), (Baldwin and Johnson [13], 1996; Sato and Nakabo [38], 2002).

16.– Fourth epibranchial morphology: EB4 has a slender proximal end and an uncinate process attached to the fourth levator externus (0), end of EB4 slender, but lacks an uncinate process (1), EB4 has an expanded proximal end capped with a large band of cartilage and an uncinate process at the middle (2), proximally expanded EB4 lacking an uncinate process (3), (Sato and Nakabo [44], 2002).

17.– Ossification of first epibranchial and ceratobranchial: well ossified and capped by a proximally short cartilage (0), ossification weak, proximal cartilaginous portions long (1), (Sato and Nakabo [46], 2002).

18.– Fifth epibranchial: EB5 absent (0), EB5 present (1), (Baldwin and Johnson [14], 1996; Sato and Nakabo [45], 2002)

19.– Dentition of fifth ceratobranchial: teeth scattered all over anterodorsal surface (0), teeth restricted to medial edge of anterodorsal surface (1), teeth restricted to medial edge of anterodorsal surface (2), without teeth (3), (Baldwin and Johnson [15], 1996).

20.– Shape of fifth ceratobranchial: CB5 not V-shaped (0), CB5 V-shaped, the medial limb slender (1), CB5 V-shaped, the medial limb robust (2), (Baldwin and Johnson [16], 1996).

21.– Gap between the fourth basibranchial cartilage and fifth ceratobranchials: no gap (0), gap between CB5s and BB4 cartilage, CB5s not articulating with reduced BB4 (1), CB5s separated from main body of BB4 by tail or small nubbins of cartilage extending posteriorly from BB4 (2), (Baldwin and Johnson [17], 1996).

22.– Third basibranchial extends beyond fourth basibranchial cartilage: BB3 terminates beneath the anterior end of BB4 cartilage (0), BB3 terminates beyond the posterior end of BB4 cartilage (1), (Baldwin and Johnson [18], 1996).

23.– Fourth basibranchial ossified: cartilaginous (0), ossified (1), (Baldwin and Johnson [19], 1996).

24.– Elongate first basibranchial: BB1 not elongate (0), BB1 elongate, ossified (1), BB1 usually elongate, comprising a short ossified anterior segment followed by a long posterior cartilage (2), (Baldwin and Johnson [20], 1996).

25.– Elongate second basibranchial: not elongate (0), elongate (1), (Baldwin and Johnson [21], 1996).

26.– Gillrakers or toothplates on third hypobranchials: present on HB3 (0), absent on HB3 (1), (Baldwin and Johnson [22], 1996).

27.– Gillrakers or toothplates on basibranchials: lacking on basibranchials (0), present on BB2, sometimes BB1 and BB3 (1), (Baldwin and Johnson [23], 1996).

28.– Gill rakers on medial surface of gill arches: present (0), absent on first arch only (1), present on first hypobranchial only (2), absent (3), (Sato and Nakabo [50], 2002).

29.– Ligament between first hypobranchial and ventral hypohyal: not ossified (0), ossified (1), (Baldwin and Johnson [24], 1996).

30.– First hypobranchial with ventrally directed processes: without ventrally directed processes (0), with a ventrally directed process (1), (Baldwin and Johnson [25], 1996).

31.– Second hypobranchial with ventrally directed process: without ventrally directed processes (0), with a ventrally directed process (1), (Baldwin and Johnson [26], 1996).

32.– Third hypobranchials fused ventrally: not fused (0), fused (1), (Baldwin and Johnson [27], 1996).

Hyoid Arch

33.– Ventral ceratohyal cartilage: anterior ceratohyal without autogenous ventral cartilage (0), anterior ceratohyal with autogenous cartilage along ventral margin (1), (Baldwin and Johnson [28], 1996).

34.– Number of branchiostegals on the posterior ceratohyal: four or fewer (0), five (1), six or more (2), (Baldwin and Johnson [29], 1996).

35.– Number of branchiostegals on the anterior ceratohyal: five or more (0), four or fewer (1), (Baldwin and Johnson [30], 1996).

36.– Proximity of posteriormost tow branchiostegals: all branchiostegals on posterior ceratohyal evenly spaced (0), two posteriormost branchiostegals close, inserting on ventral margin of posterior ceratohyal (1), two posteriormost branchiostegals close, inserting on posteroventral corner of posterior ceratohyal (2), (Baldwin and Johnson [31], 1996).

37.– 3 + 1 arrangement of branchiostegals on the anterior ceratohyal: branchiostegals on anterior ceratohyal evenly spaced (0), branchiostegals on anterior ceratohyal arranged in “3 + 1” pattern (1), (Baldwin and Johnson [32], 1996).

38.– Hypohyal branchiostegals: no branchiostegals on ventral hypohyal (0), anteriormost branchiostegal on ventral hypohyal (1), anteriormost three branchiostegals on ventral hypohyal (2), (Baldwin and Johnson [33], 1996).

39.– Basihyal morphology: basihyal oriented horizontally (0), basihyal oriented obliquely (1), basihyal oriented at 90° angle to BB1 (2), (Baldwin and Johnson [34], 1996).

40.– Basihyal teeth: absent or unmodified (0), present as large, posteriorly curved structures (1), (Baldwin and Johnson [35], 1996).

Jaws, Suspensorium, and Circumorbitals

41.– Dominant tooth-bearing bone: premaxilla (or premaxilla and maxilla) (0), premaxilla and palatine (1), palatine (2), (Baldwin and Johnson [36], 1996).

42.– Quadrate with produced anterior limb: quadrate fan-shaped (0), quadrate with produced anterior limb (1), (Baldwin and Johnson [37], 1996).

43.– Quadrate with two distinct cartilaginous heads: quadrate with single large cartilage on dorsal border (0), quadrate cartilage separated into tow condyles (1), (Baldwin and Johnson [38], 1996).

44.– Large concavity in dorsal margin of quadrate: no concavity (0), concavity between anterior and posterior cartilaginous condyles (1), (Baldwin and Johnson [39], 1996).

45.– Posterior cartilaginous condyle of quadrate articulates with hyomandibular: posterior portion of quadrate articulates dorsally with metapterygoid (0), posterior cartilaginous condyle of quadrate articulates dorsally with hyomandibular (1), (Baldwin and Johnson [40], 1996).

46.– Metapterygoid produced anteriorly: metapterygoid overlies quadrate (0), metapterygoid extends anteriorly over posterior portion of ectopterygoid (1), (Baldwin and Johnson [41], 1996).

47.– Metapterygoid free of hyomandibular: metapterygoid bound to hyomandibular (0), metapterygoid free from hyomandibular (1), (Baldwin and Johnson [42], 1996).

48.– Ectopterygoid teeth: without teeth (0), teeth on ventral margin of ectopterygoid (1), (Sato and Nakabo [20], 2002).

49.– Endopterygoid teeth: present (0), absent (1), (Sato and Nakabo [21], 2002).

50.– Hyomandibular and opercle oriented horizontally: hyomandibular oriented vertically or subvertically, opercle posterior to suspensorium (0), hyomandibular oriented ca. horizontally, opercle rotated dorsally to lie above hyomandibular (1), (Baldwin and Johnson [43], 1996).

51.– Hyomandibular condyle for articulation with skull: two condyles for articulation with skull (0), one condyle for articulation (1), (Sato and Nakabo [19], 2002).

52.– Ossification of palatine prong: well developed cartilaginous head overhanging the proximal portion of the maxilla in adult (0), mostly ossified, capped by cartilage only at its dorsal tip (1), palatine prong absent (2), (Baldwin and Johnson [44], 1996; Sato and Nakabo [5], 2002).

53.– Dorso-medially directed premaxillary process: premaxilla without dorso-medially directed process medial edge (0), premaxilla with dorso-medially directed process on medial edge (1), (Baldwin and Johnson [45], 1996).

54.– Number of infraorbitals: six (0), seven (1), eight (2), five (3), three (4), none (5), (Baldwin and Johnson [46], 1996).

55.– Long snout: snout length less than 50 percent head length (0), snout length greater than 50 percent head length (1), (Baldwin and Johnson [47], 1996).

56.– Premaxillary fenestra: no premaxillary fenestra (0), anterior premaxilla with fenestra (1), (Baldwin and Johnson [48], 1996).

57.– Palatine articulates with premaxilla: palatine without process for articulation with premaxilla (0), palatine with long process for articulation with premaxilla (1), (Baldwin and Johnson [49], 1996).

58.– Palatine morphology: ventral portion of the palatine expanded laterally (0), lateral expansion absent (1), (Sato and Nakabo [23], 2002).

59.– Position of palatinad cartilaginous facet for articulation with lateral ethmoid: facet located anteriorly (0), facet located on the posterior portion of palatine (1), absent (2), (Sato and Nakabo [24], 2002).

60.– Maxillary palatinad facet on maxilla: present (0), absent (1), (Sato and Nakabo [7], 2002).

61.– Lacrimal oriented horizontally on snout: lacrimal bordering orbit anteriorly (0), lacrimal anterior to orbit, oriented horizontally (1), (Baldwin and Johnson [50], 1996).

62.– Maxilla reduced: maxilla well developed with posterior end expanded (0), maxilla intact but slender, posterior end not expanded (1), maxilla present as posterior remnant (2), maxilla present as anterior remnant (3), (Baldwin and Johnson [51], 1996).

63.– Outer tooth patch on tip of lower jaw: absent (0), outer tooth patch exposed to the outside on tip of lower jaw (1), outer tooth patch separated from the inner tooth patch, becomes elongated along the margin of lower jaw (2), (Sato and Nakabo [8], 2002).

64.– Mandibulohyoid ligament: present (0), absent (1), (Sato and Nakabo [22], 2002).

65.– Cheek muscle: discrete A1 and A2 muscle elements (0), A1 and A2 components of the adductor mandibulae fused (1), A1 component is absent (2), (Sato and Nakabo [25], 2002).

Cranium

66.– Frontal expanded laterally over orbit: frontal not expanded laterally (0), frontal expanded laterally (1), (Baldwin and Johnson [52], 1996).

67.– Sphenotic process: sphenotic without anterior process (0), sphenotic with anterior process (1), (Baldwin and Johnson [53], 1996).

68.– Exoccipital pocess: absent (0), present (1), (Sato and Nakabo [3], 2002).

Intermuscular bones and ligaments

69.– Epipleurals extend anteriorly to first or second vertebra: epipleurals originate on V3, do not extend to V1 or V2 (0), epipleurals originate on V2 (1), epipleurals originate on V1 (2), absent (3), (Baldwin and Johnson [54], 1996; Sato and Nakabo [59], 2002).

70.– One or more epipleurals displaced dorsally into horizontal septum: all epipleurals beneath the horizontal septum (0), one or more epipleurals displaced dorsally into horizontal septum (1), (Baldwin and Johnson [55], 1996).

71.– Abrupt transition of epipleurals in and beneath the horizontal septum: no epipleurals displaced dorsally into the horizontal septum or the transition between epipleurals in and beneath the horizontal septum is gradual (0), abrupt transition between epipleurals in and beneath the horizontal septum (1), (Baldwin and Johnson [56], 1996).

72.– One or more epipleurals forked distally: epipleurals not forked distally (0), epipleurals forked distally at transition of epipleurals in and beneath the horizontal septum (1), (Baldwin and Johnson [57], 1996).

73.– Epipleurals on first and second vertebrae fused to centrum: epipleurals on V1 and V2 autogenous (0), epipleurals on V1 and V2 fused to centrum (1), (Baldwin and Johnson [58], 1996).

74.– Epipleurals not attached to axial skeleton: most or all epipleurals attached to axial skeleton (0), most epipleurals not attached to axial skeleton (1), most epipleurals are free dorsal branches (2), (Baldwin and Johnson [59], 1996).

75.– Reduced number of epipleurals: long series of epipleurals (0), epipleurals not extending posteriorly beyond V5 (1), (Baldwin and Johnson [60], 1996).

76.– Origin of epineurals: all epipleurals originate on neural arch (0), some epineurals originate on the centrum or parapophysis, these flanked anteriorly and posteriorly by epineurals originating on the neural arch (1), most or all

epineurals originate on centrum, epineurals not reascending to neural arch posteriorly (2), (Baldwin and Johnson [61], 1996).

77.– First one to three epineurals with distal end displaced ventrally: distal end of epineurals not displaced ventrally (0), distal end of first one to three epineurals displaced ventrally (1), (Baldwin and Johnson [62], 1996).

78.– Some epineurals and epipleurals forked proximally: no epineurals or epipleurals forked proximally (0), epineurals and epipleurals from about V12-V15 to near end of series forked proximally (1), epineurals and epipleurals on about V1-V5 forked proximally (2), "*Gigantura*" pattern of branching (3), (Baldwin and Johnson [63], 1996).

79.– Epineurals fused to neural arch: epineurals not fused to axial skeleton (0), epineural fused to neural arch on V1 (1), epineurals fused to neural arch on V1-V5 (2), epineurals fused to neural arch on V1-V10 (3), most epineurals fused to centrum (4), fused to neural arch on V3-V6 (or V9) (5), (Baldwin and Johnson [64], 1996; Sato and Nakabo [66], 2002).

80.– Epineurals attached to axial skeleton: most or all epineurals attached to axial skeleton (0), most epineurals unattached (1), all epineurals unattached (2), unattached epineurals represent only free ventral branches of forked epineurals (3), (Baldwin and Johnson [65], 1996).

81.– Epicentrals: epicentrals ligamentous (0), epicentrals ossified (1), epicentrals absent (2), epicentrals cartilaginous anteriorly, ligamentous posteriorly (3), ossified anteriorly, ligamentous posteriorly (4), (Baldwin and Johnson [66], 1996; Sato and Nakabo [68], 2002).

82.– Anterior epicentrals closely applied to distal end of epipleurals: all epicentrals attached to centrum or parapophyses (0), anterior epicentrals attached to distal end of epipleurals (1), (Baldwin and Johnson [67], 1996).

Postcranial axial skeleton

83.– Number of supraneurals: three or more supraneurals (0), two supraneurals (1), one supraneural (2), no supraneurals (3), (Baldwin and Johnson [68], 1996).

84.– Number of caudal vertebrae: < 25% caudal vertebrae (0), 40-60% caudal vertebrae (1), > 60% caudal vertebrae (2), (Baldwin and Johnson [69], 1996).

85.– Accessory neural arch: accessory neural arch absent (0), accessory neural arch present (1), (Baldwin and Johnson [70], 1996).

86.– First neural arch with brush-like growth: no brush-like growth on first neural arch (0), brush-like growth on first neural arch (1), (Baldwin and Johnson [71], 1996).

87.– Number of open neural arches: many neural arches open dorsally (0), neural arches open on V1 and sometimes V2-V4 (1), all neural arches closed dorsally (2), (Baldwin and Johnson [72], 1996).

88.– Origin of first rib: first rib originates on V3 (0), first rib originates on V4 (1), first rib originates on V5 (2), first rib originates on V2 (3), first rib originates on V1 (4), ribs absent (5), (Baldwin and Johnson [73], 1996).

89.– Ossification of ribs: all ribs ossify in cartilage (0), some ribs ossify in membrane bone (1), all ribs ossify in membrane bone (2), ribs absent (3), some or all ribs ligamentous (4), (Baldwin and Johnson [74], 1996).

90.– Origin of Baudelot's ligament: Baudelot's ligament originates on V1 (0), Baudelot's ligament originates on more than one vertebra (1), Baudelot's ligament originates on V1 and the occiput (2), (Baldwin and Johnson [75], 1996).

91.– Ossification of Baudelot's ligament: Baudelot's ligament is ligamentous (0), Baudelot's ligament is ossified (1), Baudelot's ligament is absent (2), (Baldwin and Johnson [76], 1996).

92.– Condition of ventral parapophyses on first vertebra: parapophyses with enlarged base (0), parapophyses without enlarged base (1), (Sato and Nakabo [58], 2002).

Caudal Fin and Rays

93.– Modified proximal segmentation of caudal-fin rays: proximal portion of principal caudal-fin rays not modified (0), proximal portion of most principal caudal rays with modified segment (1), (Baldwin and Johnson [77], 1996).

94.– Segmentation begins on distal half of each caudal ray: segmentation begins on proximal half of each caudal ray (0), segmentation begins on distal half of each caudal ray (1), caudal rays not segmented (2), (Baldwin and Johnson [78, 1996).

95.– Median caudal cartilages: two CMCs, about equal in size (0), two CMCs, the dorsal one minute (1), one CMC (2), no CMC (3), (Baldwin and Johnson [79], 1996).

96.– Urodermal: no urodermal (0), small urodermal in upper caudal lobe (1), (Baldwin and Johnson [80], 1996).

97.– Expanded neural and haemal spines on posterior vertebrae: posterior neural and haemal spine no expanded (0), neural arch and haemal spines of PU2 expanded (1), neural arch and haemal spines of PU2 and PU3 expanded (2), (Baldwin and Johnson [81], 1996).

98.– Number of hypurals: six hypurals (0), five hypurals, the sixth lost or fused (1), five hypurals, the first and second not differentiated (2), four hypurals, the first and second not differentiated, the sixth lost or fused (3), two hypurals (4), (Baldwin and Johnson [82], 1996).

99.– Number of epurals: adults with two or three epurals, if two, one split (0), adults with two epurals, neither split (1), adults with one epural (2), (Baldwin and Johnson [83], 1996).

100.– Fusion of adjacent pterygiophores: no fusion of pterygiophores of dorsal or anal fin (0), adjacent posterior anal-fin pterygiophores fused (1), adjacent dorsal-fin pterygiophores fused (2), (Baldwin and Johnson [84], 1996).

101.– Pterygiophores of dorsal fin triangular proximally: pterygiophores of anal fin not triangular proximally (0), anterior pterygiophores of anal fin triangular proximally (1), posterior pterygiophores of anal fin triangular proximally (2), (Baldwin and Johnson [85], 1996).

102.– Pterygiophores of anal fin triangular proximally: pterygiophores of anal fin not triangular proximally (0), anterior pterygiophores of anal fin triangular proximally (1), posterior pterygiophores of anal fin triangular proximally (2), (Baldwin and Johnson [86], 1996).

Pelvic and Pectoral Girdles and Fins

103.– Medial processes of the pelvic girdle joined medially by cartilage: medial processes not joined medially (0), medial processes joined medially by cartilage (1), (Baldwin and Johnson [87], 1996).

104.– Posterior processes of pelvic girdle elongate and widely separated: posterior pelvic processes small (or absent) (0), posterior pelvic processes elongate, widely separated (1), (Baldwin and Johnson [88], 1996).

105.– Posterior processes of pelvic girdle absent: ossified posterior processes of pelvic girdle present (0), posterior processes are cartilaginous (1), posterior processes of pelvic girdle absent (2), (Baldwin and Johnson [89], 1996).

106.– Lateral pelvic processes: lateral pelvic processes small (0), lateral pelvic processes large, sometimes ossifying in adults (1), (Baldwin and Johnson [90], 1996).

107.– Autogenous pelvic cartilages: autogenous pelvic cartilages absent (0), autogenous pelvic cartilages present (1), (Baldwin and Johnson [91], 1996).

108.– Ventrally directed posterior cartilage of the pelvic fin: cartilage between medial processes, if present, not terminating in ventrally directed process (0), cartilage between medial processes terminating in ventrally directed process (1), (Baldwin and Johnson [92], 1996).

109.– Posterior pelvic cartilage elongate: cartilage extending posteriorly from between medial processes, if present, not elongate (0), cartilage extending posteriorly from between medial processes elongate (1), (Baldwin and Johnson [93], 1996).

110.– Ventral surface of pelvic girdle: ventral surface of pelvic girdle is smooth (0), the pelvic girdle has a transverse keel dividing the ventral surface of the medial process area (1), (Sato and Nakabo [84], 2002).

111.– Position of pectoral and pelvic fins: pectoral fins set high on body, pelvics subthoracic (0), pectoral fins set low on body, pelvics abdominal (1), (Baldwin and Johnson [94], 1996).

112.– Relative position of abdominal pelvic fins: pelvic fins subthoracic or, if abdominal, inserting beneath or behind a vertical through the origin of the dorsal fin (0), pelvic fins abdominal, inserting anterior to vertical through dorsal fin (1), (Baldwin and Johnson [95], 1996).

113.– Number of postcleithra: two postcleithra (0), one postcleithra (1), postcleithra absent (2), three postcleithra, dorsalmost postcleithrum attaches to the posterolateral surface over dorsal margin of posterior strut of the cleithrum (3), three postcleithra, dorsalmost postcleithrum attaches to the medial surface of the cleithrum (4), (Baldwin and Johnson [96], 1996; Sato and Nakabo [77], 2002).

114.– Cleithrum with strut extending to dorsal postcleithrum: cleithrum with small rounded posterior projection or projection absent (0), cleithrum with strut extending posteriorly to postcleithrum (1), (Baldwin and Johnson [97], 1996).

115.– Orientation of pectoral-fin base: pectoral-fin base more vertical than horizontal (0), pectoral-fin base more horizontal than vertical, inserted on the ventrolateral surface of the body (1), pectoral-fin base horizontal, inserted on the dorsolateral surface of body (2), (Baldwin and Johnson [98], 1996).

116.– Greatly elongated supracleithrum: supracleithrum shorter than cleithrum (0), supracleithrum equal to or longer than cleithrum (1), (Baldwin and Johnson [99], 1996).

117.– Ventral limb of posttemporal not ossified: posttemporal forked, both branches ossified (0), posttemporal unforked, the ventral branch ligamentous (1), (Baldwin and Johnson [100], 1996).

118.– Position of cleithrum-coracoid articulation: near the anteroventral end of the cleithrum (0), joint is shifted dorsally (1), (Sato and Nakabo [76], 2002).

119.– Origin of adductor profundus: originates from the ventral or middle portion of the cleithrum (0), originates around the anterodorsal portion of the coracoid (1), (Sato and Nakabo [80], 2002).

120.– Number of adductor profundus elements: single adductor profundus (0), two adductor profundus elements (1), (Sato and Nakabo [81], 2002).

121.– Spur size on medial half of second ray of pectoral fin: spurs of the pectoral fin rays are almost equal in size (0), spur of the medial half of the second ray is more reduced than those of successive rays (1), (Sato and Nakabo [82], 2002).

External morphology

122.– Margin of anal fin indented: margin of anal fin not indented (0), margin of anal fin indented (1), (Baldwin and Johnson [101], 1996).

123.– Scales: Body and lateral-line scales present and ossified (0), body scales absent, lateral-line scales or structures at least partially ossified (1), body and lateral-line scales or structures absent (2), (Baldwin and Johnson [102], 1996).

124.– Fleshy mid-lateral keel: absent (0), single fleshy mid-lateral keel on posterior portion of body (1), pair of fleshy mid-lateral keels on caudal peduncle (2), (Baldwin and Johnson [103], 1996).

125.– Body transparent, glassy in life: appearance in life not transparent or glassy (0), appearance in life transparent, glassy (1), (Baldwin and Johnson [104], 1996).

126.– Scale pockets in continuous flap of skin: scale pockets not in continuous flap of skin (0), scale pockets in a continuous flap of marginally pigmented skin (1), (Baldwin and Johnson [105], 1996).

127.– Elliptical or keyhole aphakic space: no aphakic space (0), elliptical or keyhole shaped aphakic space (1), (Baldwin and Johnson [106], 1996).

128.– Eye morphology: eyes laterally directed, round (0), eyes slightly flattened to elliptical (1), eyes minute or absent (2), eyes dorsally directed, semitubular or tubular (3), eyes anteriorly directed, telescopic (4), eyes are broad, lensless plates on dorsal surface of head (5), (Baldwin and Johnson [107], 1996).

129.– Gular fold: gular fold tent-shaped (0), gular fold crescent-shaped (1), (Baldwin and Johnson [108], 1996).

130.– Adipose fin: present (0), absent (1), (Baldwin and Johnson [109], 1996).

131.– Mode of reproduction: separate sexes (0), synchronous hermaphrodites (1), (Baldwin and Johnson [110], 1996).

132.– Thin-walled, heavily pigmented stomach: stomach not highly distensible, with thick unpigmented walls (0), stomach highly distensible, with thin heavily pigmented walls (1), (Baldwin and Johnson [111], 1996).

133.– Swimbladder: present (0), absent (1), (Baldwin and Johnson [112], 1996).

134.– Enlarged pectoral fins: pectoral fins not enlarged in larvae (0), pectoral fins enlarged in larvae (1), (Baldwin and Johnson [113], 1996).

135.– Elongate eyes: eyes in larvae round (0), eyes in larvae elongate, the horizontal axis longer than the vertical (1), eyes in larvae elongate, the vertical axis longer than the horizontal (2), (Baldwin and Johnson [114], 1996).

136.– Head spination: head spines lacking in larvae (0), head spines present in larvae (1), (Baldwin and Johnson [115], 1996).

137.– Peritoneal pigment: absent in larvae (0), single or multiple unpaired peritoneal pigment sections in larvae (1), multiple paired peritoneal pigment sections in larvae (2), (Baldwin and Johnson [116], 1996).

138.– Ontogenetic reduction of large maxilla: maxilla not enlarged in larva, not greatly reduced ontogenetically (0), maxilla enlarged in larva, greatly reduced ontogenetically (1), (Baldwin and Johnson [117], 1996).

139.– Ontogenetic fusion of epurals: no ontogenetic fusion of epurals (0), partial ontogenetic fusion of two epurals (1), (Baldwin and Johnson [118], 1996).

APPENDIX 1.2: Morphological Data Matrix. See Appendix 1.1 for abbreviated list of characters. Y=(01), L=(12), M=(02), N=(13).

	1	2	3	4	5	6	7	8	9	10	11	12	13	14	15	16	17	18	19	20	21	22	23	24	25
Diplophos	0	0	1	0	0	0	1	0	0	0	0	0	0	0	0	0	0	?	0	0	0	0	0	0	0
Myctophidae	0	0	0	0	0	0	0	0	0	0	0	0	0	0	0	0	0	0	0	1	0	0	0	0	Y
Neoscopelus	0	0	0	0	0	0	0	0	0	0	0	0	0	0	0	0	0	0	0	1	0	0	0	0	0
Metavelifer	0	0	0	0	Y	0	0	0	0	?	0	?	0	0	0	?	?	0	0	0	0	0	0	0	0
Polymixia	0	0	0	0	0	0	0	0	0	0	0	0	0	0	0	0	0	0	0	1	0	0	0	0	0
Aulopus	1	1	0	0	0	0	0	0	0	0	0	1	0	0	0	2	0	1	0	0	2	0	0	0	0
Pseudotrichonotus	1	1	1	0	0	0	1	0	0	2	0	0	0	0	2	3	0	1	0	0	0	0	0	0	0
Synodus	1	1	1	1	1	0	0	0	0	1	0	0	0	0	0	1	0	0	0	2	2	0	0	0	0
Trachinocephalus	1	1	1	1	1	0	0	0	0	1	0	0	0	0	0	1	0	1	0	2	2	0	0	0	0
Harpadon	1	1	1	0	1	0	0	0	0	0	1	0	1	1	0	1	0	1	0	2	2	1	0	0	0
Saurida	1	1	1	0	1	0	0	0	0	0	0	0	1	1	0	1	0	1	0	2	2	1	0	0	0
Bathypterois	2	1	0	0	0	2	1	0	0	0	0	0	0	0	0	3	0	1	0	0	0	0	0	0	0
Bathymicrops	1	1	1	0	0	2	0	0	0	?	0	?	0	0	0	?	?	1	0	0	0	0	1	0	1
Bathytyphlops	1	1	0	0	2	2	1	0	0	?	0	?	0	0	0	?	?	1	0	0	0	0	0	0	1
Ipnops	1	1	0	0	0	2	1	0	0	0	0	0	0	0	0	3	0	1	0	0	0	0	1	0	0
Scopelosaurus	1	1	0	0	0	2	0	0	0	0	0	0	0	0	0	0	0	1	0	0	0	0	0	1	1
Ahliesaurus	1	1	0	0	0	2	0	0	0	?	0	?	0	0	0	?	?	1	0	0	0	0	0	1	1
Chlorophthalmus	1	1	0	0	0	1	0	0	0	0	0	0	0	0	0	0	0	1	0	0	0	0	0	0	0
Parasudis	1	1	0	0	0	1	0	0	0	0	0	0	0	0	0	0	0	1	0	0	0	0	0	0	0
Bathysauropsis	1	1	0	0	0	1	0	0	0	0	0	0	0	0	0	2	0	1	0	0	0	0	0	0	0
Omosudis	1	1	0	0	1	0	1	1	0	0	1	0	1	1	2	0	1	0	2	0	0	1	0	0	0
Alepisaurus	1	1	0	0	1	0	1	0	0	0	1	0	1	1	2	0	1	0	2	0	0	1	0	0	0
Coccorella	1	1	0	0	1	0	1	1	0	0	1	0	1	1	2	0	1	0	3	1	0	0	0	0	1
Odontostomops	1	1	0	0	1	0	1	1	0	?	0	?	1	1	0	?	?	0	2	1	0	0	0	0	1
Evermannella	1	1	0	0	1	0	1	1	0	?	0	?	1	1	0	?	?	0	2	1	0	0	0	0	1
Scopelarchus	1	1	0	0	1	0	1	0	0	?	0	?	1	1	2	?	?	0	2	0	0	0	0	0	0
Scopelarchoides	1	1	0	0	1	0	1	0	0	?	0	?	1	1	2	?	?	0	1	0	0	0	0	0	0
Benthalbella	1	1	0	0	1	0	0	0	0	0	0	0	1	1	0	0	1	0	1	0	0	0	0	0	0
Rosenblattichthys	1	1	0	0	1	0	1	0	0	?	0	?	1	1	0	?	?	0	1	0	0	0	0	0	0
Paralepis	1	1	0	0	1	0	1	0	0	0	0	0	1	1	0	0	0	0	2	0	0	0	0	2	0
Arctozenus	1	1	0	0	1	0	1	0	0	?	0	?	1	1	0	?	?	0	2	0	0	0	0	2	0
Lestrolepis	1	1	0	0	1	0	1	0	1	?	0	?	2	?	0	?	?	0	2	0	0	0	0	2	0
Lestidium	3	1	0	0	1	0	1	0	1	0	0	0	2	?	0	0	0	0	2	0	0	0	0	2	0
Stemonosudis	1	1	0	0	1	0	1	0	1	?	0	?	2	?	0	?	?	0	2	0	0	0	0	2	0
Uncisudis	1	1	0	0	1	0	1	0	1	?	0	?	2	?	0	?	?	0	2	3	3	0	0	2	0
Macroparalepis	1	1	0	0	1	0	1	0	1	?	0	?	2	?	0	?	?	0	2	0	0	0	0	2	0
Lestidiops	1	1	0	0	1	0	1	0	1	?	0	?	2	?	0	?	?	0	2	0	0	0	0	2	0
Sudis	1	1	0	0	1	0	1	0	0	?	0	?	2	?	0	?	?	0	2	0	0	0	0	2	0
Anotopterus	1	1	1	0	1	0	1	0	0	?	1	?	2	?	0	?	?	0	2	0	0	0	0	2	0
Bathysauroides	1	1	0	0	1	0	0	0	0	0	0	0	0	1	1	0	0	1	0	0	0	0	0	0	0
Bathysaurus	1	1	0	0	1	0	0	0	0	0	0	0	0	1	1	1	0	1	0	0	0	0	0	0	0
Gigantura	1	1	0	0	?	0	?	0	0	?	0	?	0	?	?	?	?	?	?	?	0	0	?	?	?
Paraulopus	1	0	0	0	0	0	?	0	?	1	0	1	?	0	0	2	0	1	?	0	0	0	?	?	?

APPENDIX 1.2 Continued: Morphological Data Matrix. See Appendix 1.1 for abbreviated list of characters. Y=(01), L=(12), M=(02), N=(13).

	26	27	28	29	30	31	32	33	34	35	36	37	38	39	40	41	42	43	44	45	46	47	48	49	50
Diplophos	0	0	1	0	0	0	0	0	0	0	0	0	1	1	0	0	0	0	0	0	0	0	0	0	0
Myctophidae	1	1	0	0	0	0	0	0	0	0	0	0	2	0	0	0	0	0	0	0	0	0	0	0	0
Neoscopelus	1	0	0	0	0	0	0	0	0	0	0	0	0	0	0	0	0	0	0	0	0	0	1	0	0
Metavelifer	1	0	?	0	0	1	0	0	0	1	0	0	0	0	0	0	0	0	0	0	0	0	?	?	0
Polymixia	1	0	0	0	0	0	0	0	0	1	0	0	0	0	0	0	0	0	0	1	0	0	1	0	0
Aulopus	1	0	0	0	0	0	0	1	2	0	0	0	0	0	0	0	0	0	0	0	0	0	1	0	0
Pseudotrichonotus	0	0	0	0	0	0	0	1	0	0	0	0	0	0	0	0	0	0	0	0	0	0	0	1	0
Synodus	0	0	0	0	1	1	0	1	2	0	0	0	0	0	0	0	1	1	1	1	1	0	0	1	0
Trachinocephalus	0	0	0	0	1	1	0	1	2	0	0	0	0	0	0	0	1	1	1	1	1	0	0	1	0
Harpadon	0	0	0	0	1	1	0	1	2	0	0	0	0	0	0	0	1	1	0	0	1	0	1	0	0
Saurida	0	0	Y	0	1	1	0	1	2	0	0	0	0	0	0	0	1	1	0	0	1	0	1	0	0
Bathypterois	1	1	1	0	0	0	0	0	1	0	0	0	0	1	0	0	0	0	0	0	0	1	Y	1	0
Bathymicrops	1	1	?	1	0	0	0	0	0	0	0	0	0	1	0	0	0	0	0	0	0	1	?	?	1
Bathytyphlops	1	1	?	1	0	0	0	0	0	0	0	0	0	1	0	0	0	0	0	0	0	1	?	?	1
Ipnops	1	1	1	0	0	0	0	0	0	0	0	0	0	1	0	0	0	0	0	0	0	1	0	1	0
Scopelosaurus	1	1	0	0	0	0	0	0	0	0	0	0	1	0	0	0	0	1	0	0	0	0	0	1	0
Ahliesaurus	1	1	?	0	0	0	0	0	0	0	0	0	1	0	0	0	0	1	0	0	0	0	?	?	0
Chlorophthalmus	0	0	1	0	1	0	0	0	0	1	0	0	0	0	0	0	0	0	0	0	0	0	0	1	0
Parasudis	1	0	1	0	0	0	0	0	0	1	0	0	0	0	0	0	0	0	0	0	0	0	0	1	0
Bathysauropsis	1	1	1	0	0	0	0	0	0	0	0	0	0	1	0	0	0	0	0	0	0	0	1	1	0
Omosudis	0	0	3	0	0	0	0	0	0	?	?	0	0	0	0	2	0	0	0	0	0	0	0	1	0
Alepisaurus	0	0	3	0	0	0	0	0	0	1	0	0	0	0	0	2	0	0	0	0	0	0	0	1	0
Coccorella	0	0	2	0	0	0	0	0	0	1	0	0	0	2	0	2	0	0	0	0	0	0	0	1	0
Odontostomops	0	0	?	0	0	0	1	0	0	1	1	0	0	2	0	2	0	0	0	0	0	0	?	?	0
Evermannella	0	0	?	0	0	0	1	0	0	1	1	0	0	2	0	2	0	0	0	0	0	0	?	?	0
Scopelarchus	0	0	?	0	0	0	0	0	0	1	0	0	0	0	1	2	0	0	0	0	0	0	?	?	0
Scopelarchoides	0	0	?	0	0	0	0	0	0	1	0	0	0	0	1	2	0	0	0	0	0	0	?	?	0
Benthalbella	0	0	3	0	0	0	0	0	0	1	0	0	0	0	1	2	0	0	0	0	0	0	0	1	0
Rosenblattichthys	0	0	?	0	0	0	0	0	0	1	0	0	0	0	1	2	0	0	0	0	0	0	?	?	0
Paralepis	1	0	0	0	0	0	0	0	0	1	2	1	0	0	0	2	0	0	0	0	0	0	0	1	0
Arctozenus	1	0	?	0	0	0	1	0	0	1	2	1	0	0	0	2	0	0	0	0	0	0	?	?	0
Lestrolepis	0	0	?	0	0	0	0	0	0	1	2	1	0	0	0	2	0	0	0	0	0	0	?	?	0
Lestidium	0	0	3	0	0	0	0	0	0	1	2	1	0	0	0	2	0	0	0	0	0	0	0	1	0
Stemonosudis	0	0	?	0	0	0	0	0	0	1	2	1	0	0	0	2	0	0	0	0	0	0	?	?	0
Uncisudis	0	0	?	0	0	0	0	0	0	1	2	1	0	0	0	2	0	0	0	0	0	0	?	?	0
Macroparalepis	0	0	?	0	0	0	0	0	0	1	2	1	0	0	0	2	0	0	0	0	0	0	?	?	0
Lestidiops	0	0	?	0	0	0	0	0	0	1	2	1	0	0	0	2	0	0	0	0	0	0	?	?	0
Sudis	0	0	?	0	0	0	0	0	0	1	2	0	0	0	0	2	0	0	0	0	0	0	?	?	0
Anotopterus	0	0	?	0	0	0	0	0	0	1	0	0	0	0	0	2	0	0	0	0	0	0	?	?	0
Bathysauroides	1	0	1	0	0	0	0	0	0	1	0	0	0	0	0	2	0	0	0	0	0	0	0	1	0
Bathysaurus	1	1	0	0	1	0	0	0	0	1	0	0	0	0	0	1	0	0	0	0	0	0	0	1	0
Gigantura	?	?	?	?	0	?	?	0	0	?	0	?	0	0	0	?	0	0	0	0	0	0	?	?	0
Paraulopus	?	?	0	?	?	?	?	0	0	0	0	0	?	0	?	0	0	0	0	0	0	0	0	0	?

APPENDIX 1.2 Continued: Morphological Data Matrix. See Appendix 1.1 for abbreviated list of characters. Y=(01), L=(12), M=(02), N=(13).

	51	52	53	54	55	56	57	58	59	60	61	62	63	64	65	66	67	68	69	70	71	72	73	74	75
Diplophos	1	2	0	0	0	0	0	0	0	0	0	0	0	0	0	0	0	0	0	0	0	0	0	0	0
Myctophidae	0	1	0	0	0	0	0	0	0	0	0	0	0	1	0	0	0	0	0	0	0	0	0	0	0
Neoscopelus	0	1	0	0	0	0	0	0	0	0	0	0	0	1	0	0	0	0	0	0	0	0	0	0	0
Metavelifer	?	?	0	5	0	0	0	?	?	?	0	0	?	?	?	0	0	?	3	?	?	?	?	?	?
Polymixia	0	0	0	0	0	0	0	0	0	0	0	0	0	1	0	0	0	0	0	0	0	0	0	0	0
Aulopus	0	0	0	0	0	0	0	1	1	1	0	0	0	0	0	0	0	0	1	1	0	0	0	0	0
Pseudotrichonotus	0	2	0	0	0	0	0	1	2	1	0	0	0	1	0	0	0	0	1	1	1	0	0	0	0
Synodus	0	1	0	0	0	0	0	1	2	0	0	1	0	0	0	0	0	0	1	1	1	0	0	0	0
Trachinocephalus	0	1	0	0	0	0	0	1	2	0	0	1	0	0	0	0	0	0	1	1	1	0	0	0	0
Harpadon	0	1	0	0	0	0	0	1	1	?	0	2	0	1	0	0	0	0	1	1	0	0	0	0	0
Saurida	0	1	0	0	0	0	0	1	1	0	0	1	0	1	0	0	0	0	1	1	0	0	0	0	0
Bathypterois	0	0	1	0	0	0	0	1	1	0	0	0	2	0	0	1	1	1	1	0	0	0	0	0	0
Bathymicrops	?	?	1	5	0	0	0	?	?	?	0	0	?	?	?	1	1	?	1	0	0	0	0	0	0
Bathytyphlops	?	?	1	3	0	0	0	?	?	?	0	0	?	?	?	1	1	?	1	1	0	0	0	0	0
Ipnops	0	0	1	3	0	0	0	1	2	0	0	0	2	0	0	?	?	1	0	?	0	0	0	0	0
Scopelosaurus	0	2	1	1	0	0	0	1	1	0	0	0	2	1	0	0	0	0	1	1	0	1	0	0	0
Ahliesaurus	?	?	1	1	0	0	0	?	?	?	0	0	?	?	?	0	0	?	1	1	0	1	0	0	0
Chlorophthalmus	1	1	1	0	0	0	0	1	1	1	0	0	1	0	1	0	0	1	1	1	0	0	0	0	0
Parasudis	1	1	1	0	0	0	0	1	1	1	0	0	1	0	1	0	0	1	1	0	0	0	0	0	0
Bathysauropsis	0	0	1	0	0	0	0	0	0	0	0	0	2	0	0	0	0	1	1	1	0	0	0	0	0
Omosudis	0	2	0	2	0	0	0	1	0	0	0	0	0	1	0	0	0	0	2	1	0	0	1	1	0
Alepisaurus	0	2	0	2	0	0	0	1	0	0	0	0	0	1	0	0	0	0	2	1	0	0	1	0	0
Coccorella	0	2	0	2	0	0	0	1	0	0	0	0	0	1	2	0	0	0	2	1	0	0	0	0	0
Odontostomops	?	?	0	2	0	0	0	?	?	?	0	0	?	?	?	0	0	?	2	1	0	0	?	0	0
Evermannella	?	?	0	2	0	0	0	?	?	?	0	0	?	?	?	0	0	?	2	1	0	0	0	0	0
Scopelarchus	?	?	0	0	0	0	0	?	?	?	0	0	?	?	?	0	0	?	2	1	0	0	0	0	0
Scopelarchoides	?	?	0	0	0	0	0	?	?	?	0	0	?	?	?	0	0	?	2	1	0	0	0	0	0
Benthalbella	0	2	0	0	0	0	0	1	0	0	0	0	0	1	2	0	0	1	2	1	0	0	0	0	0
Rosenblattichthys	?	?	0	0	0	0	0	?	?	?	0	0	?	?	?	0	0	?	2	?	0	0	0	?	0
Paralepis	0	2	0	2	1	1	1	1	1	0	1	0	0	1	2	0	0	0	2	1	0	0	1	2	0
Arctozenus	?	?	0	2	1	1	1	?	?	?	1	0	?	?	?	0	0	?	2	1	0	0	0	2	0
Lestrolepis	?	?	0	2	1	1	1	?	?	?	1	0	?	?	?	0	0	?	2	1	0	0	0	0	1
Lestidium	0	2	0	2	1	1	1	1	1	0	1	0	0	0	2	0	0	0	2	1	0	0	0	0	1
Stemonosudis	?	?	0	2	1	1	1	?	?	?	1	0	?	?	?	0	0	?	2	1	0	0	0	0	1
Uncisudis	?	?	0	2	1	1	1	?	?	?	1	0	?	?	?	0	0	?	2	?	?	0	?	?	?
Macroparalepis	?	?	0	2	1	1	1	?	?	?	1	0	?	?	?	0	0	?	2	1	0	0	0	0	1
Lestidiops	?	?	0	2	1	1	1	?	?	?	1	0	?	?	?	0	0	?	?	?	?	0	0	?	?
Sudis	?	?	0	?	1	1	1	?	?	?	?	0	?	?	?	0	0	?	2	1	0	0	0	0	1
Anotopterus	?	?	0	0	1	1	1	?	?	?	1	1	?	?	?	0	0	?	2	1	0	0	0	0	0
Bathysauroides	0	0	1	0	0	0	0	1	1	0	0	0	1	0	0	0	0	1	2	1	0	0	0	0	0
Bathysaurus	0	1	0	0	0	0	0	1	0	?	0	3	0	1	0	0	0	0	2	1	0	0	0	0	0
Gigantura	?	?	0	0	0	0	0	?	?	?	?	2	?	?	?	0	0	?	2	1	0	0	0	0	0
Paraulopus	0	0	0	?	?	0	0	1	1	1	0	0	0	0	0	?	0	0	0	0	0	?	0	0	?

APPENDIX 1.2 Continued: Morphological Data Matrix. See Appendix 1.1 for abbreviated list of characters. Y=(01), L=(12), M=(02), N=(13).

	76	77	78	79	80	81	82	83	84	85	86	87	88	89	90	91	92	93	94	95	96	97	98	99	100
Diplophos	0	0	0	2	0	0	0	0	1	1	0	0	1	0	0	0	0	0	0	0	0	0	0	0	0
Myctophidae	0	0	1	0	0	0	0	0	1	0	0	2	0	0	0	0	0	0	0	0	Y	0	0	0	0
Neoscopelus	0	0	1	0	0	0	0	0	1	0	0	2	0	0	0	0	0	0	0	2	1	0	0	0	0
Metavelifer	0	0	0	0	0	0	0	2	1	0	0	2	0	1	2	0	?	0	0	3	0	0	0	0	?
Polymixia	1	0	0	0	0	0	0	0	1	0	0	2	0	0	0	0	1	0	0	3	0	0	0	0	0
Aulopus	0	1	0	0	0	0	0	0	1	1	0	0	0	2	0	0	1	1	0	3	Y	2	0	0	0
Pseudotrichonotus	0	1	0	0	0	0	0	1	1	0	0	0	1	2	0	0	1	1	0	3	0	2	1	2	0
Synodus	0	1	0	0	0	0	0	0	0	1	1	0	2	2	0	0	1	1	0	3	0	2	1	2	0
Trachinocephalus	0	1	0	0	0	0	0	0	0	1	1	0	2	2	0	0	1	1	0	3	0	2	1	2	0
Harpadon	0	0	0	3	0	0	0	0	0	1	0	0	3	2	0	1	1	1	0	3	0	0	1	1	0
Saurida	0	0	0	3	0	0	0	0	0	1	0	0	1	2	0	1	1	1	0	3	0	2	0	1	0
Bathypterois	0	0	0	0	0	0	0	2	1	0	0	1	3	1	0	0	1	0	0	2	0	0	0	0	0
Bathymicrops	0	0	0	0	0	0	0	2	2	0	0	1	5	3	0	1	?	0	1	3	0	0	4	2	0
Bathytyphlops	0	0	0	0	0	0	0	1	2	0	0	1	3	1	0	0	?	0	0	3	0	0	0	1	0
Ipnops	0	1	0	0	0	0	0	2	2	0	0	2	3	1	0	0	0	0	1	3	0	0	2	1	0
Scopelosaurus	1	0	0	0	0	0	0	2	1	0	0	1	0	1	0	0	1	0	0	2	0	0	0	0	0
Ahliesaurus	1	0	0	0	0	0	0	2	1	0	0	1	0	1	0	0	?	0	0	2	0	0	0	0	0
Chlorophthalmus	0	1	1	0	0	0	0	1	2	0	0	1	0	1	0	0	0	0	0	0	Y	0	0	0	0
Parasudis	0	0	1	0	0	4	0	2	1	0	0	1	0	1	0	0	0	0	0	0	0	0	0	0	0
Bathysauropsis	0	0	0	0	0	0	0	0	1	0	0	1	0	1	0	0	0	0	0	0	0	0	0	0	0
Omosudis	0	0	0	?	1	1	0	2	1	0	0	1	4	2	1	0	1	0	0	?	1	0	1	0	1
Alepisaurus	0	0	0	2	1	1	0	3	1	0	0	1	4	2	1	0	1	0	0	0	0	0	1	0	1
Coccorella	1	0	0	0	0	3	1	1	2	0	0	1	0	1	0	0	1	0	0	0	0	0	0	2	0
Odontostomops	?	?	0	?	?	3	1	1	2	0	0	1	0	1	0	0	?	0	0	0	0	0	0	2	0
Evermannella	1	0	0	0	0	3	1	1	2	0	0	1	0	1	0	0	?	0	0	0	0	0	0	2	0
Scopelarchus	1	0	0	0	0	0	1	0	2	0	0	1	3	4	0	0	?	0	0	0	0	0	0	0	0
Scopelarchoides	1	0	0	0	0	0	1	0	2	0	0	1	0	4	0	0	?	0	0	0	0	0	0	0	0
Benthalbella	1	0	0	0	0	0	1	0	2	0	0	1	0	4	0	0	1	0	0	?	0	0	0	0	0
Rosenblattichthys	1	0	0	4	0	0	?	0	2	0	0	1	0	4	0	0	?	0	0	0	0	0	0	0	0
Paralepis	0	0	2	1	3	2	0	1	1	0	0	1	4	2	0	0	1	0	0	?	0	0	0	0	0
Arctozenus	0	0	2	0	3	2	0	1	1	0	0	1	0	2	1	0	?	0	0	0	0	0	2	0	0
Lestrolepis	0	0	0	0	0	2	0	1	2	0	0	1	1	2	1	0	?	0	0	2	0	0	0	?	0
Lestidium	0	0	0	0	0	2	0	1	1	0	0	1	0	2	1	0	1	0	0	1	0	0	0	0	0
Stemonosudis	0	0	0	0	0	2	0	1	1	0	0	1	1	2	1	0	?	0	0	2	0	0	0	0	0
Uncisudis	?	?	?	?	?	?	?	1	1	0	?	1	?	2	?	?	?	0	0	1	0	0	0	0	2
Macroparalepis	0	0	0	1	0	2	0	1	1	0	0	1	2	2	1	0	?	0	0	0	0	0	0	0	0
Lestidiops	0	0	?	0	0	?	?	1	1	0	0	1	1	2	0	0	?	0	0	1	0	0	0	?	0
Sudis	?	?	0	0	0	2	0	1	1	0	0	1	1	2	?	?	?	0	0	0	0	0	0	0	0
Anotopterus	0	0	0	0	2	2	0	?	1	0	0	1	3	?	1	0	?	0	0	0	?	0	N	2	0
Bathysauroides	1	1	0	0	0	0	0	0	0	0	0	1	0	1	0	0	0	0	0	0	1	2	0	0	0
Bathysaurus	2	0	0	4	0	2	0	0	0	0	0	0	3	1	0	0	1	0	0	0	1	0	0	0	0
Gigantura	2	0	3	0	0	2	0	?	0	0	0	0	5	3	?	2	?	0	2	2	0	1	0	2	0
Paraulopus	0	0	0	5	?	4	0	?	?	Y	0	0	0	1	0	0	0	1	?	2	1	1	0	?	0

APPENDIX 1.2 Continued: Morphological Data Matrix. See Appendix 1.1 for abbreviated list of characters. Y=(01), L=(12), M=(02), N=(13).

	101	102	103	104	105	106	107	108	109	110	111	112	113	114	115	116	117	118	119	120	121	122	123	124	125
Diplophos	0	0	0	0	0	0	0	0	0	0	1	1	2	0	1	0	0	0	1	0	0	0	0	0	0
Myctophidae	0	0	0	0	0	0	1	0	0	0	0	0	0	0	0	0	0	0	0	0	0	0	0	0	0
Neoscopelus	0	0	0	0	0	0	0	0	0	0	0	0	0	0	0	0	0	0	0	0	1	0	0	0	0
Metavelifer	0	0	0	0	0	0	0	0	0	?	0	0	1	0	1	0	0	?	?	?	?	0	0	0	0
Polymixia	0	0	0	0	0	0	0	0	0	0	0	0	0	0	0	0	0	0	0	0	0	0	0	0	0
Aulopus	0	0	1	1	0	0	0	0	0	0	0	0	4	0	0	0	0	0	0	1	1	0	0	0	0
Pseudotrichonotus	0	0	1	1	0	0	0	0	0	0	0	0	0	0	0	0	0	0	0	1	1	0	0	0	0
Synodus	0	0	1	1	0	0	0	0	0	0	0	0	0	0	0	0	0	0	0	1	0	0	0	0	0
Trachinocephalus	0	0	1	1	0	0	0	0	0	0	0	0	0	0	0	0	0	0	0	1	0	0	0	0	0
Harpadon	0	0	1	1	0	0	0	0	0	1	0	0	2	0	0	0	0	1	0	0	0	0	0	0	0
Saurida	0	0	1	1	0	0	0	0	0	1	0	0	0	0	0	0	0	1	0	0	0	0	0	0	0
Bathypterois	0	0	1	0	1	1	0	0	0	1	0	0	1	0	0	0	0	1	0	1	?	0	0	0	0
Bathymicrops	0	0	1	0	?	1	0	0	0	?	0	0	2	0	0	1	0	?	?	?	?	0	0	0	0
Bathytyphlops	0	0	1	0	1	1	0	0	0	?	0	0	0	0	0	1	0	?	?	?	?	0	0	0	0
Ipnops	0	0	1	0	1	1	0	0	0	0	0	0	2	0	0	0	0	1	0	0	0	0	0	0	0
Scopelosaurus	0	0	1	0	2	1	0	0	0	1	0	0	0	0	0	0	0	1	0	0	0	0	0	0	0
Ahliesaurus	0	0	1	0	2	1	0	0	0	?	0	0	0	0	0	0	0	?	?	?	?	0	0	0	0
Chlorophthalmus	0	0	1	0	2	1	0	0	0	1	0	0	3	0	0	0	0	1	0	0	0	0	0	0	0
Parasudis	0	0	1	0	2	1	0	0	0	1	0	0	0	0	0	0	0	1	0	0	0	0	0	0	0
Bathysauropsis	0	0	1	0	2	?	0	0	0	0	0	0	3	0	0	0	0	1	0	0	0	0	0	0	0
Omosudis	0	0	1	0	2	0	1	0	0	0	1	0	0	0	1	0	0	0	1	0	0	1	2	1	0
Alepisaurus	0	0	1	0	2	0	1	0	0	0	1	0	?	0	1	0	0	0	1	0	0	1	2	1	0
Coccorella	1	0	1	0	2	0	1	0	1	1	1	0	4	0	1	0	1	0	0	0	0	1	1	0	0
Odontostomops	1	1	1	0	2	0	1	0	1	?	1	0	3	0	1	0	1	?	?	?	?	1	1	0	0
Evermannella	1	1	1	0	2	0	1	0	1	?	1	0	3	0	1	0	1	?	?	?	?	1	1	0	0
Scopelarchus	0	0	1	0	2	1	0	1	0	?	1	0	0	0	1	0	1	?	?	?	?	1	0	0	0
Scopelarchoides	0	2	1	0	2	0	0	1	0	?	1	0	0	0	1	0	1	?	?	?	?	1	0	0	0
Benthalbella	0	0	1	0	2	0	1	0	0	0	1	0	3	0	1	0	0	0	0	0	0	1	0	0	0
Rosenblattichthys	0	0	1	0	2	0	0	1	0	?	1	0	0	0	1	0	1	?	?	?	?	1	0	0	0
Paralepis	0	0	1	0	2	0	1	0	0	1	1	0	4	0	1	0	0	0	1	0	0	1	0	0	0
Arctozenus	0	0	1	0	2	0	1	0	0	?	1	0	0	0	1	0	0	?	?	?	?	1	0	0	0
Lestrolepis	0	0	1	0	2	0	1	0	0	?	1	1	0	1	1	0	0	?	?	?	?	1	1	0	1
Lestidium	0	0	1	0	2	0	1	0	0	1	1	1	0	1	1	0	0	0	1	0	0	1	1	0	1
Stemonosudis	0	0	1	0	2	1	1	0	0	?	1	1	0	1	1	0	0	?	?	?	?	1	1	0	1
Uncisudis	0	0	1	0	2	0	1	0	0	?	1	1	0	1	1	0	0	?	?	?	?	1	1	0	1
Macroparalepis	0	0	1	0	2	0	1	0	0	?	1	1	0	1	1	0	0	?	?	?	?	1	1	0	1
Lestidiops	0	0	1	0	2	0	1	0	0	?	1	1	0	0	1	0	0	?	?	?	?	1	1	0	1
Sudis	0	0	1	0	2	0	1	0	0	?	1	1	?	0	1	0	0	?	?	?	?	1	1	0	1
Anotopterus	?	0	1	0	2	0	0	0	0	?	?	?	1	1	1	0	0	?	?	?	?	0	1	2	0
Bathysauroides	0	0	1	0	2	0	0	0	0	0	0	0	3	0	0	0	0	1	0	0	0	0	0	0	0
Bathysaurus	0	0	1	0	2	0	0	0	0	0	0	0	4	0	0	0	0	1	0	0	0	0	0	0	0
Gigantura	0	0	?	0	2	0	0	0	0	?	1	0	2	0	2	0	0	?	?	?	?	0	2	0	0
Paraulopus	?	?	1	?	?	1	0	?	?	0	0	?	0	?	0	?	0	0	0	1	1	0	0	0	?

APPENDIX 1.2 Continued: Morphological Data Matrix. See Appendix 1.1 for abbreviated list of characters. Y=(01), L=(12), M=(02), N=(13).

	126	127	128	129	130	131	132	133	134	135	136	137	138	139
Diplophos	0	0	0	0	1	?	0	0	0	0	0	0	0	0
Myctophidae	0	0	0	0	0	0	0	Y	0	M	0	0	0	0
Neoscopelus	0	0	0	0	0	0	0	Y	0	0	0	0	0	0
Metavelifer	0	0	0	?	1	?	0	0	0	0	0	0	0	0
Polymixia	0	0	0	1	1	0	0	0	0	0	1	0	0	0
Aulopus	0	0	0	0	0	0	0	1	0	0	0	1	0	0
Pseudotrichonotus	0	0	0	0	1	0	0	1	0	0	0	2	0	0
Synodus	0	0	0	0	0	0	0	1	0	0	0	2	0	0
Trachinocephalus	0	0	0	0	0	0	0	1	0	0	0	2	0	0
Harpadon	0	0	0	0	0	0	0	1	0	0	0	2	0	0
Saurida	0	0	0	0	0	0	0	1	0	0	0	2	0	0
Bathypterois	0	?	2	1	0	1	0	1	1	0	0	Y	0	0
Bathymicrops	0	?	2	?	1	1	0	1	1	0	0	0	0	0
Bathytyphlops	0	?	2	1	1	1	0	1	1	0	0	1	0	0
Ipnops	0	?	5	1	1	1	0	1	1	0	0	0	0	0
Scopelosaurus	0	1	1	1	0	1	0	1	0	1	0	0	0	0
Ahliesaurus	0	1	1	?	0	1	0	1	0	1	0	0	0	0
Chlorophthalmus	1	1	0	0	0	1	0	1	0	0	0	1	0	0
Parasudis	1	1	0	0	0	1	0	1	0	0	0	1	0	1
Bathysauropsis	0	1	1	0	0	1	0	?	?	?	?	?	?	0
Omosudis	0	0	0	0	0	1	1	1	0	0	1	1	0	1
Alepisaurus	0	0	0	0	0	1	1	1	0	0	1	1	0	1
Coccorella	0	0	3	0	0	1	0	1	0	2	0	1	0	0
Odontostomops	0	0	0	0	0	1	0	1	0	2	0	1	0	0
Evermannella	0	0	3	0	0	1	0	1	0	2	0	1	0	0
Scopelarchus	0	0	3	0	0	1	0	1	0	2	0	1	0	0
Scopelarchoides	0	0	3	0	0	1	0	1	0	2	0	0	0	0
Benthalbella	0	0	3	0	0	1	0	1	0	0	0	1	0	0
Rosenblattichthys	0	0	3	0	0	1	0	1	0	2	0	1	0	0
Paralepis	0	0	0	0	0	1	0	1	0	0	0	1	0	0
Arctozenus	0	0	0	0	0	1	0	1	0	0	0	1	0	0
Lestrolepis	0	0	0	0	0	1	0	1	0	0	0	1	0	1
Lestidium	0	0	0	0	0	1	0	1	0	0	0	1	0	0
Stemonosudis	0	0	0	0	0	1	0	1	0	0	0	1	0	1
Uncisudis	0	0	0	0	0	1	0	1	0	0	0	1	0	0
Macroparalepis	0	0	0	0	0	1	0	1	0	0	0	1	0	0
Lestidiops	0	0	0	0	0	1	0	1	0	0	0	1	0	1
Sudis	0	0	0	0	0	1	0	1	1	0	1	1	0	0
Anotopterus	0	0	0	0	0	1	0	1	0	0	0	1	0	0
Bathysauroides	0	1	1	0	0	1	0	1	?	?	?	?	0	0
Bathysaurus	0	0	1	0	Y	1	0	1	1	0	0	1	1	0
Gigantura	0	0	4	0	0	1	0	1	0	0	0	1	1	0
Paraulopus	0	1	?	?	0	0	0	1	?	?	?	?	?	?

APPENDIX 1.3: Morphological Character Distribution. Distributions based on the total evidence Bayesian topology (Fig. 1.7, 1.8). Results from both ACCTRAN (A) and DELTRAN (D) optimizations are provided below. The first number represents the character, while the second indicates the state.

Node A (Order Aulopiformes): 1–1^{AD}, 2–1^{A}, 16–2^{A}, 18–1^{AD}, 58–1^{AD}, 59–1^{AD}, 69–1^{A}, 70–1^{A}, 89–1^{A}, 93–1^{A}, 103–1^{AD}, 120–1^{A}, 133–1^{AD}, 137–1^{A}.

Node B (Suborder Synodontoidei): 2–1^{D}, 3–1^{A}, 21–2^{A}, 33–1^{AD}, 34–2^{A}, 69–1^{D}, 70–1^{D}, 77–1^{A}, 85–1^{A}, 88–1^{A}, 89–2^{AD}, 92–1^{AD}, 93–1^{D}, 95–3^{AD}, 97–2^{AD}, 98–1^{A}, 99–2^{A}, 104–1^{AD}, 137–2^{AD}.

Node C: 60–1^{AD}, 77–1^{D}, 120–1^{D}, 121–1^{AD}.

Node D (Family Synodontidae): 3–1^{D}, 5–1^{AD}, 16–1^{AD}, 20–2^{AD}, 21–2^{D}, 30–1^{AD}, 31–1^{AD}, 34–2^{D}, 42–1^{AD}, 43–1^{AD}, 46–1^{AD}, 52–1^{AD}, 62–1^{AD}, 84–0^{AD}, 85–1^{D}.

Node E: 4–1^{AD}, 10–1^{AD}, 44–1^{AD}, 45–1^{AD}, 49–1^{AD}, 59–2^{AD}, 71–1^{AD}, 77–1^{D}, 86–1^{AD}, 88–2^{AD}, 98–1^{D}, 99–2^{D}, 120–1^{D}.

Node F: 13–1^{AD}, 14–1^{AD}, 22–1^{AD}, 48–1^{AD}, 64–1^{AD}, 77–0^{A}, 79–3^{AD}, 91–1^{AD}, 99–1^{AD}, 110–1^{AD}, 118–1^{AD}, 120–0^{A}.

Node G: 26–1^{A}, 89–1^{D}, 105–2^{A}, 106–1^{AD}, 127–1^{AD}.

Node H (Suborder Alepisauroidei): 2–1^{D}, 16–0^{A}, 28–1^{A}, 35–1^{A}, 49–1^{AD}, 53–1^{A}, 68–1^{A}, 69–1^{D}, 70–1^{D}, 87–1^{A}, 93–0^{A}, 105–1^{D}, 118–1^{AD}, 120–1^{A}, 131–1^{AD}.

Node I: 26–1^{D}, 27–1^{A}, 113–2^{AD}, 128–1^{AD}, 134–1^{A}.

Node J: 5–1^{A}, 14–1^{A}, 15–1^{A}, 41–1^{A}, 53–0^{A}, 69–2^{AD}, 76–2^{AD}, 81–2^{A}, 84–0^{AD}, 87–0^{A}, 106–0^{AD}, 127–0^{A}, 137–1^{D}, 138–1^{A}.

Node K: 5–1^{D}, 14–1^{D}, 15–1^{D}, 35–1^{D}, 96–1^{AD}, 113–3^{A}.

Node L: 6–1^{A}, 16–2^{A}, 27–1^{D}, 28–1^{D}, 35–0^{A}, 39–1^{AD}, 53–1^{D}, 63–2^{AD}, 68–1^{D}, 87–1^{D}, 137–0^{A}.

Node M (Family Ipnopidae): 6–2^{AD}, 7–1^{AD}, 16–3^{AD}, 47–1^{AD}, 66–1^{AD}, 67–1^{AD}, 70–0^{A}, 83–2^{AD}, 88–3^{AD}, 95–2^{A}, 105–1^{AD}, 128–2^{AD}, 129–1^{AD}, 134–1^{D}.

Node N: 23–1^{A}, 54–3^{AD}, 59–2^{A}, 84–2^{AD}, 94–1^{A}, 95–3^{AD}, 99–1^{AD}, 130–1^{AD}.

Node O: 25–1^{AD}, 29–1^{AD}, 50–1^{AD}, 116–1^{AD}.

Node P: 52–1^{A}, 83–1^{A}, 87–1^{D}, 110–1^{AD}.

Node Q (Family Chlorophthalmidae): 6–1^{AD}, 28–1^{D}, 35–1^{D}, 51–1^{AD}, 52–1^{D}, 53–1^{D}, 60–1^{AD}, 63–1^{AD}, 65–1^{AD}, 68–1^{D}, 78–1^{AD}, 126–1^{AD}, 137–1^{D}.

Node R: 28–0^{A}, 52–2^{AD}, 64–1^{AD}, 68–0^{A}, 76–1^{AD}, 92–1^{AD}.

Node S (Family Notosudidae): 6–1^{AD}, 24–1^{AD}, 25–1^{AD}, 26–1^{D}, 27–1^{AD}, 35–0^{A}, 38–1^{AD}, 43–1^{AD}, 53–1^{D}, 54–1^{AD}, 63–2^{A}, 72–1^{AD}, 83–2^{AD}, 95–2^{AD}, 128–1^{AD}, 129–1^{A}, 135–1^{AD}, 137–0^{A}.

Node T (Superfamily Alepisauroidea): 5–1^{AD}, 7–1^{A}, 13–1^{AD}, 14–1^{AD}, 17–1^{AD}, 18–0^{AD}, 19–1^{A}, 26–0^{A}, 28–3^{AD}, 35–1^{D}, 41–2^{AD}, 53–0^{A}, 59–0^{AD}, 65–2^{AD}, 69–2^{AD}, 82–1^{A}, 84–2^{A}, 106–0^{AD}, 107–1^{A}, 111–1^{AD}, 115–1^{AD}, 118–0^{AD}, 122–1^{AD}, 127–0^{AD}, 137–1^{D}.

Node U (Family Scopelarchidae): 19–1^{D}, 40–1^{AD}, 68–1^{A}, 82–1^{D}, 83–0^{A}, 84–1^{D}, 89–4^{AD}, 110–0^{A},128–3^{AD}.

Node V: 7–1^{D}, 107–0^{A}, 108–1^{AD}, 117–1^{AD}, 135–2^{AD}.

Node W: 15–2^{AD}.

Node X: 7–1^{D}, 19–2^{AD}, 36–1^{A}, 54–2^{AD}, 81–2^{A}, 83–1^{D}, 107–1^{D}, 123–1^{AD}.

Node Y (Family Evermannellidae): 8–1^{AD}, 20–1^{AD}, 25–1^{AD}, 28–2^{A}, 32–1^{A}, 39–2^{AD}, 81–3^{AD}, 82–1^{D}, 84–2^{D}, 99–2^{AD}, 101–1^{AD}, 102–1^{A}, 109–1^{AD}, 113–3^{AD}, 117–1^{AD}, 135–2^{AD}.

Node Z: 128–3^{AD}.

Node AA: 13–2^{AD}, 24–2^{AD}, 36–2^{A}, 55–1^{AD}, 56–1^{A}, 57–1^{A}, 61–1^{A}, 75–1^{A}, 76–0^{A}, 81–2^{D}, 82–0^{A}, 84–1^{A}, 88–1^{A}, 89–2^{AD}, 90–1^{A}, 112–1^{A}, 119–1^{A}, 125–1^{A}.

Node BB: 76–0^{D}, 88–4^{A}, 90–1^{D}, 119–1^{D}.

Node CC (Family Alepisauridae): 11–1^{AD}, 36–0^{A}, 65–0^{A}, 75–0^{A}, 80–1^{A}, 83–2^{A}, 98–1^{AD}, 110–0^{A}, 112–0^{A}, 124–1^{A}, 125–0^{A}.

Node DD: Molecular Data Only (no morphological data for *Magnisudis*).

Node EE: 13–1^{AD}, 15–2^{AD}, 22–1^{AD}, 24–0^{AD}, 55–0^{AD}, 56–0^{A}, 57–0^{A}, 61–0^{A}, 65–0^{D}, 73–1^{AD}, 79–2^{A}, 80–1^{D}, 81–1^{AD}, 88–4^{D}, 100–1^{AD}, 110–0^{D}, 123–2^{AD}, 124–1^{D}, 132–1^{AD}, 136–1^{AD}, 139–1^{AD}.

Node FF (Family Paralepididae): 9–1^{A}, 17–0^{AD}, 36–2^{D}, 37–1^{AD}, 56–1^{D}, 57–1^{D}, 59–1^{AD}, 61–1^{D}.

Node GG: 28–0^{A}, 79–1^{A}.

Node HH: 9–0^{A}, 13–1^{AD}, 26–1^{AD}, 74–2^{AD}, 75–0^{A}, 78–2^{AD}, 80–3^{AD}, 112–0^{A}, 123–0^{AD}, 125–0^{A}.

Node II: **9**–1^{D}, 64–0^{A}, 75–1^{D}, 88–1^{AD}, 95–1^{AD}, 112–1^{D}, 125–1^{D}, 139–1^{A}.

Node JJ: 139–1^{D}.

Node KK: Molecular Data Only.

Node LL: 114–1^{AD}, 139–0^{A}.

Node MM: Molecular Data Only.

***Alepisaurus*:** 79-2^{D}, 83-3^{A}.

***Anotopterus*:** 3-1^{AD}, 54-0^{AD}, 56-1^{D}, 57-1^{D}, 61-1^{D}, 62-1^{AD}, 80-2^{AD}, 88-3^{AD}, 99-2^{AD}, 107-0^{AD}, 113-1^{AD}, 114-1^{AD}, 122-0^{AD}, 124-2^{AD}.

***Arctozenus*:** 32-1^{AD}, 79-0^{A}, 88-0^{A}, 98-2^{AD}.

***Aulopus* (Family Aulopidae):** 3-0^{A}, 12-1^{AD}, 16-2^{D}, 21-2^{D}, 26-1^{AD}, 34-2^{D}, 48-1^{AD}, 85-1^{D}, 88-0^{A}, 98-0^{A}, 99-0^{A}, 113-4^{AD}, 137-1^{AD}.

***Bathymicrops*:** 3-1^{AD}, 7-0^{AD}, 23-1^{D}, 54-5^{AD}, 88-5^{AD}, 89-3^{AD}, 91-1^{AD}, 94-1^{D}, 98-4^{AD}, 99-2^{AD}.

***Bathypterois*:** 1-2^{AD}, 34-1^{AD}, 70-0^{D}, 92-1^{AD}, 95-2^{D}, 110-1^{AD}, 113-1^{AD}, 120-1^{AD}.

***Bathytyphlops*:** 5-2^{AD}, 23-0^{A}, 70-1^{A}, 83-1^{AD}, 94-0^{A}, 113-0^{AD}, 137-1^{AD}.

***Bathysauroides* (Family Bathysauroididae):** 27-0^{A}, 28-1^{D}, 41-2^{AD}, 53-1^{AD}, 63-1^{AD}, 76-1^{AD}, 77-1^{AD}, 81-0^{A}, 87-1^{AD}, 97-2^{AD}, 113-3^{D}, 127-1^{A}, 138-0^{A}.

***Bathysauropsis* (Family Bathysauropsidae):** 6-1^{D}, 16-2^{D}, 48-1^{AD}, 58-0^{AD}, 59-0^{AD}, 113-3^{AD}.

***Bathysaurus* (Family Bathysauridae):** 16-1^{AD}, 27-1^{D}, 28-0^{A}, 30-1^{AD}, 41-1^{D}, 52-1^{AD}, 59-0^{AD}, 62-3^{AD}, 64-1^{AD}, 68-0^{A}, 79-4^{AD}, 81-2^{D}, 88-3^{AD}, 92-1^{AD}, 113-4^{AD}, 127-0^{D}, 134-1^{D}, 138-1^{D}.

***Benthalbella*:** 7-0^{A}, 68-1^{D}, 107-1^{D}, 110-0^{D}, 113-3^{AD}.

***Chlorophthalmus*:** 26-0^{A}, 30-1^{AD}, 77-1^{AD}, 83-1^{D}, 84-2^{AD}, 113-3^{AD}.

***Coccorella*:** 11-1^{AD}, 15-2^{AD}, 19-3^{AD}, 28-2^{D}, 32-0^{A}, 36-0^{A}, 102-0^{A}, 113-4^{AD}.

***Evermannella*:** 32-1^{D}, 36-1^{D}, 102-1^{D}.

***Gigantura* (Family Giganturidae):** 62-2^{AD}, 78-3^{AD}, 81-2^{D}, 88-5^{AD}, 89-3^{AD}, 91-2^{AD}, 94-2^{AD}, 95-2^{AD}, 97-1^{AD}, 99-2^{AD}, 111-1^{AD}, 115-2^{AD}, 123-2^{AD}, 127-0^{D}, 128-4^{AD}, 134-0^{A}, 138-1^{D}.

***Harpadon*:** 11-1^{AD}, 62-2^{AD}, 88-3^{AD}, 97-0^{AD}, 98-1^{D}, 113-2^{AD}.

***Ipnops*:** 23-1^{D}, 59-2^{D}, 69-0^{AD}, 77-1^{AD}, 87-2^{AD}, 94-1^{D}, 98-2^{AD}, 128-5^{AD}.

***Lestidiops*:** 90-0^{AD}, 139-1^{D}.

***Lestidium*:** 1-3^{AD}, 64-0^{D}, 88-0^{AD}.

***Lestrolepis*:** 84-2^{AD}, 95-2^{AD}, 139-1^{AD}.

***Macroparalepis*:** 9-1^{D}, 75-1^{D}, 88-2^{AD}, 95-1^{D}, 112-1^{D}, 114-1^{A}, 125-1^{D}.

***Odontostomops*:** 32-1^{D}, 36-1^{D}, 102-1^{D}.

***Omosudis*:** 8-1^{AD}, 74-1^{AD}, 83-2^{D}, 96-1^{AD}.

***Paralepis*:** 28-0^{D}, 73-1^{AD}, 79-1^{D}, 88-4^{D}, 90-0^{AD}, 113-4^{AD}.

***Parasudis*:** 26-1^{D}, 70-0^{AD}, 81-4^{AD}, 83-2^{AD}, 139-1^{AD}.

***Paraulopus* (Suborder Paraulopoidei; Family Paraulopidae):** 2-0^{A}, 10-1^{AD}, 12-1^{AD}, 16-2^{D}, 60-1^{AD}, 69-0^{A}, 70-0^{A}, 79-5^{AD}, 81-4^{AD}, 93-1^{D}, 95-2^{AD}, 96-1^{AD}, 97-1^{AD}, 120-1^{D}, 121-1^{AD}.

***Pseudotrichonotus* (Family Pseudotrichontidae):** 3-1^{D}, 7-1^{AD}, 10-2^{AD}, 15-2^{AD}, 16-3^{AD}, 21-0^{A}, 34-0^{A}, 49-1^{AD}, 52-2^{AD}, 59-2^{AD}, 64-1^{AD}, 71-1^{AD}, 83-1^{AD}, 85-0^{A}, 88-1^{D}, 98-1^{D}, 99-2^{D}, 130-1^{AD}.

***Rosenblattichthys*:** 79-4^{AD}.

***Saurida*:** 88-1^{D}, 98-0^{A}.

***Scopelarchus*:** 19-2^{AD}, 88-3^{AD}, 106-1^{AD}.

***Scopelarchoides*:** 102-2^{AD}, 137-0^{AD}.

***Scopelosaurus*:** 63-2^{D}, 129-1^{D}.

***Sudis* (Family Sudidae):** 36-2^{D}, 75-1^{D}, 88-1^{D}, 112-1^{D}, 125-1^{D}, 134-1^{AD}, 136-1^{AD}.

***Synodus*:** 18–0^{AD}

***Uncisudis*:** 20-3^{AD}, 21-3^{AD}, 100-2^{AD}.